



National Library
of Canada

Acquisitions and
Bibliographic Services Branch

395 Wellington Street
Ottawa, Ontario
K1A 0N4

Bibliothèque nationale
du Canada

Direction des acquisitions et
des services bibliographiques

395, rue Wellington
Ottawa (Ontario)
K1A 0N4

Your file *Votre référence*

Our file *Notre référence*

NOTICE

The quality of this microform is heavily dependent upon the quality of the original thesis submitted for microfilming. Every effort has been made to ensure the highest quality of reproduction possible.

If pages are missing, contact the university which granted the degree.

Some pages may have indistinct print especially if the original pages were typed with a poor typewriter ribbon or if the university sent us an inferior photocopy.

Reproduction in full or in part of this microform is governed by the Canadian Copyright Act, R.S.C. 1970, c. C-30, and subsequent amendments.

AVIS

La qualité de cette microforme dépend grandement de la qualité de la thèse soumise au microfilmage. Nous avons tout fait pour assurer une qualité supérieure de reproduction.

S'il manque des pages, veuillez communiquer avec l'université qui a conféré le grade.

La qualité d'impression de certaines pages peut laisser à désirer, surtout si les pages originales ont été dactylographiées à l'aide d'un ruban usé ou si l'université nous a fait parvenir une photocopie de qualité inférieure.

La reproduction, même partielle, de cette microforme est soumise à la Loi canadienne sur le droit d'auteur, SRC 1970, c. C-30, et ses amendements subséquents.

THE UNIVERSITY OF ALBERTA

**ANALYSIS OF ATHABASCA OIL SAND BY NEAR-INFRARED DIFFUSE
REFLECTANCE SPECTROSCOPY AND INSTRUMENTAL NEUTRON
ACTIVATION**

By

Kingsley K. Donkor

A THESIS

**SUBMITTED TO THE FACULTY OF GRADUATE STUDIES AND RESEARCH
IN PARTIAL FULFILLMENT OF THE REQUIREMENTS FOR THE DEGREE OF
DOCTOR OF PHILOSOPHY**

THE DEPARTMENT OF CHEMISTRY

**EDMONTON, ALBERTA
SPRING 1995**



National Library
of Canada

Acquisitions and
Bibliographic Services Branch

395 Wellington Street
Ottawa, Ontario
K1A 0N4

Bibliothèque nationale
du Canada

Direction des acquisitions et
des services bibliographiques

395, rue Wellington
Ottawa (Ontario)
K1A 0N4

Your title Votre référence

Our title Notre référence

The author has granted an irrevocable non-exclusive licence allowing the National Library of Canada to reproduce, loan, distribute or sell copies of his/her thesis by any means and in any form or format, making this thesis available to interested persons.

L'auteur a accordé une licence irrévocable et non exclusive permettant à la Bibliothèque nationale du Canada de reproduire, prêter, distribuer ou vendre des copies de sa thèse de quelque manière et sous quelque forme que ce soit pour mettre des exemplaires de cette thèse à la disposition des personnes intéressées.

The author retains ownership of the copyright in his/her thesis. Neither the thesis nor substantial extracts from it may be printed or otherwise reproduced without his/her permission.

L'auteur conserve la propriété du droit d'auteur qui protège sa thèse. Ni la thèse ni des extraits substantiels de celle-ci ne doivent être imprimés ou autrement reproduits sans son autorisation.

ISBN 0-612-10807-4

Canada

THE UNIVERSITY OF ALBERTA

RELEASE FORM

NAME OF AUTHOR: Kingsley K. Donkor

TITLE OF THESIS: Analysis of Athabasca Oil Sand by Near-Infrared
Diffuse Reflectance Spectroscopy and Instrumental
Neutron Activation

DEGREE : Doctor of Philosophy

YEAR: 1995

Permission is hereby granted to THE UNIVERSITY OF ALBERTA LIBRARY to reproduce single copies of this thesis and to lend or sell such copies for private, scholarly or scientific research purposes only.

The author reserves other publication rights, and neither the thesis nor extensive extracts from it may be printed or otherwise reproduced without the author's written permission.

Kingsley Donkor
(Signed)

c/o Rev. E. Ofori Donkor
Mt. Olivet Methodist Church
P.O. Box 356. U.S.T.
Kumasi. GHANA

(Permanent Address)

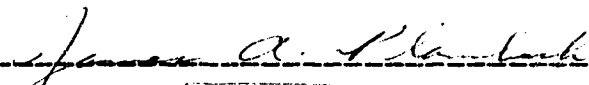
Date: November 21, 1994

**THE UNIVERSITY OF ALBERTA
FACULTY OF GRADUATE STUDIES AND RESEARCH**

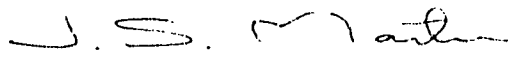
The undersigned certify that they have read, and recommend to the Faculty of Graduate Studies and Research for acceptance, a thesis entitled: ANALYSIS OF ATHABASCA OIL SAND BY NEAR INFRARED-DIFFUSE REFLECTANCE SPECTROSCOPY AND INSTRUMENTAL NEUTRON ACTIVATION submitted by KINGSLEY K. DONKOR in partial fulfilment of the requirements for the degree of Doctor of Philosophy.



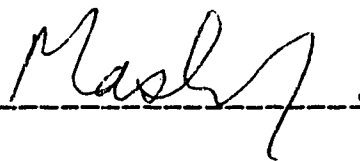
B. Kratochvil, Supervisor




J. A. Plambeck




J. S. Martin



J. Masliyah



F. F. Cantwell



R. A. Filby, External Examiner

Date: October 31, 1994

*To
my mom and Liza*

Abstract

Near-infrared diffuse reflectance spectroscopy (NIRDR) has been used to estimate the bitumen and solids content of Athabasca oil sand at a sampling resolution of 1-cm. The results made it possible to establish a detailed pattern of variability over a 15-m vertical transect of core. The resulting pattern was also used to investigate heterogeneity within the core section laterally. Factors such as effect of surface roughness and sampling frequency on the NIRDR bitumen results were evaluated. Roughness of the sample surface was found to have an important effect on the analytical results. It was also found that to attain a precision in NIR analyses for bitumen and solids of less than 5%, and to reduce errors arising from heterogeneity, measurements should be performed on a larger area than one square centimeter.

Since the accuracy of NIRDR for analyzing oil sands depends to a great extent on adequate calibration, an extensive study was carried out on the use of multivariate statistical techniques for optimizing the calibration models. The techniques investigated were Principal Component Regression (PCR) and Partial Least Squares (PLS). The results showed that these two techniques were comparable and satisfactory for this application.

The second part of the research involved the investigation of instrumental neutron activation analysis (INAA) as an alternative to the Dean-Stark technique for the determination of bitumen and fines in Athabasca oil sands. Effort was directed at possible correlation of elements determinable via their short-lived isotopes with the bitumen and fines of oil sand. Potential advantages of such a method include a fast turnaround time, elimination of the use of organic solvents, and a potential for automation. Correlations of both single elements or groups of

elements to the oil sand components on a microscopic scale were studied, using analytical test portions of a half gram. A strong correlation of decreasing slope was seen between bitumen content and a combination of six elements ($r = -0.91$). The correlations also show reasonable geochemical relationships between the major and trace elements present in oil sands.

The research also dealt with determination of trace elements in bitumen extracts via both the short and long-lived isotopes in an investigation of sources of contamination arising from micro-particulates suspended in the bitumen after Soxhlet extraction of oil sands. The results obtained offered information on the extent to which these particulate elements are associated with the inorganic and organic portions of bitumen. Vanadium, nickel and mercury were found in measurable amounts associated with the bitumen portion while the other elements were found to be largely associated with the particulate fines material suspended in the bitumen.

Acknowledgements

I wish to express my heartfelt thanks to my supervisor Professor Byron Kratochvil for his invaluable guidance and kind assistance throughout this project and for his generosity during my graduate school years in Edmonton.

My sincere appreciation to the staff of Syncrude Research for the oil sand samples and for providing space and equipment for the near-infrared part of this research. In this regard I extend my special gratitude to Mr. Gordon R. Thompson for his enthusiastic supervision, and Ms. Sylvia Gonzalez for help with the instrumentation.

I thank the staff of the University of Alberta SLOWPOKE Nuclear Reactor Facility for making available the facility for this research, particularly Dr. M.J.M. Duke for his fruitful guidance and helpful suggestions in instrumental neutron activation analysis.

It is also a pleasure to acknowledge all members of the research group for the friendly and enjoyable working atmosphere they provided throughout the project. Special thanks to Dr. Angelo Fernando for help with the statistical analysis. I also thank Dr. Monica Palcic for lending a centrifuge for use in this project.

Finally, I would like to gratefully acknowledge the Chemistry Department and the Natural Sciences and Engineering Research Council (NSERC) for financial support.

TABLE OF CONTENTS

PART 1: Analysis of Athabasca Oil Sand by Near-Infrared Diffuse Reflectance Spectroscopy

CHAPTER	PAGE
1. Introduction and Background to Method	1
1.1 General Principles of Near-Infrared Diffuse Reflectance Spectroscopy	1
1.2 Quantitative Analysis using NIR	3
1.3 Sources of Error in NIR analysis	3
1.4 Data Treatment	6
1.5 Calibration Techniques	8
1.6 Multivariate Calibration Methods	10
1.6.1 Multiple linear regression (MLR)	10
1.6.2 Full spectrum methods (PCR and PLS)	11
1.6.3 Theoretical background of Principal Component Regression (PCR)	14
1.6.4 Summary	17
2. Instrumentation and Experimental Procedure	18
2.1 Samples	18
2.2 Apparatus and Procedure for NIR Analyses	19
2.3 Soxhlet Extraction Procedure for Determination of weight percent Bitumen and Solids in Core Samples	23
3. Results and Discussion of Diffuse Reflectance Near Infrared Measurements of Athabasca Oil Sand	29
3.1 Data Analysis	29
3.2 Effect of Roughening on Bitumen Levels	46
3.3 Effect of Sampling Frequency on Error of Bitumen Results	48
4. Summary and Future Directions for NIR studies	50
4.1 Conclusions and Summary	50
4.2 Suggestions for Future NIR work	52

PART 2: Analysis of Athabasca Oil Sand by Instrumental Neutron Activation

5.	Introduction	53
5.1	Neutron Activation Analysis: Background and General Principles	53
5.1.1	Factors influencing activation with neutrons	55
5.2	Theory of Activation Analysis	57
5.2.1	Radioactive decay	57
5.2.2	Relation between measurement of radioactivity and amount of an element present in an irradiated sample....	57
5.3	Nuclear Interferences	61
5.4	Detection of gamma radiation	63
5.4.1	Mechanism	63
5.5	Detection and Measurement of Gamma radiation	64
5.5.1	Detectors	64
5.5.2	Amplification of the signal from a gamma radiation detector	66
5.5.3	Pulse height analysis	66
5.6	Gamma-ray Spectra	67
5.7	Statistical Errors in INAA	68
5.7.1	Accuracy	68
5.7.2	Detection limits	69
5.8	The University of Alberta SLOWPOKE Nuclear Reactor Facility	70
5.8.1	Description of SLOWPOKE II nuclear reactor	70
5.8.2	Sample Irradiator in the SLOWPOKE reactor	72
6.	Study of Elements Determinable in Athabasca Oil Sand by INAA: Introduction	76
6.1	Experimental Procedure	76
6.1.1	Preparation of irradiation vials for INAA	76
6.1.2	Preparation of half gram test portions of oil sand for INAA	77
6.1.3	Preparation of extracted bitumen and fines samples for INAA	77
6.1.4	Preparation of standards for INAA	78

6.1.5	Irradiation and counting of short-lived isotopes	79
6.1.6	Spectral correction and analysis	80
6.2	Results and Discussion for Correlations of Elemental Data in Raw Oil Sand and Bitumen Content	85
6.3	Analyses of Ten and Thirty Gram Test Portions of Oil Sand	105
6.3.1	Preparation and analysis of ten gram samples for INAA	105
6.3.2	Preparation and analysis of thirty gram samples for INAA	106
6.3.3	Results and discussion	106
7.	Estimation of Trace Elements in Oil Sand Bitumen by INAA: Introduction	112
7.1	Evaluation of Lateral Heterogeneity in Oil Sand Core.....	113
7.1.1	Preparation of samples and experimental conditions.....	114
7.1.2	Results and discussion	114
7.2	Determination of Trace Short-Lived Elements present in Bitumen	119
7.2.1	Sample preparation for filtration	119
7.2.2	Sample preparation for centrifugation	123
7.2.3	Results and discussion	123
7.3	Determination of Trace Long-Lived Elements present in Bitumen	135
7.3.1	Experimental procedure	135
7.3.2	Results and discussion	135
8.	Summary and Future Directions in the Characterization of Athabasca Oil Sand by INAA	139
8.1	Conclusions and Summary for INAA research	139
8.2	Suggestions for Future Work.....	142
	References	143

APPENDIX

A. Data collected on Oil Sand Core by Near-Infrared Diffuse Reflectance Spectroscopy..... 153

Glossary 154

Section 1..... 155

 Data for calibration model of *bitumen* using PCR on non-roughened surfaces 155

 Data for calibration model of *bitumen* using PLS on non-roughened surfaces 156

 Data for calibration model of *bitumen* using PCR on roughened surfaces 157

 Data for calibration model of *bitumen* using PLS on roughened surfaces 158

 Data for calibration model of *solids* using PCR on non-roughened surfaces 159

 Data for calibration model of *solids* using PLS on non-roughened surfaces 160

 Data for calibration model of *solids* using PCR on roughened surfaces 161

 Data for calibration model of *solids* using PLS on roughened surfaces 162

Section 2 163

 Data for three sets of bitumen values obtained laterally across core section, *A* 163

 Data for three sets of bitumen values obtained laterally across core section, *E* 165

 Data for three sets of bitumen values obtained laterally across core section, *J* 167

 Data for three sets of bitumen values obtained laterally across core section, *L* 169

Section 3 171

 Data for *bitumen* values estimated for the vertical transect of oil sand using PCR calibration model on non-roughened surfaces 171

	Data for <i>solids</i> values estimated for the vertical transect of oil sand using PCR calibration model on non-roughened surfaces	201
B.	Section 1	231
	Data and programs used in the analysis of a core by INAA.....	231
	Sample program used to carry out a PCA of elements in Athabasca Oil Sands.....	232
	Section 2	234
	Data for concentrations of elements in <i>half</i> gram test portions of oil sand	234
	Data for concentrations of elements in <i>ten</i> gram test portions of oil sand	239
	Data for concentrations of elements in <i>thirty</i> gram test portions of oil sand	241
	Data for RSD's of concentrations of eleven elements over nine transverse sections of oil sand core	242
	Data for concentrations of elements in bitumen determined via their long-lived isotopes	243

LIST OF TABLES

TABLE	PAGE
3.1 Correlation coefficients and optimum number of factors used for calibration models.....	32
3.2 Comparison of performance of different calibration models	34
3.3 Summary of SEC values for different calibration models using all available samples in the training set	35
3.4 Sampling error for bitumen analyses of 1 square centimeter area spaced at 2, 5, 10, 15 and 20 cm	49
6.1 Comparison of elemental concentrations measured by INAA with certified values for soil standard, SO-4	81
6.2 Comparison of elemental concentrations measured by INAA with certified values for NRC Marine Sediment Reference material, BCSS-1	82
6.3 Comparison of elemental concentrations measured by INAA with certified values for NRC Marine Sediment Reference material, MESS-1	83
6.4 Comparison of elemental concentrations measured by INAA with certified values for NRC Marine Sediment Reference material, PACS-1	84
6.5 Correlation of concentrations of elements in oil sand with weight percent bitumen	91
6.6 Principal Component Analysis of various combinations of elements	96
6.7 Correlation of elemental concentrations with fines content	99
6.8 Cross correlations of elemental concentrations present in fines	101
6.9 Correlation of concentrations of elements in oil sand with weight percent bitumen	108
6.10 Comparison of correlations of concentrations of short-lived elements with respect to bitumen for the half, ten and thirty gram test portions of oil sand	110

7.1	Weight percent bitumen and solids determined by Soxhlet extraction technique for nine transverse sections of oil sand core	117
7.2	Relative standard deviations of weight percent bitumen and solids of nine transverse sections of oil sand core determined by Soxhlet extraction method	118
7.3	Irradiation-Decay-Count scheme used for analysis of bitumen samples and filter paper	122
7.4	Concentrations, in micrograms per gram, of vanadium, aluminum and manganese in unfiltered and filtered bitumen from Soxhlet extractions	125
7.5	Concentrations of halogens ($\mu\text{g/g}$) in filtered and unfiltered bitumen, as determined by INAA	130
7.6	Ratios of concentrations of halogens in filtered and unfiltered samples of bitumen	131
7.7	Comparison of concentrations of vanadium and aluminum found by INAA in untreated and centrifuged bitumen	134

LIST OF FIGURES

FIGURE	PAGE
1.1 Flow Chart showing mathematical steps involved in Principal Component Regression (PCR)	16
2.1 Arrangement of optical system of Quantum 1200 NIR instrument	20
2.2 Schematic diagram of sampling table for analysis of oil sand	22
2.3 General set-up of micro-Soxhlet assembly for the determination of weight percent bitumen and solids in oil sand	24
2.4 Soxhlet extraction apparatus for determination of bitumen and solids contents of oil sand	25
2.5 Evaporating dishes containing bitumen residue obtained from the Soxhlet extraction of oil sand after evaporation of toluene	27
2.6 Results for analyses of training set samples showing precision of Soxhlet extraction technique	28
3.1a Standard error of prediction as a function of number of factors incorporated in model (bitumen)	30
3.1b Cumulative variance described in model as a function of number of factors (bitumen)	30
3.2 Comparison of predicted versus measured bitumen content for non-roughened samples in training set	36
3.3 Comparison of predicted versus measured bitumen content for roughened samples in training set	37
3.4 Comparison of predicted versus measured solids content for non-roughened samples in training set	38
3.5 Comparison of predicted versus measured solids content for roughened samples in training set	39
3.6 Distribution of percent bitumen residuals relative to the predicted bitumen content	40
3.7 Variation in bitumen content as a function of depth for a 15-m test section of core	42
3.8 Variation in solids content as a function of depth for a 15-m test section of core	43
3.9 Plot of standard deviation versus its location along the core sections A and E	44

3.10	Plot of standard deviation versus its location along the core sections J and L	45
3.11	Effect of surface roughening on bitumen levels in oil sand	47
5.1	University of Alberta SLOWPOKE-II reactor facility	74
5.2	Cut-away view of SLOWPOKE-II reactor critical assembly and core	75
6.1	Correlation plots of aluminum and potassium concentrations versus bitumen content for half gram portions of oil sand	86
6.2	Correlation plots of dysprosium and vanadium concentrations versus bitumen content for half gram portions of oil sand	87
6.3	Correlation plots of titanium and sodium concentrations versus bitumen content for half gram portions of oil sand.....	88
6.4	Correlation plots of samarium and europium concentrations versus bitumen content for half gram portions of oil sand	89
6.5	Correlation plots of chlorine and barium concentrations versus bitumen content for half gram portions of oil sand	90
6.6	Relationship of fines to bitumen content in oil sand	92
6.7	Cross-correlation scatter plots of europium versus dysprosium and samarium versus dysprosium for half gram test portions of oil sand	94
6.8	Cross-correlation scatter plots of sodium versus potassium and samarium versus europium for half gram test portions of oil sand	95
6.9	Combination of elements by PCA correlated with bitumen content	100
6.10	Correlation plots for aluminum and dysprosium concentrations versus fines content for half gram test portions of oil sand	102
6.11	Correlation plots for sodium and chlorine concentrations versus fines content for half gram test portions of oil sand.....	103
6.12	Cross-correlation of concentrations of europium versus dysprosium and vanadium versus sodium present in fines portion of oil sand	104

***Part 1: Analysis of Athabasca Oil Sand for Bitumen and Solids
by Near-Infrared Diffuse Reflectance Spectroscopy***

Chapter 1

Introduction and Background to Method

In a previous study [1,2], Near-Infrared Diffuse Reflectance spectroscopy (NIRDR) was successfully used for the determination of bitumen content in samples of Athabasca Oil Sand. It was shown that the technique can be used on small samples with minimal problems. However, owing to time limitations the study was limited to a 4 meter-long section of core, and so could not provide information on a typical cross section of an oil sand deposit. Therefore, it was decided to analyze a core section that passed through a complete zone of oil sand to investigate how frequently analyses of 1-cm sections needed to be done to give an acceptable estimate of the percent bitumen and solids distribution through a zone.

This chapter provides background on NIRDR as an analytical method, and on the statistical methods available for processing the analytical data obtained by the method.

1.1. General Principles of Near-Infrared Diffuse Reflectance Spectroscopy

The infrared (IR) region of the electromagnetic spectrum extends from 10 to 14300 cm^{-1} . It may be divided conveniently, both instrumentally and functionally, into near, middle and far IR as follows:

IR Region	Characteristic transitions	Wavelength range (nm)
Near	overtones/combinations	700 to 2500
Mid	fundamental vibrations	2500 to 5×10^4
Far	rotations	5×10^4 to 10^6

The near-infrared (NIR) is dominated by overtone and combination bands of fundamental molecular vibrations occurring in the mid-infrared [3-6,8,9]. Overtones and combinations arise due to the anharmonic nature of molecular vibrations, mainly hydrogen stretching modes, which show an especially large deviation from harmonic behavior because bonds involving hydrogen, the lightest atom, vibrate with large amplitude when undergoing stretching vibrations involving AHx functional groups or combinations involving stretching and bending modes of vibration of such groups [4,5].

Only molecules that possess a permanent displacement of electric charge (dipole) are capable of absorbances in the infrared region. Thus, NIR spectroscopy involves measurement of the absorbance of IR radiation through molecular vibrations which produce an oscillating electric dipole within the molecule [4].

Most NIR analyses are performed in the 1000 to 2500 nm region. This is due to the prevalent use of PbS detectors, whose sensitivity is greatest over this range. The intensities of the first overtone and combination bands are one to three orders of magnitude weaker than those of the fundamental bands. These lowered intensities require that moderately concentrated samples and longer path lengths be used. On the other hand, nonlinearity effects due to strong absorptions are less likely to occur [5-7].

Near-infrared radiation reflects from samples as either specular reflectance or diffuse reflectance[8]. Specular reflectance is mirror like; no radiation is absorbed and the angle of reflectance equals the angle of incidence. In diffuse

reflectance, the phenomenon on which most NIR is based, the incident radiation penetrates the surface of the material for a short distance, excites vibrational modes of sample molecules in this thin film of material, and is then scattered at all angles [4,9].

1.2. Quantitative Analysis using NIR

NIR is used more for quantitative measurements than qualitative work. If the bands are distinct, separate and well-characterized, a constituent may be determined by a direct application of Beer's Law. In most practical cases, however, NIR bands are broad and overlapping, and not readily assignable to a single constituent. Furthermore, scattering effects in reflectance measurements may cause nonlinearity as well as indeterminate path lengths. Hence a statistical approach to modeling the data is useful. Such an approach makes NIR analysis (NIRA) a secondary method in that the data from many wavelengths must be compared or "trained" with reference to a set of primary laboratory measurements [4,6,10]. As a result, the usual procedure for developing a quantitative NIR method involves selection of representative samples, acquisition of spectra and reference analytical data, pretreatment and statistical modeling of the data, and validation of the results.

1.3. Sources of error in NIR Analysis

The most troublesome source of error in NIR analysis is selection of appropriate samples for calibration, sampling and comparison. A set of samples used for calibration must be representative of the material to be studied in the future, and there must be enough samples in the set to permit precise estimation of the calibration constants [11-13]. The optimal size for diffuse reflectance samples has been determined as a function of detector size [14]. Sample sizes larger than

those normally used in conventional absorption analysis, in conjunction with variable size detectors, generally give the best results. Sample heterogeneity has also been found to be a major source of noise [14].

The way in which samples are packed into the cell can also have a profound influence on diffuse reflectance results [15]. It was found that when samples display a high degree of heterogeneity, repacking and rereading the samples, followed by averaging of the results, can improve the precision. Scanning the samples on a moving stage to sample a larger area has also been found to reduce the effects of nonhomogeneity [16].

Sampling errors may occur at various places in the calibration-validation process. One source of error is caused by the reference and NIR methods analyzing different subsamples; also, the two methods may look at different amounts of material. Here, however, the inverse relationship that exists between sample size and error accounts for some of the differences in precision between the methods. Also, NIR measurements can introduce sampling error because the radiation typically penetrates 2 mm or less, whereas the reference sample may take material from depths of 10 mm or more. Thus only a small portion of the material is measured [4].

Moisture levels in samples are also important because they influence scattering of radiation, a potential source of error. The scatter coefficient is proportional to the ratio of the refractive index of the particles to that of the surrounding medium. Progressively replacing air with water vapor in that medium results in a decrease in the scatter coefficient because the refractive index of water is greater than that of air. This means that variations in moisture content are accompanied by a shift in the spectra along the $\log(1/R)$ axis [4,5] where R is the reflectance. Also, significant errors occur if samples high in moisture are tested using a calibration derived from low moisture samples and vice versa. The effect

of moisture can be compensated for by calibrating with samples covering as wide a range of moisture contents as possible [5].

Particle size distribution in particulate samples may also be a source of error in NIR analyses [4,5]. Particle size and shape affect the amount of specular reflectance contributing to the observed spectrum. A change in particle size causes a change in the amount of radiation scattered by the sample. This produces a baseline shift (additive effect). Scattering (S) diminishes with increasing mean particle size (D) according to the relation $S \propto 1/D$, hence the larger the particles the smaller the scattering. As a result, the direction of the radiation does not change as often, but penetrates deeper into the sample, is absorbed to a greater extent, and results in an increase in $\log(1/R)$. In addition, strong absorbers show more change in absorbance with particle size than the weak [4,5], leading to a multiplicative effect.

Also, scattering is greater at shorter wavelengths in NIR than at longer ones. Thus a common feature of near-IR spectra is a low baseline absorbance at shorter wavelengths, increasing to higher levels as one moves toward longer wavelengths [4].

The temperature of a sample presented to the NIR instrument is recognized as another potential source of error if it is very different from that of the samples at the time of calibration [4,5]. The most satisfactory means of controlling this potential problem is to ensure that the temperature of all samples is within ± 5 °C of the temperature of the calibration samples [5]. Good calibration depends on the reference method used, so effort should be made to minimize measurement errors in the reference method.

Other sources of error which can contribute to nonlinearity arise from factors associated with the instrument itself such as amplifier noise, stray light, and

internal fluctuations in temperature which may affect the output of the lead sulfide detectors [4].

In summary, most of the important sources of error in NIR analysis can be minimized by careful calibration. It is dangerous, however, to perform a specific calibration and attempt to extrapolate it with respect to a range of constituents, particle sizes, moisture levels or temperatures that extend beyond the conditions used for the calibration set.

1.4. Data Treatment

Raw diffuse reflectance data often deviate from Beer's law because of scattering, stray light and instrumental response. The different particle sizes give rise to scattering to varying extents and this scattering can cause high intercorrelation between data at different wavelengths [17,18]. This intercorrelation, termed *multicollinearity*, (or simply *collinearity*) reduces the number of independent wavelengths available and results in a less robust calibration model [4,18-20]. Pretreatment of the raw optical data prior to calibration simplifies the multivariate mathematical model, thereby improving the ultimate performance of the method. A number of different data pretreatments have been used to convert IR data to more analytically useful forms and correct for scattering effects.

One of the most commonly used approaches is linear transformation. In this method the reflectance is converted to apparent absorbance [4,6,21], and Beer's Law is expressed as

$$A = \log (1/R) = kcl$$

Here k is a constant (molar absorptivity), c is concentration in molarity, and l is pathlength in cm. This transform was used for most of the work described in this thesis.

Another widely used transform is the Kubelka-Munk model (KM) [22];

$$f(R) = K/S = (1 - R)^2/2R$$

in which the ratio of an absorption coefficient K , and a scatter coefficient, S , is given in terms of R , the diffuse reflectance at a given wavelength (obtained from the ratio of the sample spectrum and a reference spectrum).

This function predicts a linear relationship between the absorption coefficient and the peak value of $f(R)$ for each absorbance band, provided that the scattering coefficient remains constant. For relatively dilute samples the molar absorption coefficient can be related to the concentration of the absorbing species through the expression $k = 2.303\epsilon c$, where ϵ is the molar absorptivity and c is the molar concentration. Therefore

$$f(R) = (1-R)^2/2R = c/k' = 2.303\epsilon c/s$$

where $k' = s/ 2.303\epsilon$.

With strong variation in light scatter the KM function has been found to be better than the $\log(1/R)$ relation after scatter correction [20]. Several scatter correction treatments have been applied to NIR data. Among the simplest is to divide the absorbance values at all wavelengths by that at a single reference wavelength [23]. This correction does not take into account the wavelength dependence of scattering.

Derivation is an approach which addresses two basic problems with NIR spectra, namely, overlapping peaks and large baseline variations. It minimizes the effects of scattering by removing additive offsets that change linearly with wavelength. Derivatives can also accentuate sharp spectral features, thereby helping to resolve overlapping bands [18]. Higher-order derivatives have the same basic effects and resolve overlapping bands better than lower-order ones but are more sensitive to noise [24].

Another widely used transform is the Multiplicative Scatter Correction (MSC). In this method the scatter of each spectrum is corrected to that of an "ideal" spectrum, usually the mean spectrum [25].

1.5. Calibration Techniques

The principal disadvantage of NIR analysis is that it is empirical. There is no mathematical law available to quantitatively describe in a complete way the interaction of radiation with a scattering medium containing a heterogeneous distribution of absorbing species. As a result, NIR instrument readings are arbitrary and require calibration using samples of known composition.

Calibration of an NIR instrument involves collecting an initial set of samples that are as representative as possible of the population of samples to be analyzed in future with the instrument. These initial samples, known as the training set, are then analyzed by a reliable independent reference method for the constituent(s) of interest and their NIR spectra collected. A calibration equation or model is derived from the two sets of data by statistical regression methods and applied to predict reference results for future samples measured by NIR [18-20].

Before the calibration model can be used to predict unknown samples, the quality of its possible future performance must be assessed. This can be done by a number of statistical methods, including calculation of the standard error of estimate or standard error of calibration (SEE or SEC), and the standard error of prediction (SEP). These methods are defined as follows [4,9,19].

The SEC is the standard deviation for the set of residuals resulting from differences between actual (independent laboratory analytical results) and NIR predicted values for samples *within* the calibration set. In this calculation the residual for each sample is equal to the actual chemical value minus the NIR

predicted value for all samples within the calibration set. It is an indication of the total residual error due to the particular regression equation to which it applies.

The SEP is the standard deviation for the residuals due to differences between actual and NIR predicted values for samples *outside* of the calibration set using a specific calibration equation. It is calculated as the root mean square differences (RMSD) for n degrees of freedom, and it allows for comparison between NIR observed predicted values and the reference laboratory values.

The equations for these two methods may be given as:

$$SEP = \left[\frac{\sum_{i=1}^M (y_i - \hat{y}_i)^2}{M} \right]^{1/2}$$

$$SEC = \left[\frac{\sum_{i=1}^N (y_i - \hat{y}_i)^2}{N-K-1} \right]^{1/2}$$

where N is the number of calibration samples, K is the number of parameters in regression equation, M is the number of samples in validation set, y_i is measured value of the i th sample, and \hat{y}_i the corresponding predicted value from the algorithm or regression equation.

A standard error of estimate (SEE) is calculated for the set of calibration samples, and a standard error of prediction is calculated from validation samples (samples that have not been included in the calibration set). Approximately equal values for these two statistics indicate a good calibration model. An ideal calibration model is one where both the SEC and the SEP values are equal to zero. In practice, however, a small difference between instrumental prediction and the laboratory reference value is usually present, resulting in both the SEC and SEP values being greater than zero.

Specific validation techniques are also sometimes used. These include bootstrapping and cross-validation. In bootstrapping, the prediction set is obtained from the calibration set by randomly splitting the calibration set into two and using one part as the calibration set and the other as a prediction set. In cross-validation (leave-one-out), one sample is left out of the calibration set each time and the calculation repeated until each sample is left out once [19].

1.6. Multivariate Calibration Methods

Diffuse reflectance-near infrared spectrophotometry yields non selective data because of spectral interference from strongly overlapping constituents and because of variations in light scattering. To minimize these problems the analytical equation of the near-infrared instruments has to be multivariate, that is, measurements on many different wavelengths are combined [19,20].

The calibration models used in this work were based on three statistical multivariate methods [26-38]: Multiple Linear Regression (MLR), Partial Least Squares (PLS), and Principal Component Regression (PCR). These methods are outlined briefly in the following sections.

1.6.1. Multiple linear regression

Multiple Linear Regression (MLR) is a technique in which spectral intensities at selected wavelengths are used in an inverse Beer's Law model incorporating concentration as a function of absorbance:

$$Y = b_0 + b_1X_1 + b_2X_2 + \dots + b_kX_k + E \quad (1.1)$$

Here Y is the property to be predicted (for example, weight % bitumen in an oil sand), X_i the measured spectral data values (log 1/R values at selected wavelengths), b_i the corresponding regression coefficients and E the residual

error. With this method the selection of optimum wavelengths is crucial to successful performance of the model because data compression is achieved by eliminating most of the spectral information. This means that MLR is subject to high error if the wavelengths are not well selected, and overfitting of the data (modeling of noise or random errors) can easily occur.

To apply MLR a wavelength is selected which already describes the property of interest fairly well, i.e., a wavelength which correlates well with the constituent of interest. A second wavelength which has the next best correlation and which when included improves the first correlation is then added. Succeeding wavelengths are selected and added only if they improve correlation. This process is continued until no improvement in the model is gained by inclusion of additional wavelengths. Overall the model is built from a starting wavelength and grows to yield a final model of the form shown in Equation 1.1.

1.6.2. Full spectrum methods

Partial Least Squares (PLS) and Principal Component Regression (PCR) comprise full spectrum methods. These are factor-based techniques which are becoming more commonly used because of several important advantages that they offer [19,20,26].

A major advantage of both these methods is that they make use of data from the whole spectrum so that no information is lost. Also, they employ new variables or factors which are orthogonal to each other, thereby eliminating collinearity without loss of spectral information. This produces more robust models [19,20,26,36,39]. A large portion of the noise is removed from the data because it is spread throughout all the factors, whereas the significant information is concentrated into the first few factors. Both methods have signal-averaging

capabilities and allow interpretation of underlying chemical and physical phenomena through application of spectral loadings and spectral residuals [19].

PCR and PLS are data compression techniques sharing common advantages, but they differ in the way the spectra are decomposed into the new variables, or factors. In PLS the reference laboratory data are used to guide the estimation of the factors from the near-infrared data, whereas in PCR the factors are estimated statistically from the near-infrared data only. The consequence of this difference is that PCR is more efficient at minimizing the least-squares residual. However, it should be noted that in some cases the first few factors may not contain spectral information relevant to the constituent, hence making it necessary to include the constituent data in the factoring process as in PLS. This tends to make PLS more sensitive to overfitting as compared to PCR.

Principal Component Regression (PCR) uses a form of data compression in which the data are converted into a smaller number of new variables which are linear combinations of the original spectral data, and hence contain information from the entire spectrum. These new variables, called *principal components* or *factors*, are chosen orthogonal to one another so that they are uncorrelated and account for most of the variability between samples. The first principal component is chosen to describe the maximum variability, such that the amount of spectral information in this variable is maximized. The second is that which describes the largest variability remaining after the first is mathematically removed. This procedure continues for subsequent factors in the same manner to yield principal component terms in decreasing order of importance. The significant part of the data is concentrated within the first few factors while the noise is restricted to the later factors. This allows the experimenter to build the regression model by including only those terms containing a significant part of the useful data and to eliminate much of the noise. Reference data, obtained from an independent

analysis such as Soxhlet extraction for weight % bitumen, can then be incorporated to determine regression coefficients which yield the least sum of squared errors in the calibration model. The steps involved in carrying out a PCR are outlined in Figure 1.1.

Determining the optimum number of factors to use in a PCR model is the most important step in creating the model. As the first few factors are added, the amount of predictive information increases substantially, while the noise increases to a much smaller degree. As more factors are incorporated, the increase in predictive information slows, while the increase in noise grows. Eventually a point is reached where the benefit of gaining predictive information by addition of a factor are outweighed by the increase in error introduced by the noise associated with that factor. This point indicates the optimum number of factors to be used in the model without overfitting. It is usually determined by plotting the SEP against the number of factors and selecting the number of factors which corresponds to the minimum SEP.

In PLS the first factor chosen is a linear combination of all original spectral measurements, with each one weighted proportionally to its correlation with the reference measurement. This factor is then removed statistically and a second factor generated which has maximum correlation of the residuals (difference between predicted and actual spectra). The process continues in this manner to yield the rest of the factors. The optimum number of factors are decided in the same way as in PCR. The reference data are again incorporated and regressed onto the factors to determine the regression coefficients.

The PLS and PCR methods each have particular advantages in specific situations. As will be seen, a comparison of the two methods in this work shows that comparable results are achieved by both methods.

1.6.3. Theoretical background of Principal Component Regression (PCR)

The theoretical principles behind PCR have been extensively described in the literature [19,20,26,40-50]. Figure 1.1 illustrates the mathematical steps involved in doing PCR. For a system of b components that obeys Beer's Law, the absorbance of the mixture at any wavelength will be a linear function of the absorbance of each component:

$$A = a_1C_1 + a_2C_2 + \dots + a_nC_n$$

If the absorbance is measured at n wavelengths for m samples containing b analytes, then the equation system can be expressed mathematically in matrix form as

$$A = CN + E$$

where A is the absorbance matrix ($m \times n$), C is the concentration matrix ($m \times b$), N is the absorptivity coefficient matrix ($b \times n$) and E is the residuals matrix.

In PCR calibration, the absorbance matrix, A , is first decomposed by the mathematical tool of eigenanalysis into two matrices, the scores matrix, P_S ($m \times p$), and the loadings matrix, P_L ($p \times n$).

$$A = P_S P_L + R$$

where p is the number of components and R is the residuals matrix. The scores matrix shows relationships among samples so they indicate which samples are responsible for most variation in the data set, and the loading matrix contains information about relationships among variables, i.e., they show how and the extent to which each original variable contributes to each principal component. These two matrices provide a means for deriving the best mutually independent axes (dimensions) that describe the data set. These axes are the so-called principal components or factors, and are linear combinations of the original variables that arise out of natural associations among the variables.

Mathematically, the principal component axes are derived by a rotation of the original axes such that the first few axes describe as much of the variability in the original data. The scores are an orthogonal projection of the samples (objects) on the principal component axes and the distance to origin is the score value of each sample. The loadings are cosines of the angle between the principal component axes and the original variable axes. The second step of PCR involves regressing the concentration matrix, C (in this work, the bitumen values from the extraction) onto the score matrix by the regressor matrix, G ; the regressors are determined by least-squares regression in the calibration process. Thus,

$$C = P_S G$$

$$G = (P_S^t P_S)^{-1} P_S^t C + F$$

where t denotes the transpose of the matrix, and F is the residual matrix.

To quantify an unknown, C_u , its score vector (t_u) is determined by multiplying the absorbance vector (a_u) of the unknown by the transpose of the loadings matrix. The resulting scores vector is then multiplied by the regressor matrix, G , to obtain its concentration as shown below.

$$a_u P_1^t = t_u$$

$$C_u = t_u G$$

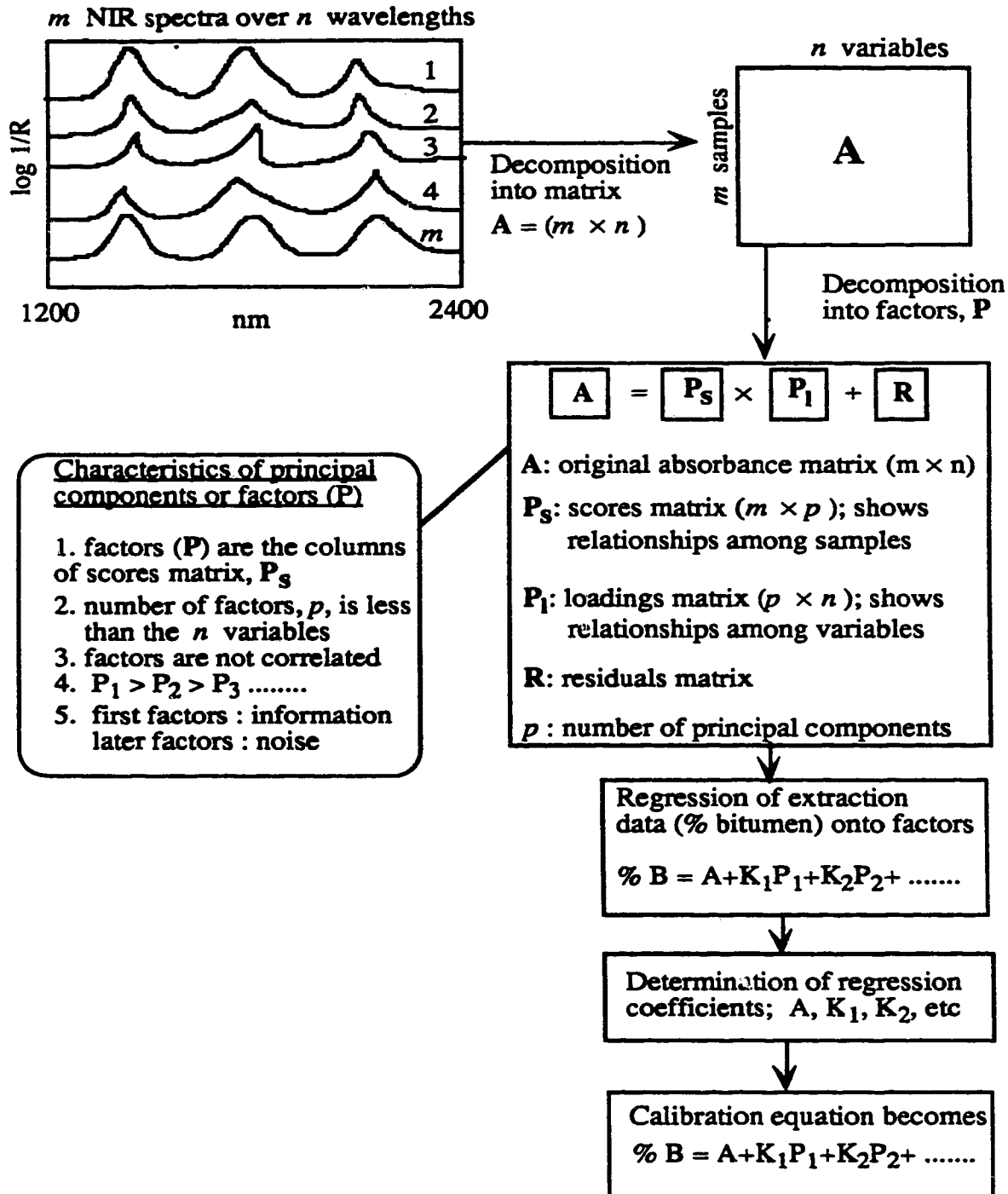


Figure 1.1. Flow chart showing mathematical steps involved in Principal Component Regression (PCR).

1.6.4. Summary

This chapter has dealt essentially with the theoretical principles of performing a NIR analysis and the sources of error involved in using NIR for quantitative analysis. The success of NIR as a technique in an application of the sort described in this thesis depends to a large extent on efficient calibration of the instrument via multivariate statistical methods. Therefore the background of various calibration techniques was also extensively covered. Based on the theoretical information gathered, the next two chapters deal with the actual experiments performed and the results obtained when NIR was used as analytical tool in analyzing oil sands.

Chapter 2

Instrumentation and Experimental Procedure

In this chapter the methodology used in the study of a selected section of core of Athabasca oil sand by diffuse reflectance-near infrared spectroscopy is outlined.

2.1. Samples

The core used in this study was provided by Syncrude Canada Ltd., and was obtained from a region of the Athabasca oil sand deposit mined by Syncrude Canada Ltd. near Fort McMurray, Alberta. The collection and preparation of the core, which was assigned the identification code 28-23-26-0-0 by the company, was arranged by Mr. Gordon Thompson of the Syncrude Research Laboratory. The core was approximately 20 m long and 7 cm in diameter, and its entire length was encased in a PVC plastic tube of wall thickness about 0.4 cm. The section of oil sands transected by the core varied in grade from 1% to 16% bitumen by weight on an anhydrous basis.

The core had been frozen and cut in half longitudinally by Syncrude to provide a uniformly textured flat surface for diffuse reflectance analysis. A section about 15 m long was selected for the NIR study as being typical of grade variations observed for a vertical transect within the deposit. The core was stored under ambient conditions in approximately 2.5-ft sections and was almost completely dry.

The Athabasca oil sands are "hydrophilic" or "water wet" with each grain of sand being surrounded by an envelope of water which, in turn, is surrounded by oil. For oil-rich zones of 12% bitumen or more, the bitumen content of the oil sample is thought to be governed by the size distribution of the solids and hence

related to the interstitial volume. Lower grade oil samples are believed to be the result of dilution with relatively oil-free sediments such as clay or coal. Hence low grade oil sand (<10% bitumen) is not a homogenous dispersion of bitumen, water and solids, but instead consists of a mixture of discrete bitumen-rich and bitumen-lean material [1].

2.2 Apparatus and Procedure for NIR Analyses

All of the commercial NIR spectrometers currently on the market have certain features in common. The radiation source is selected to generate sufficient emission in the near IR and to be stable. High-throughput optics, efficient PbS detectors and wide monochromator slits make it possible to routinely achieve a signal-to-noise (S/N) ratio of over 100,000 to 1.

The microprocessor controlled spectrophotometer used in this work, a Quantum 1200 analyzer marketed by LT Industries Inc., U.S.A, was provided by Syncrude Research Laboratories. It has a grating monochromator with a spectral response covering the range of 1200 to 2400 nm. High speed optics make it possible to acquire spectra at a rate of 5 scans per second with a resolution of 1 nm. Sample illumination is provided by a tungsten-halogen lamp, and a lead sulfide detector is used to monitor the reflected light. The arrangement of the optical system is shown in Figure 2.1. This instrument is interfaced with a Compaq Deskpro 286 computer equipped with software for in-house data acquisition, mathematical processing, modeling and graphing. The Quantum 1200 instrument is extremely rugged and can be used in any physical orientation. For this study it was positioned on end so as to direct incident radiation from the source downward onto the surface of the sample.

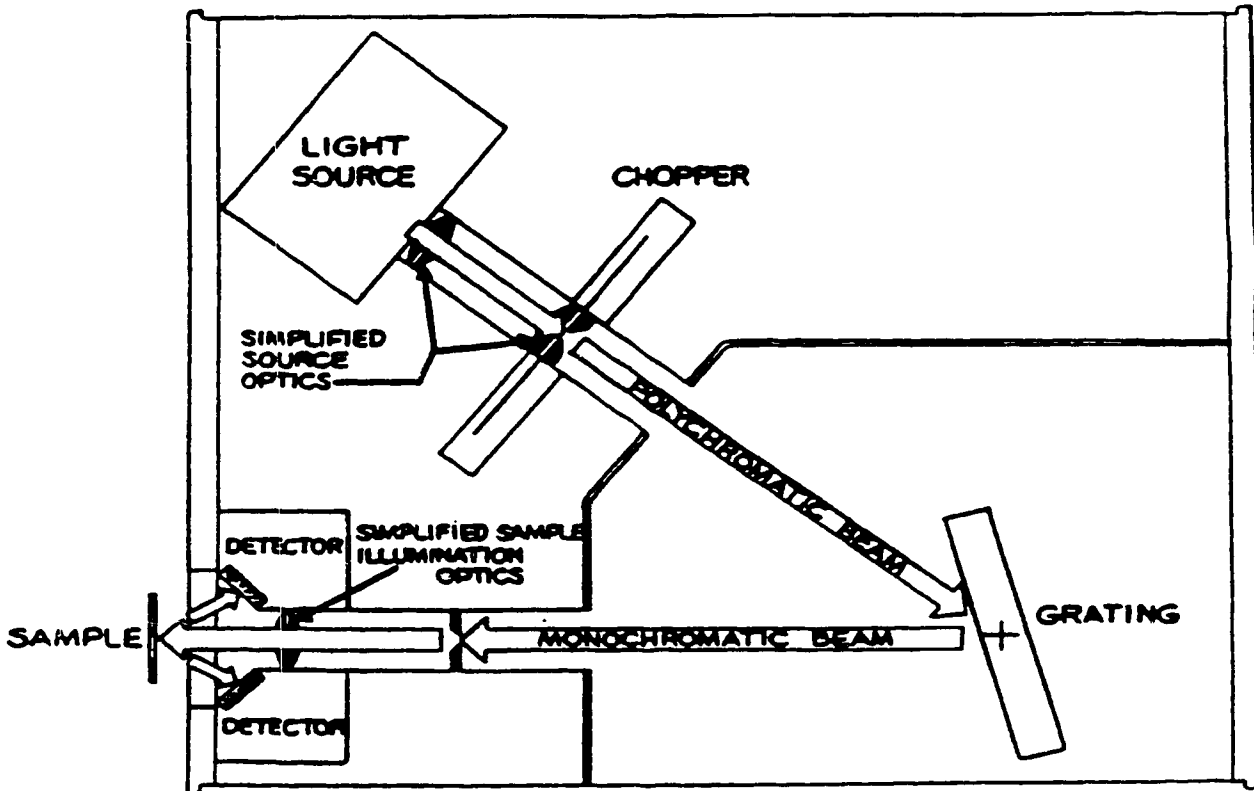


Figure 2.1. Arrangement of the optical system within the LTI Quantum 1200 NIR instrument (from Ref.1). The unit has dimensions of approximately 35X35X55 cm.

A specialized sampling table, consisting of a core holder, registration guide and bridge assembly for mounting the spectrophotometer, was used. This table, which allows the core to be rastered beneath the spectrometer viewing port in 1-cm steps, was designed by Shaw [1,2] and constructed in the machine shop of the Department of Chemistry at the University of Alberta. The viewing port was masked to provide a square sample window measuring 1-cm a side. A schematic of the sampling table and the overall arrangement of the equipment is illustrated in Figure 2.2. The operation and performance of this unit was optimized in an earlier project by Shaw [1,2] of Syncrude Research Laboratory and was further verified in this study.

To perform an analysis, about 70-cm long sections of core were scanned along their length by rastering them beneath the viewing port of the spectrophotometer. A 1-cm wide strip, starting about 1.5 cm from one edge of the core and running the length of the core, was sampled, at 1-cm intervals. Halon, a commercially available standard of bromofluorocarbon material, was used as reference. Reference spectra were taken each day before a set of measurements. Fifty scans were taken and averaged for each reading of a one square centimeter area. Both sample and standard spectra were digitized and stored on a hard disk in the computer for processing.

To assess the effect of surface roughness on the quality and accuracy of the spectra, the surface of an approximately 6-m section of core was roughened with a serrate spatula. Care was taken to minimize smearing of bitumen from one part of the surface over another region. The roughened surfaces were then rescanned to generate a new set of spectra. For another 6-m section, the above procedure was repeated on a strip down the center of the core, and again on a strip 1.5 cm from the far edge of the core. These spectra were collected as before and used to assess lateral variability in the composition of the core.

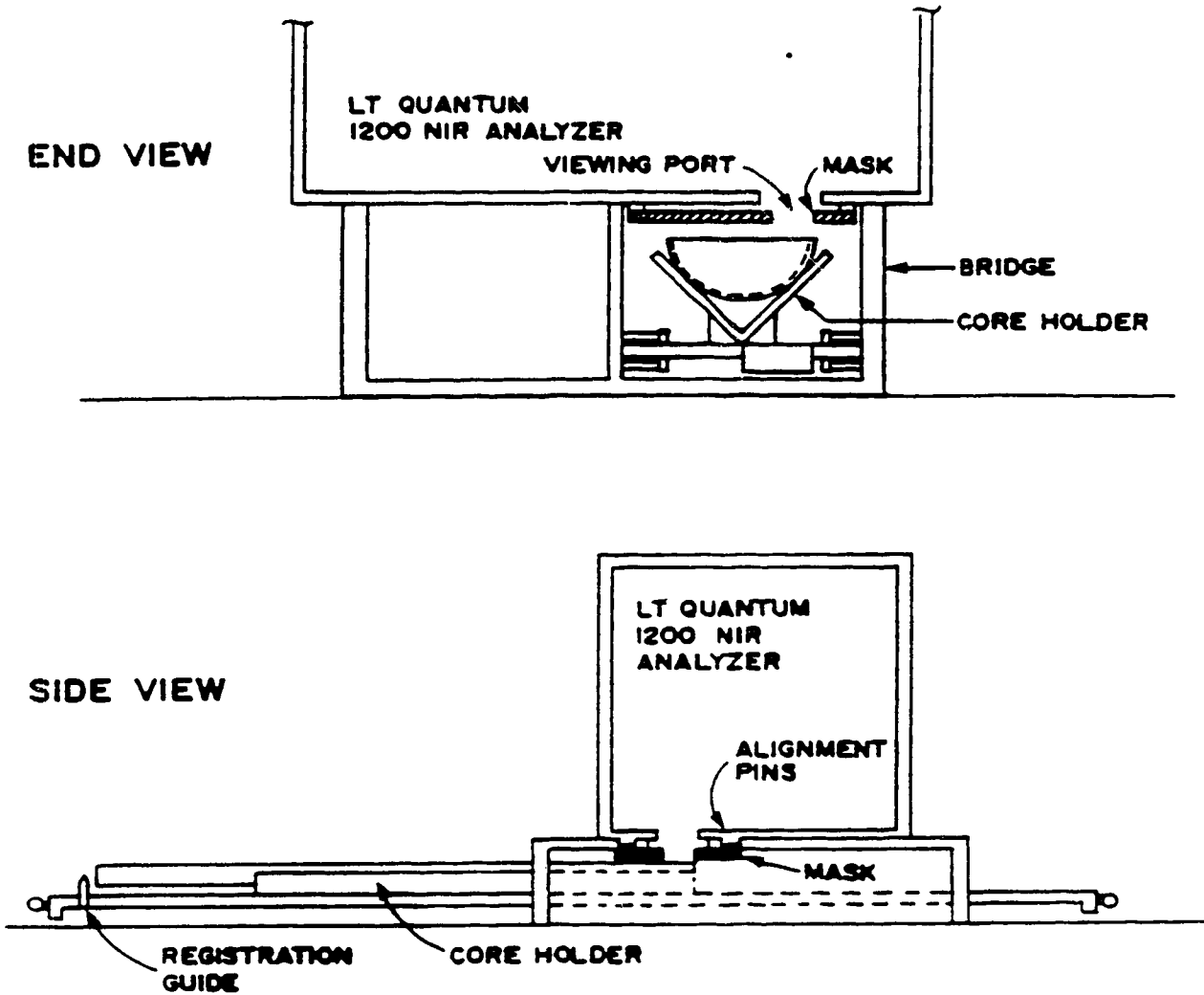


Figure 2.2. Schematic diagram of sampling table constructed for analysis of oil sand core, (adapted from Ref.1). The viewing port is a 1 cm x 1 cm square opening in the mask.

2.3. Soxhlet Extraction Procedure for Determination of Weight % Bitumen and Solids in Core Samples

Near infrared-diffuse reflectance measurements require careful calibration against a reference before they can be used for quantitative analysis. A Soxhlet extraction procedure previously developed by Shaw [1,2] was used to provide the reference composition of bitumen and solids for 1-cm square sections of core.

Two sets of samples of weights from 1 to 2 g each were removed from the core and analyzed for bitumen and solids after Soxhlet extraction to provide data for a near infrared training set. A first set of 54 samples was collected from selected sections of the core surface not previously roughened, and a second set of 42 was collected from roughened areas. The sampling locations were chosen to represent insofar as possible the overall range of bitumen and clay concentrations contained within the test section of core.

The 1 to 2-g portions were removed from the core with a scalpel and their positions along the core noted in order to match each with the NIR-DR spectrum recorded from that area. Each sample was homogenized by grinding in an agate mortar and pestle; test portions of about 1 g of the homogenized material were then taken for extraction and analysis by the Soxhlet technique.

The extraction procedure involves separation of the bitumen from the solids components of the sample by refluxing with 15 to 20 ml toluene in the extraction assembly shown in Figures 2.3 and 2.4. Each test portion was placed in a tared, single-thickness 10 x 50 mm cellulose thimble (Schleicher & Schuell, Dassel, Germany) previously dried at 60 °C for 2 hours. The thimble was then inserted in the Soxhlet unit and 20 ml of toluene added to the flask. Once the solvent is heated to reflux, the condensed toluene collects in the thimble, where it contacts the solid and dissolves the bitumen.

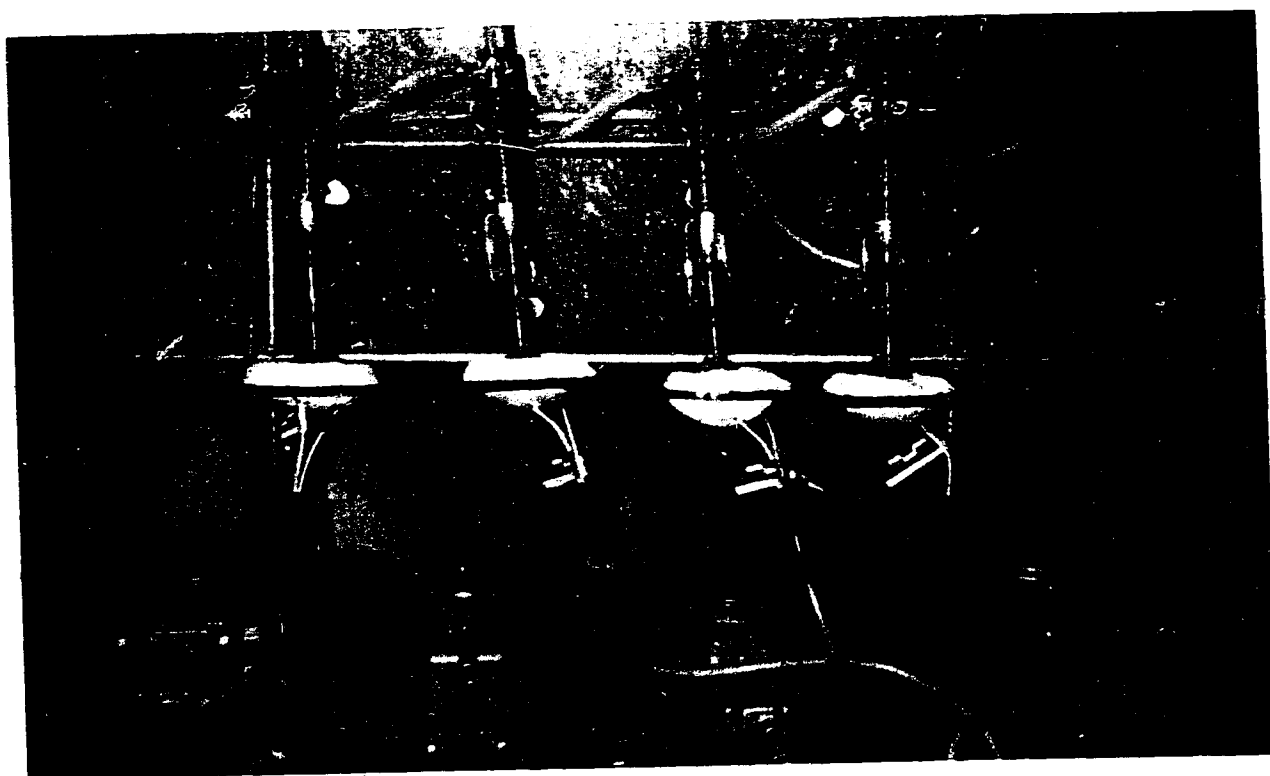
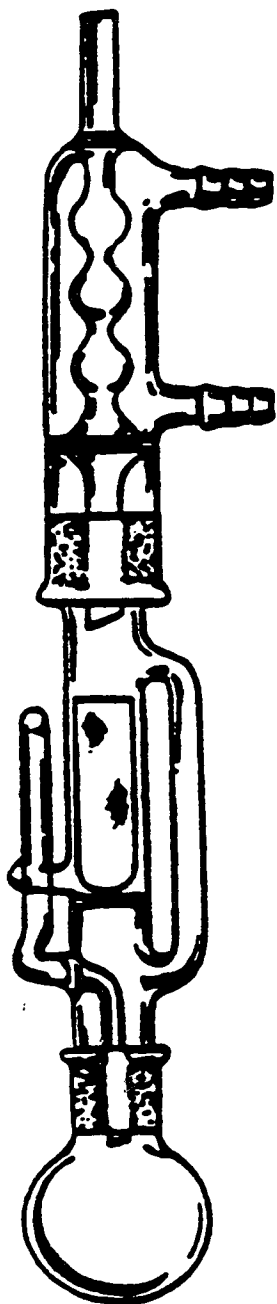


Figure 2.3. General set-up of micro-Soxhlet assembly for the determination of weight percent bitumen and solids in oil sand



Sample weight	0.5 g - 3 g
Thimble size	10 mm × 50 mm
Solvent volume	15 - 20 mL (toluene)
Extraction time	20 - 30 minutes

Figure 2.4. Micro-Soxhlet extraction apparatus used for the determination of bitumen and solids contents of oil sand; (Adapted from Ref.1).

When the toluene level in the extractor column reaches the top of the siphon arm, the solvent plus dissolved bitumen is siphoned into the refluxing flask. This process is repeated for as long as necessary to remove all the bitumen; typically about 20 to 30 minutes are required. Completion of the extraction is usually indicated when the siphoning toluene becomes light yellow.

When the extraction was complete, the thimble containing the bitumen-free solids was allowed to dry overnight in the air in a fume hood and reweighed. The extract (solvent and dissolved bitumen) was quantitatively transferred to a weighed evaporating dish, and the toluene allowed to evaporate overnight in a hood at room temperature (see Fig. 2.5). This procedure was shown by Shaw [1,2] to be valid. The dish was reweighed and the amount of bitumen in the original sample was calculated from the difference in weights of the evaporating dish before and after drying. The precision of duplicate analyses using this method is shown in Figure 2.6.

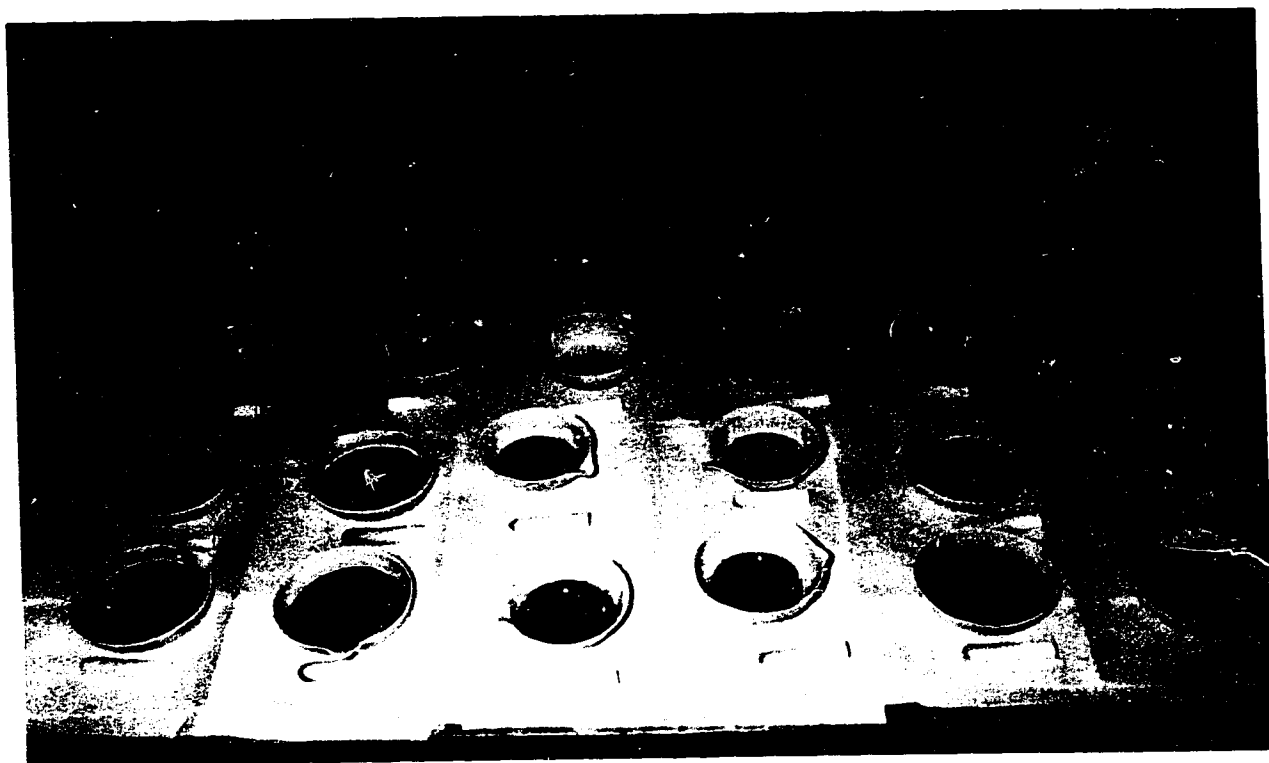


Figure 2.5. Evaporating dishes containing bitumen residue obtained from the Soxhlet extraction of oil sand after evaporation of toluene

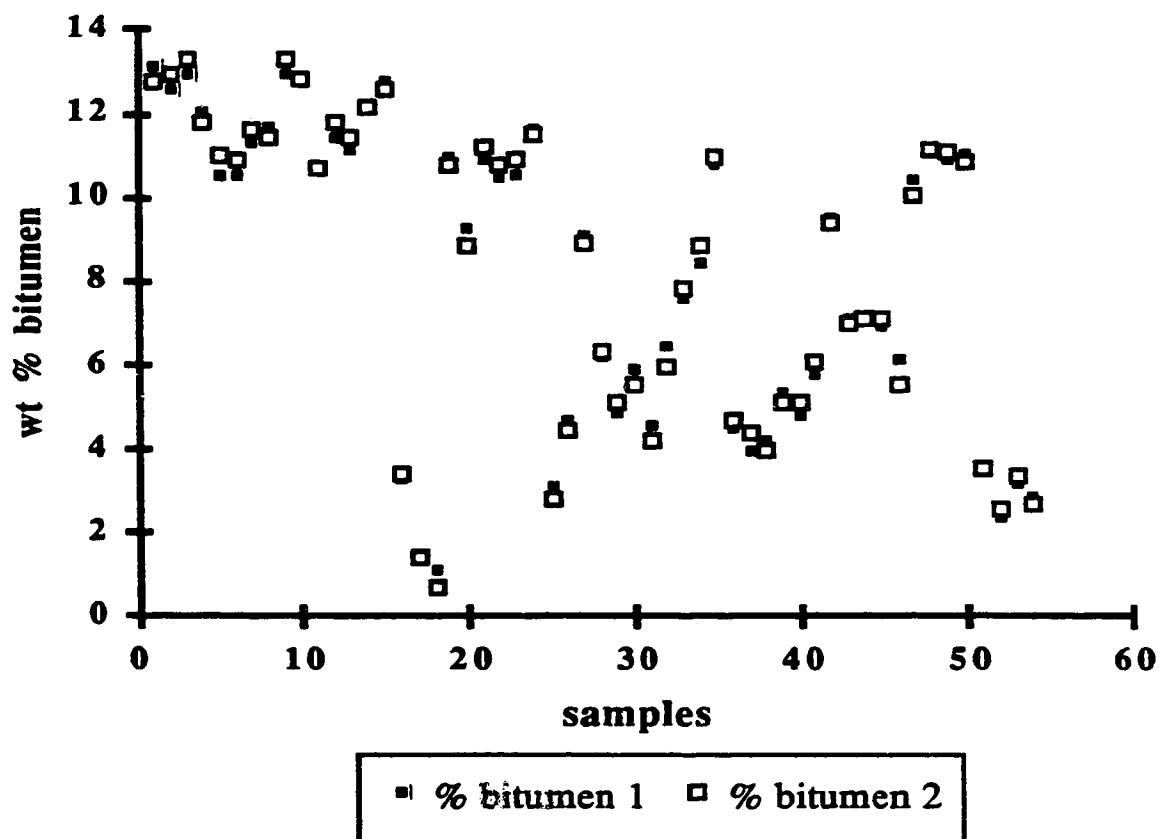


Figure 2.6. Results for analyses of training set samples showing precision of Soxhlet extraction technique. (Notice that some of the duplicate bitumen points are superimposed).

Chapter 3

Results and Discussion of Diffuse Reflectance Near Infrared Spectroscopy Measurements of Athabasca Oil Sand

3.1. Data Analysis

As indicated in the preceding chapters, present day NIR instruments require calibration before they can be used for quantitative measurement. In this work two approaches, Principal Component Regression (PCR) [19,20,26,39-50] and Partial Least Squares Regression (PLSR) [19,20,26,50-55], were used to develop calibration models for training sets for bitumen and for solids. Two training sets, one each for test portions taken from roughened and non-roughened sections of the core, were studied.

In generating each model, a decision had to be made concerning the number of factors to use during development so as to avoid a problem termed overfitting. Usually one chooses a model that minimizes the residual variance. The LighTcal Plus Package [56] provided with the Quantum NIR instrument used here is equipped with several diagnostic tools which help to determine the optimum number of factors and avoid overfitting.

One good diagnostic tool is a plot showing the standard error of prediction (SEP) as a function of the number of factors in the calibration model. The optimal number of factors to be used for the model is chosen as that number which corresponds to the minimum of the SEP curve. An example of such a plot is shown in Figure 3.1a. Here the number of factors used was 7. Of additional help in choosing the optimal number of factors is a plot showing the cumulative variance, described by the model as a function of factors (Figure 3.1b.). The criterion used here is that the difference between described variance for two consecutive numbers of factors should not be significant. An optimal model can

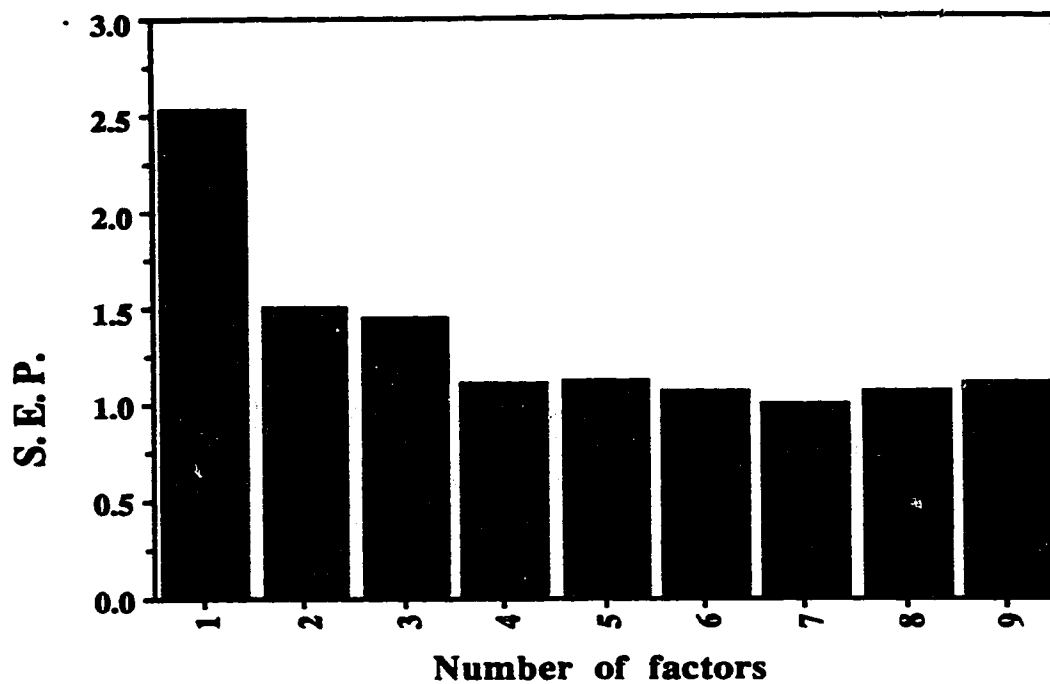


Figure 3.1 a. Standard error of prediction as a function of number of factors incorporated in the model (*bitumen*).

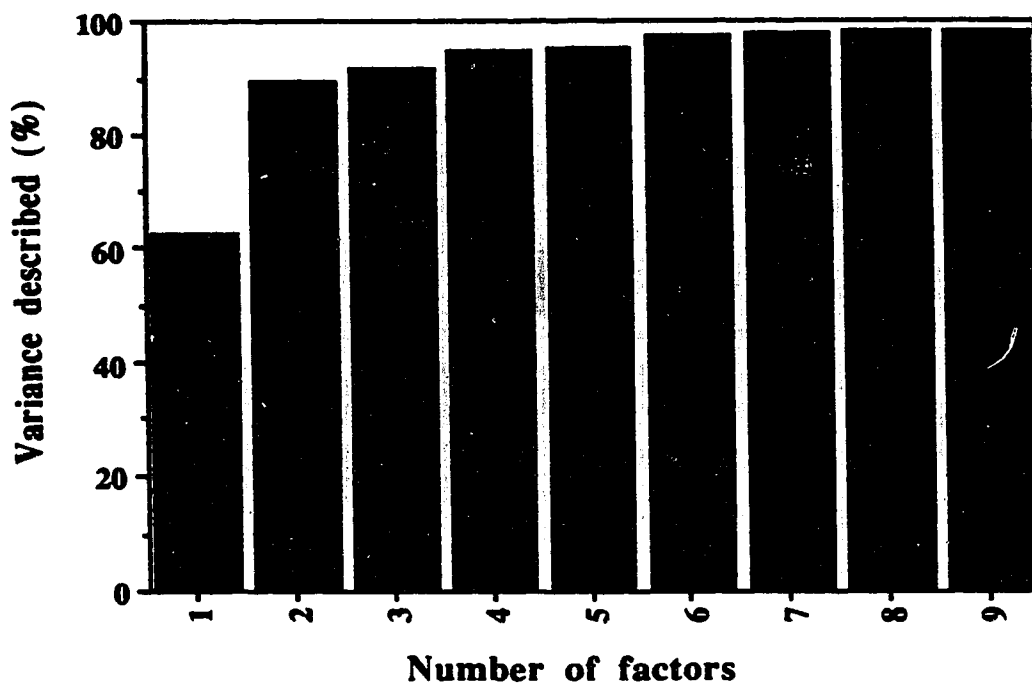


Figure 3.1 b. Cumulative variance described in model as a function of number of factors (*bitumen*).

be expected to include between 85% and 98% of the calibration set variance for the overall NIR data.

Additional diagnostics available to the user include a t-test of significance, which provides a measure of the significance of a factor in describing ingredient variation, and a plot of regression coefficients as a function of wavelength for each factor. The latter is quite useful for indicating whether or not more factors than necessary are being used in building the model.

Most of the diagnostic tools described above were used to determine the optimum number of factors for the calibration models used in this study. The calibration models produced by the LighTcal Plus software [56] are shown in Figures 3.2 to 3.5. In these figures the measured bitumen content is that determined by the Soxhlet extraction procedure, and the predicted values are those obtained from NIR-DR data. Table 3.1 shows the correlation coefficients and optimum number of factors found for each calibration.

The performance of these calibration models on future unknown samples was checked using the validation modules provided with the LighTcal Plus software package. The prediction capabilities of the different multivariate calibration models for bitumen and solids were further compared by splitting the calibration data set into calibration and prediction subsets and comparing the predicted results with the known values. This was done as follows: All of the values in the calibration set were randomized and every fourth one was pulled out and placed into the validation subset. The remaining samples constituted the calibration subset. This calibration subset was modeled and the SEC value determined. It was then applied on the validation subset and the SEP value determined. The results are shown in Table 3.2. It can be seen that the PCR and PLS methods yielded similar results for the prediction of bitumen and solids in these oil sand samples. PLS gave slightly better SEC values for bitumen and

Calibration model	r	No. of factors used
Figure 3.2. (PCR)	0.980	7
Figure 3.2. (PLS)	0.983	7
Figure 3.3. (PCR)	0.981	7
Figure 3.3. (PLS)	0.982	6
Figure 3.4. (PCR)	0.978	7
Figure 3.4. (PLS)	0.982	7
Figure 3.5. (PCR)	0.976	7
Figure 3.5. (PLS)	0.977	6

Table 3.1. Table of correlation coefficients and optimum number of factors used for calibration models.

solids, and a slightly better SEP value for bitumen, while PCR yielded slightly better SEP values for solids. The differences in the SEP values obtained by PLS and PCR were not, however, statistically different. When all the samples in the training set were combined into a single calibration set the results obtained for the SEC values were as shown in Table 3.3. Notice that inclusion of the samples from the prediction set does not change the SEC values significantly. Plots of the residual bitumen and solids concentrations against predicted values obtained with the PLS and PCR models show no prominent trends in the distribution of residuals. An example of such a plot appears in Figure 3.6. This indicates that most of the spectral nonlinearities in the data set have been modeled or accounted for.

	Bitumen (wt %)			
	Non-roughened		Roughened	
	SEC	SEP	SEC	SEP
PCR	0.74	0.4	0.99	0.16
PLS	0.69	0.4	0.95	0.15
	Solids (wt %)			
	Non-roughened		Roughened	
	SEC	SEP	SEC	SEP
PCR	0.78	0.2	1.09	0.26
PLS	0.57	0.5	1.05	0.23

Table 3.2. Comparison of performance of different calibration models. For non-roughened samples the calibration subset contained 36 samples and the validation subset 18; for the roughened samples the calibration subset had 28 samples and the validation subset 14.

	Bitumen		Number of samples
	PCR	PLS	in training set
Non-roughened	0.78	0.72	54
Roughened	0.88	0.84	42
	Solids		
	PCR	PLS	
Non-roughened	0.84	0.76	54
Roughened	1.02	0.98	42

Table 3.3. Summary of SEC values (in wt %) for different calibration models using all available samples in the training set.

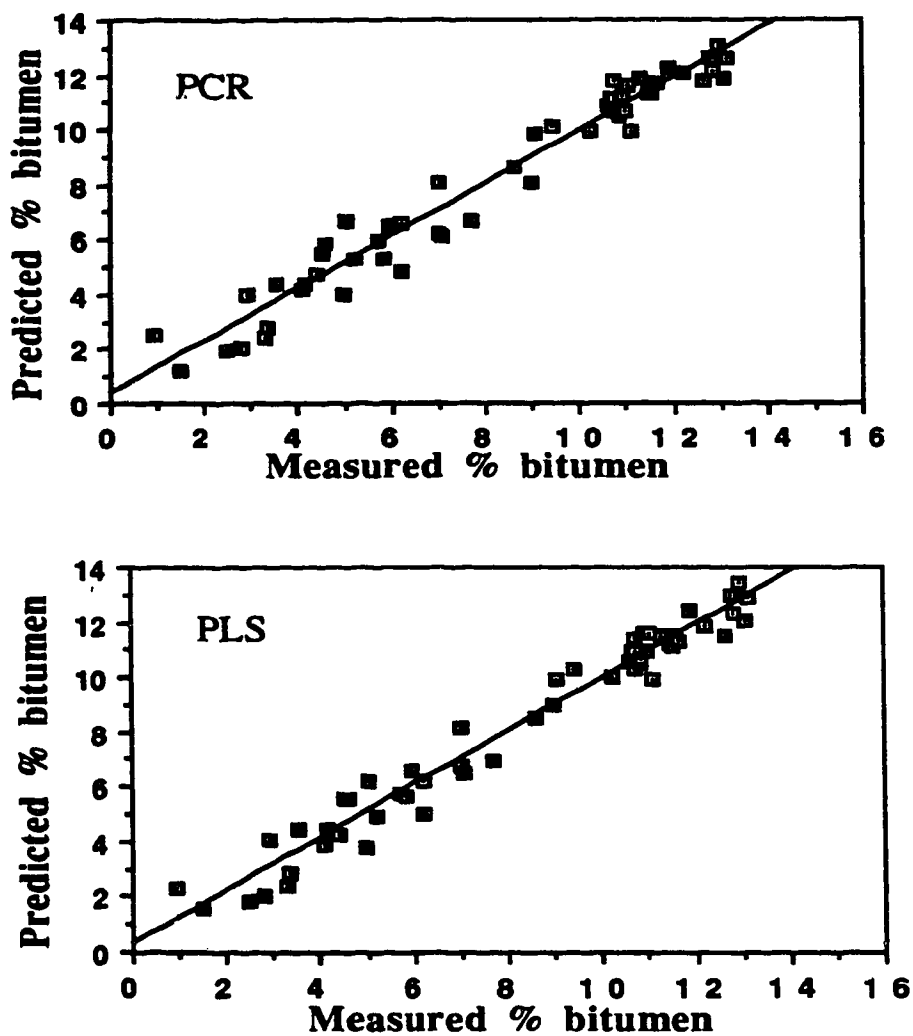


Figure 3.2. Comparison of predicted versus measured *bitumen* content for *non-roughened* samples in the training set.

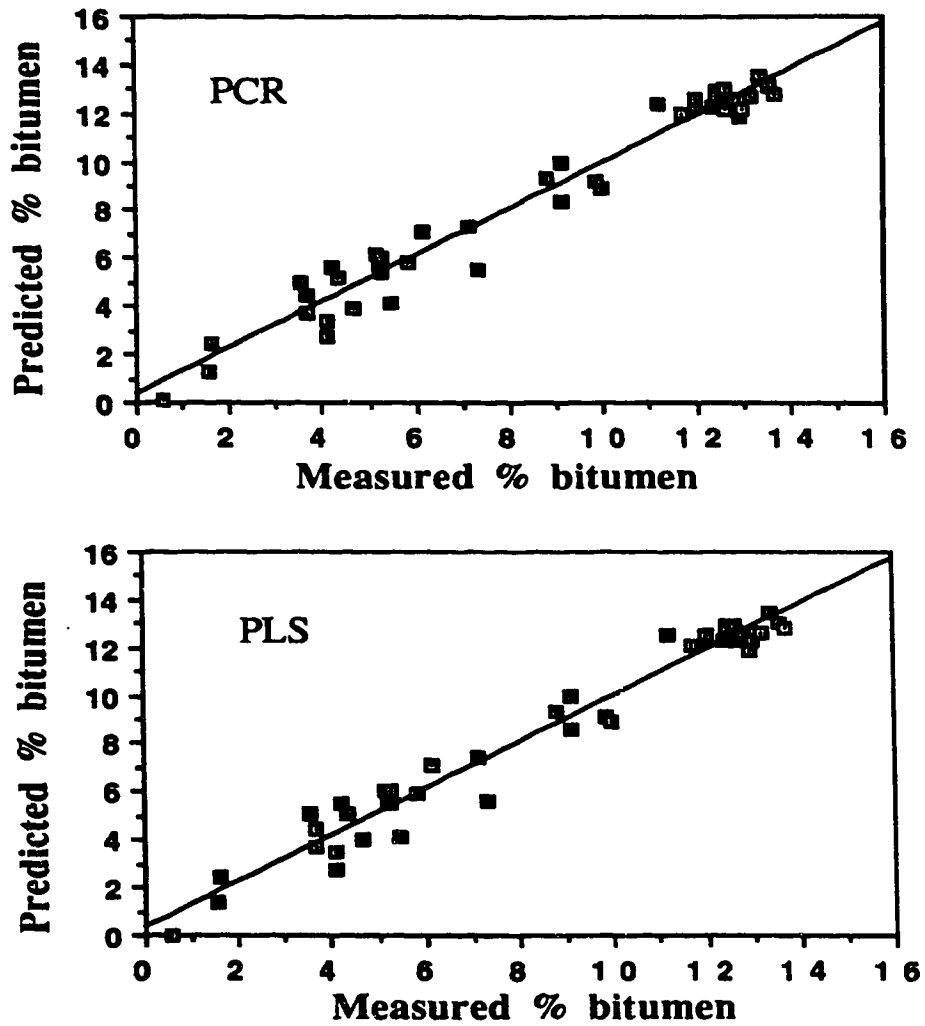


Figure 3.3. Comparison of predicted versus measured *bitumen* content for *roughened* samples in the training set.

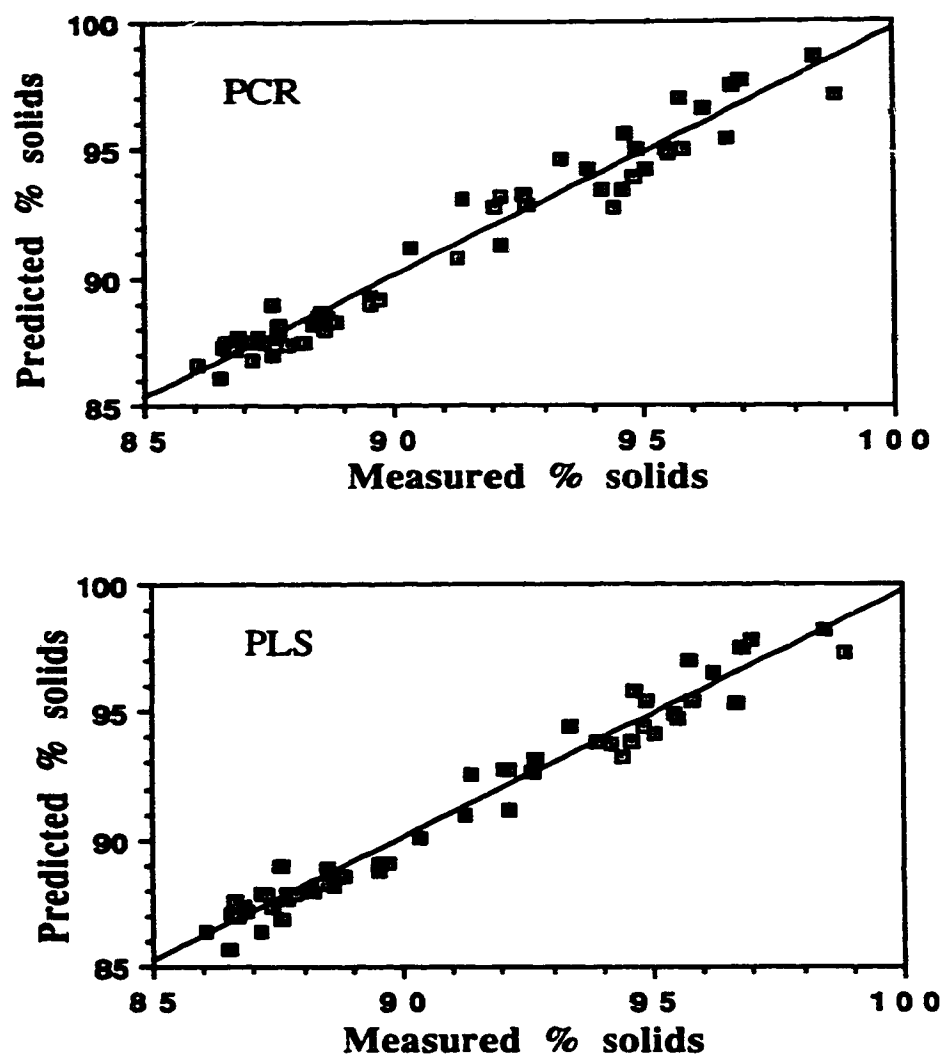


Figure 3.4. Comparison of predicted versus measured *solids* content for *non-roughened* samples in the training set.

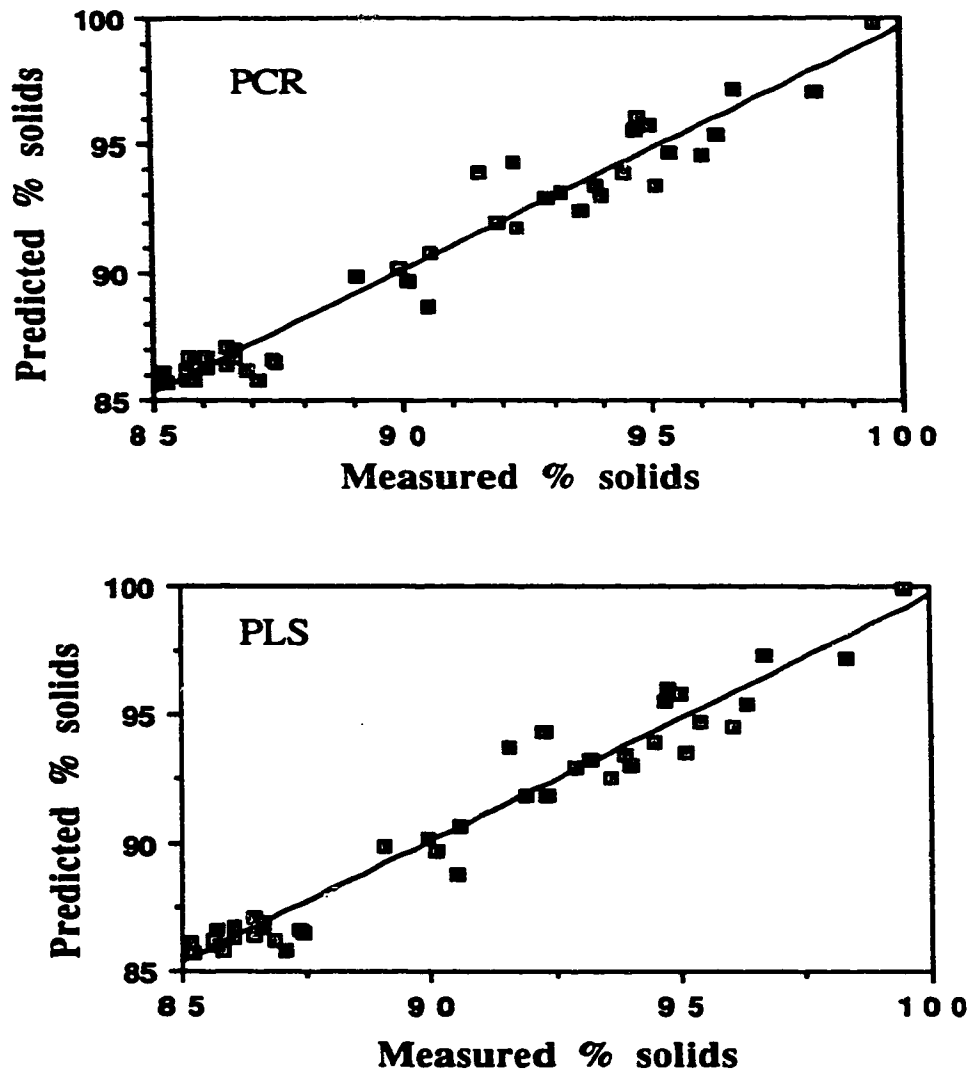


Figure 3.5. Comparison of predicted versus measured *solids* content for *roughened* samples in the training set.

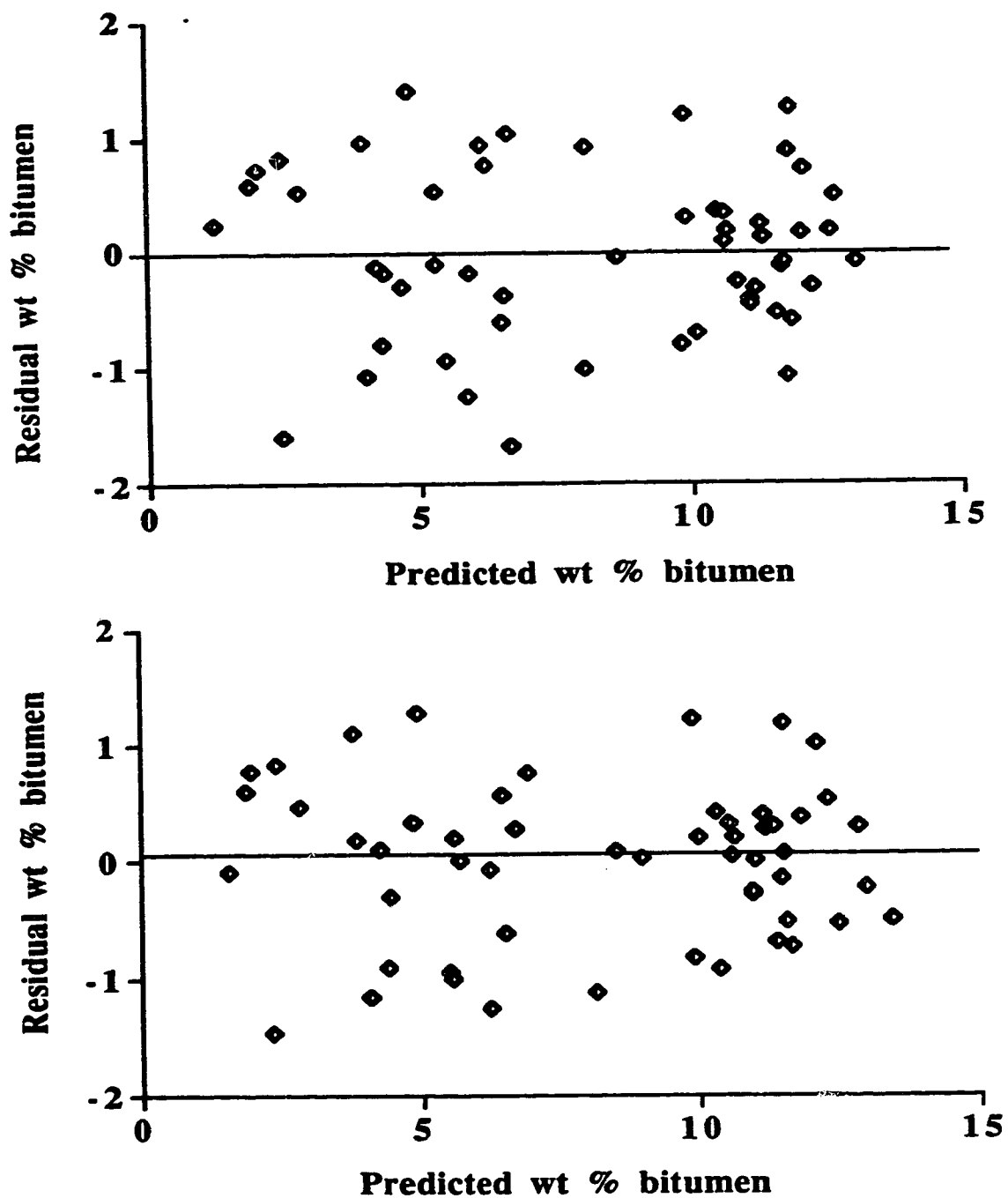


Figure 3.6. Distribution of percent bitumen residuals relative to the predicted bitumen content. (Upper figure: results obtained using seven PCR factors; lower figure: results obtained using seven PLS factors).

The models developed by the above procedure could now be used to predict bitumen and solids content in all samples analyzed by NIR-DR along the length of the test section of core. The resulting weight percent bitumen and solids data at 1-cm sampling intervals were then plotted against location along the core length to yield a high-resolution profile of grade variability. These grade profiles are shown in Figures 3.7 and 3.8. It is evident from the plots that there is a high degree of vertical variability at the centimeter level for both bitumen and solids. This longitudinal variability is most prominent near the top of the core and decreases on going down the core, indicating that the degree of heterogeneity decreases with depth in the deposit. This pattern is important because of its relevance to developing a sampling protocol for assessing bitumen and solids content by core collection and analysis. This observation that heterogeneity is greatest at the top would demand that more frequent sampling be performed at the top section than at the bottom.

The lateral variability within four core sections, each about 70 cm in length, was considered. The data were collected as outlined in Section 2.2. Figures 3.9 and 3.10 show, for the four core sections coded A, E, J, and L, plots of standard deviation for each set of three data points across the core against their location along the core. It can be seen that the absolute standard deviations for bitumen values across core are all below 1 weight percent. The average of the standard deviation values for the four sections are also shown on the plots; the value for each is about 0.3 weight percent. This indicates that the bitumen content does not vary significantly as one moves laterally across the core. The variability pattern established in this study in both lateral and vertical directions is relevant to developing a sampling protocol for assessing bitumen and solids content within a typical core hole.

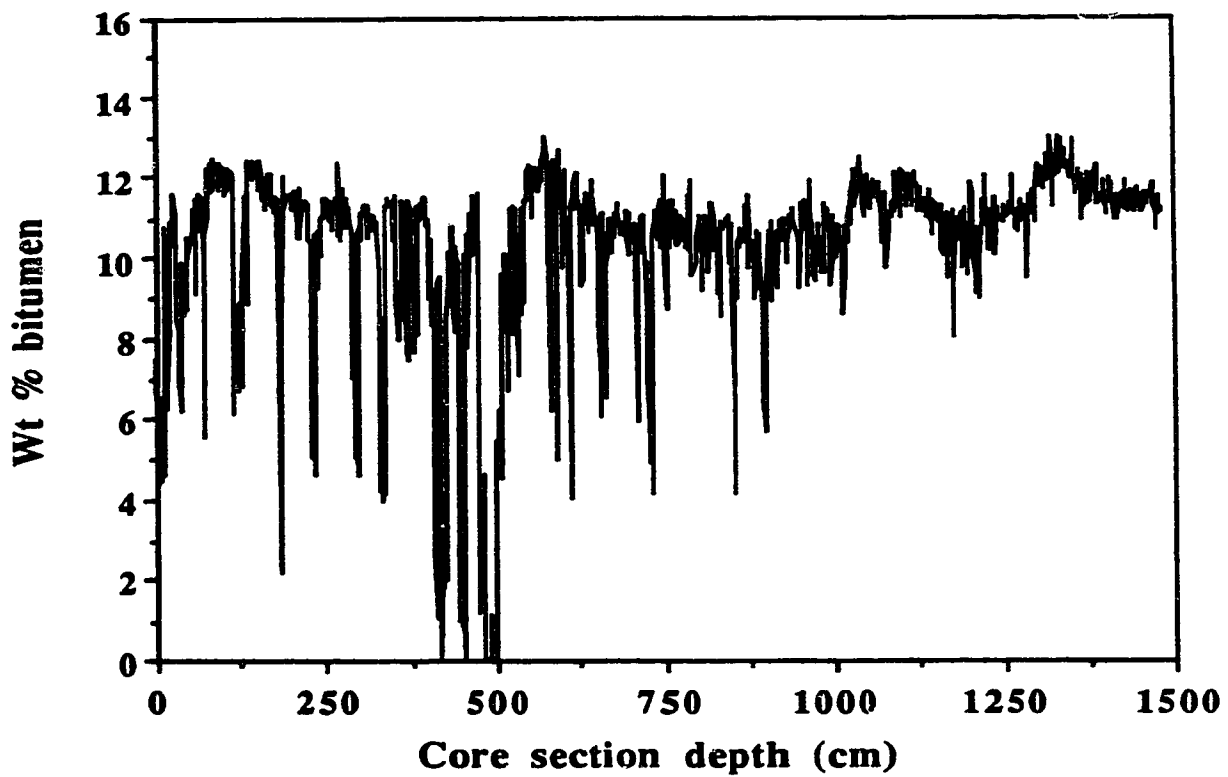


Figure 3.7. Variation in *bitumen* content as a function of depth for a 15-m test section of core. Point grade estimates were derived from NIR-DR spectral measurements at 1-cm sample spacings.

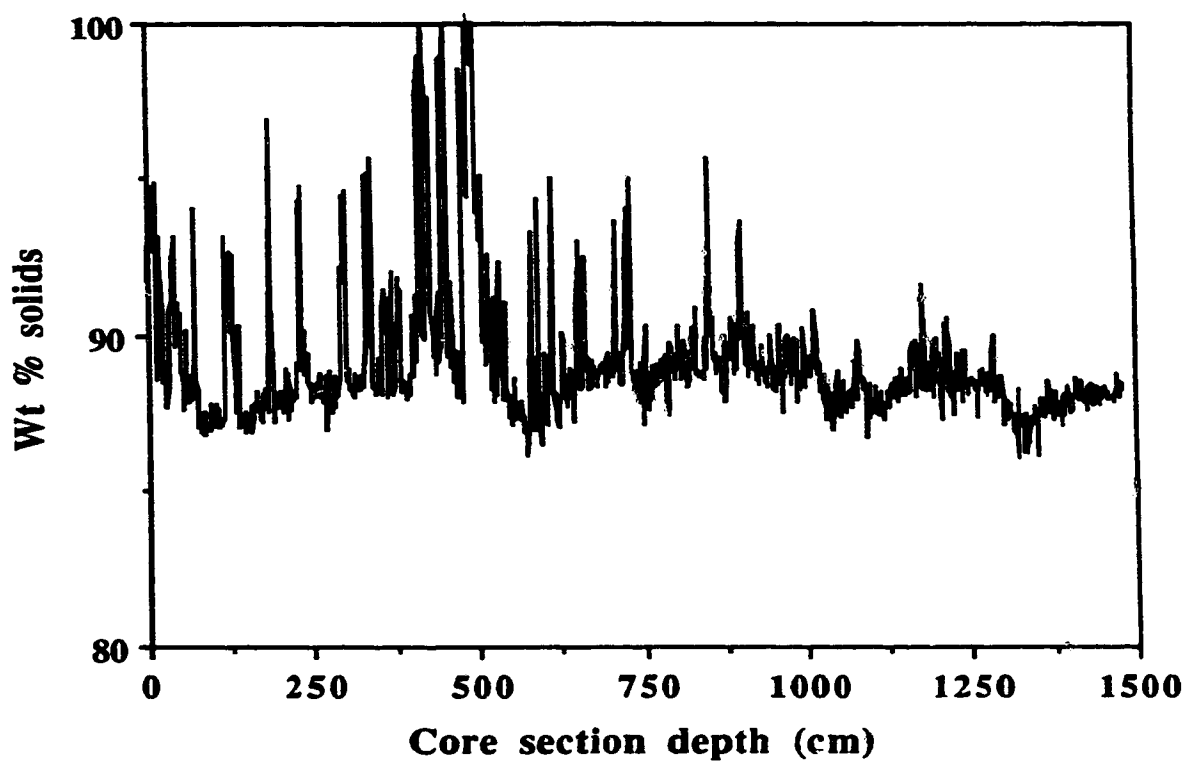


Figure 3.8. Variation in *solids* content as a function of depth for a 15-m test section of core. Point grade estimates were derived from NIR-DR spectral measurements at 1-cm sample spacings.

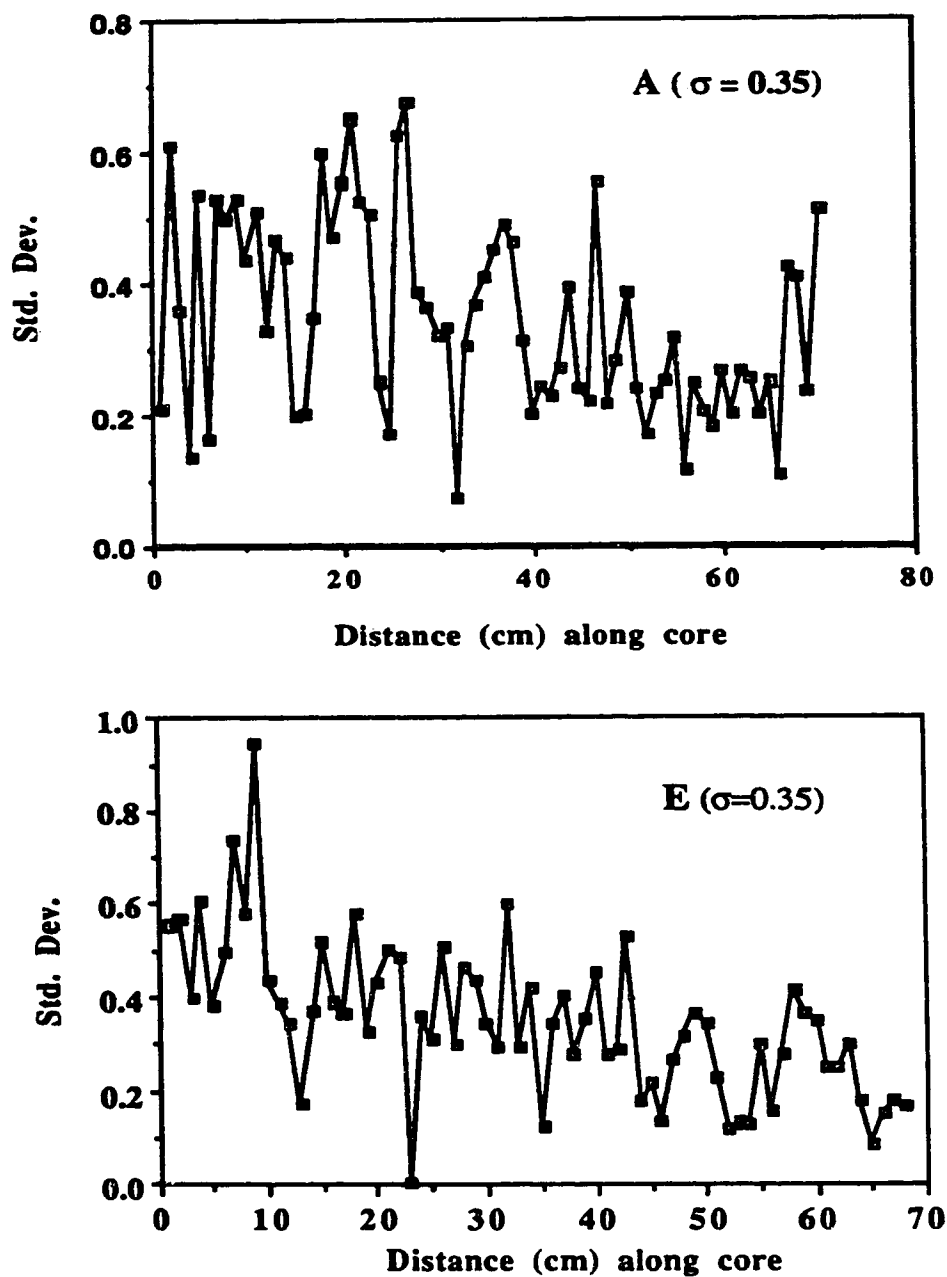


Figure 3.9. Plot of standard deviation (wt %) versus location along core sections A and E. (Standard deviation on vertical axis is that for each set of three data points taken laterally across the core; σ in plots represent average value of standard deviations for all the 70 data points).

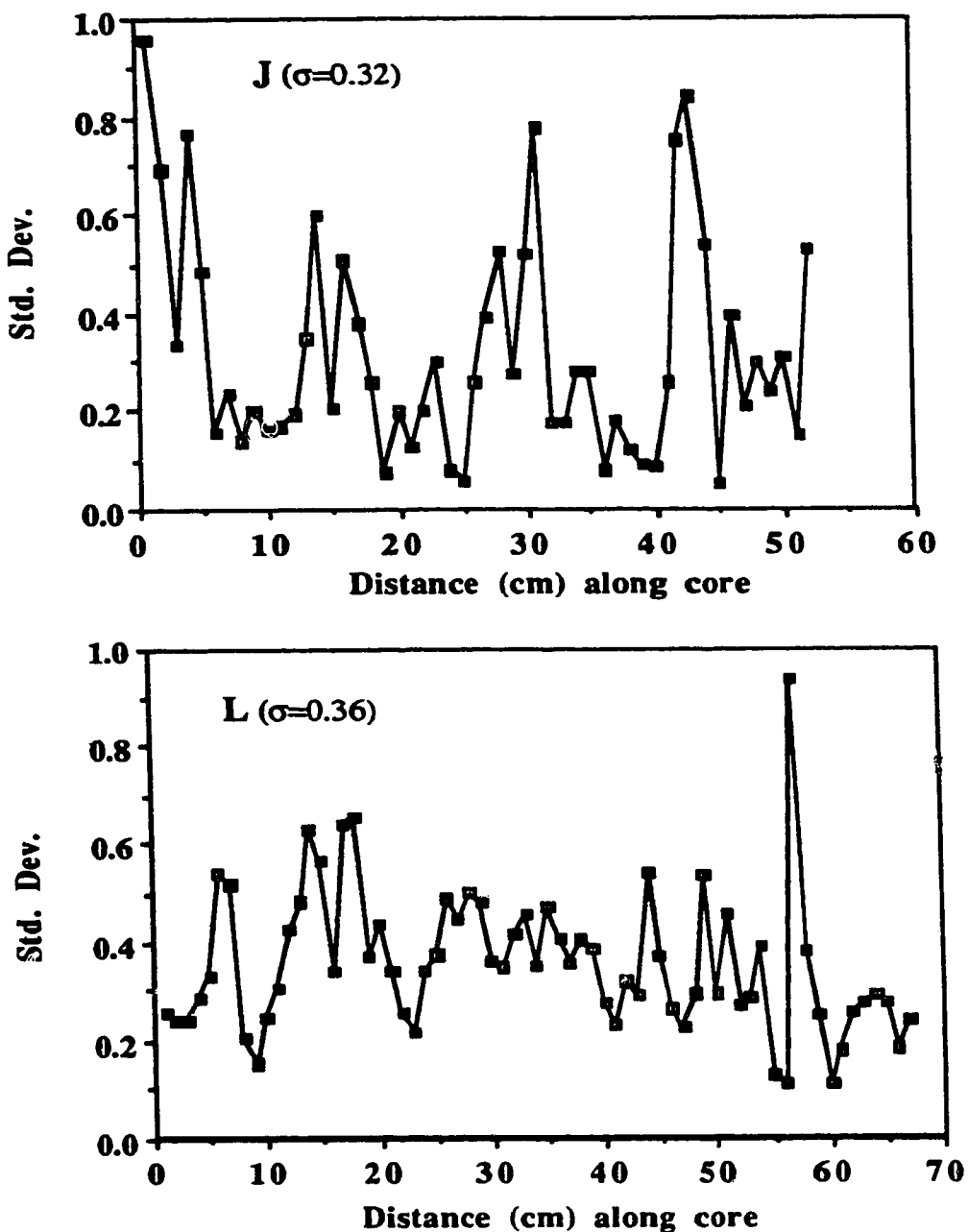


Figure 3.10. Plot of standard deviation (wt %) versus location along the core sections J and L. (Standard deviation on vertical axis is that for each set of three data points taken laterally across the core; σ in plots represent average value of standard deviations for all the 60 or 70 data points).

3.2. Effect of Roughening on Bitumen Levels

The procedure for this study was described in section 2.2 on page 21. Roughening the surface of the core appears to have a significant effect on the bitumen levels measured. In general, it was observed that for oil-rich sections, defined as sections with a bitumen content greater than 11%, roughening causes recorded bitumen levels to be elevated as compared to non-roughened values. On the other hand, for leaner sections the effect is reversed, and observed bitumen levels were lowered by roughening the core surface. This behavior is shown in Figure 3.11.

A possible explanation for the reason why roughening the surface of the oil sand prior to diffuse reflectance NIR measurement causes these effects is as follows. In oil-rich zones the bitumen tends to occur in a more or less continuous phase, whereas in oil-lean zones clay and water tend to constitute a continuous phase. The sand component does not become part of either continuous phase. When roughening oil-rich sections, therefore, the continuous bitumen phase may tend to be spread over the surface and cause the bitumen levels to appear high. In oil-lean regions, on the other hand, roughening may spread the continuous phase of clay and water, thereby producing lower bitumen levels. The medium-rich zones, which contain 8 to 11% bitumen, may consist of interbedded clay and oil. In this case a well-defined continuous phase is not present, and roughening is less likely to cause a bias in the analytical result.

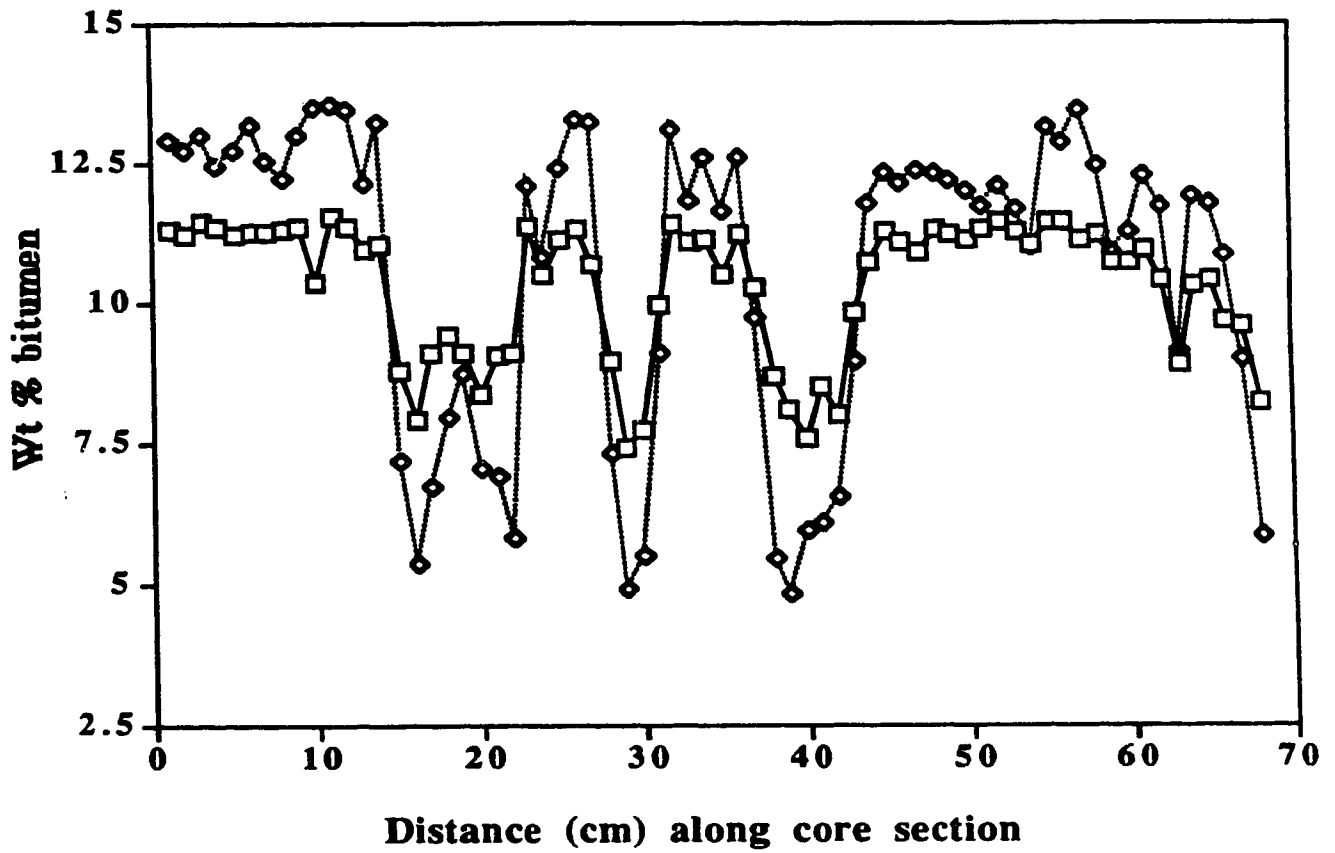


Figure 3.11. Effect of surface roughening on bitumen levels in oil sand. (Open squares are bitumen values for non-roughened surfaces; open diamonds are values for roughened surfaces).

3.3. Effect of Sampling Frequency on Error of Bitumen Results

To determine the precision for the various sample spacings of 2, 5, 10, 15 and 20 cm, a sampling procedure was adopted as follows. From the original data set of 1468 data points, every i th data point was extracted where i represents 2, 5, 10, 15 or 20 cm. This extraction of points yields five new sets of data corresponding to 2, 5, 10, 15 and 20 cm sample spacings. These data sets constitute the measured values for the different sample spacings. The same original data set of 1468 data points was divided into subsets of i samples ($i = 2, 5, 10, 15$ and 20) and the average value of each subset of i data points was calculated. These values represent the true values of each subset for the different sample spacings.

The percentage error between the measured and true values was determined. This percentage error is defined as $100[(\bar{x} - x_i)/\bar{x}]$ where \bar{x} is the true value and x_i is the measured value. The percent error values obtained were then compared with 5% and 10% error and the fraction or percentage of the total number of data points with values greater than 5 or 10 percent error was calculated. The results obtained are summarized in Table 3.4.

For the 2-cm sample spacing, it can be noticed that out of the total number of 734 points which were extracted, 122 of those had an error of 5% or greater. This is equivalent to 17% of the total number of points having an error larger than 5%. With respect to 10% error at the same 2 cm spacing, it can be seen that out of the 734 points, the number of points greater than 10% error is 55, which is equivalent to 8% of the total. As the sample spacing increased the percentage of the total number of points with error greater than 5% or 10% became even higher. This indicates how heterogenous oil sand is and the importance of proper sampling. From the above observation it can be concluded that to reduce the sampling error due to heterogeneity and to achieve improved precision, the area sampled should be larger than the 1 square centimeter used in this work.

Sample spacing	Total # of data points in set	# of data points with error > 5%	% of data points with error > 5%	# of data points with error > 10%	% of data points with error > 10%
2 cm	734	122	17	55	8
5 cm	293	91	31	50	17
10 cm	146	53	36	34	23
15 cm	97	42	43	24	25
20 cm	73	29	40	20	27

Table 3.4. Sampling error for bitumen analyses of 1 square centimeter area spaced at 2, 5, 10, 15 and 20 cm, assuming average of analyses of contiguous strip to be the true value.

Chapter 4

Summary and Future Directions for NIR Studies

4.1. Conclusions and Summary

NIR-DR spectroscopy has been used to estimate the bitumen and solids content of oil sands at high sampling resolution. The results of scans of a 15-m section of test core at 1-cm intervals allowed a detailed pattern of vertical variability to be established over a greater distance than had previously been done. The variability observed confirms earlier results of Shaw [1,2] obtained for a 4-m vertical transect of core. The degree of heterogeneity was found to be greater toward the top of the section of deposit represented by the core, and to be smaller toward the bottom. Awareness of this trend, which has been observed before at less frequent sampling intervals, could be useful in developing more refined sampling strategies for estimating the bitumen and solids content of oil sand deposits from core analyses. That is, the high degree of heterogeneity found at the top would result in poorer precision for bitumen and solids analyses in that zone than at the bottom, hence to achieve reasonable accuracy in the sampling procedure more frequent sampling would be required at the top than at the bottom of the core deposit .

Standard deviations for the averages of bitumen analyses of sets of three samples taken across a core were found to be of the order of 0.3 wt.%. These results, based on the average of 280 separate NIR transect measurements, indicate that a single NIR reading on a 1-cm square area suffices to provide a bitumen value that is representative of the 1-cm thick section of core underlying that area.

The effect of surface roughness on NIR results was evaluated. It was shown that the roughness of the sample surface can have an important effect on

NIR analytical results. To achieve satisfactory accuracy it is important that surface preparation methods be consistent from sample to sample, and between samples and reference materials. It was also found that attention must be paid to avoid the effects of specular reflection of light from sample surfaces, which can produce anomalous results in NIR analysis.

Optimization of calibration models for NIR data collected in this work by PCR and PLS techniques was found to yield reasonable results for the estimation of bitumen and solids in oil sand. SEP values indicated that the prediction capabilities of these two techniques for the modeling of oil sand components were comparable. Hence no significant advantage is obtained in using one over the other in the situation studied here. Both models were applied to a data set composed of NIR measurements at one-cm intervals on approximately 15 m of core. Residual values of less than 1% were obtained for bitumen and solids. To obtain such a low average residual value over a large data set comprising all possible variations of samples in oil sands indicates that these multivariate calibration techniques are quite robust for this application.

This research has provided an insight into the effect of sampling frequency on bitumen results. It has shown that in order to attain a precision in NIR analyses for bitumen and solids of less than the 5% desired in the oil industry, and to reduce errors arising from heterogeneity, measurements should be performed on a much larger area than one square centimeter.

In summary, NIR-DR spectroscopy has a number of advantages for estimating the bitumen and solids content of oil sand. However, its full potential can only be realized in the oil sand industry if some of its limitations, such as its inability to distinguish and identify the structural nature of *facies* (a part of a stratigraphic body differentiated from other parts by appearance or composition) or to measure directly particle size of oil sand, are overcome. Structural

information on facies in particular is important in mine planning because it yields highwall stability predictions. A direct measure of particle size affords knowledge of fines content of the deposit, which enables facies to be more easily identified and processability to be more readily predicted [57].

4.2. Suggestions for Future NIR Work

In this research, the analyses were limited to measurements on sample areas of a square centimeter. The results showed that the heterogeneity of oil sand is sufficiently high that the sampling frequency for measurements on areas this small must be large if the precision of the bitumen analyses are to reach the industry requirement of 5%. Additional work is needed, therefore, to determine whether the instrumentation can be modified to make measurements of adequate sensitivity on larger areas without affecting the precision. This may permit a reduction in the sampling frequency required to achieve the desired precision, and make the method more practical in terms of time and number of measurements.

It may be possible to develop improved methods for identification of structural facies and for the measurement of clay particle sizes. If these properties could be estimated independently in a cost-effective and rapid way it would overcome some of the limitations associated with the NIR technique in this respect.

The multivariate data analysis techniques of PCR and PLS have been quite successful in the modeling of calibrations for the determination of bitumen and solids in oil sand. Other techniques may be even more powerful, however. For example, recent advances in neural networks for modeling nonlinearities might make these systems, either singly or in combination with the approaches described here, useful for modeling calibrations for oil sand [58-62].

***Part 2: Analysis of Athabasca Oil Sand for Bitumen and Solids
by Instrumental Neutron Activation***

Chapter 5

Introduction

In the oil sand industry, knowledge of the bitumen and solids content of the mining fields is essential to processing and refining requirements. To do this, the oil sand companies each have a coring program whereby samples are taken to the laboratory and analysed for bitumen and solids. The most reliable analytical method at this time is the Dean-Stark technique. However, this method is time consuming, involves the use of organic solvents and highly humanpower intensive. Hence the objective of this project was to explore the possibility of using Instrumental Neutron Activation Analysis (INAA) to achieve the same goals of providing knowlege of bitumen and solids content and to overcome if possible some of the limitations associated with the Dean-Stark method. For this purpose INAA could have a fast turnaround time if the quantification could be done via short-lived isotopes. Also, since no sample pretreatment would be necessary, the hazards associated with the use of organic solvents could be eliminated. Finally, because for the most part the process could be automated, it would require less humanpower.

5.1. Neutron Activation Analysis: Background and General Principles

Neutron activation analysis (NAA) is a method of elemental analysis based upon modification of the nucleus by exposure to a beam of neutrons [63-69], followed by analysis of the radioactivity produced by the modified nucleus. In NAA the nuclei of stable isotopes are exposed to a neutron generating source.

Some of the nuclei capture neutrons to form radioactive species; these are referred to as radioisotopes, or most preferably, radionuclides. Radionuclides emit radiation in several ways. The emission process is called decay, and occurs with a characteristic half-life. During decay radionuclides are converted to other isotopes.

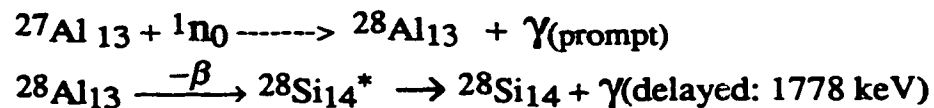
The rate of production of radionuclides (the number of activated nuclei produced) during irradiation by a neutron source depends on several factors. One factor is the half-life of the activation products. Other factors include the number of target nuclei, the number of neutrons striking the area containing the target nuclei per unit time, and the reaction cross section of the target nuclei. The reaction cross section is a function defining the probability of activation occurring for a specific reaction when a neutron strikes a nucleus. The kinetic energy of the bombarding neutrons is also a factor in determining the types of interaction that will occur and the nature of the activation products.

When a neutron is absorbed by a target nucleus, a highly energetic state in the resulting nucleus is often produced. This excess energy may be released from the nucleus in several ways. These include emission of gamma radiation, and ejection of a particle such as a proton or an alpha particle [63-65].

The most common source of neutrons for NAA is a nuclear reactor. The neutrons produced in a reactor exhibit a wide range of kinetic energies. The largest fraction have an average energy of about 0.025 eV. These neutrons have lost nearly all their kinetic energy and move in thermal equilibrium with the particles of the medium surrounding them, hence are termed *thermal* neutrons [64, 65]. Other types, classified according to their velocity, include *epithermal* neutrons, which have energies between 0.5 eV and 1 MeV, and *fast* neutrons, with energies above 1 MeV. Epithermal neutrons are fast neutrons which are in the

process of slowing down, and so are intermediate in kinetic energy between thermal and fast neutrons.

The key reaction which occurs between nuclei and thermal neutrons involves uptake of a neutron followed by emission of energy in the form of electromagnetic radiation. The shorthand notation for a process such as this is to refer to it as an (n, γ) reaction. In this process absorption of a neutron by a nucleus produces an excited state of the product nucleus which loses energy by emission of a gamma-ray, called a *prompt* gamma because it is emitted immediately after activation. Subsequently, the product nucleus emits a beta particle to form a new product which then emits another gamma-ray called *delayed* gamma as it deexcites to the stable state. A typical example is shown by ^{27}Al .



In this work, all the quantification of isotopes of the elements was done by way of delayed gamma. Fast neutrons tend to produce different reactions, and their absorption may result in one of several other decay paths. These include the emission of a proton [an (n, p) reaction], an alpha particle [an (n, α) reaction], or another neutron [an (n, 2n) reaction]. The first two of these reactions are called *transmutations* because the atomic number of the product nucleus differs from that of its parent [64].

5.1.1. Factors influencing activation with neutrons

The major factors affecting the extent of activation of nuclei with neutrons include the neutron flux ϕ , the cross-section of the target nucleus σ for a specific reaction and the number of target nuclei N . The neutron flux ϕ is defined as the product of neutron density, expressed in n cm^{-3} , and neutron velocity, expressed

in cm s^{-1} . Consequently, ϕ has the dimensions $\text{n cm}^{-2} \text{s}^{-1}$; it represents the number of neutrons flowing through a one square centimeter area in one second [65].

The cross-section σ of a nucleus is a physical parameter which measures the probability of a given nuclear reaction taking place. It is usually expressed in units of barns ($1 \text{ barn} = 10^{-24} \text{ cm}^2$) and is dependent on the velocity, or energy, of the neutron. Nuclei of low atomic number often have cross-sections which are inversely proportional to the velocity of low-energy neutrons; these are known as $1/v$ absorbers [63]. Thermal neutrons have low kinetic energy, and therefore move slowly. These slowly moving neutrons can remain within the sphere of influence of an atomic nucleus for some time and thereby have a greater probability of reacting than fast neutrons [65]. For target nuclei which are able to absorb epithermal neutrons of higher energy, the cross section is referred to as the *resonance integral* (I_r) [63]. The overall cross section for a particular target may consist of the sum of a number of partial cross sections, depending on the energy of the source neutrons and on whether the activation process involves an (n, γ) , (n, p) or (n, α) reaction. For most thermal neutron activation applications the main reaction is an (n, γ) process involving the neutron radiative capture cross section σ .

Since each isotope of an element may have a different neutron capture cross section for different reactions the number of target nuclei that undergo activation depend on the abundance of the various isotopes comprising the element of interest. For an element which is monoisotopic, such as aluminum-27, all the target nuclei are the same. On the other hand, most elements have more than one isotope. For these elements the number of target nuclei must be calculated from the % isotopic abundance (θ) of the isotope that is activated.

5.2. Theory of Activation Analysis

5.2.1. Radioactive decay

The constant fraction of the radioactive atoms produced by irradiation decay with time. The extent of this process can be calculated by the law of radioactive decay, which states that the number of atoms disintegrating per unit time ($-dN/dt$) is proportional to the total number N of radioactive atoms present [63-65], according to

$$- dN/dt = \lambda N \quad 5.1$$

where λ is called the disintegration or decay constant and has the dimension s^{-1} . This constant provides a measure of the probability of nuclear decay and has a characteristic value for each radioactive nuclide.

By integration of equation 5.1 it follows that

$$N = N_0 e^{-\lambda t} \quad 5.2$$

where N_0 is the number of radioactive atoms at time $t = 0$ and N is the number at time t . The half-life, $t_{1/2}$, is the time required for half of the initial number of radioactive atoms to decay, i.e., for N to become equal to $N_0/2$. At $t = t_{1/2}$

$$N = N_0/2 = N_0 e^{-\lambda t_{1/2}} \quad 5.3$$

which rearranges to

$$\ln 2 = \lambda t_{1/2} \quad \text{or} \quad t_{1/2} = 0.693/\lambda \quad 5.4$$

5.2.2. Relation between measurement of radioactivity and amount of an element present in an irradiated sample

In a neutron-induced nuclear reaction the growth of any given activation product depends on the number of target nuclei producing that product and on

the magnitude of the neutron flux [63-65]. A large neutron flux results in an increase in the rate at which interactions occur:

$$\text{activation rate} \propto \text{neutron flux } (\phi) \quad 5.5$$

Also, the larger the number of target nuclei is the greater the activation rate:

$$\text{activation rate} \propto \text{number of target nuclei present } (N) \quad 5.6$$

The constant relating the activation rate to the number of target nuclei and the neutron flux is called the *effective cross section* σ

$$\text{activation rate} = \sigma\phi N \quad 5.7$$

Since Avogadro's number, N_A , represents the total number of atoms in the relative atomic mass of a substance (atomic weight), A_r , of an element, then for a monoisotopic element the total number of atoms per gram, N_g , is given by

$$N_g = N_A/A_r \quad 5.8$$

and for a mass m of the element the total number of target nuclei, N , is

$$N = mN_g = mN_A/A_r \quad 5.9$$

In the case of an element with more than one isotope, the number of target nuclei must be corrected for the isotopic abundance θ . Hence

$$N = \theta mN_A/A_r \quad 5.10$$

which rearranges to

$$m = NA_r/\theta N_A \quad 5.11$$

This means that the mass of an element present as a target is proportional to the number of target nuclei, which in turn is proportional to the rate of production of the activation product. In this way the activation rate can be related to the mass of element m .

Substituting equation 5.10 into 5.7 yields

$$\text{activation rate} = \sigma\phi\theta mN_A/A_r \quad 5.12$$

For an activation product which decays with a characteristic half-life, the radionuclide is being produced at the rate described by equation 5.7, but is also

decaying according to the decay rate equation 5.1. Hence the growth in activity is given by

$$\text{rate of activation product} = \text{activation rate} - \text{decay rate} \quad 5.13$$

that is,

$$-dN^*/dt = \sigma\Phi N - \lambda N^* \quad 5.14$$

where N^* represents the number of radioactive nuclei and is related to the counts registered by the radiation measurement system.

On integration, equation 5.14 becomes

$$N^* = \{\sigma\Phi N[1 - e^{-\lambda t}]\} / \lambda \quad 5.15$$

The activity of the radioisotope A_t at a given irradiation time t can be expressed in terms of the number of disintegrations per unit time by rearranging equation 5.15 to

$$A_t = \lambda N^* = \sigma\Phi N[1 - e^{-\lambda t}] \quad 5.16$$

The growth of the induced activity with time is therefore controlled by the half-life of the activation product. The number of radioactive nuclei at the end of irradiation for a specified time t_i is given by

$$N^* = (\sigma\Phi N/\lambda) (1 - e^{-\lambda t_i}) \quad 5.17$$

Allowing for a delay time t_d from the end of irradiation to the beginning of the counting period, the number of radioactive nuclei remaining after elapsed total time, $t_i + t_d$, is given by

$$N^* = (\sigma\Phi N/\lambda) (1 - e^{-\lambda t_i}) e^{-\lambda t_d} \quad 5.18$$

A correction for the number of radioactive nuclei that decay during the counting period t_c is also necessary. Including this correction in equation 5.18, the measured activity in counts, A , (where $A = \lambda N^*$) becomes

$$A = \lambda N^* = \sigma\Phi N (1 - e^{-\lambda t_i}) e^{-\lambda t_d} (1 - e^{-\lambda t_c}) \quad 5.19$$

Allowances must also be made for the intensity of the emitted gamma rays of a specific energy I_γ and for the efficiency ϵ of the detector for that gamma ray.

With inclusion of these terms, equation 5.19 becomes

$$A = \sigma\Phi N[1 - e^{-\lambda t_i}] e^{-\lambda t_d} [1 - e^{-\lambda t_c}] I_\gamma \epsilon \quad 5.20$$

Substituting equation 5.10 for N into equation 5.20 yields

$$A = (\sigma\Phi\theta m N_A/A_r) (1 - e^{-\lambda t_i}) e^{-\lambda t_d} (1 - e^{-\lambda t_c}) I_\gamma \epsilon \quad 5.21$$

From Equation 5.21 it can be seen that activity, A , is proportional to the mass m of the element under study.

If a sample is irradiated for a length of time sufficient to make the irradiation time approach infinity relative to $t_{1/2}$, i.e. $t \gg t_{1/2}$, then $(1 - e^{-\lambda t_i})$ approaches unity and the activity expression in equation 5.17 reduces to

$$A_{\text{sat}} = \sigma\Phi N \quad 5.22$$

where A_{sat} is called the *saturation activity* and is obtained by prolonged activation ($t_{\text{irr}} \gg t_{1/2}$). The saturation activity is independent of the half-life of the activation product and depends only on the value of the neutron flux and on the cross section, and the number of atoms of the target isotope.

In this work samples and standards were analyzed at the same time under identical conditions. As a result of this approach, called the comparator method, most of the terms in equation 5.21 remain constant except the mass m and the decay term, $e^{-\lambda t_d}$. The decay term changes if samples have different decay times. Substituting k for the group of terms whose values do not change, equation 5.21 simplifies to

$$A = k m e^{-\lambda t_d} \quad 5.23$$

Dividing the counts for the unknown by those for the standard gives

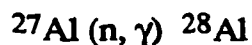
$$A_u / A_s = (m_u e^{-\lambda t_{du}}) / (m_s e^{-\lambda t_{ds}}) \quad 5.24$$

With knowledge of the other terms in above equation 5.24, the mass of the unknown m_u can be obtained.

5.3. Nuclear interferences

There are three major types of interferences in INAA. These can be classified as interfering nuclear reactions, spectral interferences and neutron self-shielding.

Interfering nuclear reactions are defined as reactions that change the relationship between the element to be determined and formation of the desired radionuclide [63]. For NAA the most important case involves the production of the radionuclide to be measured from elements in the sample other than the element being analyzed for. A good example is the analysis of a geological sample containing aluminum, silicon and phosphorus. Here ^{28}Al can be produced by any of the reactions:



The extent of the interference will depend on the cross-section of the sample nuclei for each reaction, the ratio of thermal to fast neutrons in the irradiating flux and on the concentrations of interfering elements. The interfering reactions from silicon and phosphorus can be reduced by moderating or eliminating as many of the fast neutrons in the flux as possible. A less satisfactory but still often useful alternative is to calculate and apply corrections. These interferences due to silicon and phosphorus were not however significant in this study and thus no corrections were necessary for the following reasons. Since the SLOWPOKE has a high thermal to fast neutron ratio interferences which arise mostly from fast neutrons would be negligible. Another reason is that similar matrix standards were used to analyze the standards so interferences would tend to cancel out. Besides, the matrix of the oil sand cores used is mostly SiO_2 so these interferences would not matter.

Interferences also occur in the measurement of gamma ray spectra. One type of interference is when radiation from other radionuclides interferes with the "full energy" peak of interest and causes the peak to have more than one component. This interference can be reduced or eliminated by a technique such as spectrum stripping [64]. In *spectrum stripping*, spectra of the sample and of a pure aliquot of the interferent are recorded and the activity of the pure interferent is multiplied by a factor that equates the height or area of a remote well-defined, non-interfering peak of the interferent in the two spectra. The resulting interferent spectrum is then subtracted from the original spectrum. Another method is to calculate the contribution that an interferent makes to the peak of the sample element through use of tabulated values of the relative intensities of two different photopeaks of the interferent, along with efficiency factors of the detector at both gamma energies [64,71].

Neutron self-shielding is a type of interference which occurs as a result of elements in the sample matrix competing for neutrons with the target of interest. As a result, the number of thermal neutrons from the source are reduced, the target is exposed to a lower flux, and activation does not occur to the extent expected. This interference can be detected by irradiating a range of sample masses and calculating the induced activity per unit mass. If neutron self-shielding is occurring, the activity per unit mass decreases as the mass increases [63]. Self-shielding becomes significant only when the cross sections of the interfering elements are very high. This type of interference was not a problem for the studies on oil sand reported in this work.

5.4. Detection of Gamma Radiation

5.4.1. Mechanism

As discussed before, many radionuclides emit electromagnetic radiation of high energy called gamma rays. The energies of these gamma rays, measured in units of kilo-electron volts (keV), can be used to identify the parent radionuclide, while the number of photons emitted can be used to measure the number of atoms (counts) of the parent radionuclide. To detect radioactivity it is necessary to cause the radiation emitted by decaying nuclei to interact with some material. This interaction can occur in several ways. The most important ones are the photoelectric effect, the Compton effect and pair production [63-66].

In the photoelectric effect, a gamma-ray transfers all its energy to an atom of an absorber substance, usually a semiconductor material, causing a photoelectron to be emitted. The energy of the ejected photoelectron is equal to that of the incident gamma ray, less the binding energy of the photoelectron in its original shell (usually the K-shell). The vacancy created in the inner shell of the absorber is filled through capture of an electron in the absorber. This process is accompanied by emission of a characteristic X-ray that can be detected and counted by conventional means.

The Compton effect is essentially an elastic collision in which a gamma ray photon interacts with a "free electron", that is, an electron from the interacting atom. During this interaction the photon transfers a fraction of its energy to the electron, resulting in the production of a less energetic gamma ray that is deflected at an angle from its incident direction [66]. This is called Compton scattering. Compton scattering results in production of gamma rays possessing a broad range of energies, all smaller than the energy of the original gamma ray, and all of which may interact with matter by the photoelectric effect. The result is production of a continuous background (i.e. Compton spectrum or continuum) of energy emission

which can interfere with the detection and counting of gamma rays from the decay of specific radioactive isotopes.

In pair production, highly energetic gamma rays are absorbed by interaction with the electrostatic field of an absorber nucleus to produce an electron-positron pair. Pair production usually only occurs for gamma rays with energies greater than 1.02 MeV, i.e., energy equivalent of the sum of the rest masses of an electron and a positron ($E=2mc^2$, where m is the mass of an electron or positron). The gamma ray loses all its energy to the electron-positron pair, with any energy in excess of 1.02 MeV appearing in the form of kinetic energy. The positron immediately interacts with an electron in the absorber, giving rise to two gamma photons, each with an energy of 0.511 MeV. This process is called annihilation. These gamma-rays may either be absorbed or escape from the detector. With a small detector both may escape, resulting in a detected peak with energy equal to the incident gamma ray minus 1.02 MeV. This peak is called a *double escape peak*. With a larger detector either one or none of the 511 keV photons may escape. If only one escapes then a *single escape peak* results, with an energy equal to that of the gamma ray minus 0.511 MeV.

5.5. Detection and Measurement of Gamma Radiation

5.5.1. Detectors

The gamma-ray detectors used in activation analysis convert the photons emitted by radioactive decay into an electrical signal. For this purpose a semiconductor, usually hyperpure germanium or germanium treated (drifted) with lithium, is used as the material interacting with the gamma photons. The detector is cooled [63-65] by a copper cold finger immersed in liquid nitrogen to reduce background electronic noise generated by thermal agitation of electrons in the

germanium. Lithium-drifted germanium detectors must remain immersed in liquid nitrogen at all times to prevent the lithium from drifting out of the treated zone of the crystal. Hyperpure germanium crystals do not deteriorate at room temperature and so need not be held at liquid nitrogen temperature during transport or storage [63-65].

Important specifications for gamma-ray detectors include efficiency, peak resolution, and peak-to-Compton ratio. The efficiency of a gamma-ray detector is a function of the active volume of the detector material [63]. The relative efficiency of a detector is specified by comparison of the signal from 1.33 MeV gamma rays emitted by cobalt-60 at a distance of 250 mm with that of a 76 × 76-mm sodium iodide detector for the same line at the same distance. The resolution of a spectral peak is determined by measurement of the width at half-height. This is the Full-Width-at-Half-Maximum (FWHM) [63-65]. Another important criterion for germanium detectors is the peak-to-Compton (P/C) ratio, defined as the ratio of the height of the 1.33 MeV photopeak of cobalt-60 to the highest point of the Compton spectrum at an energy just below that of the Compton edge, (the Compton edge is the sharp cut-off of the broad Compton spectrum). This ratio provides an indication of the combined resolution and efficiency of the detector, and gives an estimate of how well a gamma ray peak can be detected relative to the background. The higher the P/C ratio the better [65].

A gamma-ray detector is usually placed inside a shield of lead to reduce background counts from naturally occurring gamma ray emitters in the surrounding environment, or from radioactivity contamination. A space of at least 15 to 20 cm is maintained between the detector and shielding in all directions to minimize backscattering of gamma radiation. Typical lead shields have walls 5 to 10 cm thick, and are lined on the inside with graded sheets of cadmium (0.5 mm), copper (~0.1 mm), and sometimes clear plastic to absorb X-rays excited by β^-

radiation emitted by samples being counted or from X-rays produced as a result of gamma rays interacting with the lead.

5.5.2. Amplification of the signal from a gamma radiation detector

Measurement of the small number of electrons or the "holes" produced in a detector semiconductor requires a system for their collection and amplification. To do this a bias voltage is applied across the detector crystal by a separate high voltage unit. The electrons produced when a gamma ray strikes the detector are fed first to a preamplifier stage to amplify the very small electron pulses produced in the detector [63]. The resulting signal is usually still small, and so it is sent to a second stage for further amplification and pulse shaping.

From the preamplifier, the pulses are sent to an amplifier where they are magnified to levels of about 10V. This stage improves the signal-to-noise (S/N) ratio of the pulses and also suppresses pulse pile-up. The output from the amplifier is a set of Gaussian (voltage versus time) peaks with peak amplitudes proportional to the gamma ray energies which entered the detector. These peaks, or pulses, are sorted by a pulse height analyzer into a spectrum that can be viewed on a computer screen. The operation of the analyzer is described in the next section.

5.5.3. Pulse height analysis

The pulse height analyzer consists of an analog-to-digital converter (ADC) and a pulse-processing system, usually a multichannel analyzer (MCA). This system sorts the pulses delivered from the detector according to their energies, stores a count for each pulse in the appropriate energy channel, and makes the contents of each channel available for further processing. To do this, each pulse is converted by the ADC into a digital signal proportional to the pulse height; this

digital signal is then deposited as a count of the decay of a single nucleus into the appropriate channel number of the analyzer.

A finite time is required for the system to convert an initial pulse that enters it into a corresponding digital signal. During that time the MCA is unable to accept and count another pulse; it is said to be *busy*. The fraction of the total counting time during which the MCA is busy analyzing pulses is known as the *dead time* of the analyzer. The dead time is usually expressed as a percentage, and is calculated by the relation $(\text{dead time}/\text{live time}) \times 100$, where $\text{dead time} = (\text{clock time} - \text{live time})$. Most MCA's have inbuilt electronic circuitry that corrects automatically for this dead time. When this feature is implemented in data acquisition the MCA is said to be counting in the "Live Time" mode, where the live time is defined as the interval in which the MCA accepts pulses for counting, excluding the dead time of the analysis. The real counting time is, therefore, longer than the live time interval by the amount of the dead time [63-65].

5.6. Gamma-ray Spectra

A gamma-ray spectrum may be considered as a plot of the content of each channel in an MCA against channel number, or against the gamma ray energy (keV) corresponding to the channel number. The relationship between the analyzer channel number and the corresponding gamma-ray energy is linear (or generally a polynomial function of the channel number). For a linear function, a plot of gamma ray energy against channel number is a straight line with a slope dependent on the amplifier gain. The plot may or may not go through zero, depending on the way the ADC is set up [63].

Gamma ray spectrometers are calibrated using radionuclides such as ^{60}Co , ^{133}Ba or ^{137}Cs , all of which are available commercially as sources. These sources

are placed on the detector and the channel numbers noted for the maximum counts in the selected peaks. Energy calibration is defined by the slope (keV per channel) and the offset (keV) of a plot of the known energy of the gamma ray line against channel number.

5.7. Statistical Errors in INAA

5.7.1. Accuracy

The error in a quantitative measurement of the amount of a radionuclide in a sample (not including sampling error) is primarily due to statistics of counting. This error is typically of the order of 1 to 5 %. The statistical counting error (standard deviation), σ_N , in the absence of background is given by

$$\sigma_N = N^{1/2} \quad 5.27$$

where N is the number of the counts registered [65,72,73]. Since the relative counting error, ($\sigma_N/N = 1/N^{1/2}$) varies inversely as the square root of the counting time, any increase in counting time decreases the standard deviation of measurement [72]; thus, doubling the counting time reduces the relative error by the square root of two ($\sqrt{2}$).

The count rate for the decay of a radionuclide can be calculated by dividing the peak area by the recorded live time. The estimated count rate, σ_S , and the percent error in the count rate, $\% \sigma_S$, in the presence of background are calculated as [74]:

$$\begin{aligned} \sigma_S &= (N + 2B)^{1/2} \\ \% \sigma_S &= \{[(N + 2B)^{1/2}] / N\} 100 \end{aligned} \quad 5.28$$

where N is the net sample counts and B is the background count.

5.7.2. Detection limits

The detection limit in measurements of radioactivity may be defined as the probability of 95% of a peak being detected above the background. This corresponds to a value of about three times the standard deviation of the background [66,74]. A useful discussion on estimation of detection limit in INAA is provided by Currie [74] and is estimated as $(2.71 + 4.65 B^{1/2})$; B is background.

For a sample introduced into a detector for gamma ray counting, the detection limit is often described in terms of the minimum detectable concentration (MDC) [72], expressed as

$$MDC = (4.66 S_b) / (\epsilon P_\gamma W) \quad 5.29$$

where S_b is the estimated standard error of the net count rate; ϵ the counting efficiency of the energy of the specific nuclide (a number always ≤ 1); P_γ the absolute transition probability by gamma decay through the selected energy (also a number ≤ 1); and W is the mass of the sample in kg.

It can be seen from this equation that the factors which tend to influence the detection limits are the counting efficiency, the quantity of the sample (in terms of either mass or volume), the counting time associated with S_b , and the background. Therefore, for best detection limits the counting efficiency should be high, the sample should be as large as practicable, and the background as low as reasonably attainable. Counting efficiency is greatly influenced by sample geometry and tends to decrease as the sample-to-detector distance increases. For all but very small backgrounds, doubling the counting time improves the detection limit by a factor of the square root of two. Therefore, if one wishes to lower the detection limit by a factor of two, the counting time has to be four times as long. As mentioned earlier, proper shielding of the detector helps keep the background counts of a measurement system low. It should be kept in mind, however, that the number and type of radionuclides in a gamma spectrum will influence the level of

background in the Compton spectrum region. As a result, radionuclides with lower energies (i.e. energies in the Compton region) have higher detection limits. In addition, the concentration of an element such as potassium in samples can also influence detection limits for many radionuclides because of Compton scattering caused by the 1.46 MeV gamma ray of ^{40}K [72].

5.8. The University of Alberta SLOWPOKE Nuclear Reactor Facility

5.8.1. Description of the SLOWPOKE II nuclear reactor

SLOWPOKE is an acronym for Safe LOW POver Kritical Experiment. This reactor, a low-power moderate-flux facility developed by Atomic Energy of Canada Ltd. (AECL), is designed specifically for isotope production and neutron activation analysis. The SLOWPOKE Facility at the University of Alberta is a small pool type reactor capable of producing a neutron flux of up to $1 \times 10^{12} \text{ n cm}^{-2}\text{s}^{-1}$ [71]. A diagram of the installation is shown in Fig. 5.1.

The core of the reactor measures 22 cm in diameter by 23 cm high and contains approximately 250 fuel elements. Each fuel element consists of a pencil shaped rod of ^{235}U -enriched uranium-aluminum alloy, extrusion clad with pure aluminum. Aluminum is alloyed with uranium to provide rapid thermal conduction within the fuel rods, thereby minimizing exposure of the fuel to extreme temperatures. The aluminum cladding protects the alloy from contact with the water surrounding the rods. This avoids corrosion of the alloy and contamination of the reactor water by uranium [75].

The critical mass of enriched ^{235}U required for a sustained chain reaction in the SLOWPOKE reactor is only approximately 0.85 kg [71]. This small mass is possible because a neutron reflector of beryllium surrounds the fuel elements. Due

to its low atomic mass, beryllium reflects a fraction of the neutrons produced by the reactor core back into it. These reflected neutrons, once thermalized, may participate further in fission of the ^{235}U . The fission rate is controlled by the insertion or removal of a cadmium control rod. Cadmium is used for this purpose because it has a large thermal neutron cross section (ca. 20,000 barns) [71]. The reactor is brought to its operating power level by gradual withdrawal of the control rod from the core. During operation an approximately constant flux is maintained by automatic adjustment of the control rod position through a feedback mechanism incorporating a self-powered flux monitor [75]. The reactor is shut down by moving the control rod into the core. In the event of a fault or failure in the Cd control rod mechanism, three Cd capsules are provided with the reactor which, when placed in sample irradiation sites within the core, act as an auxiliary reactor shut-down device.

The reactor core sits within an annular beryllium reflector while resting on a lower beryllium reflector disc. Semicircular beryllium shims form the upper reflector. Additional shims are added as necessary over time to compensate for burn-up and poisoning of the fuel, thereby maintaining useful flux levels. Demineralized light water is circulated through the space between the upper and bottom reflector plates and the annular reflector to act as coolant and moderator and, most importantly, to serve as a primary safety feature for the reactor. A thermocouple, located within the beryllium annulus, monitors the temperature of the water. Water has a large "negative" temperature coefficient of reactivity [64,71], that is, its density decreases significantly as its temperature rises over most of its liquid range. As the density drops, so does its ability to moderate fission neutrons. This results in fewer fission neutrons being thermalized, (i.e. the number of these thermal neutrons which are necessary to sustain the fission process decreases). So with a sufficient temperature rise the thermal neutron flux will fall

below that required to maintain a self-sustained chain reaction. Similarly, a sudden rise in power level will cause the neutron moderating ability of the coolant to decrease, thereby lowering the thermal neutron flux and the fission rate [64]. In the event of a malfunction in the water cooling system the reactor power level will drop to a point where the amount of heat being generated by the fission process just equals that lost to the pool surroundings [71].

5.8.2. Sample irradiation in the SLOWPOKE reactor

The University of Alberta SLOWPOKE Reactor Facility has five inner radiation sites, that is, sites within the Be reflector, and one irradiation site outside the Be annulus (see Figure 5.2). The inner site can accommodate irradiation vials with a volume of 7 cm³, while vials for the larger outer site have a capacity of 27 cm³. Vials for the inner sites can each accommodate two smaller 1.5 cm³ sample vials. The U-Al alloy fuel rods are arranged in such a way as to provide an equal, stable and homogeneous neutron flux distribution over each of the five inner sites [71].

The reactor is operated via a console designed as a turnkey system. This console contains the reactor control system, radiation monitor readouts and monitors for the auxiliary systems. The reactor control system permits selection of the desired neutron flux by either automatic or manual operation of the Cd control rod. The flux, control rod position, and core temperature are monitored continuously during operation by strip chart recorders on the console.

Each polyethylene sample vial is transferred to and from the desired irradiation site in the reactor core by pressurized air. After the programmed irradiation time is over the vial is directed to a receiving station for counting.

Operation of the pneumatic device is automated, with the length of the irradiation period being controlled by a clock on each sample sending/receiving station. Once the samples have been irradiated and counted they are stored, behind lead shielding if necessary, until radiation levels have dropped to values that allow them to be disposed of.

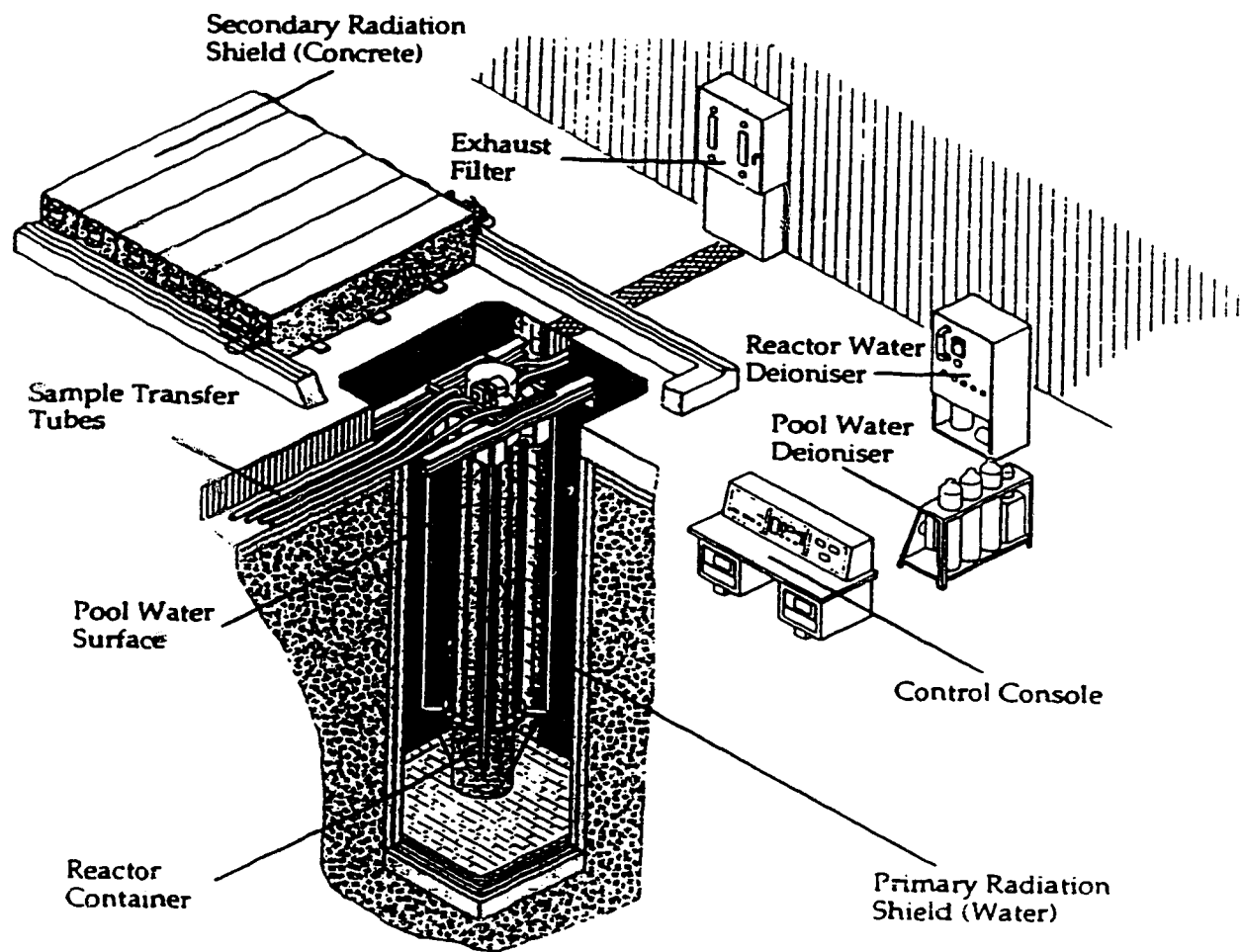


Figure 5.1. University of Alberta SLOWPOKE-II Reactor Facility
[Refs: 71,75,77].

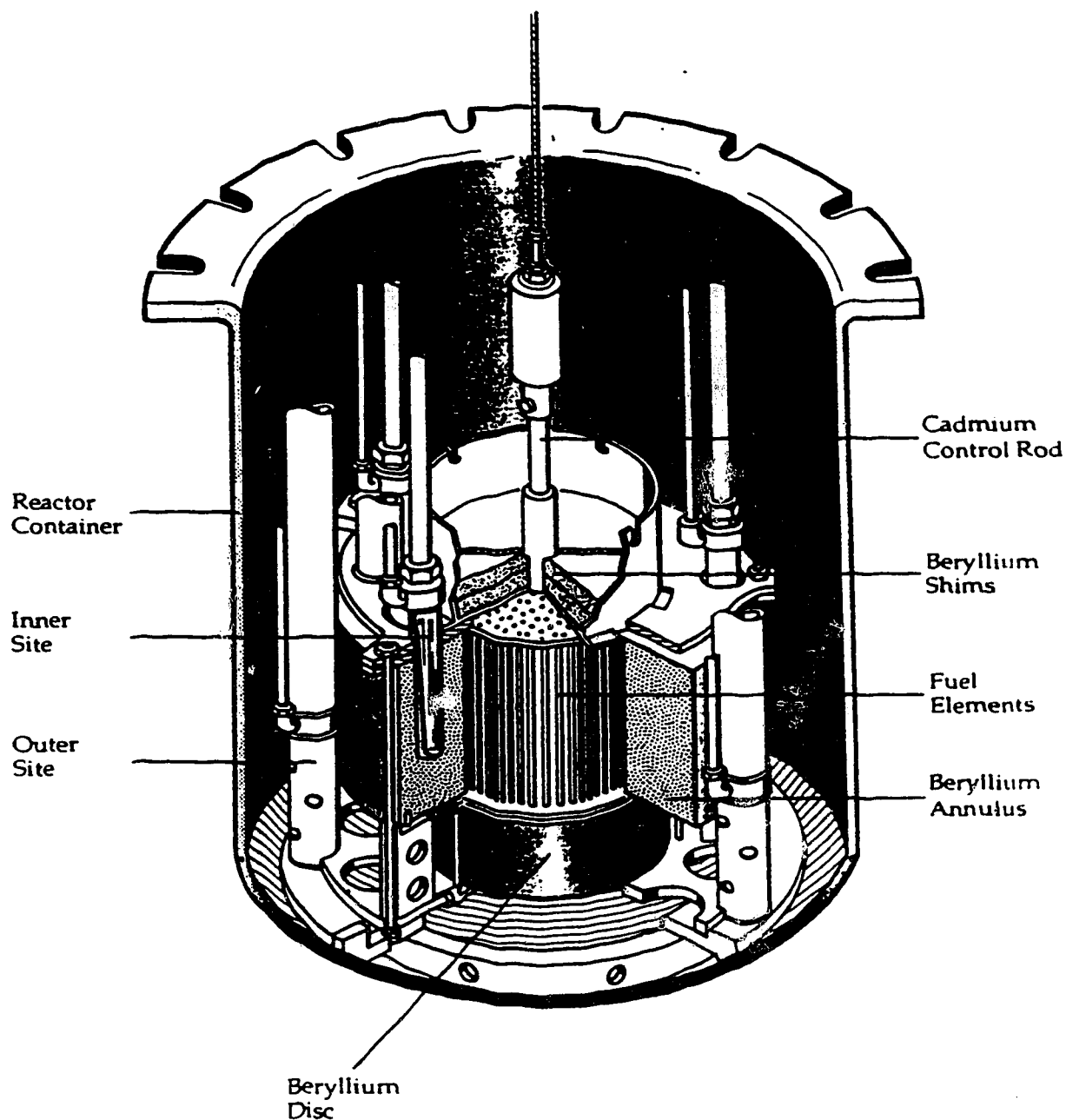


Figure 5.2. Cut-away view of SLOWPOKE-II Reactor critical assembly and core [Refs:71,75,77].

Chapter 6

Study of Elements Determinable in Athabasca Oil Sand by Instrumental Neutron Activation Analysis

Introduction

This chapter describes an INAA study of the distribution of those elements in the core of oil sand described in previous chapters amenable to detection and quantitation by a short irradiation/counting scheme. The goal of the work was to determine the degree of correlation between the INAA analyses and the levels of bitumen and fines present in the oil sand. In particular, it was of interest to determine whether INAA measurement of the concentrations of aluminum and other clay-related elements in the sands might provide a faster, more direct, and more accurate way of estimating the amounts of clay present than the currently used indirect method of particle size analysis.

6.1. Experimental Procedure

6.1.1. Preparation of irradiation vials for INAA

Polyethylene vials (Olympic Plastic Co., CA, U.S.A.) of 1.5 and 7 mL volume were soaked in 10% nitric acid for several days, rinsed several times with deionized water, and finally with nanopure water. After washing, the vials were dried overnight in an oven at about 40°C. Care was taken to handle the vials with clean gloves after they had been cleaned to prevent contamination by elements such as sodium or chlorine from the skin. Such elements would be activated upon irradiation and interfere in the measurements.

6.1.2. Preparation of half gram test portions of oil sand for INAA

Twenty-three test portions of oil sand, of approximately 0.5 g each, were removed from the core studied in the previous chapters. The samples were randomly selected, but it was important to obtain samples across the range of bitumen concentrations. In order to do this, the core was stratified into sections corresponding to regions containing different contents of bitumen. Samples were then selected randomly from each stratum and placed directly into the cleaned, dry 1.5-mL polyethylene irradiation vials. The vials were capped, each cap heat-sealed to the vial, and the sealed vials inserted into clean 7-mL polyethylene vials. Empty 1.5-mL vials were placed on top of the 1.5-mL vials containing the test portion to serve as spacers, then the 7-mL polyethylene vials were capped and the caps heat-sealed.

6.1.3. Preparation of extracted bitumen and fines samples for INAA

Another twenty-three test portions of oil sand weighing between 2 to 3 g were taken from the same regions of the core as the samples used in section 6.1.2. These were subjected to Soxhlet extraction as described in Chapter 2 to separate the bitumen from the solids. The extracted bitumen solution was centrifuged in a small bench-top centrifuge to remove particulate material or solids which might have passed through the filter thimble into the bitumen. The bitumen filtrate was pipetted with a glass Pasteur pipet into previously weighed 1.5-mL acid-washed polyethylene vials and the uncapped vials placed in a fume hood overnight to allow the toluene solvent used in the extraction to evaporate. The next day the vials were capped and reweighed to obtain the weights of the bitumen test portions. These weights ranged from 20 to 140 mg. The 1.5-mL vials were then heat-sealed and placed in 7-mL

vials. As before, empty 1.5-mL polyethylene vials were placed on top of the sample vials as spacers prior to heat-sealing of the 7-mL vials.

The twenty-three solid portions remaining in the Soxhlet extraction thimbles were removed and sieved through a 325 mesh (44 μm) stainless steel sieve to separate a finer fraction from the coarse material. This fraction smaller than 44 μm is termed "*finer*". Test portions of finer from each of the twenty-three sieve fractions, ranging between 0.05 and 0.8 g, were weighed into 1.5-mL nitric acid-washed polyethylene vials. After the vials were heat-sealed they were enclosed in 7-mL vials, empty 1.5-mL polyethylene vials inserted in each as spacers, and the 7-mL vials heat sealed for irradiation.

6.1.4. Preparation of standards for INAA

Standards were prepared from four soil reference materials: SO-1, SO-2, SO-3, and SO-4 (CANMET, Ottawa, Ontario), and from three marine sediment reference materials; BCSS-1, PACS-1, and MESS-1 (National Research Council of Canada, Ottawa, Ontario).

Portions of the standards were dried for several hours at 90°C in an oven to remove residual moisture prior to the weighing of test portions of 0.5, 10, or 30 g. For the half gram analyses, approximately 0.5-g portions were weighed into the bottom of 1.5-mL acid-washed polyethylene vials to provide about the same volume as that of the samples. This was done in order to maintain similar geometry during irradiation and counting. A few pellets of wax (Paraplast, Oxford Labware, St. Louis, Mo, USA) were placed on top of the standard material and the vials placed in an oven at a temperature of about 50 °C to melt the wax. On cooling the solid wax covering over the standards ensured that their position within the vials would remain constant during

irradiation and counting. The vials were then heat-sealed and further sealed in 7-mL vials as outlined before for the oil sand samples.

For the ten and thirty gram samples, portions of the standard materials were weighed into 7- and 27-mL vials respectively to within about 2 mm of the tops of the vials. Here the addition of wax was unnecessary because the sample heights also came to within about 2 mm of the top of the vials.

6.1.5. Irradiation and counting of short-lived isotopes

The irradiation and counting operations were performed at the SLOWPOKE-2 Reactor Facility at the University of Alberta. To analyze for short-lived isotopes, the standards and samples were individually irradiated at a thermal nominal flux of $1 \times 10^{12} \text{ n cm}^{-2} \text{ s}^{-1}$ for five minutes. Following a decay period of 20 ± 5 minutes, each sample was counted for 300 seconds (livetime) at a sample-to-detector distance of 6-cm. Elemental analysis was performed via the semi-absolute method of NAA [70].

Counting was carried out using an inhouse modified sample changer mechanism built from a Nuclear Chicago gamma counter and interfaced to a PC-based MCA card/gamma-ray spectroscopy system. The detector consisted of a Model 20180 EG &G Ortec (Oak Ridge, Tennessee, U.S.A.) vertical, closed-end, hyperpure (p-type) Ge, coaxial detector operating at +3500V. The detector specifications included a relative efficiency of 22.4%, a measured full width half maximum of 1.71 keV and a peak-to-Compton ratio of 59.3:1 for the 1332 keV photopeak of ^{60}Co . All detector specifications are quoted for a 6- μs amplifier time constant. The detector was coupled to an Aptec spectroscopy amplifier (coarse gain of 20 and shaping time of 3 μs) and an ND-575 Analog-to-Digital converter (ADC).

6.1.6. Spectral correction and analysis

Spectral peak searching was accomplished using the software program, SPAN [76]. Deadtimes of less than 10% were maintained for each sample. The spectral data were normalized with respect to weight of sample. Decay corrections and quantification of elements were performed using an inhouse BASIC program written by M.J.M Duke [77], along with two spreadsheet programs: Quattro Pro (V4.0; Borland Inc. U.S.A) and Excel (V4.0; Microsoft Corp.,U.S.A).

Statistical analysis of the resulting data was carried out using the Principal Component Analysis (PCA) module of VM SAS Statistical Package (V 120.1091) provided by the University of Alberta Computing System on the Amdahl mainframe computer.

Standard reference materials (SO-1, SO-2, SO-3) were analyzed at the same irradiation conditions as the samples. The resulting INAA data were used to create a library of decay corrected counts per microgram for the various gamma emissions of radionuclides of the elements of interest. Soil standard SO-4 and three NRCC marine sediment reference materials MESS-1, BCSS-1, and PACS-1 were analyzed and treated as unknowns. The results were then compared with literature values for quality control purposes. The data are presented in Tables 6.1 to 6.4 and as can be seen the agreement between the measured and reference data is very good.

<u>Element</u>	<u>Measured value</u>	<u>Certified value</u>
Dysprosium	3.82 ± 0.33	3.50
Samarium	4.63 ± 0.95	4.70
Europium	0.98 ± 0.21	0.97
Barium	640 ± 55	700
Titanium	3080 ± 198	3400 ± 200
Manganese	590 ± 14	600 ± 20
Sodium (wt %)	0.99 ± 0.01	1.00 ± 0.02
Vanadium	85 ± 3	90 ± 11
Potassium (wt %)	1.84 ± 0.23	1.73 ± 0.03
Aluminum (wt %)	5.8 ± 0.1	5.46 ± 0.15
Calcium (wt %)	1.1 ± 0.1	1.1 ± 0.05
Scandium	8.7 ± 0.2	8.4
Tantalum	0.65 ± 0.03	0.62
Neodymium	22.7 ± 2.1	25
Iron (wt %)	2.5 ± 0.03	2.37 ± 0.07
Cerium	53.5 ± 1.4	54
Ytterbium	2.4 ± 0.3	2.10
Chromium	71.8 ± 4.6	71 ± 6
Cesium	2.9 ± 0.1	2.88
Strontium	161 ± 17	170 ± 18
Zinc	99 ± 5	94 ± 3
Terbium	0.65 ± 0.02	0.61
Cobalt	10.3 ± 0.2	11 ± 1
Hafnium	8.0 ± 0.9	8.0

Table 6.1. Comparison of element concentrations (in microg/g unless otherwise stated) determined by INAA with certified values for CANMET soil standard, SO-4. (Uncertainties for standards represent 95% confidence limits for an individual subsample. Those values without uncertainties are consensus values. Uncertainties for measured values are one standard deviation).

<u>Element</u>	<u>Measured value</u>	<u>Certified value</u>
Aluminum (wt %)	6.53 ± 0.07	6.26 ± 0.41
Iron (wt %)	3.6 ± 0.1	3.29 ± 0.14
Potassium (wt %)	1.85 ± 0.25	1.80 ± 0.04
Sodium (wt %)	2.02 ± 0.02	2.02 ± 0.21
Titanium (wt %)	0.44 ± 0.02	0.44 ± 0.02
Chlorine (wt %)	1.11 ± 0.02	1.12 ± 0.05
Vanadium	98.5 ± 3.8	93.4 ± 4.9
Manganese	245 ± 10	229 ± 15
Cobalt	12.8 ± 0.3	11.4 ± 2.1
Arsenic	11.3 ± 1.1	11.1 ± 1.4
Chromium	129 ± 7	123 ± 14
Nickel	62.7 ± 6.7	55.3 ± 3.6

Table 6.2. Comparison of elemental concentrations (in microg/g unless otherwise stated) measured by INAA with certified values for Marine Sediment Reference material, BCSS-1. (Uncertainties for the standard represent 95% confidence limits for an individual subsample and uncertainties for measured values are one standard deviation).

<u>Element</u>	<u>Measured value</u>	<u>Certified value</u>
Aluminium (wt %)	5.95 ± 0.07	5.84 ± 0.38
Iron (wt %)	3.4 ± 0.1	3.05 ± 0.25
Potassium (wt %)	1.73 ± 0.23	1.86 ± 0.04
Sodium (wt %)	1.91 ± 0.22	1.85 ± 0.15
Titanium (wt %)	0.50 ± 0.02	0.54 ± 0.03
Chlorine (wt %)	0.82 ± 0.02	0.82 ± 0.07
Vanadium	77.9 ± 3.3	72.4 ± 17
Manganese	521 ± 14	513 ± 25
Cobalt	13.7 ± 0.3	10.8 ± 1.9
Arsenic	12.4 ± 1.3	10.6 ± 1.2
Chromium	77 ± 6	71 ± 11
Zinc	221 ± 11	191 ± 17

Table 6.3. Comparison of elemental concentrations (in microg/g unless otherwise stated) measured by INAA with certified values for NRC Marine Sediment Reference material, MESS-1. (Uncertainties for the standard represent 95% confidence limits for an individual subsample and uncertainties for measured values are one standard deviation).

<u>Element</u>	<u>Measured value</u>			<u>Certified value</u>		
Aluminium (wt %)	6.32	±	0.09	6.47	±	0.22
Iron (wt %)	4.94	±	0.1	4.87	±	0.12
Potassium (wt %)	1.14	±	0.25	1.25	±	0.09
Sodium (wt %)	3.21	±	0.03	3.26	±	0.11
Titanium (wt %)	0.40	±	0.02	0.42	±	0.01
Chlorine (wt %)	2.22	±	0.03	2.39	±	0.09
Vanadium	129	±	5	127	±	5
Manganese	477	±	14	470	±	12
Cobalt	20.8	±	0.4	17.5	±	1.1
Arsenic	198	±	20	211	±	11
Chromium	111	±	9	113	±	8
Nickel	46	±	9	44	±	2

Table 6.4. Comparison of elemental concentrations (in microg/g unless otherwise stated) measured by INAA with certified values for Marine Sediment Reference material, PACS-1. (Uncertainties for the standard represent 95% confidence limits for an individual subsample and uncertainties for measured values are one standard deviation).

6.2. Results and Discussion for Correlations of Elemental Data in Raw Oil Sand and Bitumen Content

The elements V, Al, Mn, Cl, Dy, Na, Ti, K, Ba, Sm and Eu were determined in the twenty three test portions of the raw oil sand samples using the irradiation scheme described in section 6.1.5. The concentrations of these elements in micrograms per gram of oil sand sample or in weight percent were then correlated individually with the bitumen content in the oil sand as measured by Soxhlet extraction. These correlations appear in Figs. 6.1 to 6.5. Correlation plots of all the elements against bitumen show a negative slope except for chlorine and vanadium. For chlorine there was no defined correlation i.e. zero correlation was observed. The anomalous behavior of chlorine may be due to chlorine impurities in toluene or variable sodium chloride contents in the core. Vanadium also behaved differently in that it has a decreasing correlation till the 8% bitumen mark then it levels off and that is why its r-value is relatively low compared to the other elements. Table 6.5 gives correlation values for element concentration versus bitumen content in weight percent. We notice that most of the elements have good decreasing correlations with the bitumen content of oil sand. The lanthanides (Dy, Eu and Sm) especially show very high correlations of negative slope with weight percent bitumen of oil sand.

A correlation with negative slope is also obtained between weight percent bitumen and weight percent fines, as can be seen in Fig. 6.6, confirming that the richer the grade of oil sand samples, the lower the fines content. Since with few exceptions the elemental analyses all also showed negative correlations with respect to bitumen, they parallel the amount of fines present, as expected.

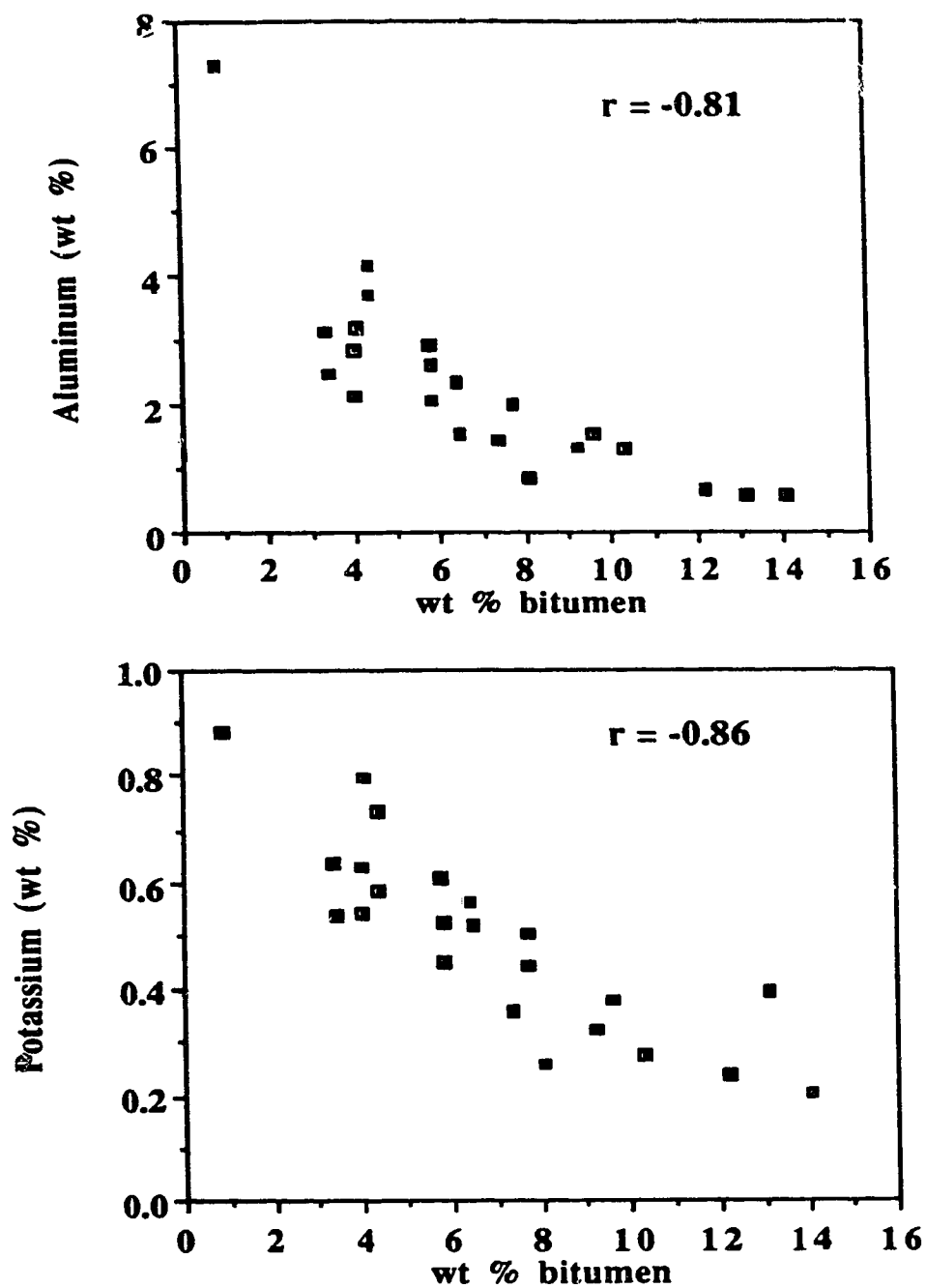


Figure 6.1. Correlation plots of aluminum (Al) and potassium (K) concentrations versus bitumen content for half gram portions of oil sand.

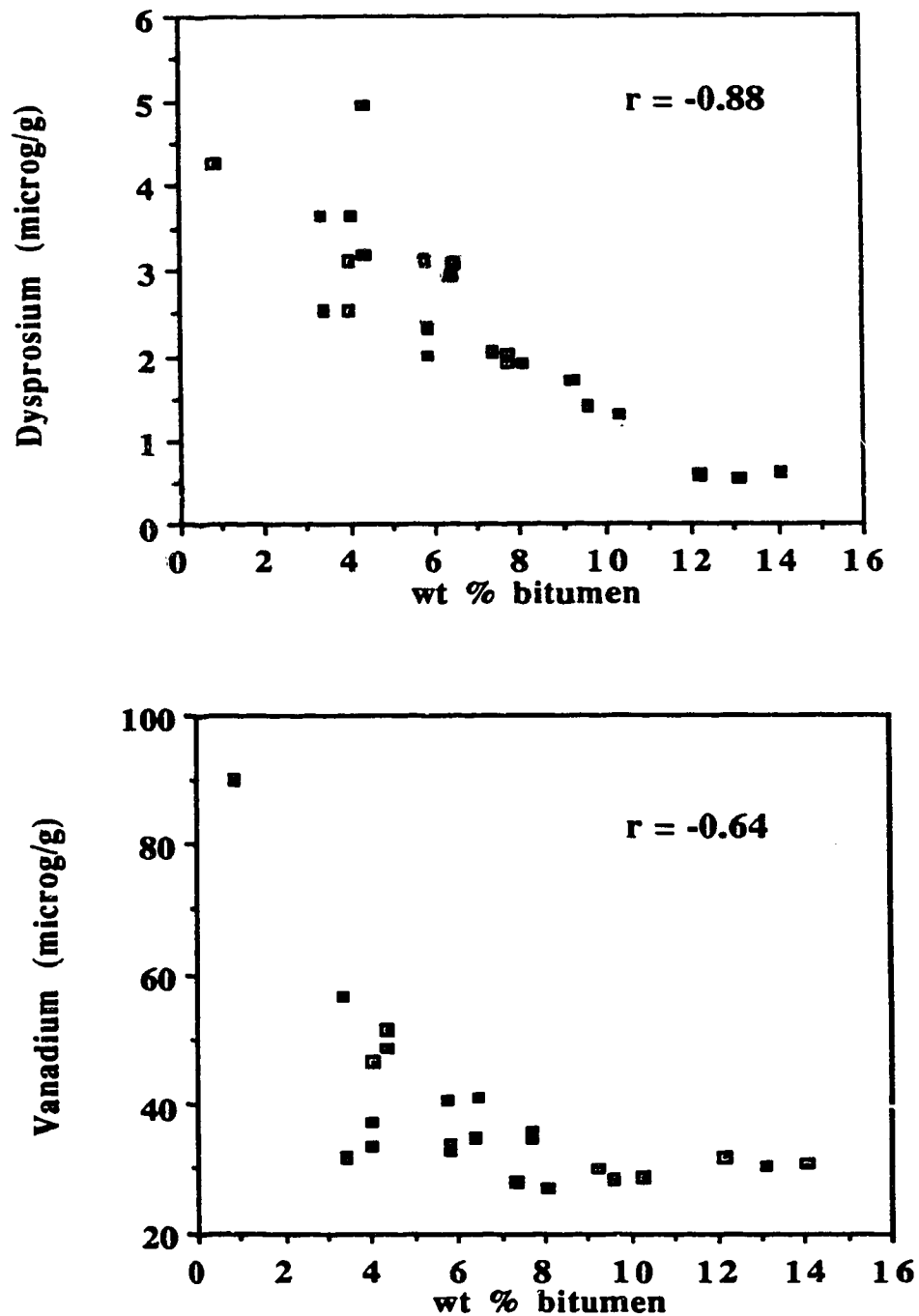


Figure 6.2. Correlation plots of dysprosium (Dy) and vanadium (V) concentrations versus bitumen content for half gram portions of oil sand.

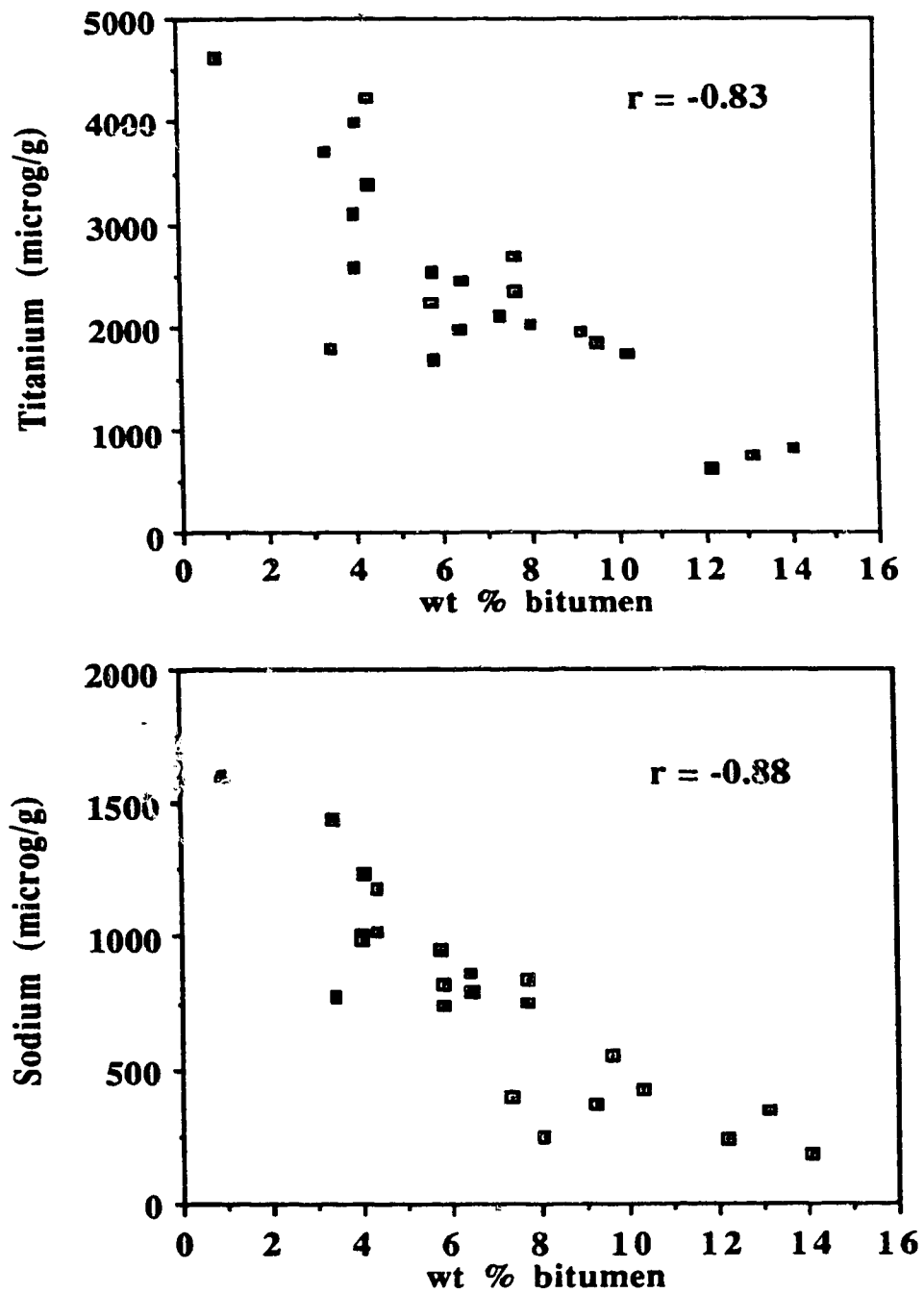


Figure 6.3. Correlation plots of titanium (Ti) and sodium (Na) concentrations versus bitumen content for half gram portions of oil sand.

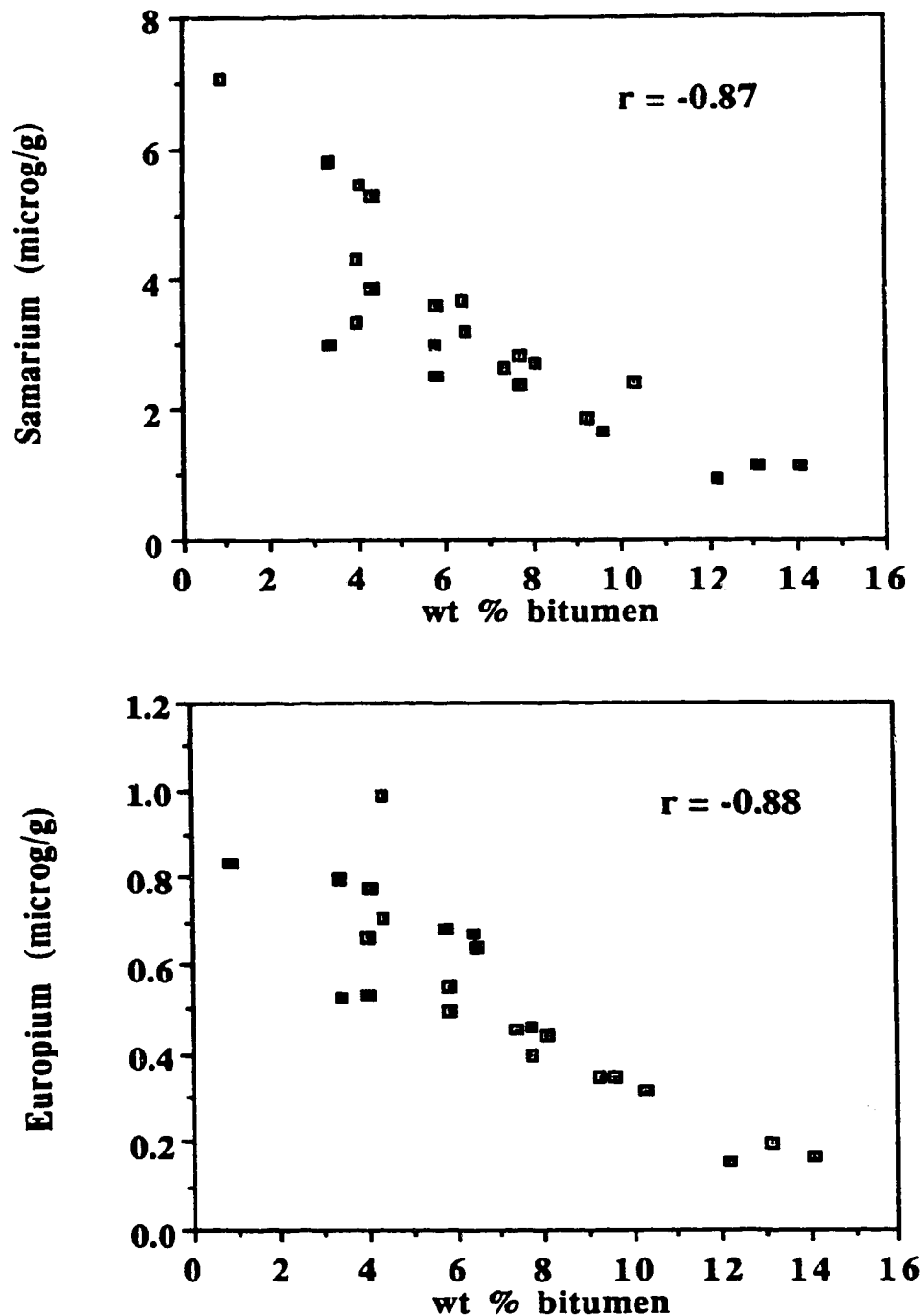


Figure 6.4. Correlation plots of samarium (Sm) and europium (Eu) concentrations versus bitumen content for half gram portions of oil sand.

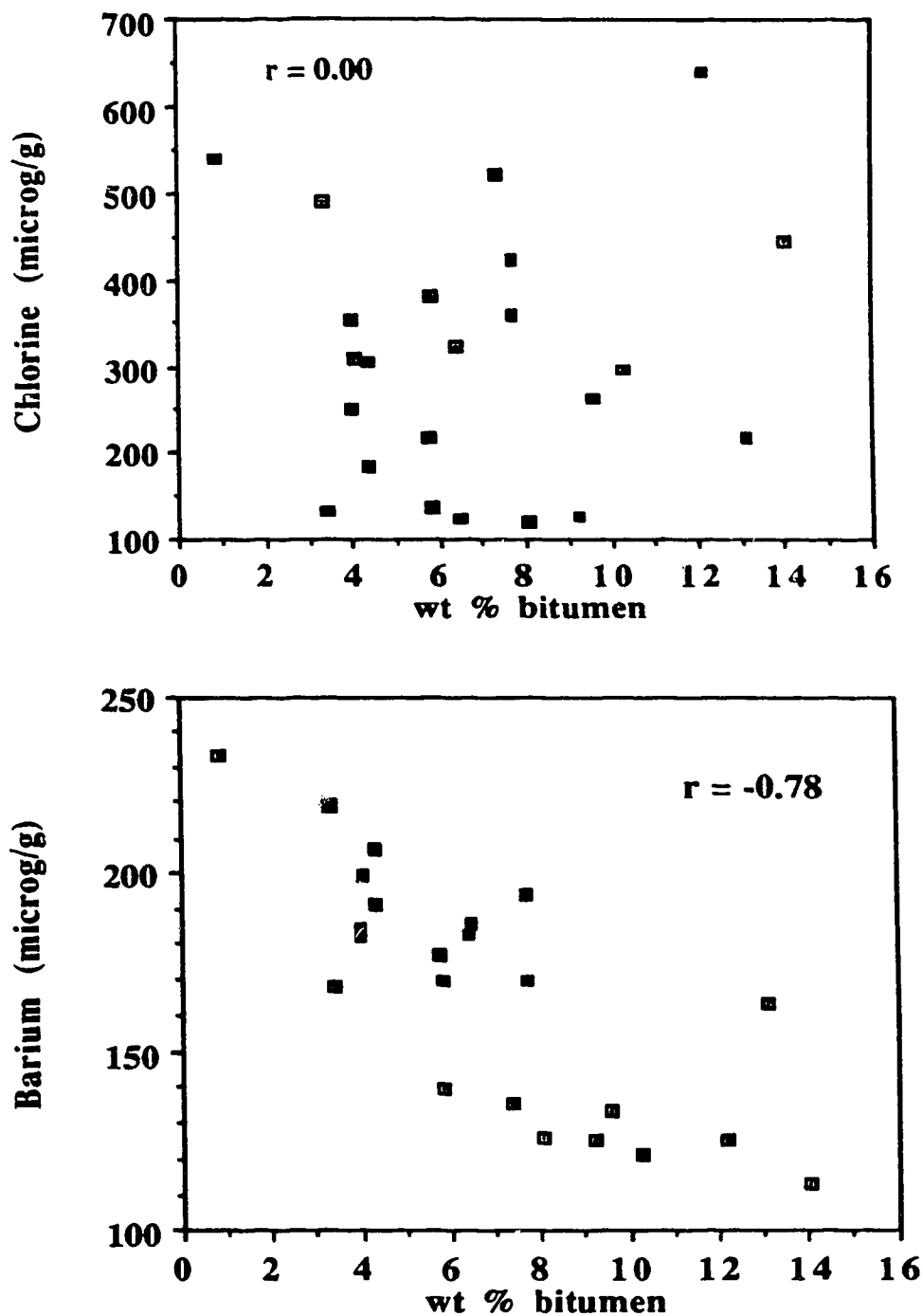


Figure 6.5. Correlation plot of chlorine (Cl) and barium (Ba) concentrations versus bitumen content for half gram portions of oil sand.

<u>element</u>	<u>r-value</u>
Vanadium (V)	-0.64
Dysprosium (Dy)	-0.88
Aluminum (Al)	-0.81
Europium (Eu)	-0.88
Samarium (Sm)	-0.87
Titanium (Ti)	-0.83
Barium (Ba)	-0.78
Potassium (K)	-0.86
Sodium (Na)	-0.88
Fines	-0.84
Chlorine (Cl)	0.00

Table 6.5. Correlation coefficients of concentrations of elements in oil sand against weight percent *bitumen*: r-values calculated for twenty-three ca. 0.5-g test portions.

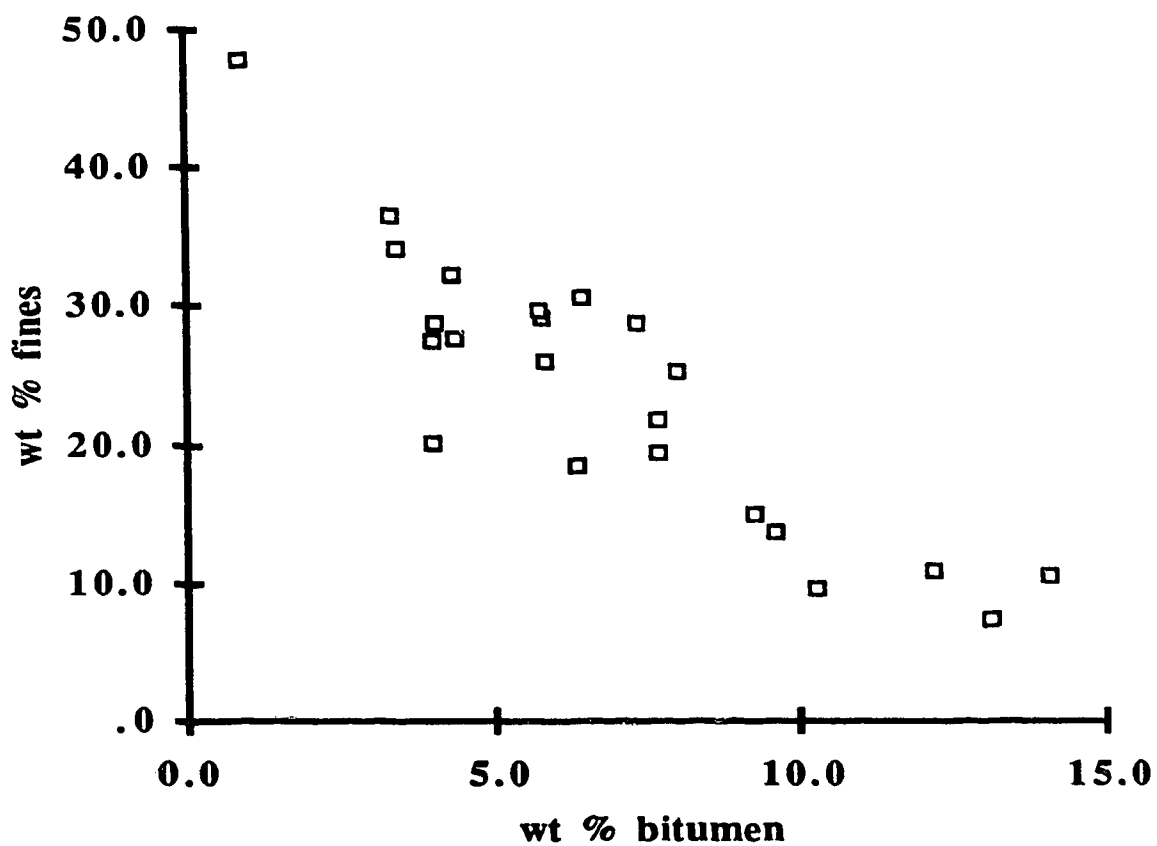


Figure 6.6. Relationship of fines to bitumen content in oil sand. (r-value = -0.84 for twenty-three ca. 0.5g test portions).

Cross correlation of the concentrations of elements in the half gram oil sand samples also yielded some interesting results. Strong positive correlations were observed among the lanthanides (Dy, Sm and Eu), and between Na and K. Plots of these correlations appear in Figs. 6.7 and 6.8.

Principal Component Analysis (PCA) was performed using the SAS program for various combinations of elements determined in the half gram oil sand samples. The statistical correlations between the resulting PCA values and the bitumen content for the various test portions were then calculated. Fig. 6.9 shows two representative correlation plots of combinations of elements, and Table 6.6 provides a summary of r-values obtained for various combinations of elements.

Comparisons of r values obtained using PCA of combined elements and those for individual elements indicate that, as expected, PCA yields better correlation values than those for any of the individual elements. This result confirms that PCA can enhance correlation models in this system by combining the predictive abilities of individual elements. The choice of elements to be incorporated in the PCA model must be carefully considered, however, in order to obtain optimum correlation. This point is illustrated in Table 6.6, from which it can be seen that the best combination ($r = -0.91$) is obtained from the PCA of Dy, Sm, Eu, K, Na and/or Al. Inclusion of an element having a poor correlation with the bitumen content in the combination can significantly degrade the model, so care in selection of the elements to include is important.

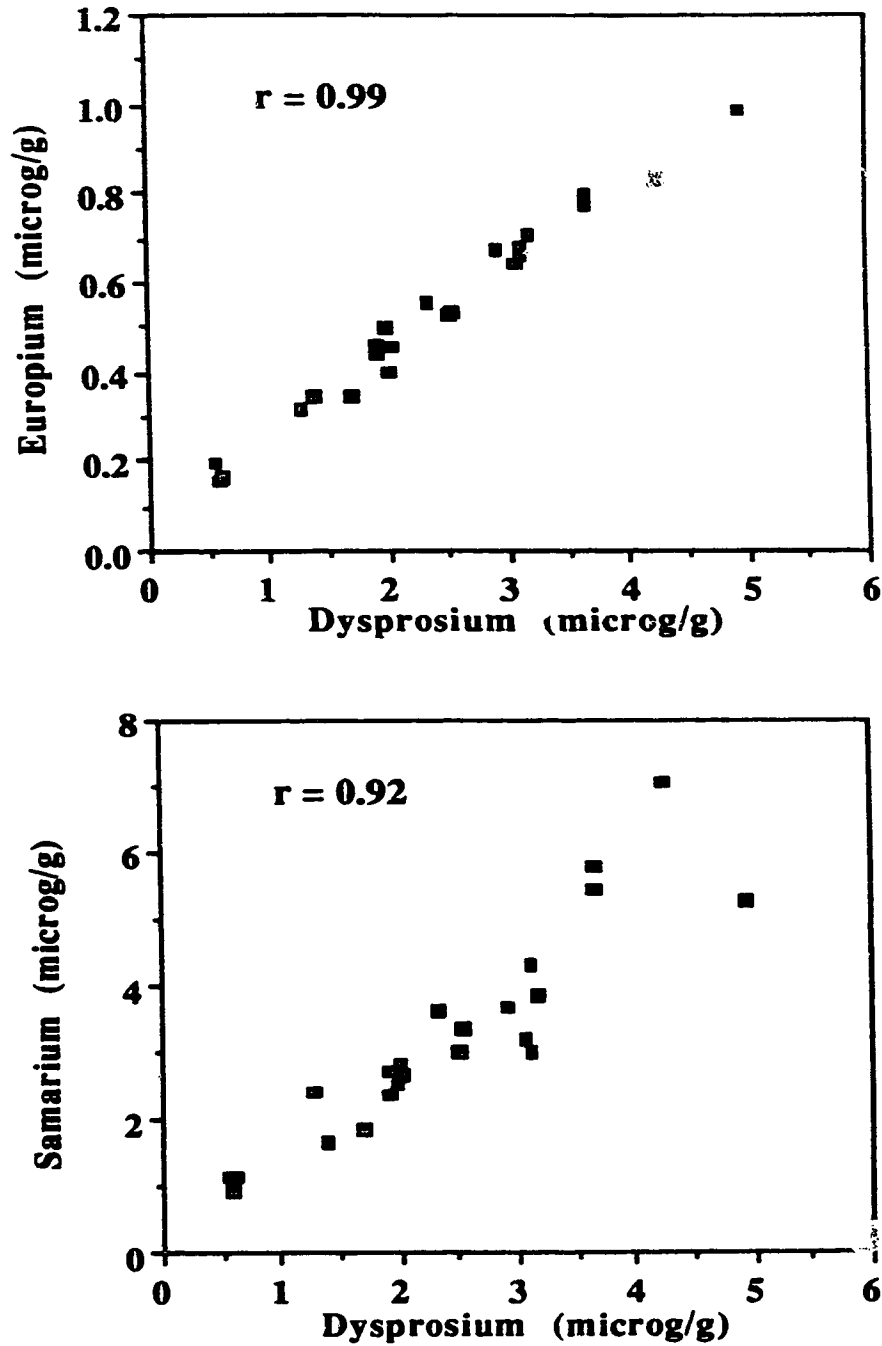


Figure 6.7. Cross-correlation plots for Eu versus Dy and Sm versus Dy of half gram test portions of oil sand.

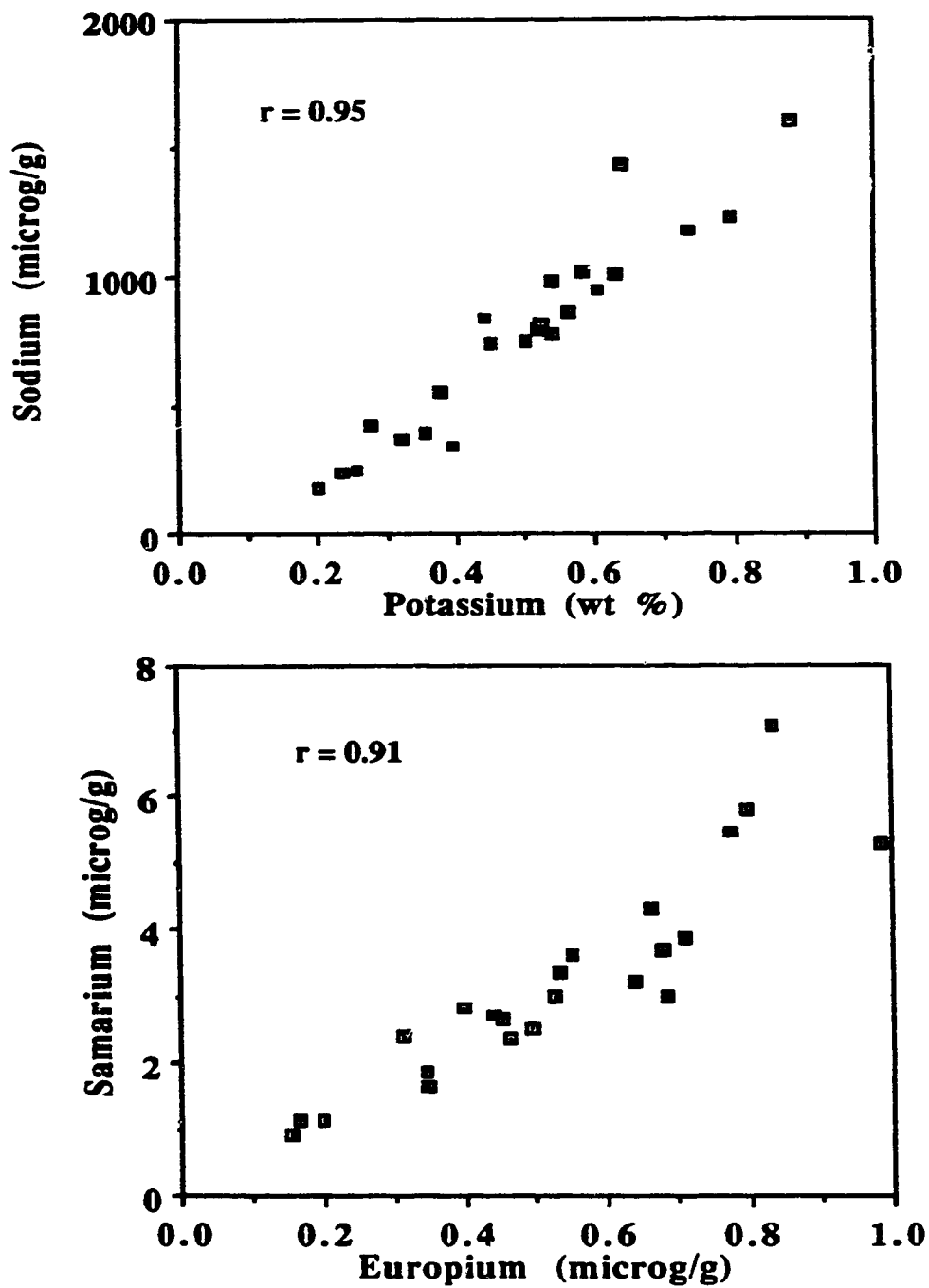


Figure 6.8. Cross-correlation plots for Na versus K and Sm versus Eu of half gram test portions of oil sand.

<u>Elements combined in PCA</u>	<u>r-value</u>
1. V,Dy,Al,Eu,Sm,Ti,Ba,K,Na,Cl,Mn	-0.88
2. V,Dy,Al,Eu,Sm,Ti,K,Na,Cl,Mn	-0.88
3. V,Dy,Al,Eu,Sm,Ti,K,Na,Cl	-0.89
4. V,Dy,Al,Eu,Sm,Ti,K,Na	-0.89
5. V,Dy,Al,Eu,Sm,K,Na	-0.89
6. V,Dy,Al,K,Na	-0.87
7. Dy,Al,Sm,Eu,K,Na	-0.91
8. Dy,Al,Sm,Eu,Ti,K,Na	-0.90
9. Dy,Sm,Eu,Ti,K,Na	-0.90
10. Dy,Sm,Eu,K,Na	-0.91
11. Dy,Sm,Eu	-0.90
12. K,Na,Al	-0.88
13. Dy,Sm,Eu,Al,Ti	-0.90
14. Dy,Sm,Eu,Al	-0.90
15. V,Ba,Cl,Mn	-0.71
16. V,Dy,Al,Sm,Eu	-0.88
17. V,Dy,Al	-0.83
18. V,Dy,Al,Eu	-0.87
19. V,Dy,Al,Sm	-0.85

Table 6.6. Principal Component Analysis results for various combinations of elements; (r-values are for ca. 0.5-g test portions of oil sand).

An example of how inclusion of a poor correlator with bitumen in the PCA degrades the model is illustrated by combination (5), where it can be seen that the addition of V to set (7) reduces the r -value from -0.91 to -0.88. Also, as expected, inclusion in the PCA of as many elements with as good negative correlations as possible tends to give a better correlation model. This is illustrated by combinations (7) through (10). Conversely, combinations of elements having poor correlations do not yield good results. In this respect V, Ba, Cl and Mn are the poorest elements in terms of correlating with bitumen content, as shown in Table 6.5, and the PCA of these elements results in a poor r -value (set 15 in Table 6.6).

The extent of correlation was also assessed for elemental concentrations in the raw oil sand portions versus fines content. In this case, concentrations were plotted against the weight percent fines for the half gram test portions and the corresponding r -values determined. These values are listed in Table 6.7, and the correlation scatter plots for Al, Dy, Na and Cl are represented in Figs 6.10 and 6.11. For the correlations with respect to fines, all elements except chlorine were found to correlate positively with the fines content, yielding r -values from 0.69 to 0.81. Chlorine concentrations had little or no correlation with fines content. We see that in general the three lanthanides readily determinable by short irradiation (Dy, Sm, and Eu) correlate well with fines content, especially dysprosium. A possible reason for this correlation may be that these elements tend to adsorb onto negatively charged areas of the clays in the fines, and the extent of adsorption is determined by the exposed surface area of these clays. If this is the case, then the greater the amount of clay present, the more dysprosium or other lanthanides would be adsorbed.

It is important to keep in mind that the fines do not consist wholly of clays but also include other mineral matter, so in that context, the degree of correlation ($r = 0.81$) obtained in this work for, say, dysprosium with fines, suggests that lanthanides such as dysprosium can be used as an indicator of clays in the fines. With respect to the potential of using a quantitative measure of one element as a measure of the clay content of oil sand, it can be concluded that of the elements studied dysprosium is the best choice.

When the element concentrations within the fines fractions were plotted against the weight percent fines in the oil sand, hardly any correlation was observed for any of the elements studied. Most of these elements are either structurally combined in the clay minerals and/or adsorbed by them [71]. They are also present in the coarser fractions of the solids to differing extents. This fact could partly explain the poor correlations observed. However, cross-correlations performed among elements in the fines yield good positive correlations, as can be seen from the r -values listed in Table 6.8. The pairs of europium versus dysprosium, and sodium versus vanadium, showed the best correlations, with r -values of 0.97. The scatter plots for these pairs appear in Fig. 6.12. In general, the lanthanides correlate well with each other, which suggests that they occur in the same matrix, probably the clay minerals in the fines.

<u>element</u>	<u>r-value</u>
Dysprosium (Dy)	0.81
Aluminum (Al)	0.77
Titanium (Ti)	0.75
Sodium (Na)	0.77
Potassium (K)	0.76
Europium (Eu)	0.80
Samarium (Sm)	0.80
Vanadium (V)	0.72
Barium (Ba)	0.69
Chlorine (Cl)	0.00

Table 6.7. Correlation coefficients of elemental concentrations versus weight percent *finer* in oil sand: r-values for twenty-three ~0.5-g test portions ranging from 5 to 50% fines.

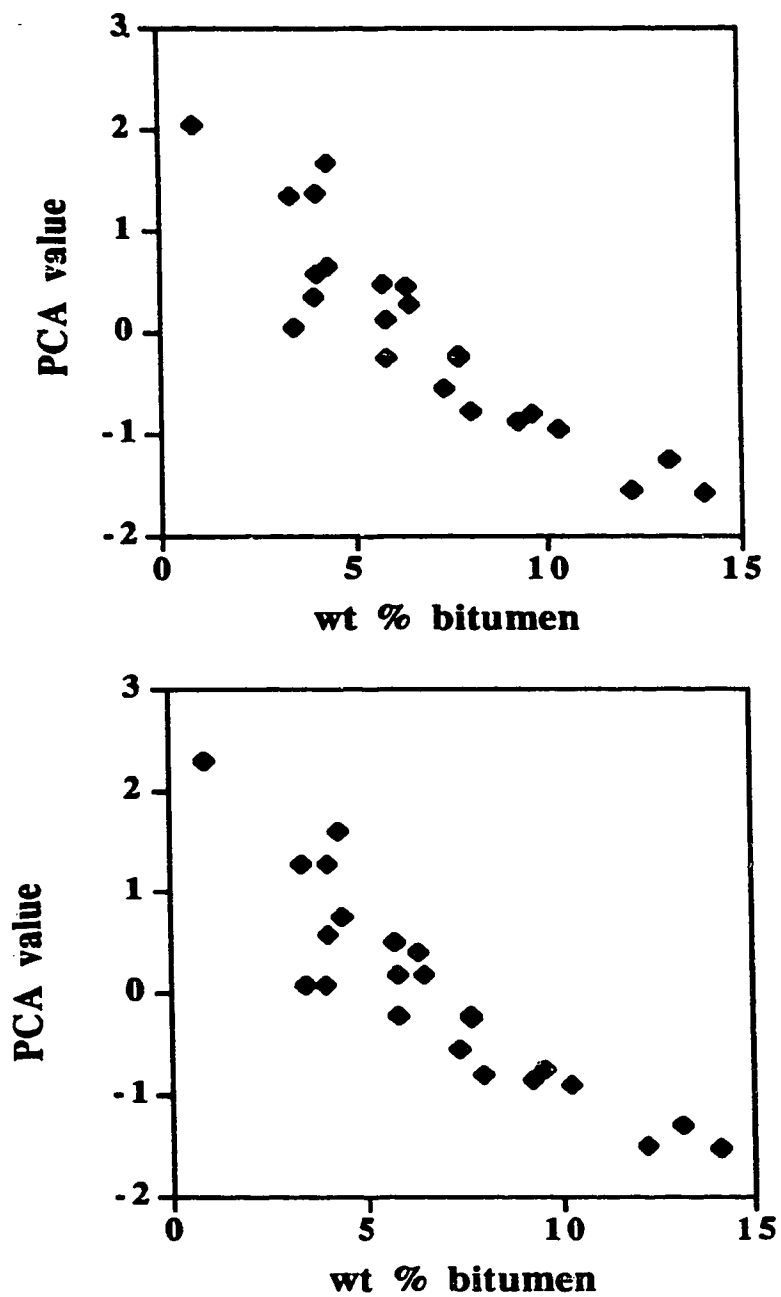


Figure 6.9. Combination of elements by PCA correlated with bitumen content. (Top: Dy, Sm, Eu, K, Na, $r = 0.91$; Bottom: Dy, Al, Sm, Eu, K, Na, $r = 0.91$).

<u>Elements in fines</u>	<u>r-value</u>
V vs Na	0.97
Eu vs Dy	0.97
Sm vs Dy	0.95
Ti vs Dy	0.95
Al vs V	0.95
Sm vs Ti	0.92
Eu vs Ti	0.91
K vs V	0.91
Eu vs Al	0.91
Na vs Al	0.89
Eu vs V	0.86
Al vs Ti	0.86
Al vs Dy	0.86
V vs Dy	0.85
Sm vs Al	0.85
V vs Ti	0.84
Na vs Eu	0.83
K vs Eu	0.83
K vs Dy	0.82
Na vs Dy	0.81
K vs Ti	0.81
V vs Sm	0.80
Na vs Ti	0.77
Na vs Sm	0.75
K vs Sm	0.72

Table 6.8. Cross correlations of elemental concentrations present in fines: r-values for twenty-three test portions ranging from 5 to 50% fines.

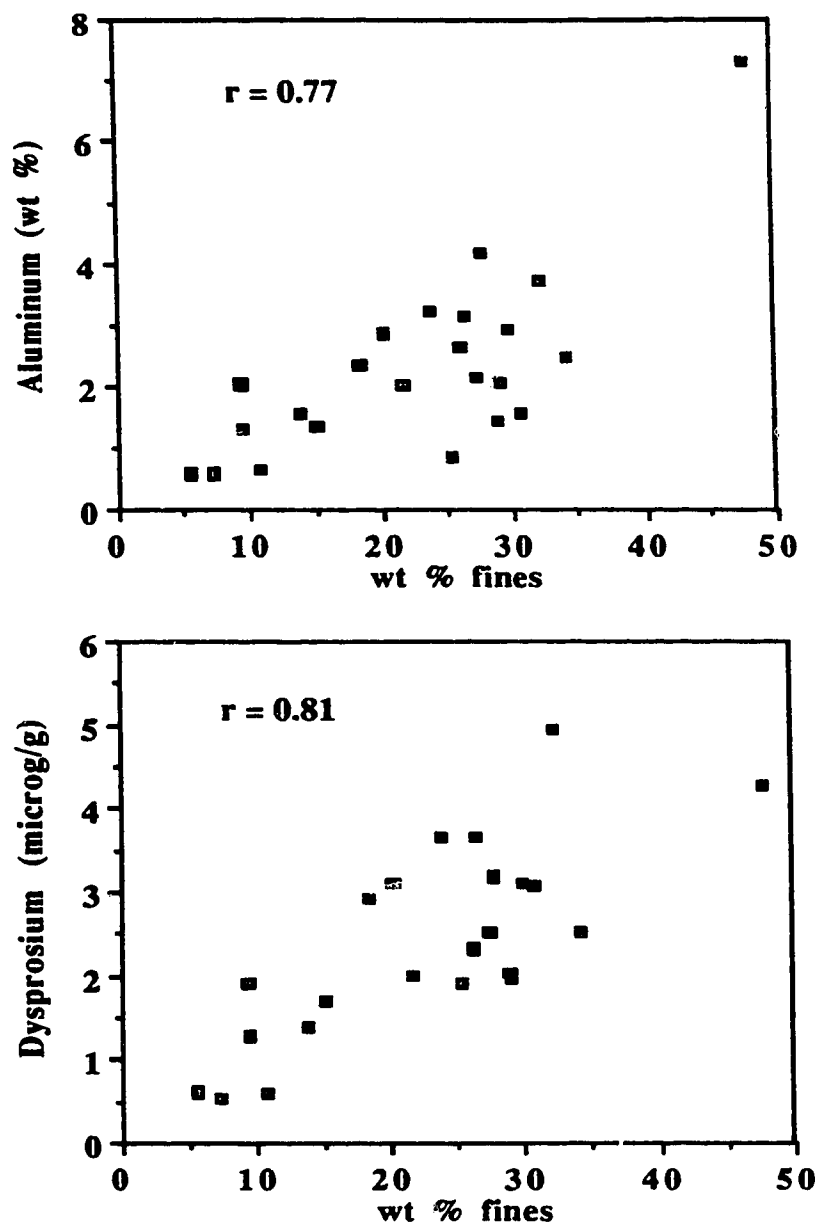


Figure 6.10. Correlation plots for aluminum (Al) and dysprosium (Dy) concentrations versus fines content for half gram test portions of oil sand.

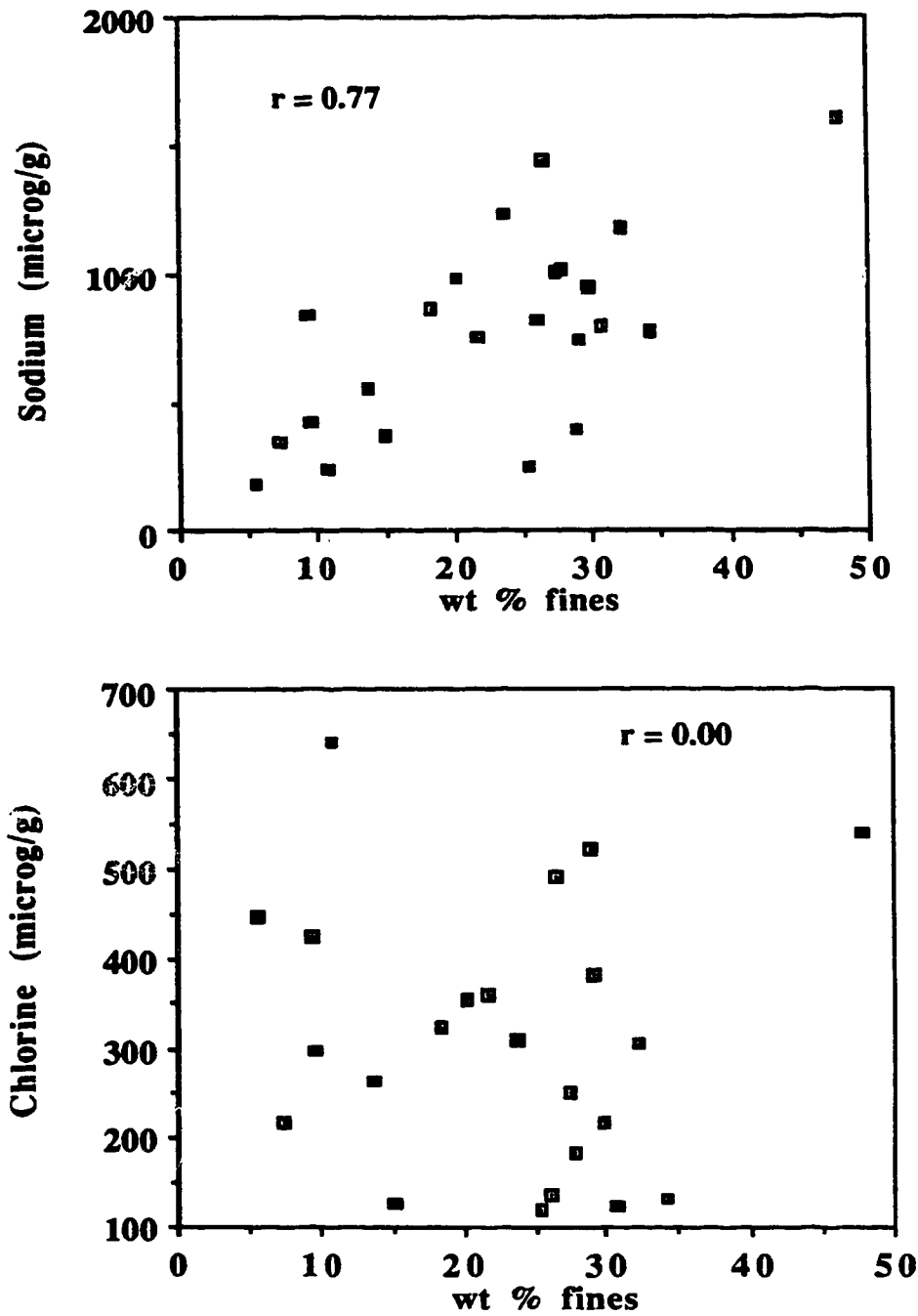


Figure 6.11. Correlation plots for sodium (Na) and chlorine (Cl) concentrations versus fines content for half gram test portions of oil sand.

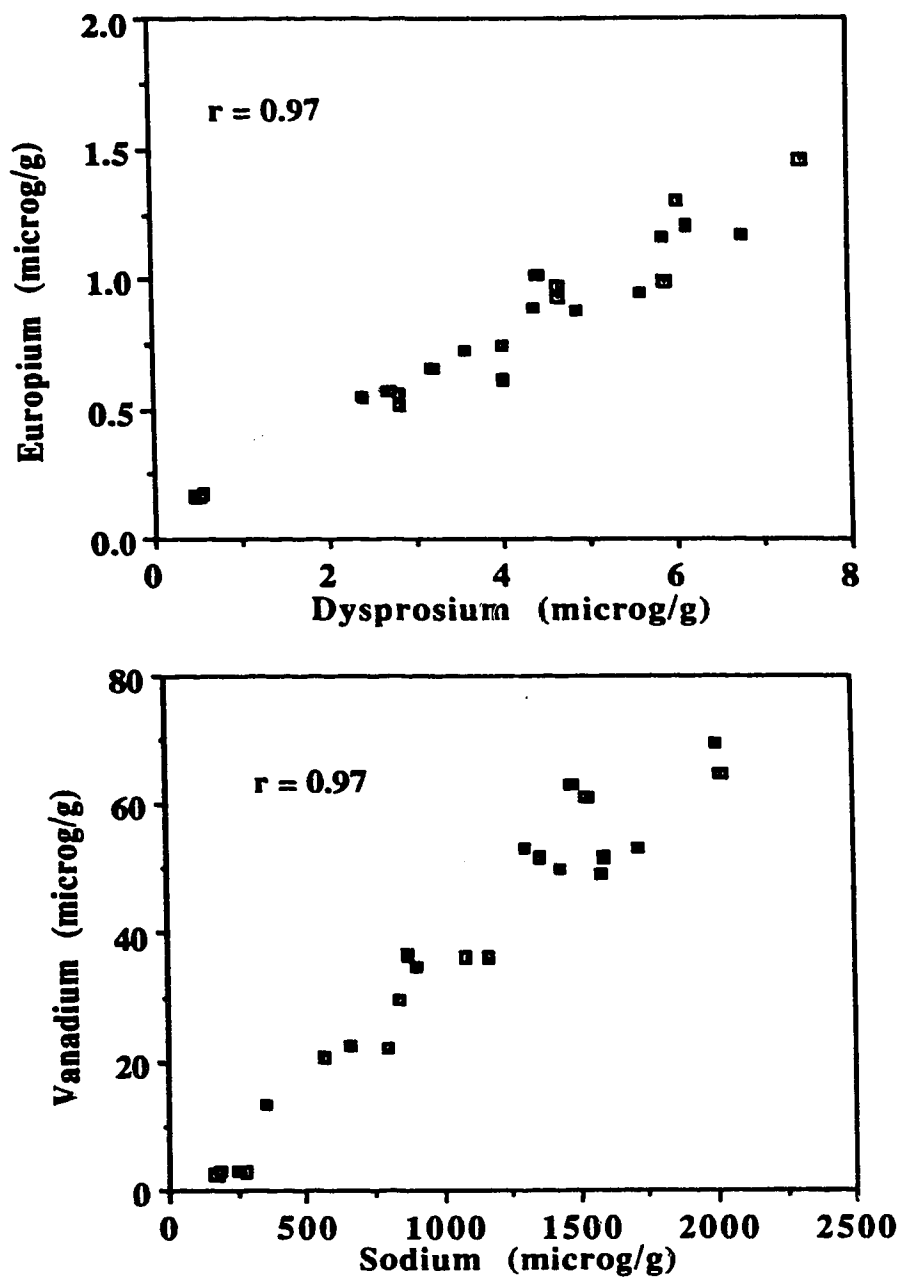


Figure 6.12. Cross correlation plots of concentrations of Eu versus Dy, and V versus Na in fines portion of oil sand.

6.3. Analyses of Ten and Thirty Gram Test Portions of Oil Sand

All of the above experimental work was done on 0.5-g portions of oil sand. Because of the heterogeneity of the material it was of interest to compare some analyses of larger portions with results obtained for the smaller ones. Therefore a small number of larger samples were taken and analyzed as for the small ones.

6.3.1. Preparation and analysis of ten gram samples by INAA

Nine test portions of oil sand weighing approximately 10g each were taken from the core. The samples were selected from locations such that three were from lean grade (< 6% bitumen), three from medium grade (6-9% bitumen) and three from rich grade regions (>9% bitumen). The test portions were weighed into 7-mL acid-washed irradiation vials, the vials capped and trimmed, and heat-sealed as before. Approximately 10-g portions of CANMET soil standards were also weighed accurately into acid-washed vials and heat-sealed in the same manner. These ten gram test portions were analyzed for both short and long-lived isotopes. To analyze for the longer-lived radioisotopes, standards and samples were individually irradiated for 16 minutes at $1 \times 10^{12} \text{ n cm}^{-2}\text{s}^{-1}$ and then counted twice, following two decay periods. The first count was for 3,600 seconds (livetime) following a decay of *ca.* 6 days, and the second count was for 25,000 seconds (livetime) after a total decay of *ca.* 21 days. Both measurements were performed at 1 cm geometry and the counting equipment used is as described in section 6.1.5. From these decay-count schemes it was possible to determine approximately seventeen elements in the samples namely As, Ce, Cr, Cs, Fe, Hf, La, Lu, Nd, Rb, Sc, Ta, Tb, Th, W, Yb and Zn.

6.3.2 Preparation and analysis of thirty gram samples by INAA

Nine test portions of oil sand weighing approximately thirty grams each were taken from regions adjacent to the locations of the ten gram samples. These samples were weighed into 27-mL acid-washed irradiation vials. The vials were heat-sealed and irradiated for five minutes in the outer site of the reactor at a thermal neutron flux of $5 \times 10^9 \text{ n cm}^{-2} \text{ s}^{-1}$ to determine elements producing short-lived isotopes. After allowing them to decay for 15 minutes they were individually counted for 300 secs (livetime) at a geometry of 10 cm to obtain data for vanadium, aluminum and titanium. Following a decay time of ca. 2 hours, each sample was recounted for 600 secs (livetime) at a geometry of 6 cm to measure additional short-lived isotopes (~~Al~~, Mn, K, Na, Dy, Eu, Ba).

6.3.3. Results and discussion

To assess the extent of correlation for the 10-g samples, scatter diagrams were developed between the INAA elemental data and percent bitumen values obtained from Soxhlet extractions. The r-values obtained for the seventeen elements determined in the analytical schemes used are presented in Table 6.9. In addition, scatter plots for some of the elements (Cr and Fe) are shown in Figure 6.13.

From these results it is seen that most of the longer-lived isotopes show strong negative correlations, with values ranging from -0.90 to -0.97. Chromium, scandium, and cesium show the highest correlation, while zinc, iron and hafnium give r-values between -0.85 and -0.87. Arsenic has the poorest correlation with bitumen content, with an r-value of -0.73.

Correlations were also calculated for elemental concentrations measurable via their short-lived isotopes for the thirty-gram samples and the results compared with those from the half- and ten-gram samples. This comparison is shown in Table 6.10. It can be seen from the table that, in general, r-values among the three weights do not differ much. In some cases there is a slight improvement in correlation with increasing test portion. For all the elements measured except vanadium the plots have a negative slope over the range of weight-percent bitumen studied.

Scatter plots for vanadium for both the half and ten-gram test portions, shown in Fig. 6.14, follow a different trend from those of the other elements in that they slope downward initially, then level off at bitumen concentrations above approximately 8%. This indicates that in oil-rich samples containing more than 8% bitumen the vanadium concentrations are independent of grade of oil sand.

<u>% bitumen vs.</u>	<u>r-value</u>
Chromium (Cr)	-0.97
Scandium (Sc)	-0.97
Cesium (Cs)	-0.96
Neodymium (Nd)	-0.95
Terbium (Tb)	-0.95
Rubidium (Rb)	-0.95
Ytterbium (Yb)	-0.95
Thorium (Th)	-0.95
Lutetium (Lu)	-0.95
Lanthanum (La)	-0.95
Tantalum (Ta)	-0.93
Cerium (Ce)	-0.93
Tungsten (W)	-0.92
Zinc (Zn)	-0.87
Iron (Fe)	-0.85
Hafnium (Hf)	-0.85
Arsenic (As)	-0.73

Table 6.9. Correlation of concentrations of long-lived elements in oil sand with weight percent bitumen : r-values are for nine *ca.* 10-g test portions.

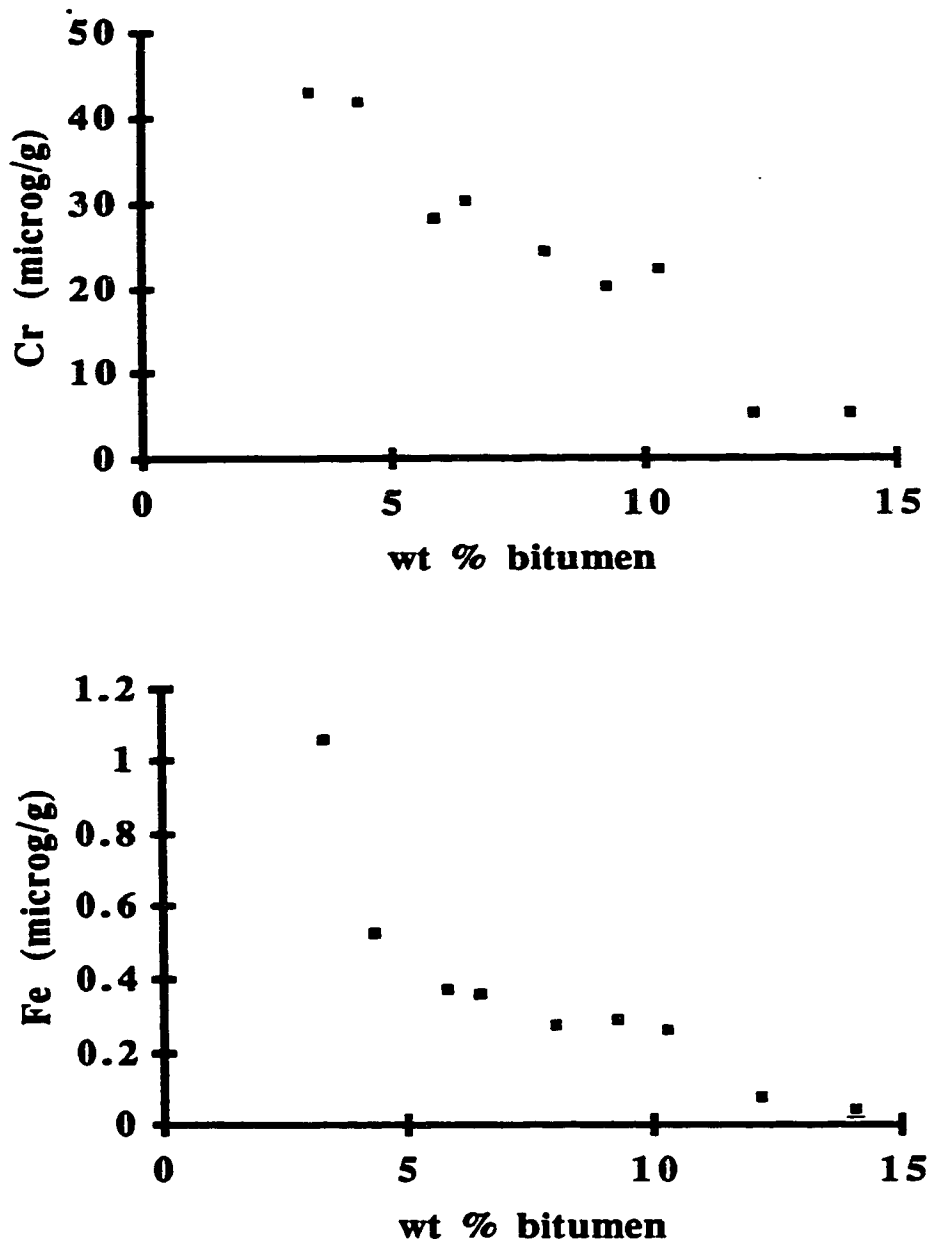


Figure 6.13. Correlation scatter plots of chromium (Cr) and iron (Fe) concentrations versus bitumen content for *ca.* ten gram test portions of oil sand; (r-values are Cr: -0.97 and Fe: -0.85).

<i>Elements</i>	<u>r (0.5 g)</u>	<u>r (10 g)</u>	<u>r (30 g)</u>
Aluminum	0.87	0.97	0.95
Barium	0.90	0.88	0.93
Dysprosium	0.91	0.94	0.94
Europium	0.93	0.91	0.96
Manganese	0.74	0.70	0.72
Potassium	0.91	0.95	0.96
Sodium	0.90	0.93	0.93
Titanium	0.94	0.96	0.89

Table 6.10. Comparison of correlations of concentrations of short-lived elements with respect to bitumen for 0.5, 10, and 30-gram test portions of oil sand (n = 9).

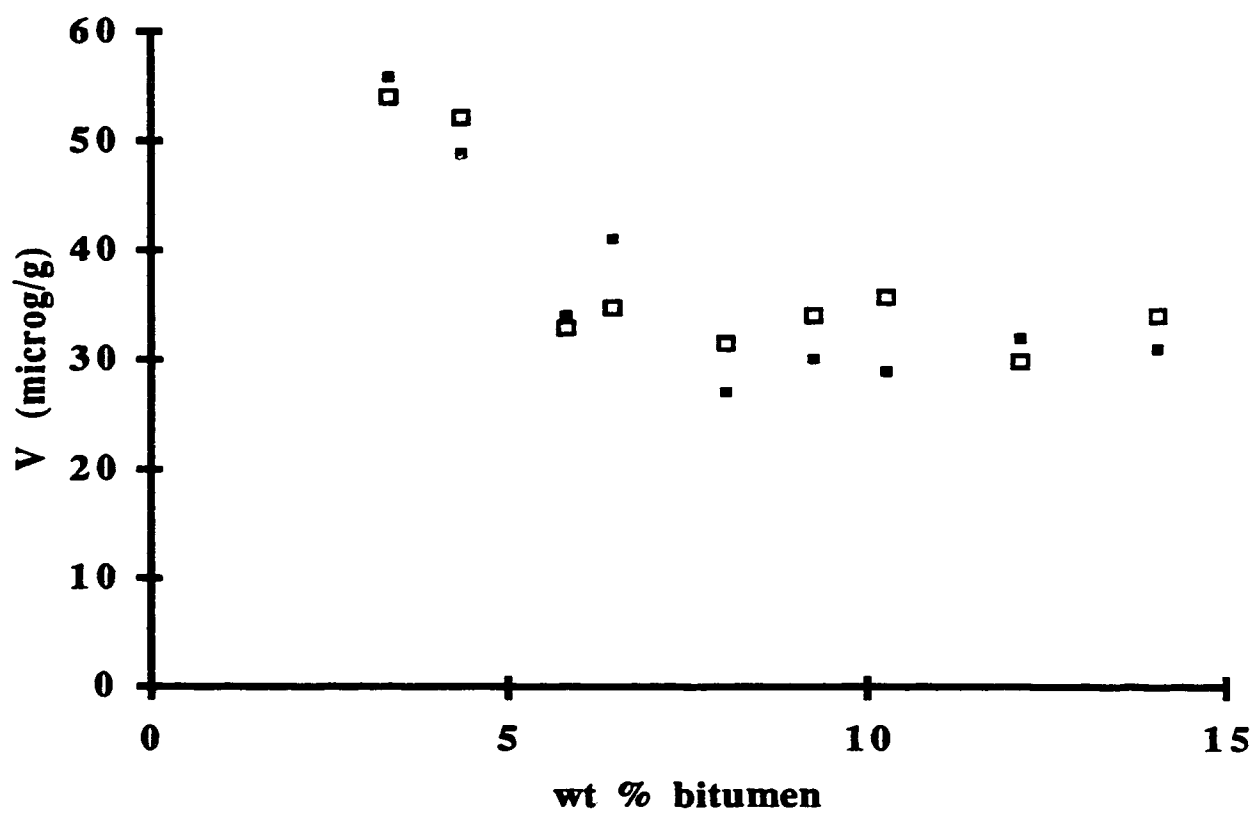


Figure 6.14. Relationship between vanadium concentrations and bitumen content for half and ten gram test portions of oil sand. (Open squares: 0.5g, dark squares: 10g).

Chapter 7

Estimation of Trace Elements in Oil Sand Bitumen by INAA

Introduction

The focus of part two of the thesis is to determine the extent of correlation between those elements in oil sand determinable by INAA and the bitumen and fines (particles less than 44 μ m). To do this, oil sand samples representing the range of bitumen values were taken from the core and analyzed for trace elements.

Accurate analysis of trace elements in oil sands and crudes has received continuing attention over the years because of the importance of trace element data in understanding the geochemistry of oil sands and the role non-hydrocarbon components play in the elucidation of mechanisms of migration and origin of oil [78-89].

Vanadium and nickel along with iron, are the most abundant trace metals in oil sands [78-80,83,84,92-94]. Vanadium and nickel have been the particular focus of research because of the problems they present in the petroleum industry [83-89]. Vanadium is surface-active[90], corrosive[91], and a catalyst poison[78-87]. Because of its catalytic poisoning effect, vanadium severely limits the life of the catalysts if not removed from heavy residues before catalytic cracking of crudes. Hence knowledge of the chemical composition of vanadium complexes in petroleum is useful in the design of efficient demetallation processes. In recent years the presence of vanadium in fuels has been of concern to environmentalists evaluating emissions from oil industries [87]. This is because the industrial combustion of fuels and the resultant emission of vanadium oxides into the

atmosphere contributes to harmful physiological effects such as lung disease [83]. The study of the short-lived trace elements is described in section 7.2.

It was also of interest to analyze the bitumen samples collected in this study for some trace long-lived elements of geochemical importance such as iron, nickel and chromium. The abundances and nature of such trace elements, particularly nickel, is important to the refining and processing of crude petroleum as they tend to affect adversely catalysts used in the cracking process[78-87]. They may also accompany the hydrocarbon through the refining processes leading to undesirable properties in the finished products[86,87]. In addition to the short-lived ones, traces of some of the long-lived elements in crudes also help to provide clues to the origin or migration/maturation of the oil [78-89]. Therefore a short study was also made of those elements which could be determined by INAA via measurement of their long-lived isotopes. This study is reported in section 7.3 of this chapter.

7.1. Evaluation of Lateral Heterogeneity in Oil Sand Core

Collection of additional samples from regions adjacent to those used in the previous NIR study made it important to assess the extent to which the heterogeneity of oil sand affected the distribution of elements laterally across the core. Hence, this study was designed to evaluate the level of lateral heterogeneity of oil sand in terms of a selected suite of elements. The results of this work should indicate the extent to which information from one sample is representative of the cross-section of core from which it was taken.

7.1.1. Preparation of samples and experimental conditions

Nine lateral zones in the core described in Chapter 2 were identified that represent a range of bitumen levels. Four subsamples of approximately 10 g were collected at random from each zone. These samples were collected with a scoop from four different regions within each strip across the core, weighed into 7-mL acid-washed irradiation vials, and sealed as described in Chapter 6. They were then analyzed by INAA for short-lived isotopes for an irradiation time of 3 minutes at a reduced thermal flux of $1 \times 10^{10} \text{ n cm}^{-2} \text{ s}^{-1}$, followed by a decay time of 15 minutes and a count time of 5 minutes. The analytical conditions were as described in Chapter 6 for the analysis of short-lived isotopes.

Upon completion of the above analyses the samples were allowed to decay for a week. After this time they no longer produced radiation significantly above background and could be handled in the laboratory without concern as to presenting a radiation hazard. The decayed samples were next analyzed for bitumen and solids by the Soxhlet method. To do this the irradiation vials were opened, test portions of 2.5 to 5 g weighed into Soxhlet extraction thimbles, and the oil sand extracted with toluene as described in Chapter 2.

7.1.2. Results and discussion

The raw data for relative standard deviation results (RSD) of the INAA analyses are shown in the Appendix on page 242. Figure 7.1 illustrates the relative standard deviations of the selected elements determined for a set of four subsamples within each of the nine transverse sections studied. It can be seen that for all test portions from the nine regions, the relative standard deviations (RSD's) of the values for vanadium are less than 10%, those for dysprosium, barium, titanium and aluminum are less than 17%, and those for potassium,

samarium and europium are less than 20%. Also, except for one value for manganese of 26% and one for sodium of 27%, the RSD's for these two elements are also less than 20%. On the other hand, chlorine shows significantly greater scatter, with RSD's ranging from 10 to 60%. Since the majority of RSD values are under 20%, with the exception of chlorine, we conclude that 10-gram test portions provide about the same precision in estimation of element distribution for all nine transverse sections of the core. As would be expected from earlier work reported in Chapter 6, vanadium showed the least variability across the core.

Results of the Soxhlet extraction analyses for bitumen and solids, shown in Table 7.1, yielded RSD values ranging from 1 to 6% for bitumen and less than 2% for solids as shown in Table 7.2. These values also showed little lateral variability across the core for the nine zones studied, and indicate that a single 10-g sample adequately represents the cross-sectional area of the core in terms of bitumen and solids distribution.

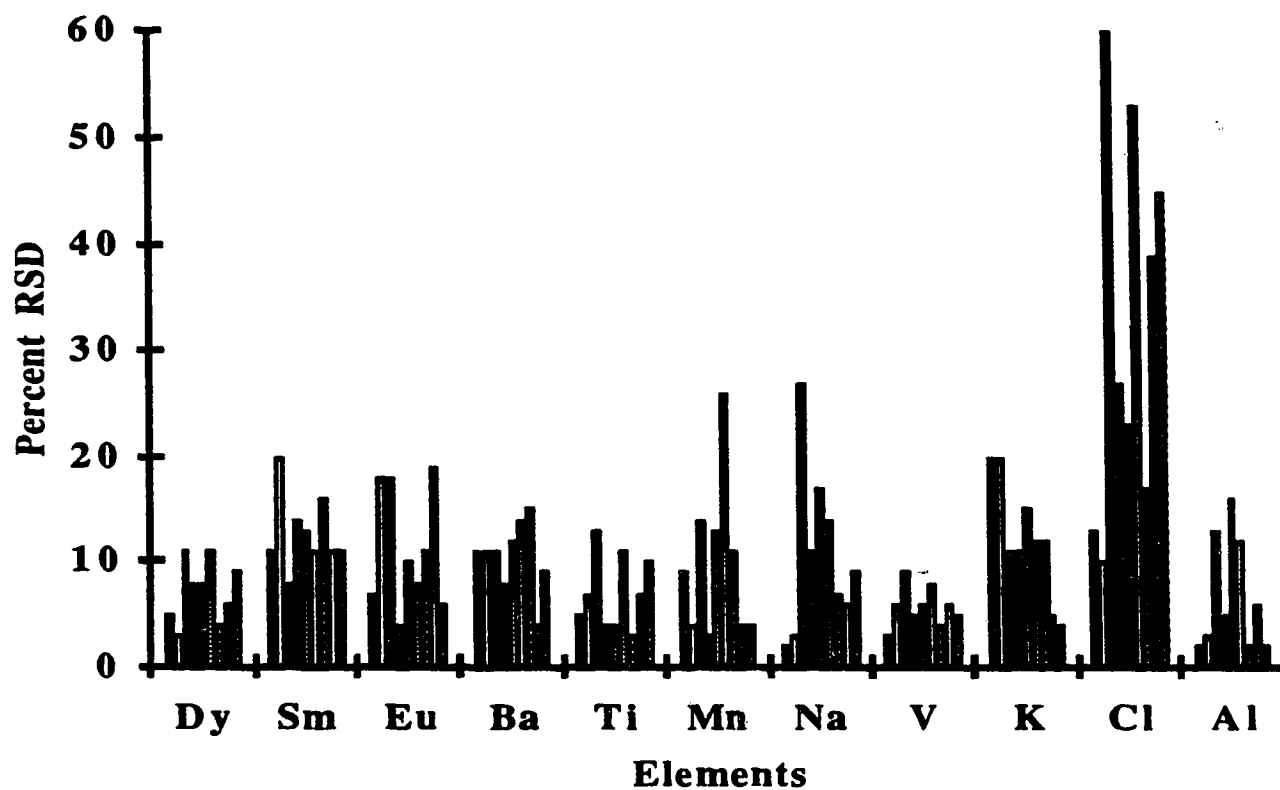


Figure 7.1. RSD's of concentrations of eleven elements over nine transverse sections of oil sand core. (Each bar represents the percent RSD value for a set of four subsamples within a single transverse section).

<u>Transverse sections</u>	<u>Wt % bitumen</u>	<u>Wt % solids</u>
1	4.0	95.6
	3.9	96.1
	4.2	95.8
	4.3	95.6
2	4.5	95.2
	4.8	95.0
	5.0	94.8
	5.1	94.5
3	5.2	92.6
	5.3	93.8
	5.9	93.6
	5.2	95.4
4	4.7	95.0
	4.4	95.0
	4.9	94.2
	4.5	94.4
5	9.3	90.8
	8.9	91.2
	9.6	90.3
	9.4	90.5
6	11.5	88.5
	11.4	88.6
	11.5	88.3
	11.1	88.7
7	10.1	89.7
	9.5	89.4
	9.9	90.0
	10.1	89.6
8	14.2	83.2
	14.8	83.3
	13.8	85.9
	14.0	85.9
9	14.8	85.0
	14.8	85.0
	14.5	85.6
	15.1	84.9

Table 7.1. Weight percent bitumen and solids determined by Soxhlet extraction technique for nine transverse sections of oil sand core.

<u>Transverse sections</u>	<u>% RSD for bitumen</u>	<u>% RSD for solids</u>
1	4.6	0.3
2	5.3	0.3
3	5.8	1.2
4	5.0	0.4
5	3.5	0.5
6	1.5	0.2
7	2.9	0.3
8	3.1	1.8
9	1.7	0.4

Table 7.2. Relative standard deviations of weight percent bitumen and solids of nine transverse sections of oil sand core determined by Soxhlet extraction method, (each value is the % RSD of four subsamples within a transverse section).

7.2. Determination of Trace Short-lived Elements present in Bitumen

This study was designed to determine the level of contamination of extracted bitumen by very small particulates (probably of colloidal dimensions), which may stay suspended in bitumen after microextraction of oil sands by the procedure used here. To estimate this fines content, elemental indicators such as aluminum and manganese were the most useful, and for the bitumen, vanadium was chosen. The results of this study also furnish geochemical information about the extent to which the elements present are associated with the inorganic particulates or organic portions of the bitumen:

7.2.1. Sample preparation for filtration

Several bitumen extracts from the Soxhlet extraction were selected arbitrarily for this study. These samples were selected from both the lean and rich grade regions. Those samples coded 3, 6, 10, 14 in the tables and figures were from the lean zones and those numbered 18, 27, 33, 35 from the oil-rich zones. Approximately 10 mL toluene was added to each portion of bitumen to replace the toluene that had been previously allowed to evaporate away. For each sample, enough of the toluene solution was pipetted to fill a preweighed acid-washed 1.5-mL irradiation vial, the toluene allowed to evaporate, and the vial reweighed to obtain the net weight of untreated bitumen.

The remaining portion of each toluene solution of bitumen was filtered through a 3-cm diameter 0.45-micron Nylon 66 membrane filter using a Millipore filtration apparatus. Each filter paper, which retained all material greater than 0.45 micron, was allowed to air dry for fifteen minutes, then was folded and placed in an acid-washed 1.5-mL irradiation vial for analysis by INAA. The filtrate from each sample was collected in an acid-washed test tube

and placed in a water bath at 50 °C to evaporate most of the toluene. A portion of the resulting solution was pipetted into a preweighed 1.5-mL irradiation vial, the residual toluene allowed to evaporate, and the net weight of filtered bitumen determined.

Standards were prepared from NIST SRM 1633A Fly Ash by weighing 39.4 mg of the material (U.S. National Institute of Standards and Technology, Gaithersburg, MD) into a 1.5-mL irradiation vial, adding a small amount of sucrose and mixing by shaking and rotating the vial. This standard was chosen rather than those used earlier because it contains all of the elements in which we were interested. A sucrose diluent was used in order to bring the volume of standard material to the same level as the samples while keeping the amount of the standard small enough that the irradiation did not produce unreasonably high radioactivity.

To ensure the filters did not contain unacceptable amounts of interfering elements such as aluminum, dysprosium or vanadium, several of the filters were analyzed for these elements by INAA. The results show virtually none of the elements of interest in this work to be present in the filter papers; in most cases they were not detected.

The irradiation-decay-count scheme used for the bitumen samples is summarized in Table 7.3. This scheme enabled the quantification of a set of short-lived isotopes, including V, Al, Mn, Ti, Ba, Na, K, Dy, Sm, Eu and the halogens. High count rates, which tend to distort the analytical spectrum through pulse pileup, were encountered for many of these samples. This problem which was avoided in previous analyses by increasing the sample-to-detector distance, could not be circumvented by this procedure for these samples, because the total counts for some elements became too low.

Pulse pileup takes place in the detector and occurs when two gamma ray emissions occur so close together in time that there is high probability that they can combine and give a signal corresponding to only one event. This process, which results in the loss of counts at the desired characteristic energy of the original element, was corrected for by placing a pulser in the detection circuit. Since the number of combined events is independent of spectral location, the pulser signal is generally positioned in a spectral region free from signals of interest. A pulser count was obtained in the absence and presence of a sample and a pulse pile-up correction factor calculated as

$$\text{Correction factor} = \frac{\text{Pulser counts (no sample)}}{\text{Pulser counts (sample)}}$$

All of the peaks in the spectrum were multiplied by this factor to correct for the pulse pile-up effect.

Livetime-Deadtime corrections [66] were also applied on the spectral data for the very short-lived isotopes such as vanadium and aluminum which were counted in the presence of the other relatively long-lived isotopes like dysprosium, samarium, manganese and others. This correction is done via the formula below [66]:

$$A_{\text{corr}} = A_m \times \{CT/LT \times [1 - \exp(-\lambda \times LT)] / [1 - \exp(-\lambda \times CT)]\}$$

where CT is the clocktime i.e. the actual time the sample was counted, LT is the livetime, which is the exact preset value of counting time, λ is the decay constant of that particular isotope and A_m is the uncorrected counts of the isotope and A_{corr} is the corrected counts.

	<u>Filter Paper</u>	<u>Unfiltered Bitumen</u>	<u>Filtered Bitumen</u>
<u>Flux</u>	1.00×10^{12}	1.00×10^{12}	1.00×10^{12}
<u>Irradiation Time</u>	180 s	300 s	300 s
<u>Decay Time</u>	variable	variable	variable
<u>Count Time</u>	180 s (~480s decay) Al, V, Ti	90 s (120 to 480s decay) Al, V	90 s (120 to 480s decay) Al, V
	300 s (~1 hr. decay) other elements	300 s (~25 min. decay) other elements	300 s (~25 min. decay.) other elements
<u>Geometry</u> (sample-to-detector)	1 cm	12 cm (90 s count)	12 cm (90 s count)
		1 cm (300 s count)	1 cm (300 s count)

Table 7.3. Irradiation-Decay-Count scheme used for analysis of bitumen samples and filter paper.

7.2.2. Sample Preparation for Centrifugation

Two approximately 30-g portions of oil sand were taken from the core, one from an area rich, and the other from an area lean, in bitumen. Each portion was homogenized manually by grinding in a mortar for several minutes. Following homogenization, five approximately 3.8-g subsamples of each grade were extracted with toluene by the Soxhlet procedure described in Chapter 2 to separate the bitumen from the solids. Approximately 1-mL portions of the toluene extract were pipetted into preweighed 1.5-mL irradiation vials, the toluene evaporated, and the residue analyzed by INAA as before. The remaining bitumen extract was centrifuged at 3000 rpm in a desk top centrifuge for 45 minutes to remove as much of the particulate material as possible. After centrifugation a portion of the bitumen extract was drawn with a Pasteur pipet from the top of each centrifuge tube and placed into a preweighed 1.5-mL irradiation vial for analysis. The remaining bitumen extract in each centrifuge tube was decanted off and the residual toluene allowed to evaporate, leaving any suspended solids behind. These suspended solids, which were presumed to consist mostly of clays, were weighed to obtain the amount of clay present in the original bitumen extracts. For the oil-rich samples, the weights of clays were of the order of 1 mg while the lean samples had about 5 mg of clays. Both the untreated and centrifuged samples were then analyzed for short lived isotopes by INAA, using the scheme outlined in Table 7.3.

7.2.3. Results and discussion

Because the suite of elements found in bitumen by INAA analysis of the Soxhlet extract would not be expected to be components of bitumen, it was suggested by Dr. John Duke of SLOWPOKE Reactor Facility that non-bitumen particulate material smaller than the pore size of the thimbles may have passed

through the thimbles used for the Soxhlet extraction. Therefore an experiment was designed to determine the level of contamination of bitumen by these extremely small particles of material, considered to most likely be clays. The elements aluminum and manganese were selected for use as indicators of the presence of clays, and vanadium as an indicator of bitumen, because these elements fit well into the INAA analytical scheme as well as into the known composition of clays and of bitumen; also, these elements were known to be present in the extracted bitumen fraction.

Table 7.4 gives the concentrations of vanadium, aluminum and manganese found by INAA in the filtered and unfiltered bitumen. The data show that the concentrations of vanadium in the two fractions (i.e. filtered and unfiltered) are not significantly different. This result, which is also shown in graphical form in Fig. 7.2, indicates that most of the vanadium is present in the bitumen in the form of toluene-soluble species. This is consistent with earlier findings that vanadium is bound in the bitumen phase [94-103].

On the other hand, filtration reduced the aluminum concentrations in bitumen to less than 1% of that in the unfiltered samples. This result indicates that upon filtration the removed solids carry with them practically all of the aluminum. Assuming the aluminum to be associated primarily with the clay fraction of the oil sand, filtration through a 0.45 micron filter renders the bitumen virtually free of clays. Support of this assumption is also provided by the observation that even though only small amounts of aluminum are left after filtration, we see from Table 7.4 and Fig. 7.3 that relatively, the lean grade samples tend to retain greater concentrations of aluminum after filtration than the rich grade samples. This is so because lean grade samples usually have more clay than the oil rich samples to start with, so it will be expected that for identical filtration conditions more clay will remain with the lean samples.

<u>ID</u>	<u>Vanadium ($\mu\text{g/g}$)</u>	
	<u>Unfiltered</u>	<u>Filtered</u>
3	188	181
6	169	170
10	198	192
14	191	176
18	239	192
27	196	218
33	248	232
35	263	206

<u>ID</u>	<u>Aluminum ($\mu\text{g/g}$)</u>	
	<u>Unfiltered</u>	<u>Filtered</u>
3	8085	105
6	15697	93
10	11942	94
14	13287	67
18	10797	26
27	34434	33
33	4231	28
35	4506	24

<u>ID</u>	<u>Manganese ($\mu\text{g/g}$)</u>	
	<u>Unfiltered</u>	<u>Filtered</u>
3	52.4	1.47
6	38.2	0.38
10	27.6	0.72
14	37.8	0.95
18	33.6	0.5
27	153.6	1.14
33	6.3	0.31
35	6	0.17

Table 7.4. Concentrations, in micrograms per gram, of vanadium, aluminum and manganese in unfiltered and filtered bitumen from Soxhlet extractions; (lean grade: 3, 6, 10, 14 and rich grade: 18, 27, 33, 35).

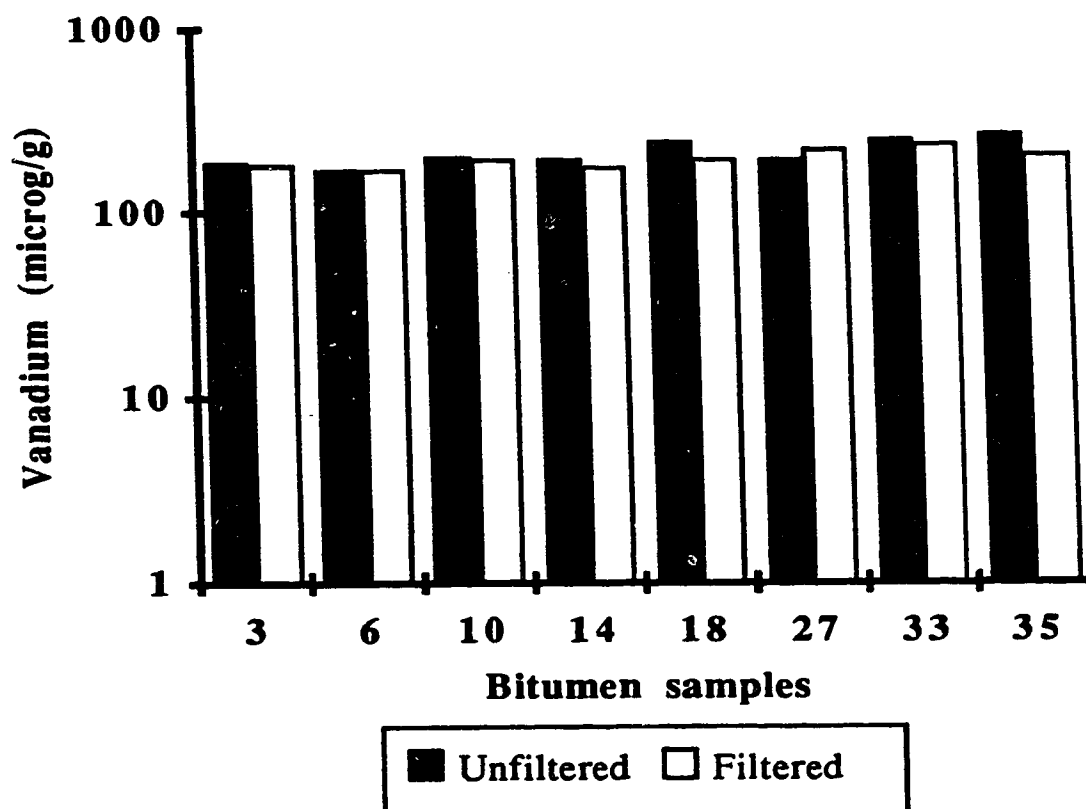


Figure 7.2. Vanadium concentrations, in micrograms per gram, in unfiltered and filtered bitumen samples. (Vertical axis is the log scale of actual concentrations obtained).

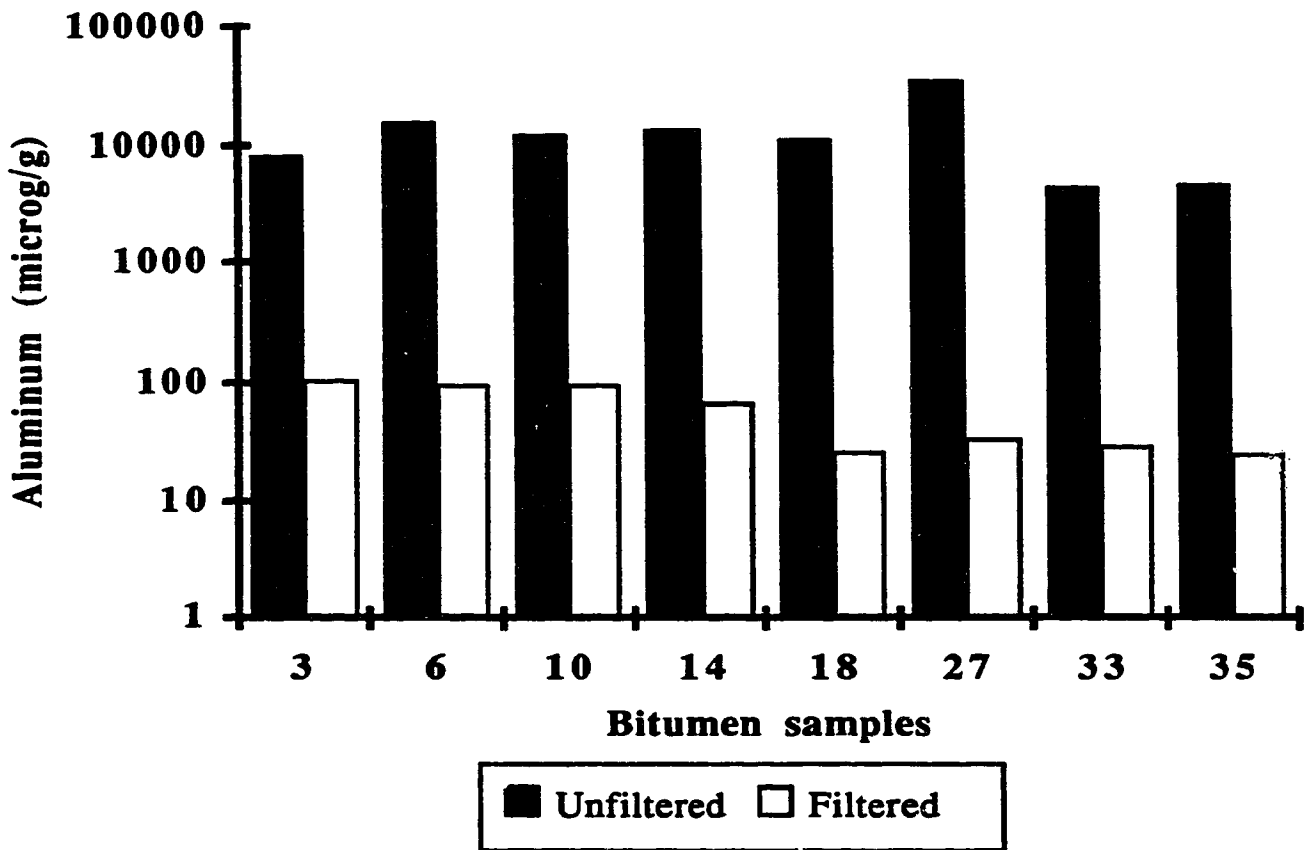


Figure 7.3. Aluminum concentrations, in micrograms per gram, in unfiltered and filtered bitumen samples. (Vertical axis is the log scale of actual concentrations obtained).

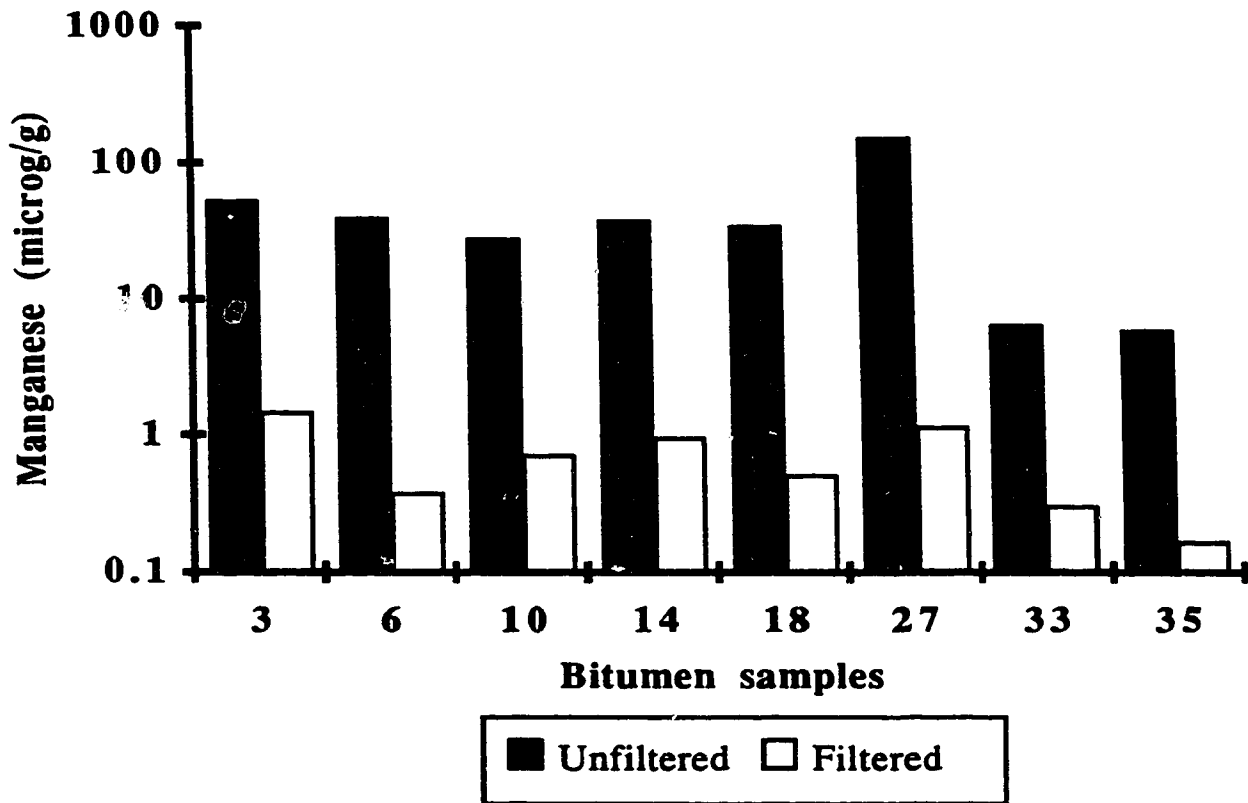


Figure 7.4. Manganese concentrations, in micrograms per gram, in unfiltered and filtered bitumen samples. (Vertical axis is the log scale of actual concentrations obtained).

The manganese data show a trend similar to that observed for aluminum, that is, manganese concentrations in filtered samples are less than 3% of the values seen for the unfiltered. Manganese is therefore also largely associated with filterable suspended material in the bitumen.

Halogen concentrations in the bitumen samples are tabulated in Table 7.5. Chlorine concentrations in all but one of the filtered bitumen samples are below the lowest value found in the unfiltered samples, although the difference is not large. This suggests that chlorine is associated with both bitumen and solids. It is known that adsorbed water is present on the surfaces of clays in oil sands, and that this water contains some dissolved chlorine compounds [57]. It is therefore possible that filtration removes this water along with the dissolved chlorides. Bromine concentrations in unfiltered and filtered samples are low but comparable. The same holds for iodine. This suggests that bromine and iodine may occur as components of the bitumen, possibly associated with water that will form a micro emulsion with toluene[104]. From Table 7.6 it can be observed that the ranges for chlorine in the filtered and unfiltered samples after being normalized relative to iodine (Cl/I) are similar among the set, whilst for chlorine normalized with bromine (Cl/Br) the ranges tend to differ. This makes it more likely that iodine is present in bitumen instead of the clays, and that bromine may be more associated with the particulate clay fraction.

It should be noticed that the study in this section does not invalidate the results obtained earlier in Chapter 6. The particulates being discussed here in Chapter 7 are those very small particles which most probably stay as colloidal suspensions in the bitumen. These constitute less than 1% of the weight of bitumen present in oil sand samples, hence their contribution to the weight of bitumen is so small that it does not affect significantly the weight % bitumen values from the Soxhlet extractions.

<u>Unfiltered ($\mu\text{g/g}$)</u>			
<u>ID</u>	<u>Cl</u>	<u>Br</u>	<u>I</u>
3	202	8	13
6	252	7	16
10	219	2	25
14	288	9	19
18	199	4	9
35	284	5	12
Range	199 to 288	2 to 9	9 to 25
<u>Filtered ($\mu\text{g/g}$)</u>			
<u>ID</u>	<u>Cl</u>	<u>Br</u>	<u>I</u>
3	128	5	11
6	157	6	16
10	212	9	25
14	177	6	16
18	91	2	7
35	133	3	8
Range	91 to 212	2 to 9	7 to 25

Table 7.5. Concentrations of halogens ($\mu\text{g/g}$) in filtered and unfiltered bitumen, as determined by INAA.

<u>Unfiltered</u>			
<u>ID</u>	<u>Cl/Br</u>	<u>Cl/I</u>	<u>I/Br</u>
3	25	15	2
6	35	16	2
10	110	9	12
14	31	15	2
18	53	22	2.5
35	62	24	2.6
Range	25 to 110	9 to 24	2 to 12
<u>Filtered</u>			
<u>ID</u>	<u>Cl/Br</u>	<u>Cl/I</u>	<u>I/Br</u>
3	28	11	2.5
6	27	10	2.7
10	24	8	2.9
14	31	11	2.9
18	40	14	2.9
35	44	16	2.8
Range	24 to 44	8 to 16	2.5 to 2.9

Table 7.6. Ratios of concentrations of chlorine, bromine and iodine in filtered and unfiltered samples of bitumen.

The above observations can be rationalized using the so-called Goldschmidt rules [105]. Clays are mostly hydrous aluminosilicates which have displaceable hydroxide groups. The substitution or replacement of these hydroxide groups by other ions depends on the similarity of ionic charge and ionic radii of the replacing ions. Since the halides have the same charge as the hydroxide ion, substitution is determined by the similarity of the ionic radii to that of the hydroxide ion. On this basis Cl^- is able to substitute most readily for hydroxide groups on clays because its ionic radius is closest to that of OH^- , while substitution becomes increasingly difficult for the larger bromide and iodide ions. This could explain why chlorine associates more strongly with clays, and why the concentrations of this element decrease in the filtered samples to the greatest extent while the bromine and iodine levels do not change very much. An alternative explanation could be considered on the basis of oil sand structure. The water layer i.e. formation water surrounding the sand particles is high in alkali metals and halogens especially chlorine. Thus during extraction these halogens will distribute between the oil and solid phases. From the results obtained in this work it seems that these halogens distribute between the two phases to differing extents. Hardly any bromine or iodine stays in the solid phase but for chlorine quite a reasonable fraction enters the solid phase which are easily removed during filtration accounting for the greater decrease in chlorine concentrations as compared to the other two halogens.

Table 7.7 gives the concentrations of vanadium and aluminum found in the untreated and centrifuged samples. We see that vanadium concentrations in the untreated and centrifuged samples for both the rich-and lean grades of oil sand are not statistically different. This again is consistent with the finding that vanadium is present primarily in the bitumen and not in the clays. As might be

expected, sampling precision for vanadium in both rich and lean samples is very high because of the homogeneity of oil sand for this element.

The aluminum data show the centrifuged samples to have considerably lower concentrations of this element in the bitumen fraction compared to the untreated samples. This indicates that centrifuging of the samples removes some aluminum-bearing clay material from the bitumen, resulting in lower aluminum concentrations in the supernate.

Also, it can be seen that aluminum concentrations in the untreated rich-grade samples are about five times smaller than those of the lean grade samples. This is as expected because lean grade bitumen is known to contain more clay than rich-grade material. On comparing the aluminum data for the filtered and centrifuged samples in Tables 7.4 and 7.7, we notice that filtration removed essentially all the aluminum, whilst centrifugation produced only a factor of five reduction. Even with the lean grade samples as much as two to seven thousand $\mu\text{g/g}$ of aluminum remained after centrifugation, as against about one hundred $\mu\text{g/g}$ with filtration. It seems that the centrifugation process used in this study removed only the larger clay particles, leaving the smaller ones still suspended in the bitumen. Filtration is therefore much more effective in removing very fine particulate material for the purpose of this work than centrifugation with a bench top centrifuge. Use of a high speed ultracentrifuge could likely provide a high degree of removal, but this was not explored further since such a process tends to remove the larger molecular weight fractions of asphaltenes.

<u>Rich grade oil sand</u>			
225	241	678	3960
203	228	618	4259
201	237	465	4479
212	221	468	2603
212	220	449	3626
Centrifuged	Untreated	Centrifuged	Untreated
Vanadium ($\mu\text{g/g}$)		Aluminum ($\mu\text{g/g}$)	
<u>Lean grade</u>			
151	169	5516	15058
156	170	2162	14131
135	161	2364	17394
152	162	4098	22025
154	165	2424	16906
Centrifuged	Untreated	Centrifuged	Untreated
Vanadium ($\mu\text{g/g}$)		Aluminum ($\mu\text{g/g}$)	

Table 7.7. Comparison of concentrations of vanadium and aluminum found by INAA in untreated and centrifuged bitumen.

7.3. Determination of Trace Long-lived Elements present in Bitumen.

7.3.1. Experimental procedure

The filtered and unfiltered bitumen samples used for the INAA analyses described in section 7.2 were used for this study. The irradiation vials, which still contained the samples, were recapped and irradiated for two hours at a neutron flux of $1 \times 10^{12} \text{ n cm}^{-2} \text{ s}^{-1}$. After allowing them to decay for six days, they were counted for 20,000 seconds at a sample-to-detector distance of 1 cm. A second count was taken after twenty-one days for 80,000 seconds at the same counting geometry. This scheme provided data for a range of geochemically-important elements including nickel, cobalt, iron and chromium.

7.3.2. Results and discussion

The results obtained for the elements that could be measured via their long-lived isotopes by the scheme used is shown in the Appendix (page 243). Figure 7.5 illustrates the values found for nickel. It is clear that concentrations of nickel in the unfiltered and filtered bitumen are not significantly different for the eight samples studied. Thus filtration did not affect the levels of nickel in bitumen, indicating that hardly any nickel is associated with the particulate suspended material. This observation is consistent with the prior knowledge that nickel is also present in the bitumen [94-103]. It has been found that less than ten micrograms per gram of nickel is present as metalloporphyrins in bitumen so most of the nickel may probably be present as naphthenates or other non-porphyrin species [104]. It can also be seen from the table that mercury behaves similarly to nickel. The concentrations of mercury before and after filtration are not significantly different, indicating that any mercury

present is largely associated with the bitumen, most probably as elemental mercury chemically complexed with the asphaltene sheets of bitumen [104].

On the other hand, there is a substantial decrease in the concentrations of the other elements after filtration. Consequently, it can be concluded that these elements are predominantly associated with the particulates in the bitumen. Figure 7.6 illustrates this behavior for iron and chromium.

In summary, with the exception of nickel and mercury, all the elements measured via their long-lived isotopes tend, as expected, to be largely associated with the clay particulate material. As mentioned earlier, nickel and vanadium are well known to occur partly as porphyrin chelates in the bitumen fraction of oil sands, but the form in which the mercury is present in the bitumen is not so well known or understood. It may exist as an elemental mercury [104].

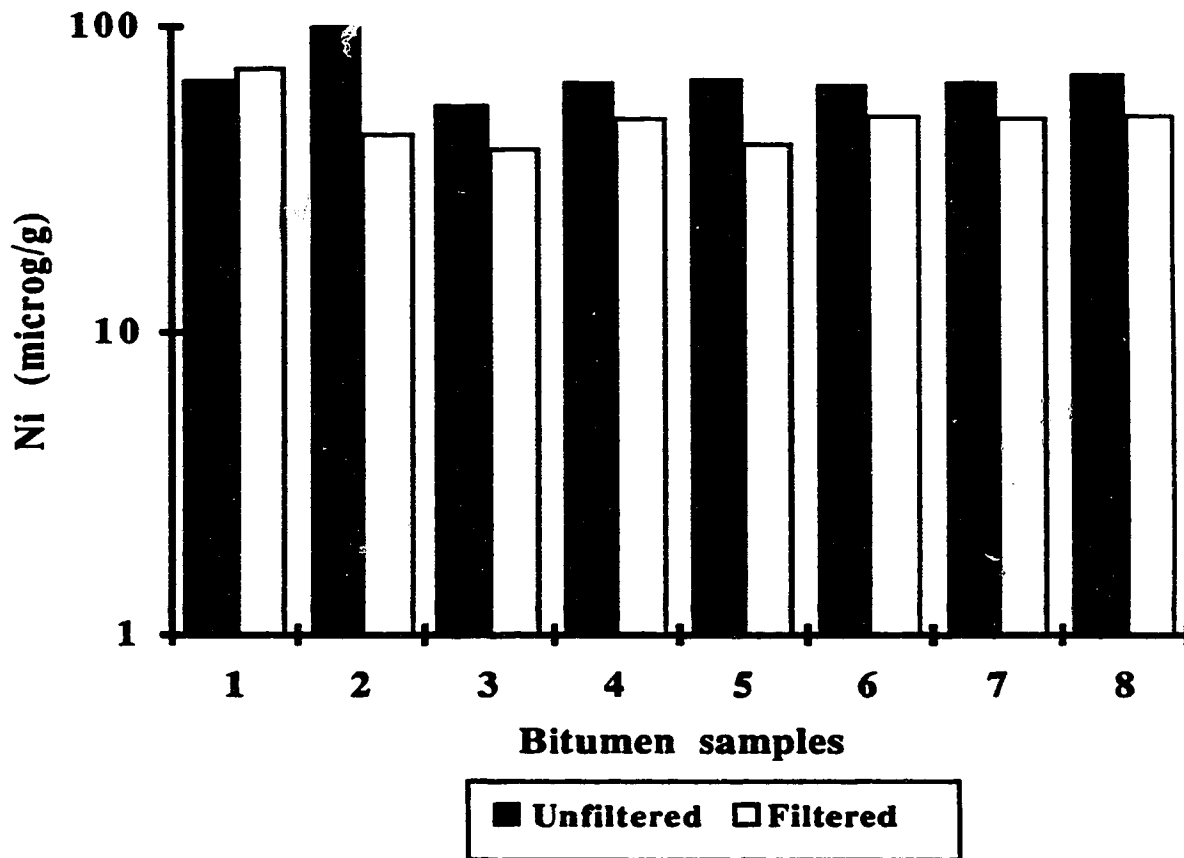


Figure 7.5. Nickel concentrations, in micrograms per gram, in unfiltered and filtered bitumen. (Vertical axis is the log scale of actual concentrations obtained).

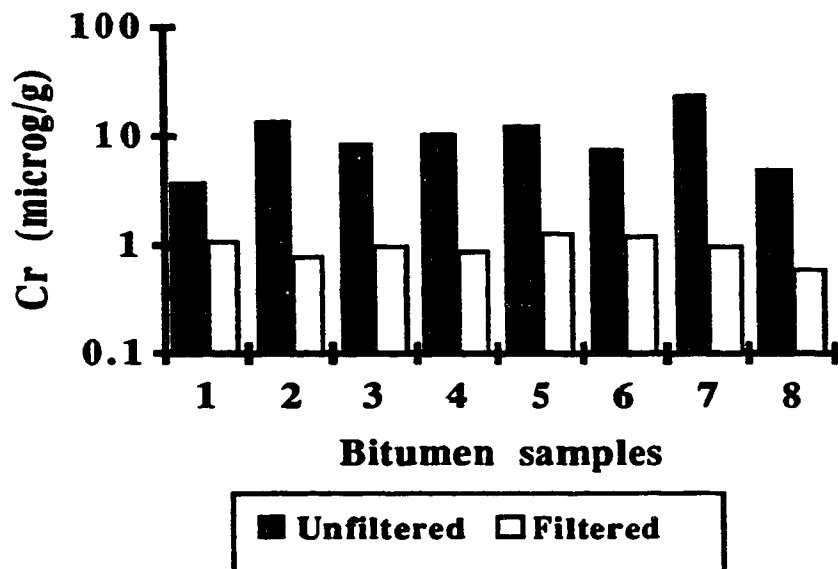
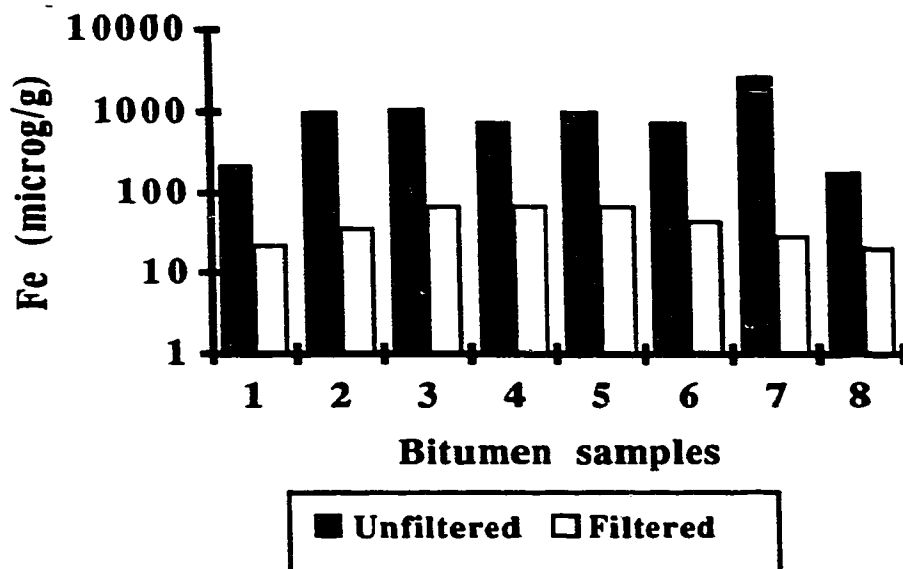


Figure 7.6. Concentrations of iron and chromium, in micrograms per gram, in unfiltered and filtered bitumen; top:iron; bottom:chromium. (Vertical axis is the log scale of actual concentrations obtained).

Chapter 8

Summary and Future Directions in the Characterization of Athabasca Oil Sand by Instrumental Neutron Activation Analysis

8.1. Conclusions and Summary for INAA research

In this research the application of Instrumental Neutron Activation Analysis (INAA) as an alternative technique to the Dean-Stark method for determining the bitumen and solids in oil sand has been extensively explored. The results show that INAA can be successfully used to relate the distribution of elements to the bitumen and solids content of oil sand, with minimal difficulties. This promising alternative offers the advantage of fast turnaround times, since quantification is possible via a set of short-lived isotopes, and is amenable to automation, thus cutting down on human power and time.

The crux of this research has dealt extensively with correlations of elements or groups of elements to the oil sand components on a microscopic scale using analytical test portions of a half gram. Even with subsamples this small, potentially useful correlations were obtained which can provide knowledge on the bitumen and solids content of oil sands. This could be done by building a model from a set of samples covering a wide range of bitumen content. The element concentrations from INAA for these calibration samples are correlated with known bitumen or fines content. Unknown samples could then be analyzed by INAA for their elemental concentrations and by way of the model, the bitumen content could be estimated. A similar model could also be developed for measurement of particles of solids (fines) whereby a model could be built from elemental data of say dysprosium or a combination of dysprosium, europium and samarium with varying particle sizes of the solids or fines.

These correlations also offer insight into the geochemical relationships between the major and trace elements present in oil sands. For instance, the strong positive correlations that were found among the lanthanides in this work are similar to those found in other geological matrices such as shales. This suggests that the lanthanides do not behave differently in oil sands relative to their behavior in other geological systems, and lends support to the belief that they bear similar chemistry and are largely associated with the same matrix as the clay minerals. Most of the other elements in oil sand, with the exception of vanadium and chlorine, were found to have reasonably good correlations of decreasing slope with the bitumen content.

The oil sand regions with high bitumen content tend to have lesser amounts of those elements commonly associated with clay minerals, as shown by the negative correlation of the fines with bitumen content. As a consequence, the correlations with bitumen have negative slopes, indicating that most of these elements are largely associated with the particulate solids. The positive correlations of these same elements with respect to fines content also support this observation. Of all the elements correlated to the fines the lanthanides, notably dysprosium, samarium and europium, tend to have the best correlations and therefore could be used as the most suitable indicators of the clay. Some of the elements measured via their long-lived isotopes, such as chromium, also yielded strong negative correlations to bitumen content, indicating their association with the solids.

Chlorine was found to have no correlation with either the bitumen or fines content. This random distribution of chlorine in the oil sand may partly be due to the variable amounts of chlorine found dissolved in pockets of water trapped within the interstices of the sand particles [57]. The correlation of vanadium with bitumen content was also unique in that it levelled off above eight percent bitumen. This indicates that in the oil-rich samples vanadium tends to concentrate

in the bitumen fraction to similar extents i.e. vanadium concentrations are independent of oil sand grade.

The statistical multivariate technique of Principal Component Analysis was also applied to various combinations of the elements. Our observations indicate that the application of this technique gives improved correlations when combinations of elements which have individually good correlations with bitumen content are used. It was also noticed that the correlations do not necessarily improve with the number of elements, especially if element(s) which correlate poorly are included.

The lateral heterogeneity study using ten-gram test portions showed that the concentrations of most of the elements did not vary significantly across the core. For the majority of the elements studied in the different transverse sections of the core, low relative standard deviation values, typically 10%, of their concentrations were obtained. This indicates that the oil sand is homogenous for most of the elements laterally across the core.

By using a simple process of filtration through membrane filters, it was confirmed that nickel and vanadium present in bitumen are largely associated with the bitumen fraction. This is consistent with the fact that they tend to form bitumen soluble metal-organic complexes. Data on mercury obtained in this research suggest that it may also largely be associated with the bitumen, again most likely as elemental mercury. Other elements which were found after Soxhlet extraction with toluene to be present in the bitumen phase were shown to be present in very small particulates which were easily removed by filtration, indicating that they are probably largely associated with fine clays that had passed through the extraction thimble.

8.2. Suggestions for Future Work

The results of the correlation models found in this research are quite encouraging. Most of the correlations, however, were studied with respect to bitumen. Those which were carried out on solids were on larger particle sizes in the 44 micron range and larger. The results obtained have laid a background for further study of smaller particle size fractions. Thus additional work needs to be pursued in the direction of developing correlation models for various fractions with particle sizes less than 44 microns. To obtain the fines fractions in this work simple hand sieving was used. This works quite well for larger particles but is tedious and inaccurate for particle sizes less than 44 microns. Thus further study is desirable to find a more sophisticated method which could quickly and accurately provide a measure of smaller particle size fractions of the solids and correlate them to INAA elemental data. This would offer direct information on the presence of minute clay particles, which is significant in that they are detrimental to the processing of bitumen from oil sand by the hot water extraction process.

Additional work should also be done on the collection of more elemental data on larger test portions of between ten and thirty grams, as was done for half gram test portions in this study. This will provide confirmation of the preliminary results obtained on larger test portions in this research.

A high degree of variability is usually associated with the bitumen content of low grade oil sand samples, so extensive study is required on the heterogeneity of oil sand zones with less than 8% bitumen content. This study should provide a better understanding of the wider range of scatter found in some zones, and also in turn possibly allow some explanation for the sampling and processing problems associated with low grade oil sand. It also may yield more insight into how large an increase in sampling size and frequency is needed in low grade zones over high grade ones to provide equivalent sampling precision and accuracy.

References

1. Shaw R. C., "Near-Infrared Diffuse Reflectance Analysis of Oil Sand", M.Sc. Thesis, University of Alberta, Edmonton, 1989.
2. Shaw R. C. and Kratochvil B., "Near-Infrared Diffuse Reflectance Analysis of Oil Sand", *Anal. Chem.* 1990, 62, 167-174.
3. Whetsel K. B., "Near-Infrared Spectrophotometry," *Appl. Spectrosc. Rev.* 1968, 2, 1-67.
4. Williams P. C. and Norris K. (Eds.), *Near-Infrared Technology in the Agricultural and Food Industries*, American Association of Cereal Chemists, St. Paul, Minneapolis, 1987.
5. Osborne B. G. and Fearn T., *Near-Infrared Spectroscopy in Food Analysis*; Longman Scientific, Essex, England, 1986.
6. Martin K. A., "Near-Infrared Reflectance Spectroscopy", *Appl. Spectrosc. Rev.* 1992, 27, 325-383.
7. Stark E., Luchter K. and Margoshes M., "Near-Infrared Analysis (NIRA): A Technology for Quantitative and Qualitative Analysis", *Appl. Spectrosc. Rev.* 1986, 22, 335-399.
8. Borman S. A., "Near-Infrared Reflectance Spectrometry: Tip of the Iceberg", *Anal. Chem.* 1984, 56 ,(8), 933A-938A.
9. Burns D.A. and Ciurczak E. W. (Eds.), *Handbook of Near-Infrared Analysis*, Marcel Dekker, Inc., N.Y., 1992.
10. Honigs D. E., Hieftje G. M. and Hirschfeld T., "Number of Samples and Wavelengths Required for the Training Set in Near-Infrared Reflectance Spectroscopy", *Appl. Spectrosc.* 1984, 38, 844-847.

11. Naes T. and Isaksson T., "Selection of Samples for calibration in Near-Infrared Spectroscopy. Part I: General Principles Illustrated by Example," *Ibid.* 1989, 43, 328-335.
12. Isaksson T. and Naes T., "Selection of Samples for Calibration in Near-Infrared Spectroscopy. Part II: Selection based on Spectral Measurements," *Ibid.* 1990, 44, 1152-1158.
13. Wetzel D. L., "Near-Infrared Reflectance Analysis-Sleeper among Spectroscopic Techniques", *Anal. Chem.* 1983, 55, 1165A-1176A.
14. Hirschfeld T., "Sample Area Optimization in a Diffuse Reflectance Near-Infrared Spectrophotometer", *Appl. Spectrosc.* 1985, 39, 1085-1086.
15. Mark H. and Workman J., "Effect of Repack on Calibrations Produced for Near-Infrared Reflectance Analysis", *Anal. Chem.* 1986, 58, 1454-1459.
16. Hall M. N., Robertson A. and Scotter C. N. G., "Near-Infrared Reflectance Prediction of Quality, Theaflavin Content and Moisture Content of Black Tea", *Food Chem.* 1988, 27, 61-75.
17. Drennen J. K., Kraemer E. G. and Lodder R. A., "Advances and Perspectives in Near-Infrared Spectrophotometry", *Crit. Rev. in Anal. Chem.* 1991, 22 (6), 443-475.
18. Stark E., "Calibration Methods for NIRS Analysis". In *Analytical Applications of Spectroscopy*; Creaser C.S. and Davies A. M. C., Eds.; 1988.
19. Martens H. and Naes T. *Multivariate Calibrations*; John Wiley, Chichester, England, 1989.
20. Martens H. and Naes T., "Multivariate Calibrations by Data Compression", Chap. 4 in Ref. 4.

21. Osborne B. G., "Comparative Study of Methods of Linearisation and Scatter Correction in Near-Infrared Reflectance Spectroscopy", *Analyst*, 1988, 113, 263-267.
22. Kubelka P. and Munk F., "Ein Beitrag zur Optik der Farbstreche", *Z. Tech. Phys.*, 1931, 12, 593.
23. Norris K. H. and Williams P. C., "Optimization of mathematical Treatments of Raw Near-Infrared Signal in the Measurement of Protein in Hard Red Spring Wheat. 1. Influence of particle size", *Cereal Chem.* 1984, 61, 158-165.
24. Weyer L. G. "The use of Derivative Nodes in Near-Infrared Spectroscopy", in *Analytical Applications of Spectroscopy* ; Creaser C.S. and Davies A.M.C; Eds., 1988.
25. Geladi P., MacDougall D. and Martens H., "Linearization and Scatter Correction for Near-Infrared Reflectance Spectra of Meat", *Appl. Spectrosc.* 1985 39, 491-500.
26. Beebe K. R. and Kowalski B. R., "An Introduction to Multivariate Calibration and Analysis", *Anal. Chem.* 1987, 59, 1007A-1017A.
27. Manly B. F. J. *Multivariate Statistical Methods; A Primer*; Chapman and Hall, 1986.
28. Thomas E. V. "A Primer on Multivariate Calibration", *Anal. Chem.* 1994, 66, 795A - 805A.
29. Anderson T. W. *An Introduction to Multivariate Statistical Analysis*; John Wiley, N.Y. 1971.
30. Seasholtz M. B. and Kowalski B. R. "The Effect of Mean Centering on Prediction in Multivariate Calibration", *J. Chemometrics*, 1992, 6, 103-111.
31. Seasholtz M. B. and Kowalski B. R. "Recent Developments in Multivariate Calibration", *J. Chemometrics*, 1991, 5, 129-145.

32. Martens H., Karstang T. and Naes T. "Improved Selectivity in Spectroscopy by Multivariate Calibration", *J. Chemometrics*, 1987, 1, 201- 219.
33. Martens H. and Naes T. "Multivariate Calibration. I. Concepts and Distinctions", *Trends in Analytical Chemistry*, 1984, 3, 204-210.
34. Martens H. and Naes T. "Multivariate Calibration. II. Chemometric methods", *Trends in Analytical Chemistry*, 1984, 3, 266-271.
35. Martens H., Wold S. and Naes T. *A Laymans Guide to Multivariate Analysis; In Food Research and Data Analysis*; Martens H. and Russwurm H. Eds. Applied Science Publishers, N.Y. 1983.
36. Mark H., "Chemometrics in Near-Infrared Spectroscopy", *Anal. Chim. Acta*, 1989, 223, 75-93.
37. Mark H. and Workman J., *Statistics in Spectroscopy*, Academic Press, Boston, 1991.
38. Barton F.E., II, "Near-Infrared Reflectance Spectroscopy. Part II. Effect of Calibration Set Selection on Accuracy of Method," *J. Assoc. Off. Anal. Chem.* 1991, 74, 853-856.
39. Mark H., "Studies of Principal Components as a Calibration Method for Near-Infrared Reflectance analysis". *Chim. Oggi.*, 1987, 9, 57-65.
40. Cowe I.A., McNicol J.W. and Cuthbertson D. C., A Designed Experiment for the Examination of Techniques used in the Analysis of Near-Infrared Spectra. Part 2. Derivation and testing of Regression Models", *Analyst*, 1985, 110, 1233-1240.
41. Cowe I.A., McNicol J. W. and Cuthbertson D. C., "Principal Component Analysis: A Chemometric Approach to the Analysis of Near-Infrared Spectra", *Anal. Proc.* 1990, 27, 61-63.
42. Daultrey S. *Principal Components Analysis; Concepts and Techniques in Modern Geography*, No 8, University of East Anglia, 1976.

43. Jackson J. E. *A User's Guide to Principal Components*, John Wiley, Chichester, 1991
44. Sutter J. M., Kalivas J. H. and Lang P. M. "Which Principal Components to utilize for Principal Component Regression", *J. Chemometrics*, 1992, 6, 217-225.
45. Gemperline P.J., Miller K. H., West T. L., Weinstein J.E., Hamilton J.C., Bray J.T. "Principal Component Analysis, Trace Elements, and Blue Crab Shell Disease", *Anal. Chem.* 1992, 64, 523A-532A.
46. Cowe I.A. McNicol J.W. and Cuthbertson D. C. "Reconstruction of Constituent Spectra Using Principal Components", *Analyst*, 1988, 113, 269-272.
47. Devaux M.F., Bertrand D. Robert P. and Qannari M. "Application of Principal Component Analysis on NIR Spectral Collection after Elimination of Interference by a Least-Squares Procedure", *Applied Spectroscopy*, 1988, 42, 1020-1023.
48. Naes T and Martens H. "Principal Component Regression in NIR Analysis: Viewpoints, Background Details and Selection of Components", *J. Chemometrics*, 1988, 2, 155-167.
49. Blanco M., Coello J., Iturriaga H., MasPOCH S. and Redon M. "Principal Component Regression for Mixture Resolution in Control Analysis by UV-Visible Spectrophotometry", *Applied Spectroscopy*, 1994, 48, 37- 43
50. Mark H. In *Handbook of Near-Infrared Analysis*, Burns D. A. and Ciurczak E.W. Eds. Marcel Decker, N.Y.,1992.
51. Haaland D.M. and Thomas E. V. "Partial Least Squares Methods for Spectral Analyses, 1. Relation to the other Quantitative Calibration Methods and the extraction of Qualitative Information. *Anal. Chem.* 1988, 60, 1193-1202.
52. Bjorsvik H-R and Martens H. In *Handbook of Near-Infrared Analysis*, Burns D. A. and Ciurczak E.W. Eds. Marcei Decker, N.Y.,1992.

53. Martens H. and Jensen S. A. In *Progress in Cereal Chemistry and Technology*, Vol. 5a; Holas J. and Kratochvil J. Eds. Elsevier, Amsterdam, 1983.
54. Haaland D. M., "Classical versus Inverse Least-Squares Methods in Quantitative Spectral analyses", *Spectroscopy*, 1987, 2, 56.
55. Thomas E. V. and Haaland D. M., "Comparison of Multivariate Calibration Methods for Quantitative Spectral Analysis", *Anal. Chem.* 1990, 62, 1091-1099.
56. LighTcal Plus V1.0 Software and Users Manual, L.T. Industries, Inc.,
57. Personal communications; Thompson G. R. Research Dept., Syncrude (Canada) Ltd. Edmonton, Alberta.
58. Gemperline P. J., Long J.R. and Gregoriou V. G. "Nonlinear Multivariate Calibration Using Principal Components Regression and Artificial Neural Networks", *Anal. Chem.* 1991, 63, 2313-2323.
59. Gemperline P. J., Long J.R. and Gregoriou V. G. "Spectroscopic Calibration and Quantification Using Artificial Neural Networks", *Anal. Chem.* 1990, 62, 1791-1797.
60. Long J.R., Mayfield H.T., Henley M. V., Kromann P. R. "*Anal. Chem.* 1991, 63, 1256-1261.
61. Sekulic S., Seasholtz M. B., Wang Z., Kowalski B. R., Lee S. E., Holt B. R. "Nonlinear Multivariate Methods in Analytical Chemistry"; *Anal. Chem.* 1993, 65, 835A-844A.
62. Bhandare P., Mendelsohn Y., Peura R.A., Janatsch G., Kruse-Jarres J. D., Marbach R., Heise H. M. "Multivariate Determination of Glucose in Whole Blood Using Partial Least Squares and Artificial Neural Networks Based on Mid-Infrared Spectroscopy"; *Applied Spectroscopy*, 1993, 47, 1214- 1221
63. Parry S.J. In *Activation Spectrometry in Chemical Analysis*; Winefordner, J.D. and Kolthoff I.M., Eds.; John Wiley and Sons, 1991.

64. Muecke G.K., Ed. *Neutron Activation Analysis in the Geosciences*; Mineral Association of Canada Short Course Handbook, Vol. 5, 1980.
65. Erdtmann G. and Petri H. *Nuclear Activation Analysis: Fundamentals and Techniques*. In *Treatise on Analytical Chemistry*, 2nd Edn, pt 1, Vol. 14, Elving P. J., Ed.; John Wiley and Sons, N.Y. 1986.
66. DeSoete D. Gibjels R. and Hoste J. *Neutron Activation Analysis*. Elving P. J. and Kolthoff I.M., Eds.; John Wiley and Sons, London, 1972.
67. Kruger P. *Principles of Neutron Activation Analysis*; John Wiley and Sons, N.Y., 1972.
68. Amiel S., Ed. *Nondestructive Activation Analysis - Studies in Analytical Chemistry*:3; Elsevier Scientific Publishing Co., The Netherlands, 1981.
69. Rakovic M., *Activation Analysis*; The Press, (Ilifte) London, 1970.
70. Bergerioux C, Kennedy G., Zikovsky L. "Use of the Semi-Absolute Method in Neutron Activation Analysis"; *J. Radioanal. Chem.* 1979, 50, 229-234.
71. Duke M.J.M., M.Sc. Thesis, University of Alberta, Edmonton, 1983.
72. International Atomic Energy Agency, *Measurement of Radionuclides in Food and the Environment*; A Guidebook, Technical Reports Series No. 295, 1989.
73. Heydorn K. *Aspects of Precision and Accuracy in Neutron Activation Analysis*; Jul. Gjellerup, Copenhagen, 1978.
74. Currie L.A. "Quantitative Determination. Application to Radiochemistry"; *Anal. Chem.*, 1986, 40, #3, 586-593.
75. Pitts S.J. Ph.D.Thesis, University of Alberta, Edmonton, 1989.

76. Wang L. "A NAA Application Software Package, SPAN"; *Nucl. Electron. Detect. Technol. (China)*, 1986, 6, 356-361.
77. Personal Communications, Duke M.J.M. SLOWPOKE Reactor Facility, University of Alberta, Edmonton, Alberta.
78. Filby R. H. In *The Role of Trace Metals in Petroleum*; T. F. Yen Ed. Ann Arbor Science Publishers Inc. Mich, U.S.A. 1975.
79. Eppolito J. and Braier H. A. In *The Role of Trace Metals in Petroleum*; T. F. Yen Ed. Ann Arbor Science Publishers Inc. Mich, U.S.A. 1975.
80. Filby R. H. and Shah K, R. In *The Role of Trace Metals in Petroleum*; T. F. Yen Ed. Ann Arbor Science Publishers Inc. Mich, U.S.A. 1975.
81. Hitchon B., Filby R. H. and Shah K. R. In *The Role of Trace Metals in Petroleum*; T. F. Yen Ed. Ann Arbor Science Publishers Inc. Mich, U.S.A. 1975.
82. Smith A. J., Rice J. O., Shaner W. C. Jr. and Cerato C. C. In *The Role of Trace Metals in Petroleum*; T. F. Yen Ed. Ann Arbor Science Publishers Inc. Mich, U.S.A. 1975.
83. Yen T. F. "Nature of Vanadium Bonding in Petroleum"; *Preprints, Div. Petrol. Chem.*, American Chemical Society, Washington D.C., 1973.
84. Filby R. H. "Trace Element Distribution in Petroleum Components"; *Preprints, Div. Petrol. Chem.*, American Chemical Society, Washington D.C., 1973.
85. Shah K. R., Filby R. H., Haller W. A. "Determination of Trace Elements in Petroleum by Neutron Activation Analysis" I. Determination of Na, S, Cl, K, Ca, V, Mn, Cu, Ga, and Br"; *J. Radioanal. Chem.* 1970, 6, 185-192.
86. Shah K. R., Filby R. H., Haller W. A. "Determination of Trace Elements in Petroleum by Neutron Activation Analysis" II. Determination of Sc, Cr, Fe, Co, Ni, Zn, As, Se, Sb, Eu, Au, Hg and U"; *J. Radioanal. Chem.* 1970, 6, 413-422.

87. Buenafama H. D. and Lubkowitz J. A. "The Stability of Trace Metals Suspensions in Heavy Crudes as determined by Neutron Activation Analysis"; *J. Radioanal. Chem.* 1977, 39, 293-300
88. Valkovic V. *Trace Elements in Petroleum*. The Petroleum Publishing Co. OK. U.S.A. 1978.
89. Jervis R. E., Ho K. L. R. and Tiefenbach B. "Trace Impurities in Canadian Oil Sands, Coals and Petroleum Products and their Fate during Extraction, Up-grading and Combustion"; *J. Radioanal. Chem.* 1982, 71, 225
90. Dunning H. N., Moore J. W. and Denekas M. O. "Interfacial Activities and Porphyrin Contents of Petroleum Extracts"; *Ind. Eng. Chem.*, 1953, 45, 1759-1765.
91. Dunning H. N. and Rabon N. A. "Porphyrin Metal Complexes in Petroleum Stocks"; *Ind. Eng. Chem.* 1956, 48, 951.
92. Barwise A. J. G. and Whitehead E. V. "Characterization of Vanadium Porphyrins in Petroleum Residues"; *Preprints, Div. Petrol. Chem.*, American Chemical Society, Washington D.C., 1980.
93. Nadkarni R. A. In *Modern Instrumental Methods of Elemental Analysis of Petroleum Products and Lubricants*. Nadkarni R. A. Ed. A.S.T.M. Pa. U.S.A. 1991.
94. Jacobs F.S. and Filby R.H. "Solvent Extraction of Oil-Sand Components for Determination of Trace Elements by Neutron Activation Analysis"; *Anal. Chem.*, 1983, 55, 74-77.
95. Filby R.H. and Strong D. In *Metal Complexes in Fossil Fuels*; Filby R.H. and Branthaver J.F.; Eds. A.C.S. Washington D.C. 1987.
96. Filby R.H. and Van Berkel J. In *Metal Complexes in Fossil Fuels*; Filby R.H. and Branthaver J.F.; Eds. A.C.S. Washington D.C. 1987.

97. Filby R.H. and Nguyen S.N. In *Metal Complexes in Fossil Fuels*; Filby R.H. and Branthaver J.F.; Eds. A.C.S. Washington D.C. 1987.
98. Quirke J.M.E. In *Metal Complexes in Fossil Fuels*; Filby R.H. and Branthaver J.F.; Eds. A.C.S. Washington D.C. 1987.
99. Branthaver J.F. In *Metal Complexes in Fossil Fuels*; Filby R.H. and Branthaver J.F.; Eds. A.C.S. Washington D.C. 1987.
100. Chicarelli M.I., Kaur S, and Maxwell J.R. In *Metal Complexes in Fossil Fuels*; Filby R.H. and Branthaver J.F.; Eds. A.C.S. Washington D.C. 1987.
101. Jacobs F.S. and Filby R. H. In *Atomic and Nuclear Methods in Fossil Energy Research*; Filby R. H. Ed. Plenum Press, N.Y. 1982.
102. Baker E. W. and Palmer S. E. In *The Porphyrins*, Vol. 1, Part A. Dolphin D. Ed. Academic Press N.Y. 1978.
103. Yen T. F. In *The Role of Trace Metals in Petroleum*; T. F. Yen Ed. Ann Arbor Science Publishers Inc. Mich, U.S.A. 1975.
104. Personal communications; Filby R. H. Department of Chemistry, Washington State University, Pullman, Washington, U.S.A.
105. Mason Brian. *Principles of Geochemistry* , 3rd ed. John Wiley and sons, Inc. N.Y. 1966. pp 132.

Appendix A

Data collected on Oil Sand Core by Near Infrared-Diffuse Reflectance Spectroscopy

This appendix deals with the Near-Infrared analysis part of the thesis. It is divided into three sections.

Appearing in Section 1 are raw data used for constructing calibration plots for bitumen and solids in oil sand. These calibration plots were modelled using Principal Components Regression (PCR) and Partial Least Squares (PLS) for data on both non-roughened and roughened surfaces of the core.

Section 2 contains the raw data for bitumen content values obtained laterally across four core sections, labelled A, E, J and L. Three test portions were collected in each lateral sampling, and the standard deviations of the three analyses were calculated. These results were used for the lateral variability studies of bitumen content in oil sand discussed in Chapter 3.

In Section 3 are raw data for predicted bitumen and solids content at 1-cm sampling intervals down the length of the vertical transect of oil sand core. These values were derived from the PCR calibration models for non-roughened surfaces.

In this appendix a number of somewhat specialized terms are used. These are defined in the glossary that follows.

Glossary

- 1. Leverage:** values showing a measure of the influence of the sample on the calibration model. The range of possible values is 0 to 1. Samples with large leverage values have a greater impact in the determination of regression coefficients than do samples with average leverage values.
- 2. Residuals:** differences between actual and predicted values for each sample.
- 3. Studentized residuals:** individual residual values divided by the estimated variance. They are used to test for outliers by comparing the values against a t-distribution for a particular significance level.
- 4. Mahalanobis distance:** a statistical description of how distant a sample is from the calibration set. It is defined as the sum of squares of the scores of the unknown samples. A score is the orthogonal projection of the samples on the principal component axes and the distance to origin is the score value of a sample. Mathematically, it is defined as the squared Euclidean distance of the sample data point from the origin in factor space. Usual values are less than 1. A value greater than 1.5 is considered large and denotes a sample which seems different.

SECTION 1

**Data for calibration model of bitumen as shown in Fig. 3.2 : PCR:
non-roughened surface.**

Sample	Leverage	Actual % bitumen	Predicted % bitumen	Residual	Studentized Residual
1	0.07	12.95	13.04	-0.09	-0.11
2	0.16	12.75	12.56	0.19	0.26
3	0.04	13.1	11.86	1.24	1.53
4	0.06	11.93	12.23	-0.3	-0.38
5	0.1	10.75	10.66	0.09	0.11
6	0.19	10.68	11.13	-0.45	-0.66
7	0.13	11.46	11.34	0.12	0.16
8	0.15	11.54	11.29	0.25	0.34
9	0.09	13.15	12.65	0.5	0.65
10	0.05	12.82	12.1	0.72	0.89
11	0.09	10.7	11.76	-1.06	-1.38
12	0.09	11.63	11.72	-0.09	-0.12
13	0.09	11.3	11.88	-0.58	-0.75
14	0.08	12.2	12.04	0.16	0.2
15	0.09	12.68	11.81	0.87	1.14
16	0.1	3.34	2.81	0.53	0.7
17	0.29	1.46	1.22	0.24	0.39
18	0.13	0.9	2.48	-1.58	-2.16
19	0.05	10.84	10.48	0.36	0.45
20	0.07	9.06	9.85	-0.79	-1
21	0.05	11.04	11.56	-0.52	-0.64
22	0.1	10.61	10.86	-0.25	-0.32
23	0.06	10.7	11.12	-0.42	-0.53
24	0.05	11.57	11.7	-0.13	-0.16
25	0.27	2.94	4	-1.06	-1.72
26	0.32	4.55	5.49	-0.94	-1.64
27	0.27	8.99	8.07	0.92	1.49
28	0.21	6.23	4.84	1.39	2.07
29	0.1	5	6.67	-1.67	-2.2
30	0.5	5.72	5.9	-0.18	-0.42
31	0.17	4.38	4.68	-0.3	-0.43
32	0.15	6.2	6.58	-0.38	-0.54
33	0.11	7.69	6.65	1.04	1.39
34	0.25	8.6	8.65	-0.05	-0.08
35	0.32	10.85	10.67	0.18	0.32
36	0.1	4.6	5.84	-1.24	-1.63
37	0.13	4.18	4.37	-0.19	-0.26
38	0.13	4.07	4.2	-0.13	-0.18
39	0.08	5.2	5.31	-0.11	-0.14
40	0.18	4.94	3.98	0.96	1.39
41	0.03	5.93	6.53	-0.6	-0.73
42	0.03	9.43	10.14	-0.71	-0.87
43	0.04	7.03	8.04	-1.01	-1.26
44	0.12	7.08	6.14	0.94	1.27
45	0.11	7.02	6.25	0.77	1.03
46	0.18	5.83	5.3	0.53	0.76
47	0.06	10.22	9.92	0.3	0.37
48	0.15	11.1	9.91	1.19	1.66
49	0.14	10.98	10.64	0.34	0.47
50	0.07	10.91	11.22	-0.31	-0.4
51	0.07	3.53	4.32	-0.79	-1
52	0.15	2.49	1.91	0.58	0.81
53	0.1	3.26	2.45	0.81	1.07
54	0.11	2.77	2.05	0.72	0.96

Data for calibration model of bitumen as shown in Fig.3.2: PLS: non-roughened.

Sample	Leverage	Actual % bitumen	Predicted % bitumen	Residual	Studentized Residual
1	0.09	12.95	13.45	-0.50	-0.72
2	0.19	12.75	12.97	-0.22	-0.35
3	0.03	13.10	12.09	1.01	1.36
4	0.06	11.93	12.46	-0.53	-0.73
5	0.12	10.75	10.33	0.42	0.61
6	0.17	10.68	10.96	-0.28	-0.44
7	0.12	11.46	11.19	0.27	0.40
8	0.12	11.54	11.14	0.40	0.60
9	0.10	13.15	12.85	0.30	0.43
10	0.06	12.82	12.30	0.52	0.72
11	0.10	10.70	11.38	-0.68	-0.99
12	0.10	11.63	11.33	0.30	0.43
13	0.12	11.30	11.45	-0.15	-0.23
14	0.09	12.20	11.83	0.37	0.52
15	0.10	12.68	11.49	1.19	1.74
16	0.09	3.34	2.87	0.47	0.67
17	0.21	1.46	1.55	-0.09	-0.15
18	0.12	0.90	2.36	-1.46	-2.15
19	0.05	10.84	10.52	0.32	0.44
20	0.05	9.06	9.88	-0.82	-1.13
21	0.05	11.04	11.55	-0.51	-0.70
22	0.12	10.61	10.57	0.04	0.06
23	0.07	10.70	10.96	-0.26	-0.37
24	0.05	11.57	11.51	0.06	0.08
25	0.26	2.94	4.08	-1.14	-2.02
26	0.25	4.55	5.55	-1.00	-1.74
27	0.41	8.99	8.96	0.03	0.07
28	0.19	6.23	4.96	1.27	2.05
29	0.14	5.00	6.24	-1.24	-1.88
30	0.40	5.72	5.72	0.00	0.00
31	0.20	4.38	4.28	0.10	0.16
32	0.14	6.20	6.26	-0.06	-0.09
33	0.12	7.69	6.94	0.75	1.11
34	0.25	8.60	8.52	0.08	0.15
35	0.25	10.85	10.65	0.20	0.35
36	0.08	4.60	5.54	-0.94	-1.33
37	0.13	4.18	4.47	-0.29	-0.43
38	0.11	4.07	3.88	0.19	0.27
39	0.10	5.20	4.87	0.33	0.48
40	0.13	4.94	3.83	1.11	1.67
41	0.03	5.93	6.54	-0.61	-0.82
42	0.03	9.43	10.34	-0.91	-1.22
43	0.02	7.03	8.13	-1.10	-1.48
44	0.15	7.08	6.51	0.57	0.87
45	0.16	7.02	6.74	0.28	0.44
46	0.19	5.83	5.62	0.21	0.33
47	0.06	10.22	10.01	0.21	0.29
48	0.15	11.10	9.88	1.22	1.87
49	0.16	10.98	10.98	0.00	-0.01
50	0.10	10.91	11.63	-0.72	-1.04
51	0.07	3.53	4.42	-0.89	-1.25
52	0.14	2.49	1.89	0.60	0.90
53	0.09	3.26	2.43	0.83	1.26
54	0.10	2.77	2.00	0.77	1.11

Data for calibration model of bitumen as shown in Fig 3.3: PCR: roughened surface

Sample	Leverage	Actual % bitumen	Predicted % bitumen	Residual	Studentized Residual
1	0.19	1.59	2.41	-0.82	-1.02
2	0.64	0.54	0.14	0.40	1.12
3	0.69	1.55	1.31	0.24	0.78
4	0.27	5.47	4.12	1.35	1.85
5	0.07	5.27	6.09	-0.82	-0.88
6	0.12	5.86	5.87	-0.01	-0.01
7	0.13	3.56	5.01	-1.45	-1.67
8	0.19	7.16	7.32	-0.16	-0.19
9	0.13	5.30	5.46	-0.16	-0.18
10	0.15	9.88	9.17	0.71	0.84
11	0.16	9.14	8.39	0.75	0.89
12	0.06	12.66	12.48	0.18	0.19
13	0.15	13.41	13.52	-0.11	-0.13
14	0.05	11.21	12.44	-1.23	-1.30
15	0.26	7.33	5.48	1.85	2.51
16	0.15	5.17	6.14	-0.97	-1.14
17	0.06	11.73	12.01	-0.28	-0.30
18	0.18	13.01	12.23	0.78	0.95
19	0.07	13.73	12.84	0.89	0.96
20	0.04	12.96	11.85	1.11	1.16
21	0.07	12.81	12.56	0.25	0.27
22	0.10	9.99	8.85	1.14	1.27
23	0.20	8.81	9.33	-0.52	-0.65
24	0.19	3.68	3.74	-0.06	-0.07
25	0.08	12.41	12.29	0.12	0.14
26	0.09	12.48	12.74	-0.26	-0.28
27	0.30	13.23	12.72	0.51	0.73
28	0.10	12.63	12.19	0.44	0.49
29	0.06	12.46	12.98	-0.52	-0.55
30	0.09	12.65	13.03	-0.38	-0.42
31	0.27	6.11	7.10	-0.99	-1.35
32	0.05	12.06	12.62	-0.56	-0.59
33	0.03	12.05	12.32	-0.27	-0.28
34	0.06	13.56	13.12	0.44	0.48
35	0.21	4.10	2.78	1.32	1.66
36	0.27	4.36	5.20	-0.84	-1.15
37	0.29	5.21	5.70	-0.49	-0.70
38	0.20	4.21	5.64	-1.43	-1.79
39	0.16	3.63	4.45	-0.82	-0.98
40	0.14	4.08	3.39	0.69	0.81
41	0.17	4.68	3.93	0.75	0.91
42	0.10	9.13	9.94	-0.81	-0.89

Data for calibration model of bitumen as shown in Fig. 3.3: PLS: roughened surface.

Sample	Leverage	Actual % bitumen	Predicted % bitumen	Residual	Studentized Residual
1	0.19	1.59	2.40	-0.81	-1.07
2	0.61	0.54	0.02	0.52	1.44
3	0.64	1.55	1.33	0.22	0.65
4	0.25	5.47	4.08	1.39	1.98
5	0.07	5.27	6.03	-0.76	-0.87
6	0.10	5.86	5.88	-0.02	-0.03
7	0.12	3.56	5.05	-1.49	-1.81
8	0.16	7.16	7.39	-0.23	-0.29
9	0.09	5.30	5.51	-0.21	-0.24
10	0.10	9.88	9.14	0.74	0.88
11	0.08	9.14	8.56	0.58	0.67
12	0.03	12.66	12.55	0.11	0.13
13	0.13	13.41	13.44	-0.03	-0.04
14	0.04	11.21	12.46	-1.25	-1.40
15	0.11	7.33	5.62	1.71	2.07
16	0.14	5.17	6.07	-0.90	-1.12
17	0.07	11.73	12.09	-0.36	-0.41
18	0.11	13.01	12.28	0.73	0.89
19	0.05	13.73	12.86	0.87	0.98
20	0.03	12.96	11.83	1.13	1.25
21	0.04	12.81	12.56	0.25	0.28
22	0.09	9.99	8.93	1.06	1.24
23	0.16	8.81	9.30	-0.49	-0.63
24	0.19	3.68	3.73	-0.05	-0.07
25	0.04	12.41	12.29	0.12	0.14
26	0.06	12.48	12.77	-0.29	-0.34
27	0.28	13.23	12.64	0.59	0.88
28	0.08	12.63	12.29	0.34	0.39
29	0.06	12.46	12.96	-0.50	-0.57
30	0.09	12.65	12.97	-0.32	-0.37
31	0.24	6.11	7.05	-0.94	-1.32
32	0.05	12.06	12.51	-0.45	-0.51
33	0.03	12.05	12.34	-0.29	-0.32
34	0.06	13.56	13.05	0.51	0.58
35	0.19	4.10	2.72	1.38	1.82
36	0.20	4.36	5.06	-0.70	-0.94
37	0.27	5.21	5.66	-0.45	-0.67
38	0.20	4.21	5.54	-1.33	-1.77
39	0.16	3.63	4.44	-0.81	-1.03
40	0.14	4.08	3.45	0.63	0.79
41	0.16	4.68	4.05	0.63	0.80
42	0.09	9.13	9.97	-0.84	-0.99

Data for calibration model of solids as shown in Fig.3.4; PCR: non-roughened.

Sample	Leverage	Actual % bitumen	Predicted % bitumen	Residual	Studentized Residual
1	0.07	86.50	86.10	0.40	0.47
2	0.16	87.15	86.78	0.37	0.48
3	0.04	86.55	87.31	-0.76	-0.86
4	0.06	87.58	87.03	0.55	0.63
5	0.10	88.46	88.48	-0.02	-0.02
6	0.19	88.63	87.98	0.65	0.86
7	0.13	87.70	87.66	0.04	0.04
8	0.15	87.27	87.71	-0.44	-0.56
9	0.09	86.06	86.60	-0.54	-0.64
10	0.05	86.70	87.15	-0.45	-0.52
11	0.09	88.16	87.52	0.64	0.76
12	0.09	88.18	87.50	0.68	0.81
13	0.09	87.86	87.40	0.46	0.55
14	0.08	86.81	87.21	-0.40	-0.48
15	0.09	87.13	87.51	-0.38	-0.45
16	0.10	96.21	96.64	-0.43	-0.52
17	0.29	98.45	98.57	-0.12	-0.18
18	0.13	98.86	97.12	1.74	2.17
19	0.05	88.52	88.68	-0.16	-0.19
20	0.07	89.54	89.28	0.26	0.31
21	0.05	87.38	87.49	-0.11	-0.13
22	0.10	88.85	88.32	0.53	0.64
23	0.06	88.36	88.16	0.20	0.23
24	0.05	86.65	87.47	-0.82	-0.94
25	0.27	96.66	95.43	1.23	1.82
26	0.32	95.06	94.27	0.79	1.26
27	0.27	90.32	91.20	-0.88	-1.31
28	0.21	93.38	94.63	-1.25	-1.71
29	0.10	94.42	92.76	1.66	1.99
30	0.50	94.19	93.44	0.75	1.64
31	0.17	94.89	94.98	-0.09	-0.12
32	0.15	92.69	92.80	-0.11	-0.14
33	0.11	91.37	93.02	-1.65	-2.01
34	0.25	91.25	90.76	0.49	0.71
35	0.32	88.66	88.52	0.14	0.23
36	0.10	94.61	93.40	1.21	1.46
37	0.13	95.53	94.84	0.69	0.86
38	0.13	95.79	95.00	0.79	0.99
39	0.08	94.80	93.90	0.90	1.07
40	0.18	94.67	95.59	-0.92	-1.21
41	0.03	92.04	92.76	-0.72	-0.81
42	0.03	89.54	88.95	0.59	0.66
43	0.04	92.18	91.22	0.96	1.09
44	0.12	92.13	93.14	-1.01	-1.25
45	0.11	92.63	93.20	-0.57	-0.70
46	0.18	93.88	94.19	-0.31	-0.41
47	0.06	89.73	89.14	0.59	0.68
48	0.15	87.53	88.95	-1.42	-1.80
49	0.14	87.69	88.19	-0.50	-0.64
50	0.07	86.87	87.73	-0.86	-1.00
51	0.07	95.48	95.08	0.40	0.47
52	0.15	96.97	97.75	-0.78	-0.99
53	0.10	95.75	97.02	-1.27	-1.53
54	0.11	96.78	97.50	-0.72	-0.87

Data for calibration model of solids as shown in Fig.3.4: PLS: non-roughened.

Sample	Leverage	Actual	Predicted % bitumen	Residual % bitumen	Studentized Residual
1	0.09	86.50	85.65	0.85	1.14
2	0.18	87.15	86.36	0.79	1.18
3	0.03	86.55	87.11	-0.56	-0.71
4	0.06	87.58	86.85	0.73	0.94
5	0.11	88.46	88.84	-0.38	-0.53
6	0.17	88.63	88.22	0.41	0.61
7	0.12	87.70	87.86	-0.16	-0.22
8	0.12	87.27	87.90	-0.63	-0.88
9	0.09	86.06	86.40	-0.34	-0.45
10	0.05	86.70	86.99	-0.29	-0.37
11	0.09	88.16	87.94	0.22	0.29
12	0.09	88.18	87.94	0.24	0.33
13	0.11	87.86	87.90	-0.04	-0.06
14	0.08	86.81	87.41	-0.60	-0.80
15	0.10	87.13	87.86	-0.73	-0.99
16	0.09	96.21	96.55	-0.34	-0.46
17	0.21	98.45	98.17	0.28	0.43
18	0.12	98.86	97.33	1.53	2.13
19	0.05	88.52	88.69	-0.17	-0.22
20	0.05	89.54	89.12	0.42	0.55
21	0.05	87.38	87.38	0.00	0.00
22	0.11	88.85	88.62	0.23	0.32
23	0.06	88.36	88.28	0.08	0.11
24	0.05	86.65	87.59	-0.94	-1.22
25	0.26	96.66	95.33	1.33	2.21
26	0.25	95.06	94.15	0.91	1.49
27	0.43	90.32	90.08	0.24	0.51
28	0.20	93.38	94.42	-1.04	-1.59
29	0.14	94.42	93.29	1.13	1.61
30	0.41	94.19	93.75	0.44	0.91
31	0.19	94.89	95.44	-0.55	-0.83
32	0.14	92.69	93.18	-0.49	-0.70
33	0.14	91.37	92.59	-1.22	-1.72
34	0.26	91.25	90.95	0.30	0.50
35	0.27	88.66	88.69	-0.03	-0.05
36	0.08	94.61	93.81	0.80	1.07
37	0.13	95.53	94.77	0.76	1.07
38	0.12	95.79	95.43	0.36	0.51
39	0.11	94.80	94.45	0.35	0.48
40	0.14	94.67	95.82	-1.15	-1.63
41	0.03	92.04	92.74	-0.70	-0.88
42	0.03	89.54	88.74	0.80	1.01
43	0.02	92.18	91.14	1.04	1.30
44	0.14	92.13	92.76	-0.63	-0.90
45	0.15	92.63	92.66	-0.03	-0.04
46	0.19	93.88	93.79	0.09	0.13
47	0.06	89.73	89.07	0.66	0.87
48	0.15	87.53	88.96	-1.43	-2.05
49	0.17	87.69	87.72	-0.03	-0.04
50	0.11	86.87	87.20	-0.33	-0.45
51	0.07	95.48	94.90	0.58	0.76
52	0.14	96.97	97.80	-0.83	-1.18
53	0.09	95.75	97.02	-1.27	-1.70
54	0.10	96.78	97.48	-0.70	-0.96

Data for calibration model of solids as shown in Fig. 3.5: PCR: roughened.

Sample	Leverage	Actual % bitumen	Predicted % bitumen	Residual	Studentized Residual
1	0.19	98.31	97.17	1.14	1.21
2	0.64	99.46	99.76	-0.30	-0.72
3	0.69	96.69	97.25	-0.56	-1.52
4	0.27	92.29	94.31	-2.02	-2.35
5	0.07	92.89	92.93	-0.04	-0.03
6	0.12	93.89	93.49	0.40	0.39
7	0.13	96.05	94.59	1.46	1.44
8	0.19	91.91	91.99	-0.08	-0.09
9	0.13	94.50	93.99	0.51	0.50
10	0.15	89.05	89.86	-0.81	-0.82
11	0.16	90.57	90.79	-0.22	-0.22
12	0.06	86.46	86.44	0.02	0.02
13	0.15	84.61	85.33	-0.72	-0.72
14	0.05	87.46	86.50	0.96	0.86
15	0.26	91.58	93.92	-2.34	-2.70
16	0.15	93.99	93.06	0.93	0.94
17	0.06	86.63	87.00	-0.37	-0.33
18	0.18	86.60	86.70	-0.10	-0.10
19	0.07	85.19	86.11	-0.92	-0.85
20	0.04	86.46	87.12	-0.66	-0.59
21	0.07	86.07	86.33	-0.26	-0.24
22	0.10	89.96	90.17	-0.21	-0.20
23	0.20	90.09	89.70	0.39	0.42
24	0.19	96.32	95.42	0.90	0.95
25	0.08	85.69	86.64	-0.95	-0.88
26	0.09	85.65	86.22	-0.57	-0.53
27	0.30	85.64	85.83	-0.19	-0.23
28	0.10	86.05	86.70	-0.65	-0.61
29	0.06	87.10	85.78	1.32	1.20
30	0.09	85.82	85.78	0.04	0.04
31	0.27	92.32	91.80	0.52	0.60
32	0.03	86.87	86.15	0.72	0.65
33	0.03	87.41	86.60	0.81	0.72
34	0.06	85.24	85.72	-0.48	-0.43
35	0.21	95.01	95.85	-0.84	-0.91
36	0.27	93.22	93.17	0.05	0.05
37	0.29	93.61	92.49	1.12	1.35
38	0.20	95.09	93.44	1.65	1.75
39	0.16	95.38	94.69	0.69	0.70
40	0.14	94.79	96.09	-1.30	-1.29
41	0.17	94.73	95.63	-0.90	-0.93
42	0.10	90.53	88.69	1.84	1.74

Data for calibration model of solids as shown in Fig.3.5: PLS: roughened.

Sample	Leverage	Actual % bitumen	Predicted % bitumen	Residual	Studentized Residual
1	0.19	98.31	97.21	1.10	1.24
2	0.57	99.46	99.91	-0.45	-0.97
3	0.63	96.69	97.28	-0.59	-1.43
4	0.25	92.29	94.33	-2.04	-2.46
5	0.07	92.89	92.92	-0.03	-0.03
6	0.09	93.89	93.44	0.45	0.46
7	0.11	96.05	94.56	1.49	1.52
8	0.13	91.91	91.87	0.04	0.04
9	0.08	94.50	93.93	0.55	0.54
10	0.10	89.05	89.86	-0.81	-0.82
11	0.06	90.57	90.68	-0.11	-0.11
12	0.04	86.46	86.42	0.04	0.04
13	0.14	84.61	85.38	-0.77	-0.81
14	0.04	87.46	86.46	1.00	0.94
15	0.13	91.58	93.78	-2.20	-2.30
16	0.15	93.99	93.06	0.93	0.99
17	0.06	86.63	86.91	-0.28	-0.28
18	0.14	86.60	86.65	-0.05	-0.05
19	0.06	85.19	86.08	-0.89	-0.86
20	0.04	86.46	87.09	-0.63	-0.59
21	0.05	86.07	86.32	-0.25	-0.24
22	0.09	89.96	90.13	-0.17	-0.17
23	0.18	90.09	89.69	0.40	0.44
24	0.19	96.32	95.46	0.86	0.96
25	0.05	85.69	86.63	-0.94	-0.90
26	0.08	85.65	86.18	-0.53	-0.52
27	0.29	85.64	85.96	-0.32	-0.42
28	0.09	86.05	86.70	-0.65	-0.65
29	0.06	87.10	85.82	1.28	1.24
30	0.09	85.82	85.84	-0.02	-0.02
31	0.25	92.32	91.83	0.49	0.59
32	0.05	86.87	86.21	0.66	0.63
33	0.03	87.41	86.57	0.84	0.79
34	0.06	85.24	85.74	-0.50	-0.49
35	0.19	95.01	95.86	-0.85	-0.95
36	0.19	93.22	93.25	-0.03	-0.03
37	0.28	93.61	92.58	1.03	1.30
38	0.20	95.09	93.53	1.56	1.77
39	0.16	95.38	94.74	0.64	0.70
40	0.14	94.79	96.05	-1.26	-1.33
41	0.15	94.73	95.52	-0.79	-0.84
42	0.09	90.53	88.73	1.80	1.81

SECTION 2

Data for three sets of bitumen values obtained laterally across core section. A. Plot is shown in Fig.3.9

<u>Distance</u> (cm)	<u>% Bitumen</u> 1	<u>% Bitumen</u> 2	<u>% Bitumen</u> 3	<u>% Bitumen</u> Mean	<u>Std. Dev.</u>
1	11.1	11.2	10.7	11.0	0.2
2	12.1	11.3	10.6	11.3	0.6
3	11.5	11.1	10.7	11.1	0.4
4	11.4	11.2	11.0	11.2	0.1
5	12.1	11.3	10.8	11.4	0.5
6	11.0	11.1	10.7	10.9	0.2
7	12.2	11.2	11.0	11.4	0.5
8	12.0	11.1	10.9	11.3	0.5
9	12.1	11.3	10.8	11.4	0.5
10	11.8	11.1	10.8	11.2	0.4
11	12.0	11.2	10.7	11.3	0.5
12	11.7	11.2	10.9	11.2	0.3
13	12.0	11.1	11.0	11.4	0.5
14	12.0	11.3	10.9	11.4	0.4
15	11.4	11.3	11.0	11.2	0.2
16	11.2	11.3	10.8	11.1	0.2
17	11.9	11.3	11.0	11.4	0.4
18	12.0	11.3	10.6	11.3	0.6
19	11.4	11.4	10.4	11.1	0.5
20	11.9	11.4	10.6	11.3	0.6
21	11.9	11.2	10.3	11.1	0.7
22	11.4	11.0	10.1	10.9	0.5
23	11.8	11.2	10.6	11.2	0.5
24	11.3	11.2	10.7	11.1	0.3
25	11.3	11.0	10.9	11.0	0.2
26	11.8	10.9	10.3	11.0	0.6
27	12.1	11.0	10.5	11.2	0.7
28	11.8	11.2	10.8	11.3	0.4
29	11.8	11.3	10.9	11.3	0.4
30	11.8	11.3	11.0	11.4	0.3
31	11.8	11.2	11.0	11.3	0.3
32	11.2	11.2	11.1	11.2	0.1
33	11.5	11.4	10.8	11.2	0.3
34	11.1	11.4	10.5	11.0	0.4
35	11.3	11.3	10.5	11.0	0.4
36	11.7	11.3	10.6	11.2	0.5
37	11.8	11.3	10.6	11.2	0.5
38	11.6	11.2	10.5	11.1	0.5

39	11.3	11.2	10.6	11.0	0.3
40	11.1	11.4	10.9	11.1	0.2
41	11.2	11.3	10.7	11.1	0.2
42	11.3	11.4	10.9	11.2	0.2
43	11.5	11.2	10.8	11.2	0.3
44	11.4	11.4	10.6	11.1	0.4
45	11.2	11.2	10.7	11.0	0.2
46	11.2	11.1	10.7	11.0	0.2
47	11.0	11.9	10.6	11.2	0.6
48	11.1	11.3	10.7	11.0	0.2
49	11.3	11.2	10.7	11.1	0.3
50	11.7	11.3	10.8	11.3	0.4
51	11.0	11.2	10.7	11.0	0.2
52	11.0	11.3	11.4	11.2	0.2
53	10.8	11.3	10.8	11.0	0.2
54	10.5	11.1	10.9	10.9	0.3
55	11.3	11.3	10.6	11.1	0.3
56	11.1	11.0	10.9	11.0	0.1
57	11.4	11.4	10.9	11.2	0.3
58	11.2	11.3	10.8	11.1	0.2
59	11.3	11.4	10.9	11.2	0.2
60	11.3	11.4	10.8	11.2	0.3
61	11.3	11.4	10.9	11.2	0.2
62	10.8	11.4	10.9	11.1	0.3
63	11.1	11.5	10.8	11.1	0.3
64	11.0	11.3	10.8	11.0	0.2
65	11.2	11.4	10.8	11.1	0.3
66	11.2	11.3	11.0	11.2	0.1
67	11.3	11.5	10.5	11.1	0.4
68	10.7	11.3	10.3	10.8	0.4
69	10.8	11.2	10.7	10.9	0.2
70	10.1	11.4	10.7	10.7	0.5

Data for three sets of bitumen values obtained laterally across core section. E. Plot is shown in Fig.3.9

<u>Distance</u> (cm)	<u>% Bitumen</u> 1	<u>% Bitumen</u> 2	<u>% Bitumen</u> 3	<u>% Bitumen</u> Mean	<u>Std. Dev.</u>
1	12.2	11.3	10.9	11.5	0.6
2	12.2	11.2	10.8	11.4	0.6
3	11.9	11.1	11.0	11.3	0.4
4	12.3	11.4	10.8	11.5	0.6
5	11.9	11.1	11.1	11.4	0.4
6	12.2	11.1	11.1	11.5	0.5
7	12.6	11.0	11.0	11.5	0.7
8	12.2	11.1	10.9	11.4	0.6
9	12.9	11.0	10.9	11.6	0.9
10	12.1	11.0	11.3	11.5	0.4
11	12.0	11.1	11.5	11.5	0.4
12	11.7	11.1	11.0	11.2	0.3
13	11.6	11.2	11.2	11.3	0.2
14	11.6	11.0	10.7	11.1	0.4
15	11.8	11.1	10.5	11.1	0.5
16	11.7	10.9	10.9	11.2	0.4
17	11.8	11.2	11.0	11.3	0.4
18	12.1	11.0	10.9	11.3	0.6
19	11.7	11.2	10.9	11.3	0.3
20	11.9	11.0	11.0	11.3	0.4
21	12.0	11.0	10.9	11.3	0.5
22	11.9	11.0	10.8	11.3	0.5
23	10.9	10.9	10.9	10.9	0.0
24	11.2	11.1	10.4	10.9	0.4
25	11.2	10.9	10.5	10.9	0.3
26	11.8	11.2	10.6	11.2	0.5
27	11.6	11.2	10.8	11.2	0.3
28	11.9	11.3	10.7	11.3	0.5
29	11.8	10.9	10.9	11.2	0.4
30	11.7	11.0	11.0	11.3	0.4
31	11.3	11.3	10.7	11.1	0.3
32	12.1	11.1	10.7	11.3	0.6
33	11.6	11.2	10.9	11.2	0.3
34	11.8	11.0	10.8	11.2	0.4
35	11.3	11.1	11.0	11.2	0.1
36	11.8	11.3	11.0	11.4	0.4
37	12.0	11.3	11.1	11.5	0.4
38	11.7	11.2	11.0	11.3	0.3
39	11.9	11.2	11.1	11.4	0.4
40	12.1	11.2	11.0	11.4	0.5

41	11.7	11.1	11.1	11.3	0.3
42	11.7	11.1	11.2	11.3	0.3
43	12.3	11.2	11.1	11.5	0.5
44	11.6	11.2	11.2	11.3	0.2
45	11.6	11.4	11.1	11.3	0.2
46	11.3	11.2	11.0	11.2	0.1
47	11.6	11.1	11.0	11.3	0.3
48	11.8	11.3	11.1	11.4	0.3
49	11.9	11.2	11.1	11.4	0.4
50	11.8	11.1	10.9	11.3	0.4
51	11.3	11.2	10.8	11.1	0.2
52	11.2	11.2	11.0	11.1	0.1
53	11.1	11.2	10.9	11.1	0.1
54	11.1	11.3	11.0	11.1	0.1
55	11.6	11.2	10.9	11.2	0.3
56	11.4	11.2	11.0	11.2	0.2
57	11.5	11.2	10.8	11.2	0.3
58	11.9	11.3	10.9	11.4	0.4
59	11.8	11.2	10.9	11.3	0.4
60	11.8	11.2	10.9	11.3	0.4
61	11.8	11.2	11.7	11.6	0.3
62	11.6	11.2	11.0	11.3	0.3
63	11.6	11.2	10.9	11.2	0.3
64	11.4	11.2	10.9	11.2	0.2
65	11.0	11.2	11.0	11.0	0.1
66	11.1	11.3	10.9	11.1	0.2
67	10.9	11.3	11.0	11.1	0.2
68	11.4	11.3	11.0	11.2	0.2

Data for three sets of bitumen values obtained laterally across core section. I. Plot is shown in Fig.3.10

<u>Distance</u> (cm)	<u>% Bitumen</u> 1	<u>% Bitumen</u> 2	<u>% Bitumen</u> 3	<u>% Bitumen</u> Mean	<u>Std. Dev.</u>
1	9.2	11.3	11.2	10.6	1.0
2	9.6	11.2	10.9	10.6	0.7
3	10.6	11.3	11.4	11.1	0.3
4	9.7	11.2	11.3	10.7	0.8
5	10.8	12.0	11.5	11.4	0.5
6	10.9	11.3	11.1	11.1	0.2
7	10.7	11.3	11.1	11.1	0.2
8	10.9	11.2	10.9	11.0	0.1
9	10.8	11.3	11.0	11.0	0.2
10	10.8	11.1	11.0	11.0	0.2
11	11.0	11.4	11.1	11.2	0.2
12	10.8	11.2	11.1	11.0	0.2
13	10.4	11.1	11.2	10.9	0.4
14	10.4	11.9	11.3	11.2	0.6
15	10.8	11.2	11.2	11.0	0.2
16	9.8	11.1	10.5	10.5	0.5
17	10.2	11.1	11.0	10.8	0.4
18	10.7	11.3	11.3	11.1	0.3
19	11.0	11.1	11.2	11.1	0.1
20	10.9	11.2	11.3	11.1	0.2
21	11.0	11.2	11.3	11.2	0.1
22	10.9	11.1	11.4	11.1	0.2
23	11.1	11.2	11.8	11.3	0.3
24	11.3	11.2	11.4	11.3	0.1
25	11.0	11.0	11.2	11.1	0.1
26	10.9	11.2	10.6	10.9	0.3
27	10.4	11.2	11.3	10.9	0.4
28	10.3	11.1	11.6	11.0	0.5
29	10.5	11.2	10.8	10.8	0.3
30	9.9	11.2	10.7	10.6	0.5
31	9.2	11.1	10.4	10.2	0.8
32	10.7	11.0	11.1	11.0	0.2
33	10.8	11.2	10.9	11.0	0.2
34	11.3	11.1	10.7	11.0	0.3
35	10.6	11.3	10.9	10.9	0.3
36	10.9	11.1	11.0	11.0	0.1
37	11.4	11.3	11.0	11.2	0.2
38	11.3	11.4	11.1	11.3	0.1
39	11.2	11.2	11.0	11.1	0.1
40	11.0	11.2	11.0	11.1	0.1

41	10.5	11.1	11.0	10.8	0.3
42	9.3	11.0	10.6	10.3	0.8
43	9.3	11.0	11.1	10.5	0.8
44	10.1	11.2	11.2	10.9	0.5
45	11.1	11.0	10.9	11.0	0.1
46	11.9	11.1	11.0	11.3	0.4
47	10.9	11.3	11.0	11.0	0.2
48	11.2	11.4	10.7	11.1	0.3
49	10.4	11.0	10.6	10.7	0.2
50	10.8	10.9	10.2	10.6	0.3
51	10.8	11.1	11.0	11.0	0.2
52	9.8	10.7	11.1	10.5	0.5

Data for three sets of bitumen values obtained laterally across core section. L. Plot is shown in Fig.3.10

<u>Distance</u> (cm)	<u>% Bitumen</u> 1	<u>% Bitumen</u> 2	<u>% Bitumen</u> 3	<u>% Bitumen</u> Mean	<u>Std. Dev.</u>
1	11.5	11.3	10.9	11.2	0.3
2	11.0	11.4	10.8	11.1	0.2
3	10.8	11.3	10.9	11.0	0.2
4	11.6	11.4	10.9	11.3	0.3
5	11.9	11.5	11.1	11.5	0.3
6	12.2	11.5	10.8	11.5	0.5
7	11.8	11.3	10.6	11.2	0.5
8	11.5	11.3	11.0	11.3	0.2
9	11.2	11.4	11.0	11.2	0.2
10	11.6	11.3	11.0	11.3	0.3
11	11.5	11.6	10.9	11.3	0.3
12	11.7	11.6	10.8	11.4	0.4
13	11.9	11.5	10.8	11.4	0.5
14	12.4	11.6	10.8	11.6	0.6
15	12.2	11.5	10.9	11.5	0.6
16	11.6	11.4	10.8	11.3	0.3
17	12.4	11.5	10.8	11.6	0.6
18	12.4	11.5	10.8	11.6	0.7
19	11.6	11.6	10.8	11.3	0.4
20	12.0	11.4	11.0	11.5	0.4
21	11.7	11.3	10.9	11.3	0.3
22	11.3	11.4	10.8	11.2	0.3
23	11.0	11.4	10.9	11.1	0.2
24	11.4	11.5	10.7	11.2	0.3
25	11.5	11.5	10.7	11.3	0.4
26	11.8	11.6	10.7	11.3	0.5
27	11.9	11.5	10.9	11.4	0.5
28	12.0	11.6	10.8	11.5	0.5
29	11.9	11.5	10.8	11.4	0.5
30	11.7	11.5	10.9	11.4	0.4
31	11.7	11.4	10.9	11.3	0.4
32	11.2	11.6	10.6	11.1	0.4
33	11.7	11.6	10.7	11.3	0.5
34	11.7	11.5	10.9	11.4	0.4
35	11.6	11.6	10.6	11.3	0.5
36	11.8	11.7	10.9	11.5	0.4
37	11.6	11.7	10.9	11.4	0.4
38	11.8	11.6	10.9	11.4	0.4
39	11.9	11.6	11.0	11.5	0.4
40	11.5	11.4	10.9	11.2	0.3

41	11.5	11.5	11.0	11.3	0.2
42	11.6	11.5	10.9	11.3	0.3
43	11.7	11.6	11.1	11.5	0.3
44	11.7	12.2	10.9	11.6	0.5
45	11.8	11.6	10.9	11.4	0.4
46	11.6	11.5	11.0	11.3	0.3
47	11.3	11.4	10.9	11.2	0.2
48	11.6	11.3	10.9	11.2	0.3
49	11.7	11.4	10.4	11.2	0.5
50	11.0	11.3	10.6	11.0	0.3
51	10.3	11.4	10.9	10.9	0.5
52	10.9	11.6	11.1	11.2	0.3
53	11.4	11.6	11.0	11.3	0.3
54	11.6	11.6	10.8	11.3	0.4
55	11.3	11.3	11.0	11.2	0.1
56	11.2	11.1	10.9	11.1	0.1
57	9.7	11.9	11.0	10.9	0.9
58	10.6	11.5	11.0	11.0	0.4
59	11.1	11.5	10.9	11.2	0.3
60	10.9	11.2	11.0	11.0	0.1
61	10.9	11.2	10.8	10.9	0.2
62	11.1	11.5	10.8	11.1	0.3
63	11.0	11.6	11.0	11.2	0.3
64	11.4	11.6	10.9	11.3	0.3
65	11.3	11.6	11.0	11.3	0.3
66	11.2	11.5	11.1	11.3	0.2
67	11.4	11.5	11.0	11.3	0.2

SECTION 3

Data for bitumen values estimated for the vertical transect of oil sand using the PCR calibration model on non-roughened surfaces. The estimated wt % bitumen values were used to construct the plot illustrated in Fig. 3.7

<u>Sample #</u>	<u>Estimated Wt % bitumen</u>	<u>Estimated Error</u>	<u>Mahalanobis Distance</u>	<u>Spectral Residual (%)</u>
<u>Top of core</u>				
1	7.51	0.1	0.11	0.2
2	6.63	0.1	0.11	0.2
3	5.87	0.09	0.11	0.16
4	4.47	0.08	0.09	0.07
5	4.4	0.11	0.13	0.09
6	5.42	0.14	0.16	0.12
7	4.46	0.14	0.16	0.18
8	5.98	0.12	0.13	0.21
9	5.27	0.08	0.08	0.19
10	6.3	0.16	0.19	0.18
11	6.55	0.13	0.15	0.25
12	4.57	0.18	0.2	0.23
13	4.98	0.24	0.27	0.24
14	10.68	0.07	0.05	0.3
15	10.79	0.06	0.04	0.27
16	8.36	0.04	0.03	0.21
17	6.23	0.03	0.03	0.15
18	6.59	0.05	0.05	0.16
19	6.87	0.14	0.17	0.15
20	8.38	0.07	0.07	0.24
21	10.09	0.07	0.06	0.31
22	10.91	0.07	0.06	0.44
23	10.83	0.08	0.07	0.48
24	10.26	0.11	0.11	0.48
25	10.41	0.06	0.05	0.44
26	10.93	0.07	0.05	0.44
27	11.44	0.06	0.04	0.42
28	11.65	0.07	0.06	0.45
29	11.1	0.07	0.06	0.39
30	10.58	0.06	0.06	0.22
31	10.87	0.04	0.02	0.25
32	9.9	0.02	0.02	0.12
33	8.52	0.05	0.05	0.09
34	8.22	0.05	0.06	0.08
35	6.89	0.16	0.18	0.22
36	6.81	0.11	0.11	0.21
37	7.09	0.13	0.14	0.21
38	6.3	0.18	0.2	0.23

39	6.17	0.2	0.23	0.25
40	8.24	0.06	0.06	0.14
41	9.8	0.09	0.09	0.24
42	9.89	0.25	0.3	0.35
43	9.58	0.22	0.26	0.33
44	8.53	0.31	0.36	0.4
45	9.42	0.61	0.72	0.66
46	9.45	0.86	1.02	0.87
47	8.67	0.37	0.43	0.37
48	10.54	0.07	0.06	0.27
49	9.82	0.05	0.05	0.13
50	9.96	0.13	0.15	0.12
51	10.67	0.05	0.05	0.15
52	10.84	0.05	0.05	0.18
53	11.01	0.11	0.12	0.19
54	10.44	0.1	0.12	0.15
55	11.23	0.15	0.18	0.19
56	10.77	0.05	0.05	0.23
57	9.1	0.06	0.06	0.25
58	11.48	0.12	0.12	0.54
59	11	0.12	0.12	0.49
60	10.65	0.07	0.06	0.38
61	11.39	0.13	0.13	0.6
62	10.99	0.07	0.06	0.45
63	11.24	0.1	0.1	0.54
64	11.62	0.13	0.13	0.62
65	10.97	0.14	0.15	0.57
66	11.42	0.17	0.18	0.64
67	11.58	0.12	0.12	0.58
68	11.5	0.09	0.08	0.47
69	9.8	0.21	0.24	0.53
70	10.74	0.29	0.33	0.58
71	10.27	0.66	0.77	0.8
72	5.51	0.24	0.27	0.57
73	10.59	0.12	0.11	0.63
74	10.94	0.11	0.11	0.68
75	11.49	0.11	0.1	0.64
76	12.18	0.11	0.1	0.71
77	12.03	0.09	0.08	0.61
78	11.61	0.12	0.12	0.68
79	11.72	0.14	0.14	0.68
80	12.31	0.12	0.12	0.64
81	11.91	0.09	0.08	0.61
82	12.15	0.11	0.1	0.66
83	12.44	0.13	0.13	0.74
84	11.69	0.1	0.09	0.65
85	12.46	0.12	0.11	0.72
86	12.21	0.11	0.1	0.65
87	12.31	0.13	0.13	0.71
88	12.14	0.12	0.11	0.65

89	12.37	0.13	0.12	0.68
90	12.14	0.12	0.12	0.5
91	12.09	0.11	0.11	0.5
92	12.06	0.12	0.13	0.62
93	11.68	0.2	0.22	0.66
94	12.33	0.12	0.12	0.64
95	12.33	0.11	0.11	0.63
96	12.12	0.12	0.12	0.65
97	11.97	0.08	0.07	0.58
98	12.08	0.13	0.13	0.71
99	12.21	0.11	0.11	0.67
100	12.23	0.12	0.12	0.7
101	12.21	0.13	0.13	0.73
102	11.58	0.1	0.1	0.59
103	11.79	0.14	0.15	0.69
104	11.72	0.1	0.09	0.59
105	12.05	0.09	0.08	0.55
106	12.08	0.12	0.11	0.64
107	12.22	0.09	0.09	0.59
108	12.2	0.09	0.09	0.54
109	11.91	0.09	0.08	0.46
110	12.07	0.13	0.13	0.68
111	12.16	0.09	0.09	0.54
112	12.13	0.1	0.1	0.61
113	12.02	0.11	0.1	0.59
114	12.01	0.1	0.09	0.58
115	6.66	0.4	0.47	0.26
116	6.06	1.42	1.68	0.57
117	8.91	0.38	0.45	0.29
118	7.41	1.08	1.26	0.6
119	6.76	0.57	0.66	0.36
120	7.33	0.28	0.31	0.36
121	8.14	0.25	0.28	0.31
122	8.15	0.52	0.6	0.39
123	7.69	0.33	0.37	0.37
124	6.66	0.29	0.31	0.36
125	8.85	0.3	0.34	0.35
126	8.29	0.24	0.26	0.35
127	6.82	0.16	0.16	0.31
128	7.06	0.16	0.16	0.33
129	7.77	0.12	0.11	0.27
130	9.33	0.2	0.22	0.28
131	10.91	0.25	0.3	0.13
132	11.54	0.16	0.19	0.22
133	10.71	0.09	0.1	0.19
134	9.48	0.09	0.05	0.25
135	8.83	0.23	0.25	0.37
136	10.97	0.07	0.06	0.39
137	11.79	0.13	0.14	0.56
138	12.27	0.12	0.13	0.56

139	12.39	0.14	0.14	0.61
140	12	0.13	0.14	0.57
141	12.22	0.17	0.19	0.7
142	12.2	0.2	0.23	0.75
143	12.21	0.18	0.19	0.69
144	12.31	0.15	0.17	0.64
145	11.88	0.14	0.15	0.57
146	12.4	0.12	0.13	0.55
147	12.21	0.13	0.14	0.52
148	12.22	0.14	0.16	0.39
149	12.18	0.13	0.14	0.5
150	12.01	0.13	0.14	0.55
151	12.06	0.14	0.15	0.61
152	12.13	0.15	0.17	0.66
153	12.34	0.15	0.16	0.63
154	11.7	0.13	0.14	0.53
155	11.96	0.13	0.14	0.56
156	12.08	0.14	0.15	0.59
157	12.43	0.14	0.15	0.59
158	11.97	0.13	0.14	0.55
159	11.9	0.13	0.14	0.47
160	11.73	0.13	0.13	0.48
161	11.45	0.09	0.08	0.54
162	11.81	0.16	0.16	0.72
163	11.18	0.1	0.09	0.52
164	11.56	0.11	0.11	0.6
165	11.72	0.1	0.1	0.58
166	11.71	0.12	0.13	0.59
167	12.05	0.12	0.12	0.65
168	11.64	0.13	0.14	0.6
169	11.9	0.11	0.11	0.53
170	11.86	0.11	0.11	0.49
171	11.97	0.13	0.14	0.61
172	11.76	0.12	0.12	0.53
173	12.06	0.12	0.12	0.52
174	11.27	0.11	0.11	0.51
175	11.32	0.1	0.1	0.51
176	11.09	0.09	0.09	0.43
177	11.49	0.12	0.14	0.44
178	11.48	0.08	0.07	0.44
179	11.57	0.08	0.08	0.39
180	11.23	0.07	0.06	0.33
181	11.34	0.06	0.05	0.38
182	11.52	0.08	0.09	0.27
183	10.64	0.13	0.14	0.29
184	2.15	1.48	1.74	0.51
185	2.94	0.8	0.92	0.44
186	2.66	0.65	0.75	0.42
187	4.22	0.45	0.52	0.39
188	8.34	0.2	0.23	0.23

189	11.23	0.08	0.08	0.41
190	12.04	0.08	0.06	0.44
191	11.6	0.1	0.09	0.47
192	11.2	0.09	0.09	0.41
193	11.41	0.07	0.05	0.4
194	11.53	0.1	0.1	0.5
195	11.5	0.07	0.05	0.4
196	11.56	0.06	0.05	0.36
197	11.49	0.09	0.08	0.48
198	11.2	0.09	0.08	0.4
199	11.63	0.07	0.06	0.41
200	11.35	0.06	0.04	0.36
201	11.38	0.08	0.07	0.42
202	11.32	0.08	0.06	0.44
203	11.35	0.06	0.04	0.39
204	11.66	0.06	0.04	0.43
205	11.44	0.06	0.06	0.29
206	10.88	0.07	0.07	0.33
207	10.48	0.06	0.05	0.26
208	10.73	0.06	0.04	0.29
209	10.99	0.07	0.05	0.35
210	10.77	0.04	0.03	0.28
211	11.76	0.08	0.07	0.35
212	10.44	0.06	0.06	0.24
213	11.17	0.05	0.03	0.32
214	10.68	0.04	0.02	0.28
215	11.21	0.08	0.07	0.47
216	11.34	0.05	0.03	0.39
217	11.26	0.08	0.07	0.44
218	11.41	0.08	0.08	0.27
219	11.37	0.06	0.05	0.41
220	11.3	0.06	0.04	0.39
221	11.15	0.08	0.08	0.41
222	11.26	0.1	0.09	0.48
223	11.4	0.08	0.07	0.44
224	11.17	0.08	0.07	0.44
225	11.39	0.08	0.08	0.46
226	11.27	0.07	0.06	0.45
227	10.35	0.07	0.06	0.32
228	10.41	0.05	0.04	0.34
229	10.25	0.04	0.03	0.26
230	9.06	0.05	0.06	0.19
231	7.21	0.21	0.23	0.31
232	5.03	0.77	0.9	0.7
233	5.17	1.18	1.38	0.85
234	4.58	0.91	1.06	0.63
235	10.57	0.08	0.08	0.32
236	10.11	0.07	0.08	0.29
237	9.21	0.07	0.07	0.3
238	10.23	0.09	0.1	0.31

239	10.45	0.09	0.09	0.32
240	10.66	0.12	0.13	0.33
241	9.83	0.21	0.24	0.35
242	10.74	0.08	0.07	0.3
243	9.97	0.07	0.07	0.29
244	10.71	0.07	0.06	0.32
245	10.95	0.09	0.09	0.38
246	11.07	0.09	0.08	0.39
247	11.4	0.08	0.07	0.4
248	11.51	0.13	0.14	0.45
249	11.41	0.14	0.15	0.5
250	10.96	0.1	0.1	0.43
251	11.41	0.08	0.06	0.41
252	11.47	0.12	0.11	0.52
253	11.33	0.16	0.18	0.57
254	11.33	0.09	0.09	0.35
255	10.9	0.07	0.05	0.46
256	11.3	0.1	0.1	0.48
257	11.39	0.11	0.1	0.46
258	11.4	0.14	0.15	0.57
259	10.66	0.07	0.06	0.41
260	11.35	0.08	0.08	0.39
261	11.29	0.13	0.14	0.53
262	11.1	0.09	0.08	0.42
263	11.03	0.08	0.07	0.4
264	11.37	0.08	0.07	0.44
265	11.37	0.11	0.11	0.48
266	11.49	0.07	0.05	0.39
267	11.36	0.07	0.05	0.44
268	11.52	0.11	0.1	0.53
269	11.37	0.09	0.08	0.46
270	10.52	0.07	0.07	0.25
271	11.52	0.08	0.06	0.43
272	12.37	0.11	0.1	0.62
273	11.24	0.09	0.08	0.48
274	10.37	0.06	0.01	0.37
275	11.56	0.07	0.05	0.33
276	10.6	0.11	0.12	0.28
277	11.13	0.07	0.06	0.31
278	11.74	0.07	0.06	0.43
279	11.43	0.09	0.09	0.5
280	11.43	0.09	0.09	0.48
281	11.02	0.07	0.06	0.38
282	11.52	0.07	0.07	0.32
283	11.38	0.07	0.06	0.39
284	10.73	0.08	0.07	0.4
285	11.27	0.05	0.03	0.37
286	11.23	0.08	0.06	0.38
287	11.06	0.05	0.04	0.32
288	11.13	0.06	0.04	0.34

289	11.04	0.05	0.04	0.36
290	10.62	0.05	0.03	0.34
291	9.27	0.03	0.03	0.19
292	9.72	0.13	0.14	0.37
293	7	0.26	0.3	0.3
294	7.46	0.17	0.2	0.23
295	7.39	0.15	0.18	0.18
296	6.93	0.15	0.17	0.24
297	5.06	0.33	0.39	0.24
298	5.33	0.2	0.22	0.25
299	4.81	0.42	0.49	0.3
300	4.9	0.31	0.36	0.32
301	4.55	0.17	0.2	0.23
302	10.46	0.06	0.06	0.17
303	10.58	0.06	0.06	0.16
304	10.78	0.06	0.05	0.29
305	10.41	0.06	0.06	0.3
306	10.8	0.07	0.06	0.33
307	11.09	0.06	0.04	0.41
308	11.13	0.14	0.15	0.54
309	11.02	0.08	0.08	0.36
310	11.21	0.08	0.07	0.36
311	11.28	0.1	0.1	0.43
312	11.32	0.07	0.06	0.34
313	10.97	0.11	0.13	0.17
314	10.73	0.07	0.08	0.21
315	10.48	0.07	0.08	0.24
316	10.65	0.08	0.08	0.3
317	10.63	0.11	0.11	0.24
318	10.88	0.07	0.06	0.26
319	10.97	0.07	0.07	0.26
320	11.07	0.08	0.08	0.33
321	11.02	0.06	0.05	0.28
322	10.74	0.09	0.1	0.25
323	10.88	0.09	0.09	0.27
324	10.99	0.08	0.07	0.28
325	10.64	0.07	0.07	0.3
326	10.89	0.07	0.07	0.28
327	10.88	0.06	0.05	0.3
328	10.5	0.07	0.07	0.18
329	10.67	0.07	0.07	0.19
330	9.51	0.12	0.14	0.21
331	9.67	0.06	0.06	0.19
332	8.08	0.11	0.12	0.2
333	5.98	0.28	0.32	0.32
334	4.18	0.46	0.54	0.29
335	6.97	0.13	0.14	0.16
336	8.51	0.07	0.08	0.14
337	5.23	0.31	0.35	0.27
338	3.92	0.55	0.64	0.33

339	4.46	0.55	0.65	0.31
340	4.11	0.45	0.53	0.26
341	8.99	0.18	0.21	0.2
342	11.33	0.19	0.21	0.58
343	11.23	0.15	0.17	0.55
344	11.49	0.14	0.15	0.55
345	11.39	0.16	0.17	0.53
346	11.26	0.19	0.21	0.56
347	11.31	0.2	0.22	0.59
348	11.31	0.2	0.22	0.58
349	11.33	0.17	0.19	0.54
350	11.4	0.18	0.2	0.59
351	10.41	0.21	0.23	0.62
352	11.55	0.24	0.27	0.71
353	11.39	0.17	0.19	0.57
354	10.99	0.12	0.13	0.48
355	11.07	0.17	0.19	0.52
356	8.79	0.14	0.15	0.33
357	7.91	0.1	0.11	0.29
358	9.09	0.06	0.06	0.2
359	9.41	0.08	0.09	0.22
360	9.1	0.11	0.12	0.24
361	8.4	0.11	0.13	0.17
362	9.07	0.09	0.09	0.26
363	9.11	0.09	0.09	0.27
364	11.4	0.08	0.06	0.42
365	10.53	0.09	0.09	0.44
366	11.18	0.13	0.14	0.51
367	11.35	0.15	0.16	0.56
368	10.73	0.09	0.08	0.41
369	8.98	0.08	0.09	0.21
370	7.43	0.09	0.08	0.31
371	7.76	0.09	0.07	0.3
372	9.98	0.05	0.02	0.27
373	11.44	0.14	0.14	0.57
374	11.12	0.12	0.12	0.47
375	11.14	0.2	0.22	0.56
376	10.51	0.22	0.25	0.51
377	11.24	0.15	0.16	0.54
378	10.28	0.21	0.23	0.5
379	8.69	0.11	0.12	0.24
380	8.12	0.1	0.11	0.24
381	7.59	0.08	0.08	0.2
382	8.51	0.05	0.03	0.18
383	8.01	0.09	0.07	0.31
384	9.86	0.05	0.01	0.23
385	10.76	0.08	0.08	0.39
386	11.32	0.11	0.11	0.48
387	11.12	0.16	0.17	0.54
388	10.92	0.08	0.07	0.47

389	11.33	0.15	0.16	0.55
390	11.26	0.14	0.14	0.49
391	11.15	0.08	0.06	0.44
392	11.36	0.12	0.12	0.53
393	11.46	0.09	0.07	0.44
394	11.28	0.13	0.13	0.47
395	11.04	0.07	0.06	0.43
396	11.46	0.17	0.19	0.59
397	11.48	0.14	0.14	0.53
398	11.18	0.19	0.21	0.55
399	11.27	0.16	0.18	0.55
400	10.77	0.07	0.06	0.35
401	10.75	0.1	0.1	0.4
402	10.98	0.15	0.16	0.53
403	10.41	0.11	0.11	0.4
404	8.94	0.13	0.14	0.29
405	10.36	0.11	0.12	0.42
406	10.44	0.14	0.15	0.42
407	9.7	0.12	0.13	0.39
408	9.59	0.12	0.13	0.25
409	8.26	0.11	0.12	0.25
410	8.68	0.1	0.11	0.24
411	6.44	0.07	0.08	0.21
412	9.23	0.07	0.07	0.28
413	2.34	0.36	0.42	0.37
414	1.03	0.37	0.43	0.32
415	3.95	0.09	0.1	0.18
416	7.78	0.04	0.04	0.17
417	8.66	0.05	0.04	0.18
418	9.32	0.04	0.03	0.2
419	9.51	0.06	0.06	0.22
420	8.65	0.14	0.16	0.26
421	4.45	0.31	0.37	0.3
422	4.13	0.07	0.07	0.14
423	1.77	0.13	0.16	0.07
424	2.38	0.09	0.11	0.08
425	2.69	0.09	0.1	0.08
426	1.96	0.09	0.11	0.1
427	5.31	0.08	0.09	0.17
428	4.14	0.2	0.23	0.3
429	4.56	0.19	0.22	0.27
430	8.46	0.07	0.08	0.23
431	9.35	0.05	0.05	0.25
432	10.04	0.04	0.02	0.29
433	10.1	0.05	0.04	0.3
434	9.55	0.06	0.05	0.3
435	9.21	0.07	0.06	0.3
436	10.16	0.07	0.06	0.39
437	10.79	0.1	0.09	0.49
438	10.64	0.11	0.12	0.46

439	9.04	0.08	0.08	0.3
440	8.08	0.08	0.08	0.27
441	9.39	0.08	0.07	0.3
442	9.51	0.09	0.1	0.28
443	10.22	0.15	0.17	0.34
444	9.62	0.14	0.16	0.36
445	9.88	0.12	0.13	0.36
446	9.45	0.16	0.18	0.34
447	7.68	0.28	0.33	0.33
448	0.96	0.3	0.35	0.23
449	2.29	0.13	0.15	0.12
450	3.06	0.1	0.11	0.14
451	0.88	0.15	0.18	0.16
452	1.86	0.16	0.19	0.15
453	5.14	0.24	0.28	0.25
454	10	0.06	0.06	0.23
455	10.08	0.08	0.08	0.3
456	8.18	0.09	0.09	0.28
457	7.72	0.04	0.03	0.18
458	9.08	0.05	0.04	0.23
459	10.6	0.14	0.15	0.43
460	7.96	0.11	0.12	0.3
461	10.17	0.06	0.05	0.38
462	10.88	0.16	0.18	0.54
463	11.11	0.14	0.15	0.52
464	10.14	0.09	0.09	0.36
465	10.54	0.12	0.13	0.41
466	10.2	0.12	0.13	0.41
467	10.01	0.12	0.12	0.49
468	11.55	0.13	0.12	0.61
469	10.8	0.19	0.21	0.53
470	10.93	0.19	0.22	0.57
471	10.42	0.18	0.2	0.48
472	10.41	0.1	0.11	0.4
473	10.16	0.16	0.18	0.43
474	10.78	0.19	0.21	0.53
475	11.3	0.18	0.2	0.52
476	11.48	0.18	0.2	0.56
477	11.63	0.19	0.21	0.57
478	1.11	0.2	0.23	0.25
479	2.78	0.41	0.48	0.49
480	3.77	1.1	1.3	0.63
481	2.01	2.83	3.34	1.08
482	2.31	2.39	2.82	1
483	4.63	1.95	2.3	1.1
484	1.1	0.25	0.29	0.14
485	2.59	0.11	0.12	0.29
486	3.26	0.19	0.2	0.38
487	5.4	0.08	0.08	0.24
488	5.3	0.09	0.1	0.21

489	6.03	0.07	0.06	0.24
490	6.21	0.15	0.15	0.36
491	5.14	0.08	0.08	0.19
492	5.07	0.09	0.09	0.26
493	6.75	0.11	0.12	0.28
494	4.48	0.14	0.15	0.24
495	6.32	0.12	0.14	0.26
496	9.61	0.07	0.06	0.35
497	9.11	0.08	0.07	0.38
498	10.06	0.1	0.11	0.29
499	8.2	0.19	0.23	0.23
500	9.31	0.21	0.24	0.25
501	8.03	0.28	0.33	0.3
502	6.65	0.28	0.33	0.28
503	9.23	0.23	0.28	0.21
504	7.66	0.19	0.21	0.29
505	9.82	0.12	0.14	0.25
506	9.18	0.09	0.09	0.36
507	11.26	0.1	0.1	0.54
508	11.21	0.09	0.08	0.51
509	10.76	0.08	0.07	0.36
510	8.03	0.11	0.12	0.32
511	10.13	0.06	0.06	0.25
512	11.27	0.06	0.04	0.3
513	10.97	0.06	0.04	0.38
514	11.21	0.07	0.06	0.42
515	9.9	0.05	0.03	0.35
516	9.83	0.09	0.09	0.23
517	8.92	0.09	0.09	0.23
518	8.81	0.06	0.06	0.15
519	7.08	0.12	0.14	0.21
520	9.03	0.81	0.95	0.74
521	8.72	0.46	0.55	0.42
522	10.32	0.23	0.27	0.42
523	10.65	0.28	0.32	0.49
524	11.22	0.35	0.39	0.59
525	10.46	0.34	0.39	0.56
526	8.54	0.84	0.98	0.78
527	8.81	1.06	1.24	0.94
528	8.9	0.56	0.66	0.59
529	11.45	0.12	0.13	0.44
530	10.05	0.14	0.16	0.31
531	11.14	0.11	0.12	0.44
532	11.59	0.17	0.18	0.58
533	12.08	0.14	0.15	0.58
534	12.1	0.12	0.12	0.53
535	12.07	0.16	0.18	0.65
536	12.18	0.17	0.18	0.66
537	11.95	0.13	0.14	0.55
538	11.82	0.13	0.13	0.53

539	12.3	0.13	0.13	0.62
540	11.44	0.12	0.13	0.5
541	12.24	0.14	0.15	0.67
542	11.26	0.12	0.12	0.48
543	10.99	0.14	0.15	0.49
544	11.66	0.14	0.15	0.56
545	11.9	0.12	0.12	0.53
546	11.96	0.15	0.16	0.63
547	12.18	0.19	0.21	0.73
548	12.17	0.2	0.22	0.75
549	11.93	0.18	0.19	0.67
550	12.17	0.14	0.14	0.61
551	11.63	0.12	0.13	0.47
552	11.91	0.13	0.13	0.57
553	11.6	0.13	0.14	0.52
554	12.21	0.12	0.11	0.56
555	11.84	0.12	0.12	0.53
556	12.07	0.11	0.11	0.49
557	12.42	0.13	0.13	0.53
558	12.19	0.13	0.13	0.65
559	12.59	0.14	0.14	0.67
560	12.2	0.13	0.13	0.58
561	12.19	0.12	0.12	0.63
562	13.02	0.15	0.16	0.68
563	12.29	0.17	0.18	0.77
564	11.95	0.18	0.19	0.75
565	11.9	0.1	0.1	0.54
566	10.35	0.16	0.18	0.42
567	6.16	0.17	0.19	0.55
568	9.33	0.12	0.13	0.45
569	12.3	0.1	0.1	0.48
570	12.19	0.13	0.13	0.66
571	12.18	0.19	0.2	0.82
572	12.4	0.12	0.12	0.7
573	12.37	0.13	0.12	0.71
574	11.19	0.08	0.07	0.47
575	11.13	0.08	0.08	0.44
576	9.89	0.11	0.1	0.54
577	4.99	0.24	0.27	0.55
578	11.84	0.1	0.1	0.56
579	12.28	0.11	0.11	0.51
580	11.92	0.09	0.08	0.58
581	12.67	0.13	0.12	0.66
582	12.14	0.1	0.09	0.54
583	11.88	0.1	0.09	0.5
584	12.04	0.12	0.12	0.55
585	11.14	0.09	0.08	0.5
586	12.05	0.12	0.12	0.52
587	10.18	0.1	0.09	0.46
588	9.68	0.21	0.23	0.53

589	12.15	0.11	0.11	0.51
590	11.56	0.14	0.15	0.44
591	11.3	0.12	0.12	0.51
592	11.01	0.11	0.12	0.34
593	10.96	0.11	0.12	0.29
594	10.92	0.15	0.16	0.5
595	10.37	0.11	0.12	0.35
596	9.97	0.08	0.08	0.34
597	9.77	0.28	0.33	0.48
598	4.12	0.41	0.47	0.63
599	4	0.28	0.31	0.6
600	8.41	0.26	0.29	0.52
601	10.54	0.12	0.14	0.36
602	11.22	0.07	0.06	0.47
603	11.54	0.08	0.08	0.42
604	11.42	0.1	0.11	0.45
605	11.14	0.08	0.09	0.37
606	11.84	0.08	0.06	0.57
607	12.07	0.1	0.1	0.52
608	11.98	0.15	0.16	0.52
609	11.85	0.13	0.14	0.47
610	11.83	0.08	0.08	0.48
611	11.49	0.07	0.05	0.5
612	11.15	0.08	0.07	0.46
613	10.29	0.18	0.2	0.34
614	9.54	0.22	0.25	0.39
615	9.24	0.11	0.12	0.38
616	9.49	0.07	0.07	0.32
617	10.11	0.08	0.07	0.39
618	10.61	0.07	0.07	0.39
619	11.02	0.06	0.05	0.38
620	11.48	0.06	0.05	0.42
621	11.23	0.06	0.05	0.39
622	11.6	0.07	0.05	0.45
623	11.51	0.09	0.06	0.54
624	11.37	0.09	0.08	0.46
625	10.68	0.17	0.19	0.49
626	11.43	0.09	0.08	0.57
627	10.61	0.08	0.07	0.39
628	11.16	0.09	0.08	0.51
629	11.38	0.08	0.06	0.48
630	11.88	0.23	0.27	0.38
631	10.98	0.13	0.13	0.47
632	10.76	0.14	0.15	0.47
633	11.59	0.08	0.06	0.43
634	10.58	0.11	0.11	0.36
635	10.58	0.07	0.06	0.26
636	9.06	0.07	0.08	0.19
637	8.51	0.1	0.1	0.28
638	7.03	0.13	0.12	0.39

639	5.99	0.76	0.89	0.65
640	9.94	0.11	0.12	0.18
641	10.54	0.06	0.07	0.19
642	11.02	0.04	0.03	0.28
643	11.11	0.13	0.14	0.46
644	10.92	0.11	0.11	0.43
645	9.28	0.19	0.22	0.45
646	10.65	0.09	0.09	0.35
647	9.98	0.14	0.16	0.2
648	7.59	0.1	0.11	0.24
649	6.49	0.41	0.47	0.34
650	9.81	0.06	0.07	0.2
651	10.12	0.08	0.08	0.23
652	10.52	0.09	0.09	0.22
653	10.59	0.1	0.11	0.22
654	10.97	0.07	0.07	0.25
655	10.48	0.08	0.09	0.24
656	10.06	0.11	0.12	0.18
657	10.97	0.06	0.04	0.34
658	10.99	0.07	0.06	0.34
659	10.69	0.09	0.09	0.28
660	10.97	0.14	0.15	0.49
661	11	0.12	0.11	0.47
662	10.68	0.12	0.12	0.4
663	10.46	0.1	0.09	0.36
664	11.1	0.12	0.11	0.54
665	10.9	0.16	0.17	0.54
666	11.37	0.21	0.23	0.67
667	10.98	0.14	0.15	0.46
668	11.12	0.2	0.22	0.62
669	10.65	0.15	0.17	0.42
670	10.85	0.12	0.13	0.43
671	10.83	0.17	0.19	0.5
672	10.51	0.13	0.14	0.37
673	10.83	0.31	0.36	0.65
674	10.84	0.18	0.2	0.56
675	10.72	0.14	0.16	0.45
676	10.69	0.17	0.19	0.47
677	10.5	0.15	0.16	0.44
678	10.61	0.12	0.13	0.39
679	11.18	0.13	0.13	0.51
680	10.65	0.21	0.24	0.55
681	10.43	0.14	0.15	0.38
682	9.98	0.15	0.16	0.3
683	10.68	0.15	0.17	0.45
684	11.09	0.16	0.16	0.57
685	10.75	0.1	0.1	0.36
686	10.86	0.1	0.1	0.35
687	10.5	0.14	0.16	0.32
688	10.62	0.12	0.13	0.34

689	10.35	0.15	0.17	0.38
690	10.58	0.11	0.12	0.35
691	10.87	0.12	0.11	0.43
692	10.36	0.13	0.14	0.28
693	10.58	0.18	0.2	0.48
694	10.71	0.11	0.11	0.37
695	9.94	0.09	0.05	0.44
696	5.86	1.23	1.45	0.9
697	10.74	0.26	0.3	0.59
698	10.79	0.19	0.21	0.54
699	10.35	0.13	0.14	0.37
700	10.05	0.17	0.2	0.4
701	10.91	0.11	0.11	0.42
702	10.65	0.15	0.17	0.29
703	10.63	0.05	0.04	0.23
704	10.96	0.09	0.08	0.36
705	11.05	0.09	0.09	0.39
706	10.73	0.11	0.11	0.38
707	10.85	0.14	0.15	0.47
708	10.56	0.15	0.16	0.45
709	9.01	0.31	0.36	0.48
710	9.86	0.23	0.27	0.34
711	9.2	0.25	0.29	0.27
712	7.19	0.16	0.18	0.26
713	5.47	0.24	0.26	0.42
714	4.21	0.68	0.8	0.39
715	5.29	0.14	0.16	0.31
716	5.29	0.22	0.26	0.33
717	8.56	0.24	0.15	0.28
718	6.1	0.3	0.33	0.46
719	4.11	0.9	1.05	0.59
720	8.98	0.15	0.16	0.38
721	10.5	0.11	0.12	0.31
722	10.94	0.09	0.1	0.39
723	11.18	0.09	0.09	0.41
724	11	0.1	0.11	0.32
725	10.94	0.11	0.12	0.41
726	10.62	0.12	0.13	0.34
727	10.4	0.16	0.18	0.36
728	10.44	0.21	0.25	0.32
729	10.83	0.1	0.11	0.29
730	11.12	0.08	0.08	0.34
731	11.43	0.06	0.04	0.35
732	10.7	0.1	0.1	0.36
733	10.17	0.3	0.35	0.31
734	10.25	0.15	0.17	0.36
735	10.81	0.1	0.11	0.42
736	12.03	0.27	0.32	0.46
737	11.17	0.14	0.16	0.3
738	10.88	0.16	0.18	0.31

739	10.11	0.45	0.53	0.4
740	8.72	0.46	0.54	0.27
741	10.63	0.1	0.11	0.22
742	10.4	0.1	0.12	0.22
743	11.16	0.18	0.21	0.26
744	10.22	0.18	0.16	0.47
745	11.46	0.17	0.2	0.3
746	10.47	0.16	0.19	0.24
747	10.8	0.07	0.07	0.32
748	11.21	0.07	0.06	0.32
749	11.44	0.08	0.08	0.39
750	11.1	0.11	0.11	0.42
751	10.44	0.1	0.1	0.32
752	10.87	0.11	0.11	0.41
753	11.02	0.09	0.08	0.38
754	10.97	0.09	0.09	0.38
755	11.18	0.11	0.11	0.43
756	10.91	0.11	0.11	0.44
757	10.28	0.16	0.18	0.34
758	10.31	0.13	0.14	0.31
759	10.76	0.12	0.14	0.33
760	11.06	0.11	0.12	0.45
761	10.98	0.12	0.12	0.48
762	10.98	0.14	0.15	0.53
763	10.79	0.2	0.22	0.57
764	10.42	0.14	0.16	0.41
765	10.75	0.11	0.12	0.33
766	10.91	0.15	0.16	0.48
767	10.2	0.18	0.21	0.3
768	10.3	0.13	0.15	0.34
769	10.86	0.11	0.11	0.41
770	10.24	0.15	0.16	0.33
771	10.37	0.2	0.22	0.5
772	11.54	0.09	0.07	0.43
773	10.12	0.12	0.12	0.3
774	10.46	0.12	0.13	0.34
775	11.9	0.09	0.07	0.5
776	10.88	0.13	0.13	0.43
777	11.25	0.12	0.12	0.38
778	10.44	0.22	0.25	0.39
779	9.51	0.25	0.3	0.25
780	9.8	0.19	0.22	0.28
781	10.45	0.12	0.12	0.42
782	9.77	0.23	0.26	0.24
783	10.5	0.09	0.08	0.31
784	10.86	0.16	0.17	0.52
785	11.05	0.15	0.16	0.51
786	10.85	0.15	0.16	0.47
787	10.23	0.14	0.15	0.37
788	10.97	0.14	0.15	0.49

789	10.04	0.13	0.14	0.31
790	9.43	0.19	0.22	0.18
791	9.17	0.17	0.2	0.2
792	9.97	0.14	0.16	0.35
793	10.07	0.13	0.14	0.33
794	11.06	0.17	0.19	0.55
795	10.76	0.19	0.21	0.52
796	10.65	0.12	0.13	0.39
797	10.52	0.13	0.15	0.41
798	10.96	0.2	0.22	0.58
799	10.93	0.22	0.24	0.59
800	11	0.16	0.16	0.54
801	9.58	0.13	0.15	0.2
802	10.79	0.12	0.12	0.44
803	10.1	0.12	0.13	0.25
804	10.96	0.23	0.26	0.63
805	11.34	0.23	0.25	0.69
806	10.92	0.15	0.16	0.49
807	10.09	0.14	0.15	0.38
808	10.87	0.15	0.16	0.57
809	10.82	0.16	0.17	0.56
810	10.65	0.12	0.12	0.47
811	10.1	0.12	0.13	0.33
812	10.2	0.09	0.1	0.29
813	9.08	0.22	0.25	0.24
814	9.48	0.12	0.14	0.22
815	10.78	0.11	0.11	0.41
816	10.92	0.18	0.2	0.56
817	10.09	0.12	0.13	0.41
818	8.51	0.1	0.09	0.36
819	10.82	0.12	0.12	0.5
820	10.71	0.08	0.06	0.4
821	10.82	0.11	0.11	0.49
822	10.66	0.11	0.1	0.45
823	10.85	0.1	0.09	0.45
824	10.78	0.11	0.1	0.44
825	10.85	0.11	0.1	0.47
826	10.86	0.1	0.1	0.5
827	10.96	0.13	0.13	0.54
828	10.7	0.11	0.11	0.43
829	11.04	0.15	0.15	0.54
830	10.67	0.2	0.22	0.53
831	10.23	0.15	0.17	0.41
832	9.8	0.18	0.21	0.39
833	10.83	0.21	0.23	0.56
834	10.12	0.16	0.17	0.41
835	10.53	0.14	0.15	0.41
836	8.81	0.28	0.32	0.55
837	6.76	0.58	0.69	0.62
838	6.18	0.51	0.6	0.39

839	4.44	0.51	0.6	0.33
840	4.09	0.88	1.04	0.42
841	9.46	0.11	0.13	0.3
842	8.94	0.07	0.07	0.28
843	9.87	0.24	0.27	0.49
844	10.39	0.11	0.11	0.43
845	10.27	0.11	0.11	0.36
846	10.5	0.14	0.15	0.45
847	10.26	0.1	0.1	0.37
848	10.16	0.12	0.12	0.36
849	10.74	0.1	0.1	0.36
850	10.23	0.09	0.1	0.34
851	10.54	0.08	0.07	0.37
852	10.39	0.11	0.12	0.36
853	10.63	0.12	0.13	0.38
854	10.37	0.15	0.16	0.41
855	10.47	0.16	0.18	0.44
856	10.49	0.17	0.19	0.43
857	10.32	0.19	0.22	0.45
858	11.32	0.15	0.16	0.56
859	10.5	0.18	0.2	0.45
860	10.61	0.19	0.21	0.46
861	10.45	0.19	0.21	0.45
862	9.67	0.24	0.27	0.43
863	11.53	0.1	0.09	0.53
864	9.92	0.11	0.11	0.39
865	10.1	0.08	0.07	0.43
866	9.87	0.15	0.17	0.41
867	9.96	0.16	0.18	0.42
868	10.36	0.11	0.12	0.49
869	10.09	0.13	0.14	0.51
870	9.08	0.16	0.18	0.41
871	8.92	0.15	0.16	0.37
872	9.07	0.18	0.21	0.45
873	9.25	0.13	0.14	0.37
874	9.61	0.08	0.07	0.39
875	9.88	0.09	0.08	0.4
876	10.68	0.08	0.06	0.39
877	9.68	0.09	0.09	0.36
878	10.6	0.09	0.08	0.42
879	10.39	0.07	0.04	0.37
880	9.69	0.1	0.09	0.4
881	9.89	0.11	0.12	0.46
882	8.61	0.12	0.12	0.39
883	9.34	0.11	0.11	0.37
884	8.01	0.15	0.16	0.41
885	6.41	0.23	0.25	0.45
886	5.63	0.29	0.33	0.46
887	7.68	0.4	0.45	0.63
888	6.9	0.3	0.34	0.48

889	8.82	0.12	0.13	0.36
890	10.3	0.12	0.11	0.45
891	9.72	0.15	0.16	0.41
892	10.64	0.24	0.27	0.58
893	10.55	0.21	0.24	0.55
894	10.62	0.19	0.21	0.5
895	10.53	0.21	0.24	0.52
896	8.89	0.15	0.18	0.28
897	10.12	0.1	0.1	0.33
898	10.92	0.13	0.14	0.48
899	9.94	0.1	0.1	0.36
900	9.36	0.14	0.15	0.34
901	9.89	0.16	0.17	0.43
902	10.08	0.18	0.2	0.43
903	10.37	0.2	0.22	0.47
904	9.2	0.18	0.2	0.45
905	9.59	0.11	0.12	0.39
906	10.62	0.12	0.11	0.51
907	9.67	0.07	0.06	0.39
908	10.82	0.13	0.13	0.43
909	10.92	0.14	0.14	0.45
910	10.74	0.13	0.13	0.45
911	10.94	0.13	0.14	0.47
912	10.76	0.14	0.14	0.48
913	10.75	0.14	0.15	0.49
914	10.99	0.16	0.17	0.48
915	10.77	0.13	0.13	0.47
916	10.4	0.13	0.13	0.5
917	10.4	0.11	0.11	0.48
918	10.75	0.12	0.12	0.49
919	9.82	0.09	0.09	0.44
920	10.24	0.16	0.17	0.49
921	10.74	0.14	0.15	0.5
922	11.02	0.14	0.15	0.48
923	10.87	0.15	0.16	0.5
924	11	0.17	0.18	0.5
925	10.9	0.17	0.18	0.5
926	11.05	0.16	0.17	0.52
927	11.26	0.17	0.18	0.54
928	11.03	0.14	0.15	0.51
929	10.92	0.16	0.17	0.48
930	10.39	0.15	0.16	0.5
931	10.3	0.16	0.18	0.47
932	10.51	0.11	0.11	0.43
933	9.91	0.09	0.06	0.49
934	9.23	0.1	0.06	0.54
935	10.71	0.06	0.04	0.36
936	10.83	0.16	0.17	0.47
937	11.34	0.18	0.19	0.54
938	10.57	0.16	0.15	0.55

939	10.93	0.17	0.18	0.56
940	11.44	0.18	0.19	0.62
941	11.28	0.19	0.2	0.6
942	11.16	0.17	0.18	0.53
943	11.02	0.16	0.17	0.5
944	10.48	0.19	0.21	0.47
945	9.25	0.18	0.2	0.55
946	9.26	0.25	0.29	0.45
947	10.08	0.1	0.09	0.37
948	11.05	0.15	0.16	0.46
949	11.86	0.13	0.11	0.57
950	10.85	0.12	0.12	0.43
951	11.17	0.15	0.15	0.52
952	10.39	0.14	0.15	0.45
953	10.81	0.16	0.17	0.48
954	10.75	0.14	0.11	0.56
955	9.84	0.19	0.21	0.41
956	9.52	0.15	0.16	0.38
957	9.37	0.16	0.17	0.38
958	10.08	0.13	0.15	0.39
959	10.28	0.15	0.16	0.51
960	9.71	0.12	0.13	0.31
961	10.72	0.12	0.12	0.46
962	10.2	0.14	0.15	0.46
963	10.52	0.12	0.13	0.39
964	10.86	0.11	0.11	0.41
965	10.6	0.17	0.19	0.4
966	9.59	0.15	0.16	0.44
967	10.21	0.2	0.23	0.41
968	10.44	0.13	0.13	0.35
969	9.97	0.14	0.14	0.39
970	9.58	0.09	0.08	0.35
971	10.1	0.12	0.12	0.42
972	11.33	0.06	0.04	0.46
973	10.66	0.11	0.11	0.46
974	10.63	0.1	0.1	0.39
975	10.65	0.1	0.11	0.32
976	10.7	0.11	0.11	0.34
977	11.08	0.09	0.08	0.42
978	11.25	0.11	0.1	0.51
979	10.75	0.11	0.11	0.43
980	10.76	0.11	0.12	0.33
981	10.03	0.11	0.12	0.38
982	9.29	0.14	0.16	0.36
983	9.98	0.15	0.13	0.48
984	10.25	0.08	0.08	0.28
985	11.01	0.07	0.06	0.46
986	9.81	0.19	0.21	0.51
987	9.91	0.11	0.12	0.31
988	9.96	0.13	0.12	0.51

989	10.48	0.09	0.07	0.47
990	10.48	0.09	0.09	0.36
991	10.76	0.09	0.07	0.45
992	10.78	0.1	0.08	0.45
993	10.19	0.1	0.11	0.36
994	10.33	0.13	0.14	0.41
995	10.27	0.16	0.18	0.47
996	10.28	0.12	0.13	0.43
997	10.47	0.11	0.11	0.4
998	10.04	0.1	0.09	0.4
999	9.13	0.14	0.16	0.3
1000	8.56	0.14	0.16	0.32
1001	9.61	0.12	0.13	0.33
1002	10.5	0.13	0.14	0.41
1003	10.81	0.14	0.16	0.48
1004	10.32	0.13	0.14	0.45
1005	10.49	0.11	0.11	0.45
1006	10.33	0.13	0.13	0.44
1007	11.07	0.1	0.09	0.45
1008	11.04	0.09	0.07	0.48
1009	10.9	0.1	0.07	0.51
1010	11.47	0.17	0.18	0.59
1011	11.04	0.16	0.15	0.5
1012	10.8	0.16	0.18	0.4
1013	11.61	0.19	0.2	0.57
1014	11.9	0.19	0.21	0.61
1015	12.15	0.19	0.21	0.51
1016	11.83	0.17	0.18	0.57
1017	11.53	0.17	0.19	0.53
1018	11.21	0.22	0.25	0.56
1019	11.58	0.2	0.22	0.6
1020	11.49	0.22	0.24	0.66
1021	11.7	0.17	0.19	0.58
1022	11.91	0.24	0.26	0.79
1023	12.35	0.16	0.16	0.72
1024	12.23	0.18	0.19	0.72
1025	11.6	0.3	0.35	0.8
1026	12.37	0.21	0.22	0.84
1027	12.44	0.15	0.15	0.66
1028	11.56	0.14	0.15	0.45
1029	12.03	0.16	0.17	0.61
1030	11.73	0.17	0.19	0.58
1031	11.33	0.2	0.23	0.59
1032	10.95	0.29	0.33	0.67
1033	11.42	0.2	0.23	0.61
1034	11.52	0.19	0.21	0.65
1035	11.77	0.17	0.19	0.58
1036	11.94	0.14	0.15	0.5
1037	12.01	0.15	0.15	0.61
1038	11.91	0.23	0.24	0.85

1039	11.7	0.17	0.18	0.68
1040	11.71	0.19	0.2	0.69
1041	11.15	0.23	0.26	0.63
1042	11.65	0.24	0.26	0.8
1043	11.69	0.26	0.3	0.82
1044	11.61	0.2	0.22	0.68
1045	11.84	0.17	0.19	0.65
1046	11.61	0.24	0.27	0.73
1047	11.81	0.21	0.24	0.7
1048	11.91	0.16	0.17	0.6
1049	11.51	0.16	0.16	0.64
1050	11.47	0.27	0.31	0.8
1051	11.62	0.2	0.22	0.65
1052	11.71	0.18	0.2	0.62
1053	11.72	0.19	0.21	0.73
1054	11.83	0.15	0.15	0.66
1055	11.55	0.19	0.21	0.67
1056	11.34	0.22	0.25	0.65
1057	11.56	0.16	0.17	0.64
1058	11.67	0.17	0.19	0.71
1059	11	0.22	0.24	0.62
1060	10.29	0.14	0.14	0.51
1061	10.91	0.11	0.11	0.46
1062	11.43	0.14	0.14	0.58
1063	11.64	0.16	0.18	0.69
1064	11.26	0.14	0.15	0.62
1065	11.16	0.15	0.16	0.62
1066	9.66	0.12	0.13	0.44
1067	10.59	0.11	0.11	0.42
1068	11.09	0.18	0.19	0.56
1069	10.9	0.2	0.22	0.63
1070	10.89	0.11	0.11	0.49
1071	11.1	0.23	0.26	0.68
1072	10.97	0.18	0.2	0.59
1073	11.35	0.17	0.17	0.67
1074	11.26	0.31	0.35	0.81
1075	11.22	0.37	0.42	0.86
1076	11.41	0.2	0.21	0.71
1077	11.13	0.16	0.18	0.4
1078	12.11	0.84	0.99	0.48
1079	11.54	0.16	0.18	0.59
1080	11.38	0.19	0.21	0.65
1081	12.07	0.12	0.13	0.51
1082	10.97	0.13	0.15	0.34
1083	12.16	0.19	0.21	0.68
1084	12.04	0.23	0.26	0.77
1085	12.06	0.23	0.25	0.75
1086	11.82	0.17	0.18	0.56
1087	11.97	0.19	0.21	0.65
1088	11.66	0.19	0.21	0.58

1089	12.02	0.22	0.25	0.73
1090	11.98	0.2	0.22	0.65
1091	11.41	0.21	0.24	0.63
1092	11.23	0.21	0.23	0.57
1093	11.86	0.16	0.18	0.59
1094	12.04	0.16	0.18	0.59
1095	11.43	0.14	0.16	0.44
1096	11.9	0.14	0.15	0.46
1097	11.87	0.15	0.16	0.53
1098	11.39	0.18	0.2	0.56
1099	11.8	0.18	0.19	0.58
1100	11.32	0.19	0.21	0.49
1101	11.26	0.14	0.15	0.4
1102	11.81	0.17	0.19	0.57
1103	12.1	0.16	0.18	0.55
1104	11.77	0.16	0.18	0.55
1105	11.79	0.22	0.25	0.7
1106	11.8	0.18	0.19	0.57
1107	11.77	0.17	0.18	0.52
1108	11.21	0.17	0.19	0.43
1109	11.51	0.15	0.16	0.44
1110	11.11	0.16	0.18	0.35
1111	11.31	0.15	0.17	0.32
1112	11.66	0.16	0.18	0.43
1113	11.75	0.16	0.17	0.49
1114	11.57	0.16	0.18	0.52
1115	11.26	0.19	0.21	0.46
1116	11.09	0.18	0.19	0.49
1117	11.17	0.12	0.13	0.36
1118	11.33	0.17	0.19	0.53
1119	11.45	0.17	0.18	0.52
1120	11.41	0.11	0.12	0.35
1121	11.16	0.1	0.1	0.31
1122	11.2	0.13	0.15	0.41
1123	10.99	0.21	0.24	0.52
1124	11.08	0.19	0.22	0.52
1125	11.34	0.18	0.2	0.52
1126	11.71	0.17	0.19	0.57
1127	11.01	0.14	0.16	0.43
1128	10.99	0.14	0.16	0.42
1129	10.81	0.13	0.15	0.36
1130	10.53	0.13	0.15	0.28
1131	11.28	0.15	0.16	0.44
1132	11.14	0.12	0.13	0.4
1133	11.42	0.13	0.14	0.42
1134	11.17	0.12	0.13	0.35
1135	11.27	0.12	0.13	0.38
1136	11.34	0.13	0.14	0.39
1137	11.25	0.14	0.15	0.42
1138	10.81	0.11	0.11	0.33

1139	11.12	0.17	0.19	0.43
1140	10.97	0.13	0.15	0.34
1141	11.18	0.16	0.18	0.32
1142	11.2	0.14	0.16	0.34
1143	11.27	0.15	0.18	0.34
1144	10.7	0.12	0.14	0.3
1145	10.84	0.17	0.19	0.33
1146	10.13	0.18	0.2	0.37
1147	9.98	0.22	0.25	0.41
1148	10.37	0.19	0.22	0.38
1149	10.07	0.35	0.41	0.28
1150	10.51	0.12	0.13	0.29
1151	11.08	0.13	0.14	0.26
1152	9.46	0.23	0.27	0.13
1153	10.3	0.11	0.13	0.18
1154	10.96	0.1	0.1	0.3
1155	9.77	0.11	0.12	0.25
1156	10.94	0.09	0.1	0.18
1157	10.64	0.1	0.11	0.27
1158	10.67	0.1	0.11	0.31
1159	10.32	0.11	0.11	0.22
1160	10.72	0.17	0.2	0.19
1161	8.88	0.27	0.31	0.27
1162	11.19	0.08	0.08	0.31
1163	7.96	0.2	0.24	0.21
1164	9.33	0.3	0.35	0.11
1165	10.67	0.09	0.11	0.23
1166	10.75	0.16	0.19	0.24
1167	10.94	0.12	0.14	0.18
1168	10.91	0.14	0.17	0.22
1169	10.77	0.12	0.13	0.28
1170	10.36	0.13	0.15	0.37
1171	10.83	0.07	0.07	0.26
1172	10.95	0.08	0.08	0.3
1173	10.86	0.12	0.13	0.29
1174	11.08	0.07	0.08	0.27
1175	10.92	0.12	0.14	0.39
1176	10.79	0.14	0.15	0.35
1177	9.65	0.16	0.18	0.29
1178	9.96	0.11	0.13	0.18
1179	11.22	0.14	0.16	0.28
1180	10.98	0.1	0.11	0.34
1181	10.8	0.14	0.15	0.46
1182	10.75	0.13	0.14	0.45
1183	10.36	0.15	0.15	0.47
1184	9.56	0.22	0.25	0.52
1185	10.63	0.09	0.08	0.35
1186	9.9	0.18	0.21	0.37
1187	9.98	0.23	0.27	0.52
1188	10.67	0.24	0.28	0.42

1189	10.82	0.14	0.15	0.39
1190	11.85	0.39	0.44	0.6
1191	11.54	0.55	0.65	0.72
1192	11.48	0.4	0.46	0.66
1193	11.16	0.46	0.53	0.62
1194	11.11	0.41	0.48	0.54
1195	9.89	0.28	0.32	0.43
1196	9.52	0.21	0.21	0.58
1197	9.07	0.44	0.49	0.64
1198	10.06	0.22	0.22	0.54
1199	10.73	0.52	0.62	0.49
1200	10.07	0.57	0.67	0.32
1201	10.7	0.92	1.08	0.43
1202	8.97	0.1	0.11	0.18
1203	9.47	0.08	0.09	0.25
1204	9.88	0.06	0.06	0.24
1205	10.85	0.11	0.12	0.3
1206	11.41	0.13	0.14	0.46
1207	10.88	0.13	0.14	0.43
1208	11.1	0.17	0.19	0.53
1209	10.75	0.13	0.14	0.4
1210	11.99	0.1	0.09	0.54
1211	11.24	0.15	0.16	0.49
1212	11.32	0.13	0.14	0.49
1213	10.98	0.15	0.16	0.47
1214	10.99	0.14	0.16	0.46
1215	10.15	0.15	0.16	0.38
1216	10.36	0.12	0.14	0.37
1217	10.55	0.11	0.12	0.3
1218	10.53	0.16	0.18	0.23
1219	10.35	0.11	0.12	0.34
1220	11.17	0.13	0.14	0.43
1221	10.12	0.14	0.16	0.38
1222	11.52	0.09	0.07	0.48
1223	10.81	0.12	0.13	0.42
1224	10.88	0.13	0.14	0.44
1225	10.68	0.09	0.1	0.28
1226	9.97	0.17	0.2	0.27
1227	11.24	0.19	0.22	0.54
1228	10.93	0.13	0.14	0.45
1229	11.1	0.11	0.12	0.43
1230	11.05	0.14	0.15	0.44
1231	10.83	0.14	0.14	0.6
1232	10.96	0.14	0.15	0.41
1233	11.31	0.13	0.14	0.41
1234	11.1	0.15	0.16	0.48
1235	11.14	0.18	0.19	0.52
1236	11.06	0.14	0.16	0.43
1237	10.95	0.16	0.17	0.47
1238	11.16	0.14	0.15	0.47

1239	10.97	0.14	0.15	0.46
1240	11.12	0.12	0.13	0.44
1241	11.34	0.15	0.16	0.51
1242	11.02	0.15	0.16	0.47
1243	11.08	0.14	0.15	0.43
1244	11.42	0.13	0.14	0.46
1245	11.42	0.13	0.13	0.47
1246	12	0.09	0.07	0.52
1247	11.4	0.14	0.16	0.44
1248	11.02	0.16	0.18	0.5
1249	11.2	0.18	0.2	0.59
1250	10.73	0.16	0.17	0.46
1251	11.2	0.19	0.21	0.58
1252	10.68	0.15	0.16	0.46
1253	10.9	0.12	0.13	0.42
1254	10.72	0.16	0.18	0.47
1255	10.56	0.1	0.1	0.35
1256	11.16	0.16	0.18	0.52
1257	10.76	0.09	0.09	0.35
1258	11.46	0.17	0.19	0.57
1259	11.17	0.15	0.16	0.49
1260	10.86	0.16	0.17	0.48
1261	10.83	0.17	0.19	0.51
1262	11.29	0.15	0.16	0.52
1263	11.32	0.15	0.16	0.5
1264	11.25	0.16	0.18	0.52
1265	11.26	0.14	0.15	0.51
1266	11.25	0.14	0.15	0.49
1267	11.07	0.16	0.18	0.5
1268	10.97	0.11	0.11	0.41
1269	10.14	0.12	0.14	0.38
1270	9.49	0.15	0.17	0.34
1271	11.55	0.16	0.17	0.45
1272	11.53	0.17	0.18	0.6
1273	11.2	0.13	0.13	0.5
1274	11.11	0.17	0.19	0.56
1275	11.13	0.2	0.22	0.49
1276	11.28	0.22	0.25	0.54
1277	11.68	0.22	0.25	0.56
1278	11.04	0.21	0.23	0.47
1279	11.29	0.25	0.29	0.58
1280	11.5	0.2	0.22	0.53
1281	11.11	0.21	0.24	0.5
1282	10.83	0.19	0.21	0.37
1283	11.6	0.16	0.18	0.41
1284	12.26	0.14	0.15	0.44
1285	12.01	0.14	0.15	0.49
1286	12.27	0.18	0.2	0.59
1287	11.88	0.19	0.21	0.57
1288	11.73	0.18	0.2	0.48

1289	11.89	0.19	0.21	0.56
1290	12.19	0.16	0.18	0.43
1291	11.73	0.21	0.23	0.57
1292	12.07	0.15	0.16	0.42
1293	11.98	0.17	0.19	0.51
1294	11.72	0.19	0.21	0.48
1295	11.87	0.17	0.18	0.48
1296	12.13	0.19	0.22	0.57
1297	12.1	0.17	0.19	0.46
1298	12.37	0.14	0.15	0.37
1299	11.81	0.27	0.31	0.3
1300	12.49	0.14	0.14	0.45
1301	12.55	0.15	0.17	0.46
1302	11.9	0.15	0.17	0.31
1303	12.25	0.17	0.19	0.41
1304	12.24	0.13	0.14	0.38
1305	12.97	0.27	0.31	0.29
1306	12.25	0.15	0.17	0.24
1307	11.2	0.15	0.17	0.28
1308	12.25	0.13	0.14	0.39
1309	12.24	0.16	0.17	0.48
1310	12.23	0.18	0.2	0.58
1311	12.37	0.17	0.19	0.56
1312	11.96	0.15	0.17	0.36
1313	12.03	0.14	0.15	0.41
1314	12.09	0.17	0.18	0.51
1315	12.98	0.16	0.17	0.41
1316	12.2	0.15	0.17	0.29
1317	12.32	0.16	0.17	0.46
1318	12.15	0.17	0.19	0.49
1319	12.04	0.19	0.21	0.59
1320	12.27	0.17	0.18	0.56
1321	12.21	0.15	0.16	0.5
1322	12.95	0.16	0.18	0.44
1323	12.3	0.16	0.17	0.5
1324	12.7	0.17	0.2	0.42
1325	12.42	0.16	0.18	0.61
1326	12.53	0.15	0.16	0.45
1327	12.12	0.19	0.21	0.63
1328	12.21	0.2	0.22	0.68
1329	12.23	0.16	0.18	0.51
1330	12.37	0.17	0.19	0.54
1331	12.21	0.21	0.23	0.69
1332	12.18	0.17	0.18	0.56
1333	11.89	0.23	0.26	0.69
1334	12.28	0.18	0.2	0.63
1335	11.91	0.18	0.2	0.59
1336	12.16	0.18	0.2	0.63
1337	12.55	0.2	0.23	0.49
1338	12.22	0.15	0.16	0.61

1339	12.93	0.24	0.28	0.45
1340	12.05	0.17	0.18	0.56
1341	12.02	0.17	0.19	0.56
1342	11.73	0.2	0.22	0.6
1343	11.56	0.18	0.2	0.57
1344	11.56	0.18	0.2	0.56
1345	11.77	0.16	0.18	0.56
1346	11.71	0.18	0.2	0.56
1347	11.8	0.19	0.21	0.55
1348	12.14	0.17	0.19	0.58
1349	11.7	0.2	0.22	0.59
1350	11.9	0.17	0.19	0.56
1351	12.04	0.18	0.2	0.62
1352	11.94	0.15	0.17	0.5
1353	10.89	0.17	0.2	0.35
1354	11.22	0.14	0.15	0.33
1355	11.22	0.14	0.15	0.29
1356	11.82	0.15	0.17	0.4
1357	11.57	0.2	0.23	0.61
1358	11.85	0.18	0.2	0.57
1359	11.8	0.2	0.22	0.59
1360	11.73	0.17	0.19	0.52
1361	11.3	0.17	0.19	0.48
1362	12.11	0.17	0.19	0.51
1363	11.6	0.19	0.21	0.55
1364	11.77	0.14	0.15	0.48
1365	11.33	0.18	0.2	0.52
1366	11.83	0.14	0.15	0.48
1367	12.01	0.16	0.17	0.56
1368	11.66	0.15	0.17	0.5
1369	11.85	0.17	0.19	0.57
1370	12.05	0.2	0.23	0.69
1371	11.73	0.21	0.24	0.65
1372	11.73	0.18	0.2	0.58
1373	12.26	0.18	0.2	0.5
1374	11.59	0.16	0.18	0.52
1375	11.59	0.18	0.2	0.54
1376	11.27	0.13	0.15	0.4
1377	11.61	0.16	0.18	0.52
1378	11.81	0.16	0.17	0.56
1379	11.9	0.12	0.13	0.45
1380	11.75	0.19	0.21	0.6
1381	11.34	0.22	0.25	0.58
1382	11.24	0.16	0.17	0.47
1383	11.12	0.17	0.19	0.45
1384	11.06	0.14	0.16	0.36
1385	11.63	0.19	0.22	0.39
1386	11.35	0.16	0.18	0.48
1387	11.51	0.16	0.18	0.55
1388	11.94	0.17	0.18	0.59

1389	11.82	0.16	0.17	0.55
1390	11.75	0.17	0.19	0.57
1391	11.8	0.16	0.18	0.56
1392	11.61	0.19	0.21	0.59
1393	11.62	0.16	0.17	0.53
1394	11.35	0.19	0.21	0.54
1395	10.97	0.2	0.22	0.49
1396	11.06	0.17	0.19	0.46
1397	10.91	0.12	0.14	0.34
1398	11.44	0.19	0.21	0.56
1399	11.53	0.16	0.18	0.49
1400	11.4	0.15	0.16	0.51
1401	11.07	0.14	0.16	0.44
1402	10.95	0.11	0.13	0.28
1403	10.91	0.15	0.17	0.41
1404	11.25	0.18	0.2	0.52
1405	11.39	0.16	0.18	0.53
1406	11.55	0.17	0.19	0.57
1407	11.57	0.14	0.15	0.47
1408	11.34	0.18	0.2	0.54
1409	11.43	0.16	0.18	0.51
1410	11.65	0.16	0.17	0.54
1411	11.32	0.13	0.14	0.52
1412	11.14	0.14	0.15	0.46
1413	11.29	0.18	0.2	0.55
1414	11.85	0.13	0.14	0.51
1415	11.47	0.11	0.11	0.45
1416	11.53	0.13	0.14	0.47
1417	11.38	0.18	0.2	0.54
1418	11.55	0.16	0.17	0.52
1419	11.1	0.17	0.18	0.5
1420	11.48	0.14	0.15	0.49
1421	11.68	0.14	0.14	0.47
1422	11.69	0.17	0.19	0.59
1423	11.48	0.13	0.14	0.46
1424	11.14	0.14	0.16	0.45
1425	11.4	0.14	0.16	0.48
1426	11.37	0.17	0.19	0.53
1427	11.11	0.15	0.16	0.47
1428	11.35	0.17	0.18	0.51
1429	11.46	0.17	0.19	0.53
1430	11.79	0.19	0.21	0.63
1431	11.29	0.17	0.18	0.53
1432	11.29	0.14	0.16	0.48
1433	11.24	0.15	0.16	0.51
1434	11.37	0.16	0.17	0.5
1435	11.55	0.19	0.21	0.57
1436	11.56	0.16	0.18	0.54
1437	11.38	0.2	0.22	0.57
1438	11.1	0.13	0.14	0.5

1439	11.23	0.11	0.11	0.47
1440	11.3	0.12	0.12	0.45
1441	11.29	0.14	0.15	0.51
1442	11.6	0.16	0.18	0.56
1443	11.58	0.17	0.18	0.58
1444	11.63	0.15	0.16	0.55
1445	11.32	0.16	0.18	0.51
1446	11.44	0.15	0.16	0.51
1447	11.6	0.22	0.24	0.65
1448	11.51	0.15	0.17	0.54
1449	11.55	0.18	0.2	0.57
1450	11.53	0.2	0.22	0.6
1451	11.55	0.18	0.2	0.57
1452	11.79	0.22	0.25	0.67
1453	11.49	0.2	0.23	0.58
1454	11.43	0.15	0.16	0.48
1455	11.4	0.15	0.17	0.46
1456	11.28	0.21	0.24	0.52
1457	11.13	0.23	0.27	0.57
1458	10.62	0.13	0.15	0.31
1459	11.42	0.13	0.14	0.46
1460	11.46	0.18	0.2	0.56
1461	11.55	0.16	0.17	0.52
1462	11.4	0.17	0.19	0.53
1463	11.07	0.17	0.19	0.51
1464	11.38	0.19	0.22	0.55
1465	11.16	0.23	0.26	0.58
1466	11.24	0.19	0.21	0.55
1467	11.08	0.15	0.17	0.46
1468	11.21	0.12	0.13	0.43

**Bottom of
core**

Data for solids values estimated for the vertical transect of oil sand using the PCR calibration model on non-roughened surfaces. The estimated wt % solids values were used to construct the plot illustrated in Fig. 3.8

<u>Sample #</u>	<u>Estimated Wt % solids</u>	<u>Estimated Error</u>	<u>Mahalanobis Distance</u>	<u>Spectral Residual (%)</u>
<u>Top of core</u>				
1	91.71	0.11	0.11	0.2
2	92.69	0.11	0.11	0.2
3	93.36	0.1	0.11	0.16
4	94.79	0.09	0.09	0.07
5	94.81	0.12	0.13	0.09
6	93.63	0.15	0.16	0.12
7	94.69	0.15	0.16	0.18
8	93.09	0.13	0.13	0.21
9	93.94	0.09	0.08	0.19
10	92.67	0.18	0.19	0.18
11	92.67	0.14	0.15	0.25
12	94.88	0.19	0.2	0.23
13	94.57	0.26	0.27	0.24
14	88.62	0.07	0.05	0.3
15	88.49	0.06	0.04	0.27
16	91	0.05	0.03	0.21
17	93.13	0.04	0.03	0.15
18	92.66	0.05	0.05	0.16
19	92.15	0.15	0.17	0.15
20	90.73	0.08	0.07	0.24
21	89	0.07	0.06	0.31
22	88.41	0.08	0.06	0.44
23	88.56	0.09	0.07	0.48
24	89.17	0.12	0.11	0.48
25	88.91	0.07	0.05	0.44
26	88.32	0.08	0.05	0.44
27	87.78	0.07	0.04	0.42
28	87.59	0.08	0.06	0.45
29	88.22	0.08	0.06	0.39
30	88.48	0.06	0.06	0.22
31	88.32	0.05	0.02	0.25
32	89.25	0.03	0.02	0.12
33	90.67	0.05	0.05	0.09
34	91.01	0.05	0.06	0.08
35	92.23	0.18	0.18	0.22
36	92.52	0.12	0.11	0.21
37	92.09	0.14	0.14	0.21
38	92.97	0.2	0.2	0.23
39	93.15	0.23	0.23	0.25

40	91.07	0.06	0.06	0.14
41	89.53	0.1	0.09	0.24
42	89.62	0.28	0.3	0.35
43	90.02	0.25	0.26	0.33
44	91.02	0.34	0.36	0.4
45	90	0.67	0.72	0.66
46	90.03	0.94	1.02	0.87
47	90.69	0.4	0.43	0.37
48	88.77	0.08	0.06	0.27
49	89.26	0.05	0.05	0.13
50	88.89	0.14	0.15	0.12
51	88.38	0.05	0.05	0.15
52	88.17	0.06	0.05	0.18
53	87.84	0.12	0.12	0.19
54	88.43	0.11	0.12	0.15
55	87.53	0.17	0.18	0.19
56	88.27	0.06	0.05	0.23
57	90.09	0.07	0.06	0.25
58	87.93	0.13	0.12	0.54
59	88.48	0.13	0.12	0.49
60	88.69	0.08	0.06	0.38
61	88.04	0.14	0.13	0.6
62	88.3	0.08	0.06	0.45
63	88.16	0.12	0.1	0.54
64	87.79	0.15	0.13	0.62
65	88.55	0.16	0.15	0.57
66	88.08	0.19	0.18	0.64
67	87.82	0.14	0.12	0.58
68	87.82	0.1	0.08	0.47
69	89.27	0.23	0.24	0.53
70	88.12	0.31	0.33	0.58
71	88.64	0.72	0.77	0.8
72	94.04	0.26	0.27	0.57
73	88.47	0.13	0.11	0.63
74	88.16	0.13	0.11	0.68
75	87.58	0.12	0.1	0.64
76	86.91	0.12	0.1	0.71
77	87.15	0.11	0.08	0.61
78	87.41	0.14	0.12	0.68
79	87.24	0.16	0.14	0.68
80	86.81	0.13	0.12	0.64
81	87.3	0.11	0.08	0.61
82	87.1	0.12	0.1	0.66
83	86.8	0.15	0.13	0.74
84	87.53	0.12	0.09	0.65
85	86.67	0.13	0.11	0.72
86	86.93	0.12	0.1	0.65
87	86.96	0.15	0.13	0.71
88	87.13	0.13	0.11	0.65
89	86.88	0.14	0.12	0.68

90	86.94	0.13	0.12	0.5
91	87.04	0.12	0.11	0.5
92	87.24	0.14	0.13	0.62
93	87.77	0.22	0.22	0.66
94	86.89	0.13	0.12	0.64
95	86.9	0.13	0.11	0.63
96	87.17	0.14	0.12	0.65
97	87.21	0.1	0.07	0.58
98	87.26	0.15	0.13	0.71
99	87.04	0.13	0.11	0.67
100	87.05	0.14	0.12	0.7
101	87.09	0.15	0.13	0.73
102	87.76	0.12	0.1	0.59
103	87.61	0.16	0.15	0.69
104	87.58	0.11	0.09	0.59
105	87.13	0.1	0.08	0.55
106	87.18	0.13	0.11	0.64
107	86.94	0.11	0.09	0.59
108	86.93	0.11	0.09	0.54
109	87.25	0.1	0.08	0.46
110	87.26	0.14	0.13	0.68
111	87.01	0.11	0.09	0.54
112	87.11	0.12	0.1	0.61
113	87.24	0.12	0.1	0.59
114	87.24	0.11	0.09	0.58
115	92.86	0.44	0.47	0.26
116	93.11	1.56	1.68	0.57
117	90.2	0.42	0.45	0.29
118	91.51	1.18	1.26	0.6
119	92.33	0.63	0.66	0.36
120	91.89	0.31	0.31	0.36
121	91	0.28	0.28	0.31
122	90.74	0.58	0.6	0.39
123	91.43	0.36	0.37	0.37
124	92.62	0.32	0.31	0.36
125	90.08	0.33	0.34	0.35
126	90.75	0.27	0.26	0.35
127	92.59	0.18	0.16	0.31
128	92.36	0.18	0.16	0.33
129	91.68	0.14	0.11	0.27
130	89.95	0.22	0.22	0.28
131	88.23	0.27	0.3	0.13
132	87.42	0.18	0.19	0.22
133	88.47	0.1	0.1	0.19
134	89.82	0.1	0.05	0.25
135	90.32	0.26	0.25	0.37
136	88.36	0.08	0.06	0.39
137	87.63	0.15	0.14	0.56
138	87.02	0.14	0.13	0.56
139	86.92	0.15	0.14	0.61

140	87.37	0.15	0.14	0.57
141	87.2	0.19	0.19	0.7
142	87.26	0.22	0.23	0.75
143	87.22	0.19	0.19	0.69
144	87.05	0.17	0.17	0.64
145	87.53	0.15	0.15	0.57
146	86.79	0.13	0.13	0.55
147	87.07	0.14	0.14	0.52
148	86.95	0.15	0.16	0.39
149	87.08	0.14	0.14	0.5
150	87.33	0.14	0.14	0.55
151	87.31	0.15	0.15	0.61
152	87.25	0.17	0.17	0.66
153	86.94	0.16	0.16	0.63
154	87.69	0.14	0.14	0.53
155	87.38	0.14	0.14	0.56
156	87.27	0.16	0.15	0.59
157	86.79	0.15	0.15	0.59
158	87.37	0.15	0.14	0.55
159	87.39	0.14	0.14	0.47
160	87.45	0.14	0.13	0.48
161	87.76	0.1	0.08	0.54
162	87.54	0.18	0.16	0.72
163	88.2	0.11	0.09	0.52
164	87.8	0.12	0.11	0.6
165	87.58	0.11	0.1	0.58
166	87.67	0.14	0.13	0.59
167	87.21	0.13	0.12	0.65
168	87.77	0.15	0.14	0.6
169	87.37	0.12	0.11	0.53
170	87.39	0.12	0.11	0.49
171	87.38	0.15	0.14	0.61
172	87.44	0.13	0.12	0.53
173	87.08	0.13	0.12	0.52
174	88.11	0.12	0.11	0.51
175	88.03	0.11	0.1	0.51
176	88.25	0.11	0.09	0.43
177	87.61	0.14	0.14	0.44
178	87.78	0.09	0.07	0.44
179	87.59	0.1	0.08	0.39
180	87.99	0.08	0.06	0.33
181	87.86	0.07	0.05	0.38
182	87.4	0.09	0.09	0.27
183	88.46	0.14	0.14	0.29
184	96.93	1.62	1.74	0.51
185	96.21	0.87	0.92	0.44
186	96.86	0.71	0.75	0.42
187	95.31	0.5	0.52	0.39
188	90.78	0.22	0.23	0.23
189	88.11	0.09	0.08	0.41

190	87.09	0.09	0.06	0.44
191	87.7	0.11	0.09	0.47
192	88.18	0.11	0.09	0.41
193	87.83	0.08	0.05	0.4
194	87.82	0.11	0.1	0.5
195	87.73	0.08	0.05	0.4
196	87.63	0.07	0.05	0.36
197	87.84	0.1	0.08	0.48
198	88.16	0.1	0.08	0.4
199	87.6	0.08	0.06	0.41
200	87.87	0.07	0.04	0.36
201	87.94	0.09	0.07	0.42
202	88	0.09	0.06	0.44
203	87.85	0.07	0.04	0.39
204	87.46	0.07	0.04	0.43
205	87.62	0.07	0.06	0.29
206	88.44	0.08	0.07	0.33
207	88.86	0.07	0.05	0.26
208	88.58	0.06	0.04	0.29
209	88.35	0.08	0.05	0.35
210	88.45	0.05	0.03	0.28
211	87.2	0.09	0.07	0.35
212	88.71	0.07	0.06	0.24
213	88.02	0.05	0.03	0.32
214	88.51	0.05	0.02	0.28
215	88.13	0.09	0.07	0.47
216	87.82	0.06	0.03	0.39
217	88.07	0.09	0.07	0.44
218	87.5	0.08	0.08	0.27
219	87.83	0.07	0.05	0.41
220	87.87	0.06	0.04	0.39
221	88.14	0.09	0.08	0.41
222	88.08	0.11	0.09	0.48
223	87.87	0.09	0.07	0.44
224	88.15	0.09	0.07	0.44
225	87.9	0.09	0.08	0.46
226	88.02	0.08	0.06	0.45
227	89.08	0.08	0.06	0.32
228	88.8	0.06	0.04	0.34
229	88.95	0.05	0.03	0.26
230	90.13	0.06	0.06	0.19
231	92.49	0.23	0.23	0.31
232	94.31	0.85	0.9	0.7
233	94.19	1.29	1.38	0.85
234	94.8	0.99	1.06	0.63
235	88.83	0.09	0.08	0.32
236	89.24	0.08	0.08	0.29
237	90.15	0.08	0.07	0.3
238	89.15	0.1	0.1	0.31
239	88.87	0.1	0.09	0.32

240	88.64	0.13	0.13	0.33
241	89.43	0.23	0.24	0.35
242	88.59	0.09	0.07	0.3
243	89.4	0.08	0.07	0.29
244	88.53	0.08	0.06	0.32
245	88.43	0.1	0.09	0.38
246	88.27	0.1	0.08	0.39
247	87.85	0.09	0.07	0.4
248	87.77	0.14	0.14	0.45
249	87.95	0.16	0.15	0.5
250	88.4	0.11	0.1	0.43
251	87.89	0.09	0.06	0.41
252	87.92	0.13	0.11	0.52
253	88.13	0.18	0.18	0.57
254	87.9	0.1	0.09	0.35
255	88.43	0.08	0.05	0.46
256	88.08	0.12	0.1	0.48
257	88	0.12	0.1	0.46
258	88.06	0.16	0.15	0.57
259	88.72	0.08	0.06	0.41
260	87.9	0.1	0.08	0.39
261	88.17	0.15	0.14	0.53
262	88.29	0.1	0.08	0.42
263	88.33	0.09	0.07	0.4
264	87.95	0.09	0.07	0.44
265	88.05	0.12	0.11	0.48
266	87.78	0.08	0.05	0.39
267	87.91	0.08	0.05	0.44
268	87.86	0.12	0.1	0.53
269	87.96	0.1	0.08	0.46
270	88.66	0.08	0.07	0.25
271	87.75	0.09	0.06	0.43
272	86.85	0.13	0.1	0.62
273	88.13	0.1	0.08	0.48
274	88.82	0.07	0.01	0.37
275	87.57	0.08	0.05	0.33
276	88.55	0.12	0.12	0.28
277	88	0.08	0.06	0.31
278	87.44	0.08	0.06	0.43
279	87.92	0.11	0.09	0.5
280	87.92	0.11	0.09	0.48
281	88.14	0.08	0.06	0.38
282	87.59	0.08	0.07	0.32
283	87.86	0.08	0.06	0.39
284	88.65	0.09	0.07	0.4
285	87.91	0.06	0.03	0.37
286	87.99	0.09	0.06	0.38
287	88.17	0.06	0.04	0.32
288	88.09	0.07	0.04	0.34
289	88.05	0.06	0.04	0.36

290	88.54	0.05	0.03	0.34
291	89.96	0.04	0.03	0.19
292	89.29	0.14	0.14	0.37
293	92.18	0.28	0.3	0.3
294	91.73	0.19	0.2	0.23
295	91.71	0.17	0.18	0.18
296	92.31	0.17	0.17	0.24
297	94.43	0.36	0.39	0.24
298	93.99	0.21	0.22	0.25
299	94.48	0.46	0.49	0.3
300	94.28	0.34	0.36	0.32
301	94.6	0.19	0.2	0.23
302	88.63	0.06	0.06	0.17
303	88.51	0.06	0.06	0.16
304	88.42	0.06	0.05	0.29
305	88.92	0.07	0.06	0.3
306	88.47	0.08	0.06	0.33
307	88.2	0.07	0.04	0.41
308	88.37	0.16	0.15	0.54
309	88.31	0.09	0.08	0.36
310	88.09	0.09	0.07	0.36
311	88.08	0.11	0.1	0.43
312	87.93	0.08	0.06	0.34
313	88.04	0.12	0.13	0.17
314	88.45	0.08	0.08	0.21
315	88.74	0.08	0.08	0.24
316	88.65	0.09	0.08	0.3
317	88.49	0.12	0.11	0.24
318	88.34	0.07	0.06	0.26
319	88.14	0.08	0.07	0.26
320	88.23	0.09	0.08	0.33
321	88.13	0.07	0.05	0.28
322	88.42	0.1	0.1	0.25
323	88.33	0.1	0.09	0.27
324	88.17	0.09	0.07	0.28
325	88.69	0.08	0.07	0.3
326	88.28	0.08	0.07	0.28
327	88.31	0.07	0.05	0.3
328	88.69	0.07	0.07	0.18
329	88.51	0.07	0.07	0.19
330	89.72	0.14	0.14	0.21
331	89.56	0.07	0.06	0.19
332	91.22	0.12	0.12	0.2
333	93.14	0.31	0.32	0.32
334	95.07	0.5	0.54	0.29
335	92.41	0.14	0.14	0.16
336	90.79	0.08	0.08	0.14
337	93.96	0.34	0.35	0.27
338	95.22	0.6	0.64	0.33
339	94.56	0.61	0.65	0.31

340	95.69	0.5	0.53	0.26
341	90.11	0.2	0.21	0.2
342	88.22	0.21	0.21	0.58
343	88.27	0.17	0.17	0.55
344	87.96	0.16	0.15	0.55
345	88.1	0.18	0.17	0.53
346	88.29	0.21	0.21	0.56
347	88.25	0.22	0.22	0.59
348	88.25	0.22	0.22	0.58
349	88.19	0.19	0.19	0.54
350	88.11	0.2	0.2	0.59
351	89.23	0.23	0.23	0.62
352	88.03	0.26	0.27	0.71
353	88.12	0.19	0.19	0.57
354	88.49	0.14	0.13	0.48
355	88.49	0.19	0.19	0.52
356	90.8	0.15	0.15	0.33
357	91.43	0.11	0.11	0.29
358	90.22	0.07	0.06	0.2
359	90.03	0.09	0.09	0.22
360	90.5	0.12	0.12	0.24
361	91.16	0.12	0.13	0.17
362	90.38	0.1	0.09	0.26
363	90.07	0.1	0.09	0.27
364	87.9	0.09	0.06	0.42
365	88.92	0.11	0.09	0.44
366	88.29	0.15	0.14	0.51
367	88.14	0.17	0.16	0.56
368	88.69	0.1	0.08	0.41
369	90.54	0.09	0.09	0.21
370	91.99	0.11	0.08	0.31
371	91.47	0.1	0.07	0.3
372	89.26	0.06	0.02	0.27
373	88.03	0.15	0.14	0.57
374	88.23	0.14	0.12	0.47
375	88.44	0.22	0.22	0.56
376	89.17	0.24	0.25	0.51
377	88.27	0.17	0.16	0.54
378	89.37	0.23	0.23	0.5
379	90.66	0.12	0.12	0.24
380	91.23	0.12	0.11	0.24
381	91.83	0.09	0.08	0.2
382	90.86	0.05	0.03	0.18
383	91.42	0.1	0.07	0.31
384	89.35	0.06	0.01	0.23
385	88.64	0.1	0.08	0.39
386	88.1	0.12	0.11	0.48
387	88.41	0.18	0.17	0.54
388	88.47	0.1	0.07	0.47
389	88.16	0.17	0.16	0.55

390	88.22	0.15	0.14	0.49
391	88.2	0.09	0.06	0.44
392	88.08	0.13	0.12	0.53
393	87.85	0.1	0.07	0.44
394	88.17	0.14	0.13	0.47
395	88.29	0.08	0.06	0.43
396	88.05	0.19	0.19	0.59
397	87.96	0.15	0.14	0.53
398	88.38	0.21	0.21	0.55
399	88.26	0.18	0.18	0.55
400	88.62	0.08	0.06	0.35
401	88.72	0.11	0.1	0.4
402	88.56	0.16	0.16	0.53
403	89.11	0.12	0.11	0.4
404	90.64	0.14	0.14	0.29
405	89.15	0.12	0.12	0.42
406	89.09	0.15	0.15	0.42
407	89.76	0.13	0.13	0.39
408	89.78	0.13	0.13	0.25
409	91.27	0.12	0.12	0.25
410	90.7	0.11	0.11	0.24
411	93.08	0.08	0.08	0.21
412	90.1	0.08	0.07	0.28
413	97.53	0.39	0.42	0.37
414	98.92	0.4	0.43	0.32
415	95.6	0.1	0.1	0.18
416	91.5	0.05	0.04	0.17
417	90.51	0.05	0.04	0.18
418	89.99	0.05	0.03	0.2
419	89.77	0.07	0.06	0.22
420	90.82	0.15	0.16	0.26
421	95.04	0.34	0.37	0.3
422	95.31	0.07	0.07	0.14
423	97.92	0.14	0.16	0.07
424	97.11	0.1	0.11	0.08
425	96.79	0.09	0.1	0.08
426	97.6	0.1	0.11	0.1
427	93.9	0.09	0.09	0.17
428	95.21	0.22	0.23	0.3
429	94.73	0.21	0.22	0.27
430	90.66	0.08	0.08	0.23
431	90	0.06	0.05	0.25
432	89.24	0.05	0.02	0.29
433	89.27	0.06	0.04	0.3
434	89.88	0.07	0.05	0.3
435	90.23	0.08	0.06	0.3
436	89.27	0.08	0.06	0.39
437	88.65	0.11	0.09	0.49
438	88.85	0.13	0.12	0.46
439	90.44	0.09	0.08	0.3

440	91.38	0.09	0.08	0.27
441	90.04	0.09	0.07	0.3
442	89.92	0.1	0.1	0.28
443	89.09	0.16	0.17	0.34
444	89.79	0.16	0.16	0.36
445	89.58	0.13	0.13	0.36
446	89.93	0.18	0.18	0.34
447	91.72	0.31	0.33	0.33
448	98.88	0.33	0.35	0.23
449	97.35	0.14	0.15	0.12
450	96.56	0.11	0.11	0.14
451	98.96	0.17	0.18	0.16
452	97.85	0.18	0.19	0.15
453	94.33	0.26	0.28	0.25
454	89.25	0.07	0.06	0.23
455	89.26	0.09	0.08	0.3
456	91.27	0.1	0.09	0.28
457	91.64	0.04	0.03	0.18
458	90.31	0.06	0.04	0.23
459	88.87	0.15	0.15	0.43
460	91.59	0.12	0.12	0.3
461	89.13	0.07	0.05	0.38
462	88.67	0.18	0.18	0.54
463	88.37	0.16	0.15	0.52
464	89.21	0.1	0.09	0.36
465	88.69	0.14	0.13	0.41
466	89.17	0.14	0.13	0.41
467	89.47	0.14	0.12	0.49
468	87.91	0.14	0.12	0.61
469	88.8	0.21	0.21	0.53
470	88.6	0.22	0.22	0.57
471	89.08	0.2	0.2	0.48
472	89.03	0.12	0.11	0.4
473	89.39	0.18	0.18	0.43
474	88.75	0.21	0.21	0.53
475	88.1	0.2	0.2	0.52
476	87.9	0.2	0.2	0.56
477	87.74	0.21	0.21	0.57
478	98.56	0.22	0.23	0.25
479	96.89	0.46	0.48	0.49
480	95.96	1.2	1.3	0.63
481	97.3	3.09	3.34	1.08
482	96.96	2.61	2.82	1
483	94.39	2.14	2.3	1.1
484	98.58	0.27	0.29	0.14
485	96.89	0.13	0.12	0.29
486	96.24	0.21	0.2	0.38
487	93.91	0.09	0.08	0.24
488	94.09	0.1	0.1	0.21
489	93.27	0.08	0.06	0.24

490	92.94	0.17	0.15	0.36
491	94.42	0.09	0.08	0.19
492	94.46	0.1	0.09	0.26
493	92.78	0.13	0.12	0.28
494	95.09	0.15	0.15	0.24
495	93.09	0.13	0.14	0.26
496	89.69	0.08	0.06	0.35
497	90.25	0.09	0.07	0.38
498	89	0.11	0.11	0.29
499	90.81	0.21	0.23	0.23
500	89.62	0.23	0.24	0.25
501	91.06	0.31	0.33	0.3
502	92.57	0.31	0.33	0.28
503	89.8	0.26	0.28	0.21
504	91.34	0.21	0.21	0.29
505	89.32	0.13	0.14	0.25
506	90	0.1	0.09	0.36
507	88.16	0.12	0.1	0.54
508	88.16	0.1	0.08	0.51
509	88.48	0.09	0.07	0.36
510	91.2	0.12	0.12	0.32
511	89.1	0.07	0.06	0.25
512	87.78	0.07	0.04	0.3
513	88.3	0.07	0.04	0.38
514	88.01	0.08	0.06	0.42
515	89.37	0.06	0.03	0.35
516	89.35	0.09	0.09	0.23
517	90.33	0.1	0.09	0.23
518	90.48	0.06	0.06	0.15
519	92.32	0.14	0.14	0.21
520	90.76	0.89	0.95	0.74
521	91.23	0.51	0.55	0.42
522	89.02	0.25	0.27	0.42
523	88.47	0.31	0.32	0.49
524	87.85	0.38	0.39	0.59
525	88.8	0.38	0.39	0.56
526	91.03	0.91	0.98	0.78
527	90.73	1.16	1.24	0.94
528	91.05	0.61	0.66	0.59
529	87.86	0.14	0.13	0.44
530	89.39	0.15	0.16	0.31
531	88.25	0.12	0.12	0.44
532	87.93	0.19	0.18	0.58
533	87.31	0.16	0.15	0.58
534	87.26	0.14	0.12	0.53
535	87.38	0.18	0.18	0.65
536	87.27	0.19	0.18	0.66
537	87.46	0.15	0.14	0.55
538	87.57	0.14	0.13	0.53
539	87	0.14	0.13	0.62

540	87.98	0.14	0.13	0.5
541	87.15	0.16	0.15	0.67
542	88.17	0.13	0.12	0.48
543	88.55	0.16	0.15	0.49
544	87.8	0.16	0.15	0.56
545	87.48	0.14	0.12	0.53
546	87.49	0.17	0.16	0.63
547	87.3	0.21	0.21	0.73
548	87.32	0.23	0.22	0.75
549	87.56	0.2	0.19	0.67
550	87.2	0.16	0.14	0.61
551	87.79	0.14	0.13	0.47
552	87.49	0.15	0.13	0.57
553	87.84	0.15	0.14	0.52
554	87.01	0.13	0.11	0.56
555	87.39	0.13	0.12	0.53
556	87.16	0.12	0.11	0.49
557	86.78	0.14	0.13	0.53
558	87.14	0.15	0.13	0.65
559	86.68	0.15	0.14	0.67
560	87.12	0.14	0.13	0.58
561	87.12	0.14	0.12	0.63
562	86.03	0.17	0.16	0.68
563	87.12	0.19	0.18	0.77
564	87.53	0.2	0.19	0.75
565	87.33	0.12	0.1	0.54
566	88.74	0.18	0.18	0.42
567	93.27	0.19	0.19	0.55
568	89.85	0.14	0.13	0.45
569	86.86	0.11	0.1	0.48
570	87.17	0.14	0.13	0.66
571	87.27	0.21	0.2	0.82
572	86.89	0.14	0.12	0.7
573	86.92	0.14	0.12	0.71
574	88.09	0.09	0.07	0.47
575	88.19	0.09	0.08	0.44
576	89.31	0.12	0.1	0.54
577	94.37	0.27	0.27	0.55
578	87.23	0.12	0.1	0.56
579	86.82	0.13	0.11	0.51
580	87.32	0.11	0.08	0.58
581	86.38	0.15	0.12	0.66
582	87.08	0.11	0.09	0.54
583	87.28	0.11	0.09	0.5
584	87.23	0.14	0.12	0.55
585	88.12	0.11	0.08	0.5
586	87.12	0.13	0.12	0.52
587	88.93	0.12	0.09	0.46
588	89.37	0.23	0.23	0.53
589	87.01	0.12	0.11	0.51

590	87.43	0.16	0.15	0.44
591	87.8	0.14	0.12	0.51
592	88.09	0.13	0.12	0.34
593	88.06	0.12	0.12	0.29
594	88.17	0.17	0.16	0.5
595	88.71	0.12	0.12	0.35
596	89.1	0.1	0.08	0.34
597	88.99	0.31	0.33	0.48
598	94.81	0.45	0.47	0.63
599	95.05	0.3	0.31	0.6
600	90.38	0.28	0.29	0.52
601	88.38	0.14	0.14	0.36
602	87.97	0.08	0.06	0.47
603	87.49	0.1	0.08	0.42
604	87.61	0.12	0.11	0.45
605	88.05	0.09	0.09	0.37
606	87.26	0.09	0.06	0.57
607	86.9	0.12	0.1	0.52
608	86.91	0.17	0.16	0.52
609	87.01	0.14	0.14	0.47
610	87.24	0.1	0.08	0.48
611	87.71	0.08	0.05	0.5
612	88.02	0.09	0.07	0.46
613	88.72	0.19	0.2	0.34
614	89.53	0.24	0.25	0.39
615	90	0.12	0.12	0.38
616	89.73	0.08	0.07	0.32
617	88.94	0.09	0.07	0.39
618	88.42	0.08	0.07	0.39
619	88.08	0.07	0.05	0.38
620	87.65	0.07	0.05	0.42
621	88.02	0.07	0.05	0.39
622	87.59	0.08	0.05	0.45
623	87.8	0.1	0.06	0.54
624	88	0.1	0.08	0.46
625	88.92	0.19	0.19	0.49
626	87.93	0.11	0.08	0.57
627	88.81	0.09	0.07	0.39
628	88.22	0.1	0.08	0.51
629	87.88	0.09	0.06	0.48
630	87.08	0.25	0.27	0.38
631	88.51	0.14	0.13	0.47
632	88.77	0.15	0.15	0.47
633	87.74	0.09	0.06	0.43
634	88.89	0.12	0.11	0.36
635	88.71	0.07	0.06	0.26
636	90.19	0.08	0.08	0.19
637	90.78	0.11	0.1	0.28
638	92.18	0.14	0.12	0.39
639	93	0.83	0.89	0.65

640	89.14	0.12	0.12	0.18
641	88.55	0.07	0.07	0.19
642	88.13	0.05	0.03	0.28
643	88.34	0.14	0.14	0.46
644	88.53	0.12	0.11	0.43
645	90.35	0.21	0.22	0.45
646	88.73	0.11	0.09	0.35
647	89.28	0.15	0.16	0.2
648	91.6	0.11	0.11	0.24
649	92.48	0.45	0.47	0.34
650	89.32	0.07	0.07	0.2
651	89.15	0.09	0.08	0.23
652	88.71	0.1	0.09	0.22
653	88.6	0.11	0.11	0.22
654	88.19	0.08	0.07	0.25
655	88.79	0.09	0.09	0.24
656	89.11	0.12	0.12	0.18
657	88.25	0.06	0.04	0.34
658	88.25	0.08	0.06	0.34
659	88.63	0.1	0.09	0.28
660	88.55	0.16	0.15	0.49
661	88.45	0.13	0.11	0.47
662	88.81	0.13	0.12	0.4
663	88.96	0.11	0.09	0.36
664	88.35	0.14	0.11	0.54
665	88.65	0.17	0.17	0.54
666	88.21	0.23	0.23	0.67
667	88.53	0.15	0.15	0.46
668	88.48	0.22	0.22	0.62
669	88.89	0.17	0.17	0.42
670	88.64	0.14	0.13	0.43
671	88.76	0.19	0.19	0.5
672	88.99	0.14	0.14	0.37
673	88.92	0.34	0.36	0.65
674	88.75	0.2	0.2	0.56
675	88.73	0.16	0.16	0.45
676	88.88	0.19	0.19	0.47
677	89.02	0.17	0.16	0.44
678	88.81	0.14	0.13	0.39
679	88.28	0.15	0.13	0.51
680	88.99	0.23	0.24	0.55
681	89.04	0.15	0.15	0.38
682	89.37	0.16	0.16	0.3
683	88.89	0.17	0.17	0.45
684	88.45	0.18	0.16	0.57
685	88.59	0.11	0.1	0.36
686	88.47	0.11	0.1	0.35
687	88.88	0.16	0.16	0.32
688	88.75	0.13	0.13	0.34
689	89.17	0.16	0.17	0.38

690	88.83	0.13	0.12	0.35
691	88.56	0.13	0.11	0.43
692	88.91	0.14	0.14	0.28
693	89.05	0.2	0.2	0.48
694	88.63	0.12	0.11	0.37
695	89.19	0.1	0.05	0.44
696	93.67	1.35	1.45	0.9
697	88.96	0.29	0.3	0.59
698	88.84	0.21	0.21	0.54
699	89.08	0.14	0.14	0.37
700	89.39	0.19	0.2	0.4
701	88.42	0.12	0.11	0.42
702	88.57	0.16	0.17	0.29
703	88.57	0.06	0.04	0.23
704	88.38	0.1	0.08	0.36
705	88.32	0.1	0.09	0.39
706	88.71	0.12	0.11	0.38
707	88.66	0.16	0.15	0.47
708	88.99	0.16	0.16	0.45
709	90.4	0.34	0.36	0.48
710	89.44	0.25	0.27	0.34
711	90.09	0.27	0.29	0.27
712	92.06	0.18	0.18	0.26
713	93.74	0.26	0.26	0.42
714	94.02	0.75	0.8	0.39
715	90.5	0.16	0.16	0.31
716	90.01	0.24	0.26	0.33
717	90.55	0.15	0.15	0.28
718	92.95	0.33	0.33	0.46
719	95.04	0.98	1.05	0.59
720	89.96	0.17	0.16	0.38
721	88.73	0.12	0.12	0.31
722	88.31	0.11	0.1	0.39
723	88.2	0.1	0.09	0.41
724	88.26	0.12	0.11	0.32
725	88.52	0.13	0.12	0.41
726	88.77	0.14	0.13	0.34
727	88.84	0.17	0.18	0.36
728	88.72	0.23	0.25	0.32
729	88.32	0.11	0.11	0.29
730	88.07	0.09	0.08	0.34
731	87.72	0.07	0.04	0.35
732	88.66	0.12	0.1	0.36
733	88.92	0.33	0.35	0.31
734	89.09	0.16	0.17	0.36
735	88.59	0.12	0.11	0.42
736	86.99	0.3	0.32	0.46
737	87.96	0.15	0.16	0.3
738	88.24	0.18	0.18	0.31
739	88.94	0.49	0.53	0.4

740	90.31	0.5	0.54	0.27
741	88.48	0.11	0.11	0.22
742	88.75	0.11	0.12	0.22
743	87.63	0.2	0.21	0.26
744	88.7	0.2	0.16	0.47
745	87.48	0.19	0.2	0.3
746	88.41	0.18	0.19	0.24
747	88.34	0.08	0.07	0.32
748	87.98	0.08	0.06	0.32
749	87.82	0.1	0.08	0.39
750	88.32	0.12	0.11	0.42
751	88.97	0.11	0.1	0.32
752	88.56	0.12	0.11	0.41
753	88.29	0.1	0.08	0.38
754	88.36	0.1	0.09	0.38
755	88.21	0.12	0.11	0.43
756	88.49	0.12	0.11	0.44
757	88.99	0.17	0.18	0.34
758	89.01	0.14	0.14	0.31
759	88.51	0.14	0.14	0.33
760	88.36	0.13	0.12	0.45
761	88.41	0.13	0.12	0.48
762	88.46	0.16	0.15	0.53
763	88.82	0.22	0.22	0.57
764	89.14	0.16	0.16	0.41
765	88.52	0.13	0.12	0.33
766	88.61	0.16	0.16	0.48
767	89.1	0.2	0.21	0.3
768	89.18	0.15	0.15	0.34
769	88.56	0.12	0.11	0.41
770	89.15	0.16	0.16	0.33
771	89.27	0.22	0.22	0.5
772	87.78	0.1	0.07	0.43
773	89.2	0.13	0.12	0.3
774	89.04	0.13	0.13	0.34
775	87.37	0.1	0.07	0.5
776	88.62	0.14	0.13	0.43
777	87.98	0.13	0.12	0.38
778	88.65	0.24	0.25	0.39
779	89.71	0.28	0.3	0.25
780	89.47	0.2	0.22	0.28
781	89.01	0.14	0.12	0.42
782	89.37	0.25	0.26	0.24
783	88.84	0.1	0.08	0.31
784	88.7	0.18	0.17	0.52
785	88.48	0.17	0.16	0.51
786	88.69	0.16	0.16	0.47
787	89.33	0.15	0.15	0.37
788	88.55	0.16	0.15	0.49
789	89.35	0.14	0.14	0.31

790	89.85	0.2	0.22	0.18
791	90.26	0.19	0.2	0.2
792	89.55	0.16	0.16	0.35
793	89.41	0.14	0.14	0.33
794	88.51	0.19	0.19	0.55
795	88.85	0.21	0.21	0.52
796	88.84	0.13	0.13	0.39
797	89.01	0.15	0.15	0.41
798	88.65	0.22	0.22	0.58
799	88.71	0.24	0.24	0.59
800	88.55	0.18	0.16	0.54
801	89.82	0.14	0.15	0.2
802	88.69	0.13	0.12	0.44
803	89.08	0.13	0.13	0.25
804	88.69	0.26	0.26	0.63
805	88.26	0.25	0.25	0.69
806	88.61	0.16	0.16	0.49
807	89.42	0.15	0.15	0.38
808	88.68	0.17	0.16	0.57
809	88.73	0.17	0.17	0.56
810	88.81	0.13	0.12	0.47
811	89.21	0.13	0.13	0.33
812	88.93	0.11	0.1	0.29
813	90.21	0.24	0.25	0.24
814	89.87	0.14	0.14	0.22
815	88.68	0.12	0.11	0.41
816	88.67	0.2	0.2	0.56
817	89.4	0.14	0.13	0.41
818	90.87	0.12	0.09	0.36
819	88.69	0.14	0.12	0.5
820	88.67	0.09	0.06	0.4
821	88.67	0.13	0.11	0.49
822	88.82	0.12	0.1	0.45
823	88.6	0.11	0.09	0.45
824	88.7	0.12	0.1	0.44
825	88.62	0.12	0.1	0.47
826	88.6	0.12	0.1	0.5
827	88.55	0.15	0.13	0.54
828	88.81	0.13	0.11	0.43
829	88.49	0.17	0.15	0.54
830	88.98	0.22	0.22	0.53
831	89.39	0.17	0.17	0.41
832	89.88	0.2	0.21	0.39
833	88.81	0.23	0.23	0.56
834	89.49	0.17	0.17	0.41
835	89.02	0.15	0.15	0.41
836	91	0.31	0.32	0.55
837	93.3	0.64	0.69	0.62
838	93.63	0.56	0.6	0.39
839	95.39	0.56	0.6	0.33

840	95.66	0.97	1.04	0.42
841	89.99	0.13	0.13	0.3
842	90.53	0.08	0.07	0.28
843	89.66	0.26	0.27	0.49
844	89.1	0.12	0.11	0.43
845	89.23	0.12	0.11	0.36
846	89.06	0.16	0.15	0.45
847	89.19	0.11	0.1	0.37
848	89.36	0.13	0.12	0.36
849	88.68	0.11	0.1	0.36
850	89.18	0.1	0.1	0.34
851	88.8	0.09	0.07	0.37
852	89.09	0.13	0.12	0.36
853	88.85	0.13	0.13	0.38
854	89.19	0.16	0.16	0.41
855	89.09	0.18	0.18	0.44
856	89.07	0.19	0.19	0.43
857	89.26	0.21	0.22	0.45
858	88.11	0.17	0.16	0.56
859	89.06	0.2	0.2	0.45
860	88.93	0.21	0.21	0.46
861	89.13	0.2	0.21	0.45
862	89.98	0.26	0.27	0.43
863	87.76	0.12	0.09	0.53
864	89.61	0.12	0.11	0.39
865	89.35	0.1	0.07	0.43
866	89.71	0.17	0.17	0.41
867	89.65	0.18	0.18	0.42
868	89.15	0.13	0.12	0.49
869	89.47	0.15	0.14	0.51
870	90.51	0.17	0.18	0.41
871	90.54	0.16	0.16	0.37
872	90.41	0.2	0.21	0.45
873	90.25	0.14	0.14	0.37
874	89.7	0.09	0.07	0.39
875	89.39	0.1	0.08	0.4
876	88.66	0.09	0.06	0.39
877	89.75	0.1	0.09	0.36
878	88.79	0.11	0.08	0.42
879	88.94	0.08	0.04	0.37
880	89.6	0.11	0.09	0.4
881	89.6	0.13	0.12	0.46
882	90.79	0.13	0.12	0.39
883	89.77	0.12	0.11	0.37
884	91.33	0.17	0.16	0.41
885	92.92	0.25	0.25	0.45
886	93.64	0.32	0.33	0.46
887	91.27	0.44	0.45	0.63
888	92.77	0.33	0.34	0.48
889	90.72	0.13	0.13	0.36

890	89.23	0.13	0.11	0.45
891	89.9	0.16	0.16	0.41
892	89.04	0.26	0.27	0.58
893	89.12	0.23	0.24	0.55
894	89.01	0.21	0.21	0.5
895	89.15	0.24	0.24	0.52
896	90.7	0.17	0.18	0.28
897	89.38	0.11	0.1	0.33
898	88.57	0.15	0.14	0.48
899	89.55	0.12	0.1	0.36
900	90.24	0.16	0.15	0.34
901	89.74	0.18	0.17	0.43
902	89.53	0.2	0.2	0.43
903	89.26	0.22	0.22	0.47
904	90.27	0.19	0.2	0.45
905	89.96	0.13	0.12	0.39
906	88.82	0.14	0.11	0.51
907	89.72	0.08	0.06	0.39
908	88.59	0.14	0.13	0.43
909	88.51	0.15	0.14	0.45
910	88.7	0.14	0.13	0.45
911	88.48	0.15	0.14	0.47
912	88.72	0.15	0.14	0.48
913	88.7	0.16	0.15	0.49
914	88.35	0.18	0.17	0.48
915	88.64	0.14	0.13	0.47
916	89.08	0.14	0.13	0.5
917	89.08	0.13	0.11	0.48
918	88.66	0.13	0.12	0.49
919	89.66	0.11	0.09	0.44
920	89.36	0.18	0.17	0.49
921	88.75	0.16	0.15	0.5
922	88.41	0.16	0.15	0.48
923	88.61	0.17	0.16	0.5
924	88.51	0.19	0.18	0.5
925	88.62	0.18	0.18	0.5
926	88.44	0.18	0.17	0.52
927	88.21	0.18	0.18	0.54
928	88.44	0.16	0.15	0.51
929	88.55	0.17	0.17	0.48
930	89.13	0.16	0.16	0.5
931	89.21	0.18	0.18	0.47
932	88.9	0.12	0.11	0.43
933	89.46	0.1	0.06	0.49
934	89.99	0.12	0.06	0.54
935	88.59	0.07	0.04	0.36
936	88.65	0.18	0.17	0.47
937	88.13	0.2	0.19	0.54
938	88.98	0.17	0.15	0.55
939	88.63	0.19	0.18	0.56

940	88.06	0.2	0.19	0.62
941	88.27	0.21	0.2	0.6
942	88.32	0.19	0.18	0.53
943	88.46	0.18	0.17	0.5
944	89.07	0.21	0.21	0.47
945	90.26	0.2	0.2	0.55
946	90.25	0.27	0.29	0.45
947	89.32	0.11	0.09	0.37
948	88.41	0.17	0.16	0.46
949	87.4	0.14	0.11	0.57
950	88.55	0.13	0.12	0.43
951	88.32	0.17	0.15	0.52
952	89.12	0.16	0.15	0.45
953	88.7	0.17	0.17	0.48
954	88.6	0.15	0.11	0.56
955	89.55	0.2	0.21	0.41
956	89.8	0.16	0.16	0.38
957	89.95	0.18	0.17	0.38
958	89.26	0.15	0.15	0.39
959	88.93	0.17	0.16	0.51
960	89.65	0.13	0.13	0.31
961	88.61	0.13	0.12	0.46
962	89.12	0.15	0.15	0.46
963	88.63	0.13	0.13	0.39
964	88.32	0.12	0.11	0.41
965	88.57	0.18	0.19	0.4
966	89.85	0.16	0.16	0.44
967	88.81	0.2	0.23	0.41
968	88.65	0.14	0.13	0.35
969	89.32	0.15	0.14	0.39
970	89.82	0.1	0.08	0.35
971	89.34	0.13	0.12	0.42
972	87.78	0.07	0.04	0.46
973	88.67	0.12	0.11	0.46
974	88.71	0.11	0.1	0.39
975	88.61	0.11	0.11	0.32
976	88.57	0.12	0.11	0.34
977	88.24	0.1	0.08	0.42
978	88.13	0.12	0.1	0.51
979	88.68	0.12	0.11	0.43
980	88.53	0.12	0.12	0.33
981	89.49	0.12	0.12	0.38
982	90.24	0.16	0.16	0.36
983	89.22	0.17	0.13	0.48
984	89.03	0.09	0.08	0.28
985	88.24	0.08	0.06	0.46
986	89.46	0.21	0.21	0.51
987	89.16	0.12	0.12	0.31
988	89.24	0.14	0.12	0.51
989	88.72	0.11	0.07	0.47

990	88.74	0.1	0.09	0.36
991	88.62	0.11	0.07	0.45
992	88.61	0.11	0.08	0.45
993	89.22	0.11	0.11	0.36
994	89.17	0.15	0.14	0.41
995	89.31	0.18	0.18	0.47
996	89.11	0.13	0.13	0.43
997	88.92	0.12	0.11	0.4
998	89.21	0.11	0.09	0.4
999	90.1	0.15	0.16	0.3
1000	90.77	0.15	0.16	0.32
1001	89.82	0.13	0.13	0.33
1002	88.93	0.15	0.14	0.41
1003	88.67	0.16	0.16	0.48
1004	89.17	0.14	0.14	0.45
1005	88.96	0.12	0.11	0.45
1006	88.96	0.15	0.13	0.44
1007	88.1	0.11	0.09	0.45
1008	88.24	0.1	0.07	0.48
1009	88.43	0.11	0.07	0.51
1010	88.07	0.2	0.18	0.59
1011	88.38	0.17	0.15	0.5
1012	88.65	0.18	0.18	0.4
1013	87.92	0.21	0.2	0.57
1014	87.6	0.21	0.21	0.61
1015	87.15	0.21	0.21	0.51
1016	87.67	0.19	0.18	0.57
1017	88.01	0.19	0.19	0.53
1018	88.44	0.24	0.25	0.56
1019	87.99	0.22	0.22	0.6
1020	88.11	0.24	0.24	0.66
1021	87.81	0.19	0.19	0.58
1022	87.66	0.26	0.26	0.79
1023	87.04	0.18	0.16	0.72
1024	87.22	0.2	0.19	0.72
1025	88.07	0.33	0.35	0.8
1026	87.09	0.23	0.22	0.84
1027	86.84	0.17	0.15	0.66
1028	87.8	0.15	0.15	0.45
1029	87.34	0.18	0.17	0.61
1030	87.74	0.19	0.19	0.58
1031	88.27	0.22	0.23	0.59
1032	88.79	0.32	0.33	0.67
1033	88.17	0.22	0.23	0.61
1034	88.02	0.21	0.21	0.65
1035	87.68	0.19	0.19	0.58
1036	87.29	0.16	0.15	0.5
1037	87.33	0.17	0.15	0.61
1038	87.64	0.25	0.24	0.85
1039	87.79	0.19	0.18	0.68

1040	87.79	0.21	0.2	0.69
1041	88.48	0.25	0.26	0.63
1042	87.93	0.26	0.26	0.8
1043	87.92	0.29	0.3	0.82
1044	87.95	0.22	0.22	0.68
1045	87.59	0.19	0.19	0.65
1046	87.98	0.26	0.27	0.73
1047	87.72	0.24	0.24	0.7
1048	87.46	0.18	0.17	0.6
1049	87.93	0.17	0.16	0.64
1050	88.18	0.3	0.31	0.8
1051	87.91	0.22	0.22	0.65
1052	87.76	0.2	0.2	0.62
1053	87.79	0.21	0.21	0.73
1054	87.59	0.17	0.15	0.66
1055	87.98	0.21	0.21	0.67
1056	88.25	0.24	0.25	0.65
1057	87.89	0.18	0.17	0.64
1058	87.8	0.19	0.19	0.71
1059	88.62	0.24	0.24	0.62
1060	89.16	0.15	0.14	0.51
1061	88.43	0.12	0.11	0.46
1062	87.95	0.15	0.14	0.58
1063	87.81	0.18	0.18	0.69
1064	88.23	0.16	0.15	0.62
1065	88.34	0.17	0.16	0.62
1066	89.8	0.14	0.13	0.44
1067	88.81	0.12	0.11	0.42
1068	88.46	0.19	0.19	0.56
1069	88.71	0.22	0.22	0.63
1070	88.55	0.13	0.11	0.49
1071	88.53	0.25	0.26	0.68
1072	88.58	0.2	0.2	0.59
1073	88.16	0.19	0.17	0.67
1074	88.44	0.34	0.35	0.81
1075	88.53	0.4	0.42	0.86
1076	88.14	0.22	0.21	0.71
1077	88.19	0.18	0.18	0.4
1078	86.61	0.92	0.99	0.48
1079	87.87	0.18	0.18	0.59
1080	88.11	0.21	0.21	0.65
1081	87.26	0.14	0.13	0.51
1082	88.43	0.15	0.15	0.34
1083	87.28	0.21	0.21	0.68
1084	87.48	0.26	0.26	0.77
1085	87.44	0.25	0.25	0.75
1086	87.62	0.18	0.18	0.56
1087	87.49	0.21	0.21	0.65
1088	87.84	0.21	0.21	0.58
1089	87.46	0.24	0.25	0.73

1090	87.5	0.22	0.22	0.65
1091	88.16	0.23	0.24	0.63
1092	88.33	0.23	0.23	0.57
1093	87.57	0.18	0.18	0.59
1094	87.34	0.18	0.18	0.59
1095	87.97	0.16	0.16	0.44
1096	87.35	0.15	0.15	0.46
1097	87.5	0.17	0.16	0.53
1098	88.1	0.2	0.2	0.56
1099	87.63	0.2	0.19	0.58
1100	88.05	0.21	0.21	0.49
1101	88.15	0.15	0.15	0.4
1102	87.6	0.19	0.19	0.57
1103	87.22	0.18	0.18	0.55
1104	87.64	0.18	0.18	0.55
1105	87.75	0.25	0.25	0.7
1106	87.63	0.19	0.19	0.57
1107	87.6	0.18	0.18	0.52
1108	88.15	0.18	0.19	0.43
1109	87.88	0.16	0.16	0.44
1110	88.16	0.18	0.18	0.35
1111	87.89	0.16	0.17	0.32
1112	87.61	0.17	0.18	0.43
1113	87.57	0.17	0.17	0.49
1114	87.86	0.18	0.18	0.52
1115	88.2	0.21	0.21	0.46
1116	88.37	0.2	0.19	0.49
1117	88.21	0.13	0.13	0.36
1118	88.18	0.19	0.19	0.53
1119	88.03	0.19	0.18	0.52
1120	87.9	0.13	0.12	0.35
1121	88.15	0.11	0.1	0.31
1122	88.25	0.15	0.15	0.41
1123	88.61	0.24	0.24	0.52
1124	88.48	0.21	0.22	0.52
1125	88.17	0.2	0.2	0.52
1126	87.76	0.19	0.19	0.57
1127	88.5	0.16	0.16	0.43
1128	88.5	0.16	0.16	0.42
1129	88.69	0.15	0.15	0.36
1130	88.91	0.14	0.15	0.28
1131	88.17	0.16	0.16	0.44
1132	88.27	0.13	0.13	0.4
1133	87.98	0.15	0.14	0.42
1134	88.19	0.13	0.13	0.35
1135	88.08	0.14	0.13	0.38
1136	88.03	0.14	0.14	0.39
1137	88.17	0.15	0.15	0.42
1138	88.61	0.12	0.11	0.33
1139	88.34	0.19	0.19	0.43

1140	88.44	0.15	0.15	0.34
1141	88.15	0.18	0.18	0.32
1142	88.15	0.15	0.16	0.34
1143	88.06	0.17	0.18	0.34
1144	88.7	0.14	0.14	0.3
1145	88.56	0.19	0.19	0.33
1146	89.42	0.2	0.2	0.37
1147	89.67	0.24	0.25	0.41
1148	89.19	0.21	0.22	0.38
1149	89.32	0.38	0.41	0.28
1150	89.32	0.38	0.41	0.28
1151	88.78	0.13	0.13	0.29
1152	87.93	0.14	0.14	0.26
1153	89.76	0.25	0.27	0.13
1154	88.98	0.12	0.13	0.18
1155	88.39	0.11	0.1	0.3
1156	89.59	0.12	0.12	0.25
1157	88.22	0.1	0.1	0.18
1158	88.66	0.11	0.11	0.27
1159	88.75	0.11	0.11	0.31
1160	88.89	0.12	0.11	0.22
1161	88.48	0.19	0.2	0.19
1162	90.24	0.29	0.31	0.27
1163	88.12	0.09	0.08	0.31
1164	91.61	0.22	0.24	0.21
1165	89.88	0.33	0.35	0.11
1166	88.55	0.1	0.11	0.23
1167	88.26	0.18	0.19	0.24
1168	88.15	0.13	0.14	0.18
1169	88.17	0.16	0.17	0.22
1170	88.4	0.13	0.13	0.28
1171	89.08	0.14	0.15	0.37
1172	88.47	0.08	0.07	0.26
1173	88.38	0.09	0.08	0.3
1174	88.41	0.13	0.13	0.29
1175	88.16	0.08	0.08	0.27
1176	88.52	0.14	0.14	0.39
1177	88.56	0.15	0.15	0.35
1178	89.76	0.17	0.18	0.29
1179	89.23	0.12	0.13	0.18
1180	87.89	0.16	0.16	0.28
1181	88.32	0.11	0.11	0.34
1182	88.55	0.16	0.15	0.46
1183	88.51	0.14	0.14	0.45
1184	89.01	0.16	0.15	0.47
1185	89.87	0.24	0.25	0.52
1186	88.62	0.1	0.08	0.35
1187	89.37	0.2	0.21	0.37
1188	89.33	0.26	0.27	0.52
1189	88.57	0.27	0.28	0.42

1190	88.53	0.15	0.15	0.39
1191	87.19	0.42	0.44	0.6
1192	87.49	0.61	0.65	0.72
1193	87.59	0.44	0.46	0.66
1194	87.94	0.5	0.53	0.62
1195	87.98	0.45	0.48	0.54
1196	89.33	0.31	0.32	0.43
1197	89.93	0.24	0.21	0.58
1198	90.37	0.48	0.49	0.64
1199	89.31	0.24	0.22	0.54
1200	88.28	0.57	0.62	0.49
1201	88.94	0.62	0.67	0.32
1202	88.1	1	1.08	0.43
1203	90.5	0.11	0.11	0.18
1204	90.02	0.09	0.09	0.25
1205	89.54	0.07	0.06	0.24
1206	88.47	0.12	0.12	0.3
1207	87.89	0.14	0.14	0.46
1208	88.59	0.14	0.14	0.43
1209	88.45	0.19	0.19	0.53
1210	88.71	0.14	0.14	0.4
1211	87.32	0.11	0.09	0.54
1212	88.23	0.16	0.16	0.49
1213	88.13	0.15	0.14	0.49
1214	88.54	0.16	0.16	0.47
1215	88.53	0.16	0.16	0.46
1216	89.4	0.16	0.16	0.38
1217	89.09	0.14	0.14	0.37
1218	88.74	0.12	0.12	0.3
1219	88.61	0.17	0.18	0.23
1220	89	0.12	0.12	0.34
1221	88.2	0.15	0.14	0.43
1222	89.44	0.16	0.16	0.38
1223	87.76	0.1	0.07	0.48
1224	88.64	0.14	0.13	0.42
1225	88.58	0.15	0.14	0.44
1226	88.61	0.1	0.1	0.28
1227	89.46	0.19	0.2	0.27
1228	88.27	0.21	0.22	0.54
1229	88.54	0.15	0.14	0.45
1230	88.31	0.13	0.12	0.43
1231	88.42	0.15	0.15	0.44
1232	88.49	0.16	0.14	0.6
1233	88.44	0.16	0.15	0.41
1234	88.03	0.14	0.14	0.41
1235	88.41	0.17	0.16	0.48
1236	88.4	0.19	0.19	0.52
1237	88.39	0.16	0.16	0.43
1238	88.58	0.18	0.17	0.47
1239	88.33	0.16	0.15	0.47

1240	88.52	0.15	0.15	0.46
1241	88.3	0.14	0.13	0.44
1242	88.13	0.17	0.16	0.51
1243	88.48	0.17	0.16	0.47
1244	88.33	0.15	0.15	0.43
1245	88.01	0.15	0.14	0.46
1246	88	0.14	0.13	0.47
1247	87.26	0.1	0.07	0.52
1248	87.99	0.16	0.16	0.44
1249	88.5	0.18	0.18	0.5
1250	88.35	0.2	0.2	0.59
1251	88.82	0.18	0.17	0.46
1252	88.34	0.21	0.21	0.58
1253	88.83	0.17	0.16	0.46
1254	88.53	0.14	0.13	0.42
1255	88.83	0.18	0.18	0.47
1256	88.89	0.11	0.1	0.35
1257	88.37	0.18	0.18	0.52
1258	88.65	0.1	0.09	0.35
1259	88.06	0.19	0.19	0.57
1260	88.32	0.17	0.16	0.49
1261	88.68	0.17	0.17	0.48
1262	88.72	0.19	0.19	0.51
1263	88.2	0.17	0.16	0.52
1264	88.15	0.16	0.16	0.5
1265	88.26	0.18	0.18	0.52
1266	88.19	0.16	0.15	0.51
1267	88.2	0.15	0.15	0.49
1268	88.45	0.18	0.18	0.5
1269	88.42	0.12	0.11	0.41
1270	89.29	0.14	0.14	0.38
1271	89.92	0.17	0.17	0.34
1272	87.77	0.17	0.17	0.45
1273	87.94	0.18	0.18	0.6
1274	88.25	0.14	0.13	0.5
1275	88.43	0.19	0.19	0.56
1276	88.47	0.22	0.22	0.49
1277	88.34	0.24	0.25	0.54
1278	87.91	0.24	0.25	0.56
1279	88.57	0.23	0.23	0.47
1280	88.39	0.28	0.29	0.58
1281	88.02	0.22	0.22	0.53
1282	88.52	0.23	0.24	0.5
1283	88.67	0.21	0.21	0.37
1284	87.81	0.18	0.18	0.41
1285	87.04	0.15	0.15	0.44
1286	87.39	0.16	0.15	0.49
1287	87.15	0.2	0.2	0.59
1288	87.65	0.21	0.21	0.57
1289	87.77	0.19	0.2	0.48

1290	87.63	0.21	0.21	0.56
1291	87.22	0.18	0.18	0.43
1292	87.82	0.23	0.23	0.57
1293	87.34	0.16	0.16	0.42
1294	87.51	0.19	0.19	0.51
1295	87.78	0.2	0.21	0.48
1296	87.55	0.19	0.18	0.48
1297	87.36	0.21	0.22	0.57
1298	87.31	0.19	0.19	0.46
1299	86.88	0.16	0.15	0.37
1300	87.29	0.3	0.31	0.3
1301	86.82	0.15	0.14	0.45
1302	86.78	0.17	0.17	0.46
1303	87.44	0.16	0.17	0.31
1304	87.04	0.19	0.19	0.41
1305	87.02	0.14	0.14	0.38
1306	85.95	0.3	0.31	0.29
1307	86.94	0.16	0.17	0.24
1308	88.21	0.17	0.17	0.28
1309	87.06	0.14	0.14	0.39
1310	87.15	0.17	0.17	0.48
1311	87.21	0.2	0.2	0.58
1312	87.03	0.19	0.19	0.56
1313	87.4	0.16	0.17	0.36
1314	87.34	0.15	0.15	0.41
1315	87.35	0.18	0.18	0.51
1316	86.13	0.17	0.17	0.41
1317	87.01	0.16	0.17	0.29
1318	86.99	0.17	0.17	0.46
1319	87.25	0.19	0.19	0.49
1320	87.43	0.21	0.21	0.59
1321	87.12	0.19	0.18	0.56
1322	87.16	0.16	0.16	0.5
1323	86.12	0.18	0.18	0.44
1324	87.05	0.17	0.17	0.5
1325	86.48	0.19	0.2	0.42
1326	86.93	0.18	0.18	0.61
1327	86.68	0.16	0.16	0.45
1328	87.35	0.21	0.21	0.63
1329	87.26	0.22	0.22	0.68
1330	87.14	0.18	0.18	0.51
1331	86.98	0.19	0.19	0.54
1332	87.26	0.23	0.23	0.69
1333	87.19	0.18	0.18	0.56
1334	87.65	0.25	0.26	0.69
1335	87.1	0.2	0.2	0.63
1336	87.54	0.2	0.2	0.59
1337	87.24	0.2	0.2	0.63
1338	86.6	0.22	0.23	0.49
1339	87.12	0.17	0.16	0.61

1340	86.03	0.26	0.28	0.45
1341	87.34	0.19	0.18	0.56
1342	87.38	0.19	0.19	0.56
1343	87.78	0.22	0.22	0.6
1344	87.93	0.2	0.2	0.57
1345	87.95	0.2	0.2	0.56
1346	87.67	0.18	0.18	0.56
1347	87.76	0.2	0.2	0.56
1348	87.65	0.21	0.21	0.55
1349	87.23	0.19	0.19	0.58
1350	87.8	0.22	0.22	0.59
1351	87.52	0.19	0.19	0.56
1352	87.39	0.2	0.2	0.62
1353	87.4	0.17	0.17	0.5
1354	88.5	0.19	0.2	0.35
1355	88	0.15	0.15	0.33
1356	87.93	0.15	0.15	0.29
1357	87.42	0.17	0.17	0.4
1358	87.97	0.22	0.23	0.61
1359	87.6	0.2	0.2	0.57
1360	87.67	0.22	0.22	0.59
1361	87.69	0.19	0.19	0.52
1362	88.18	0.19	0.19	0.48
1363	87.14	0.19	0.19	0.51
1364	87.88	0.21	0.21	0.55
1365	87.56	0.16	0.15	0.48
1366	88.19	0.2	0.2	0.52
1367	87.49	0.16	0.15	0.48
1368	87.35	0.17	0.17	0.56
1369	87.72	0.17	0.17	0.5
1370	87.58	0.19	0.19	0.57
1371	87.4	0.22	0.23	0.69
1372	87.79	0.23	0.24	0.65
1373	87.74	0.2	0.2	0.58
1374	86.99	0.2	0.2	0.5
1375	87.85	0.18	0.18	0.52
1376	87.89	0.2	0.2	0.54
1377	88.08	0.15	0.15	0.4
1378	87.85	0.18	0.18	0.52
1379	87.62	0.17	0.17	0.56
1380	87.36	0.14	0.13	0.45
1381	87.74	0.21	0.21	0.6
1382	88.24	0.25	0.25	0.58
1383	88.21	0.17	0.17	0.47
1384	88.36	0.18	0.19	0.45
1385	88.3	0.16	0.16	0.36
1386	87.64	0.21	0.22	0.39
1387	88.11	0.18	0.18	0.48
1388	87.96	0.18	0.18	0.55
1389	87.46	0.18	0.18	0.59

1390	87.59	0.18	0.17	0.55
1391	87.69	0.19	0.19	0.57
1392	87.62	0.18	0.18	0.56
1393	87.88	0.21	0.21	0.59
1394	87.82	0.18	0.17	0.53
1395	88.17	0.21	0.21	0.54
1396	88.59	0.22	0.22	0.49
1397	88.45	0.19	0.19	0.46
1398	88.49	0.14	0.14	0.34
1399	88.09	0.21	0.21	0.56
1400	87.86	0.18	0.18	0.49
1401	88.07	0.16	0.16	0.51
1402	88.41	0.16	0.16	0.44
1403	88.38	0.13	0.13	0.28
1404	88.53	0.17	0.17	0.41
1405	88.27	0.2	0.2	0.52
1406	88.1	0.18	0.18	0.53
1407	87.94	0.19	0.19	0.57
1408	87.84	0.15	0.15	0.47
1409	88.18	0.2	0.2	0.54
1410	88.04	0.18	0.18	0.51
1411	87.78	0.17	0.17	0.54
1412	88.14	0.15	0.14	0.52
1413	88.33	0.16	0.15	0.46
1414	88.22	0.2	0.2	0.55
1415	87.49	0.14	0.14	0.51
1416	87.87	0.12	0.11	0.45
1417	87.87	0.14	0.14	0.47
1418	88.14	0.2	0.2	0.54
1419	87.92	0.17	0.17	0.52
1420	88.41	0.18	0.18	0.5
1421	87.96	0.15	0.15	0.49
1422	87.69	0.15	0.14	0.47
1423	87.77	0.19	0.19	0.59
1424	87.92	0.14	0.14	0.46
1425	88.33	0.16	0.16	0.45
1426	88.04	0.16	0.16	0.48
1427	88.13	0.19	0.19	0.53
1428	88.36	0.17	0.16	0.47
1429	88.1	0.19	0.18	0.51
1430	88.01	0.19	0.19	0.53
1431	87.68	0.21	0.21	0.63
1432	88.22	0.18	0.18	0.53
1433	88.17	0.16	0.16	0.48
1434	88.24	0.17	0.16	0.51
1435	88.08	0.17	0.17	0.5
1436	87.95	0.2	0.21	0.57
1437	87.9	0.18	0.18	0.54
1438	88.16	0.22	0.22	0.57
1439	88.35	0.15	0.14	0.5

1440	88.15	0.13	0.11	0.47
1441	88.1	0.13	0.12	0.45
1442	88.17	0.16	0.15	0.51
1443	87.88	0.18	0.18	0.56
1444	87.9	0.19	0.18	0.58
1445	87.81	0.17	0.16	0.55
1446	88.16	0.18	0.18	0.51
1447	88.04	0.17	0.16	0.51
1448	87.94	0.24	0.24	0.65
1449	87.97	0.17	0.17	0.54
1450	87.93	0.2	0.2	0.57
1451	87.99	0.22	0.22	0.6
1452	87.95	0.2	0.2	0.57
1453	87.72	0.24	0.25	0.67
1454	88.03	0.22	0.23	0.58
1455	87.96	0.16	0.16	0.48
1456	87.97	0.17	0.17	0.46
1457	88.26	0.24	0.24	0.52
1458	88.47	0.26	0.27	0.57
1459	88.77	0.15	0.15	0.31
1460	88	0.15	0.14	0.46
1461	88.05	0.2	0.2	0.56
1462	87.89	0.18	0.17	0.52
1463	88.09	0.19	0.19	0.53
1464	88.46	0.19	0.19	0.51
1465	88.13	0.21	0.22	0.55
1466	88.45	0.25	0.26	0.58
1467	88.3	0.21	0.21	0.55
1468	88.42	0.17	0.17	0.46

**Bottom of
core**

Appendix B

Data and Programs used in the Analysis of a Core from the Syncrude Lease in the Athabasca Oil Sands by Instrumental Neutron Activation Analysis

This appendix provides the raw data, and the programs used to process the data, for the INAA experiments performed in this thesis. All of the work was done on a core of oil sand from the Syncrude lease in the Athabasca oil sand deposit. The core was supplied by Syncrude Canada Ltd.

There are two sections in Appendix B. Section 1 deals with sample programs and other information used for data processing. In Section 2 appear the INAA raw data obtained for the experiments done on the oil sand and its components.

Sample program used to carry out a Principal Component Analysis of elements in Athabasca oil sand. This program was part of an SAS software package available from the University of Alberta Computing Network Services.

```

1.  data oilsand;
2.      infile 'oil1 prn';
3.      input V Dy Al Eu Sm Ti Ba K;
4.      infile 'oil2 prn';
5.      input Na Cl Mn Bit Fines;
6.  proc princomp standard out = tar1;
7.      var V Dy Al Eu Sm Ti Ba K Na Cl Mn;
8.  proc sort;
9.      by prin1;
10. proc print;
11.     var bitumen prin1 V Dy Al Eu Sm Ti Ba K Na Cl Mn;
12.     title1 'samples listed in order as determined by prin1';
13. proc print;
14.     print data = tar1;
15. proc plot;
16.     plot prin1*Bit;
17.     plot prin1*Fines;
18. run;
19. submit;

```

Explanation of Program Commands in SAS Software Used in this Work

Line 1: **data** denotes a name to describe the analysis.

Lines 2-5: If the data file is too large, as was the case here, it is advisable to break it into two. Hence oil1 prn and oil2 prn. A data file is identified by starting it with the command **infile**. Oil1 prn contains V, Dy, Al, Eu, Sm, Ti, Ba, and K values, while Oil2 prn has Na, Cl, Mn, Bit, and Fines values. These are prefixed by **input**.

Line 6: **proc** is a command used in SAS to execute a procedure. This line executes the principal component analysis with values standardized and outputs results in file tar1.

- Line 7: var command denotes which elements to be used in the PCA.
- Lines 8,9: these lines sort the result according to the principal component values.
- Line 10: used to execute printing.
- Line 11: var here denotes how the results are to be printed.
- Line 12: this provides an option for a title for the printed results.
- Lines 13,14: print command, which prints output of the PCA results.
- Line 15: command to plot.
- Lines 16,17: some plot options, e.g. plot of principal component 1 values versus Bitumen and Fines values.
- Line 18: run command initiates the running of the entire program.
- Line 19: submit offers the program for execution. Instead of the word submit , can press F9 after the run command.

Also notice that in SAS each statement is ended with a semi-colon (;)

Data for concentrations of elements (microg/g, unless otherwise stated) in half gram test portions of oil sand

<u>Sample ID</u>	<u>Wt. % bitumen</u>	<u>Wt. % fines</u>	<u>Vanadium</u>	<u>Dysprosium</u>	<u>Aluminum (%)</u>	<u>Europium</u>
1F3	6.4	18.4	35	2.9	2.34	0.68
1F5	4.4	32.2	49	4.9	3.73	0.99
1F7	4.0	20.2	37	3.1	2.85	0.66
1F9	4.0	27.4	33	2.5	2.15	0.53
1F32	10.3	9.6	29	1.3	1.30	0.31
1F34	9.6	13.7	28	1.4	1.54	0.35
1F36	5.8	29.1	33	2.0	2.06	0.50
1F39	7.7	21.7	36	2.0	1.99	0.40
1F50	9.3	15.0	30	1.7	1.35	0.35
1F35	7.7	19.4	35	1.9	2.05	0.46
2B15	4.1	28.8	47	3.7	3.19	0.78
2B17	3.3	36.5	56	3.7	3.12	0.80
2B42	0.9	47.7	90	4.3	7.29	0.83
1D1	3.4	34.2	32	2.5	2.48	0.53
1D3	6.5	30.7	41	3.1	1.55	0.64
1D5	5.8	26.1	34	2.3	2.64	0.55
1D7	5.8	29.7	41	3.1	2.93	0.68
1D10	4.4	27.8	51	3.2	4.16	0.71
1D15	7.4	28.9	28	2.0	1.43	0.45
1D16	8.0	25.4	27	1.9	0.85	0.44
4A5	12.2	10.9	32	0.6	0.64	0.16
4A15	14.1	10.6	31	0.6	0.59	0.17
4A45	13.1	7.4	30	0.5	0.59	0.20

Data for concentrations of elements (microg/g. unless otherwise stated) in half gram test portions of oil sand

<u>Samarium</u>	<u>Titanium</u>	<u>Barium</u>	<u>Potassium (%)</u>	<u>Sodium</u>	<u>Chlorine</u>	<u>Manganese</u>
3.7	1987	183	0.57	866	321	52
5.3	4233	207	0.73	1184	306	71
4.3	3113	182	0.54	981	354	57
3.3	2583	185	0.63	1008	250	68
2.4	1739	121	0.28	421	295	36
1.6	1846	134	0.38	553	262	53
2.5	1683	139	0.45	738	382	102
2.8	2703	170	0.50	747	358	269
1.9	1967	125	0.33	367	125	39
2.4	2342	194	0.45	837	423	93
5.4	3982	199	0.80	1232	309	235
5.8	3698	219	0.64	1439	491	227
7.1	4620	233	0.88	1600	539	121
3.0	1796	168	0.54	778	132	59
3.2	2456	186	0.52	795	122	47
3.6	2553	170	0.52	819	135	68
3.0	2240	177	0.61	946	215	62
3.8	3382	191	0.59	1016	184	131
2.7	2119	136	0.36	393	523	36
2.7	2036	126	0.26	249	118	25
0.9	628	125	0.24	244	640	12
1.1	824	113	0.20	179	447	9
1.1	751	163	0.40	342	218	16

Data for concentrations of elements (microg/g, unless otherwise stated) in fines

<u>Sample ID</u>	<u>Wt % Bitumen</u>	<u>Wt % Fines</u>	<u>Dysprosium</u>	<u>Aluminum (%)</u>	<u>Samarium</u>	<u>Europium</u>
1F3	6.39	18.4	7.46	4.70	7.32	1.46
1F5	4.35	32.2	6.80	4.93	6.26	1.17
1F7	4.02	20.2	6.15	5.53	6.09	1.21
1F9	3.99	27.4	5.90	6.11	6.38	1.16
1F32	10.28	9.6	4.88	3.06	5.12	0.88
1F34	9.59	13.7	5.62	3.29	5.39	0.95
1F36	5.82	29.1	6.07	5.68	5.44	1.31
1F39	7.71	21.7	4.68	4.48	4.28	0.98
1F50	9.26	15.0	4.03	2.76	3.56	0.61
1F35	7.73	19.4	3.21	2.70	3.44	0.65
2B15	4.05	28.8	4.69	4.61	5.39	0.93
2B17	3.34	36.5	4.38	3.79	4.66	0.89
2B42	0.89	47.7	4.04	3.83	5.01	0.74
1D1	3.43	34.2	4.45	4.66	6.01	1.11
1D3	6.47	30.7	3.58	3.19	4.82	0.73
1D5	5.84	26.1	2.70	1.90	2.75	0.57
1D7	5.78	29.7	2.83	2.13	2.44	0.55
1D10	4.38	27.8	2.82	1.19	2.71	0.51
1D15	7.38	28.9	5.92	2.91	7.34	0.99
1D16	8.04	25.4	2.37	0.08	2.28	0.54
4A5	12.17	10.9	0.55	0.53	1.01	0.18
4A15	14.06	10.6	0.47	0.53	0.85	0.16
4A45	13.12	7.4	0.53	0.65	0.81	0.16

Data for concentrations of elements (microg/g, unless otherwise stated) in fines

<u>Titanium</u>	<u>Vanadium</u>	<u>Sodium</u>	<u>Potassium (%)</u>	<u>Chlorine</u>	<u>Manganese</u>	<u>Barium</u>
6327	53.13	1717	1.17	452	115	325
6150	61.11	1536	0.95	310	115	279
6423	63.22	1478	1.05	277	118	296
4916	69.15	2003	1.15	435	164	334
5328	36.08	1081	0.89	379	94	243
5289	36.35	1164	1.08	526	109	272
4564	64.49	2021	1.27	944	308	320
4797	53.24	1301	1.37	529	330	284
4238	29.58	839	0.71	316	74	235
3179	49.13	1581	1.07	671	181	271
4120	51.63	1361	0.74	278	348	218
4564	49.93	1436	0.84	357	345	236
4363	51.65	1590	0.93	359	155	237
5203	36.57	877	0.75	95	83	214
3049	20.59	562	0.47	91	42	164
2795	22.57	659	0.54	84	54	197
3004	22.00	796	0.63	132	72	202
2899	13.60	345	0.34	61	41	166
5155	34.76	899	0.73	204	81	227
1023	2.67	273	0.31	44	36	128
728	3.20	185	0.24	56	8	109
601	2.58	168	0.21	65	7	132
622	3.01	253	0.34	71	8	149

Data for concentrations of elements (microg/g, unless otherwise stated) in ten gram test portions of oil sand

ID	% Bitumen	Dy	Sm	Eu	Mn	Na	Y	K(%)	Cl	Ti	Al(%)	Ba
2B17	3.3	3.7	3.1	0.6	266	1386	54	1.1	196	4062	3.7	236
1F5	4.4	4.8	6.3	0.8	75	1252	52	1.0	127	4426	3.8	218
1D5	5.8	3.0	3.0	0.6	57	712	34	1.0	51	2761	2.7	156
1D3	6.5	3.3	3.6	0.7	51	689	35	0.7	52	3028	2.7	181
1D16	8.0	2.7	3.9	0.5	41	482	32	0.6	52	2434	1.8	135
1F50	9.3	1.8	2.5	0.4	59	597	34	0.6	120	2294	2.1	180
1F32	10.3	2.1	2.2	0.4	47	515	36	0.4	93	2256	1.7	158
4A5	12.2	0.7	1.1		13	220	30	0.3	77	820	0.6	115
4A15	14.1	0.6	0.9	0.1	9	153	34	0.3	61	705	0.6	99

**Data for concentrations of long-lived elements in ten gram portions
of oil sand**

<u>Sample ID</u>	<u>% Bitumen</u>	<u>Cerium</u>	<u>Iron</u>	<u>Ytterbium</u>
2B17	3.3	54	1.1	2.3
1F5	4.4	65	0.5	2.8
1D5	5.8	40	0.4	1.7
1D3	6.5	52	0.4	2.0
1D16	8.0	46	0.3	1.8
1F50	9.3	27	0.3	1.2
1F32	10.3	30	0.3	1.2
4A5	12.2	13	0.1	0.3
4A15	14.1	11	0.0	0.4
<u>Sample ID</u>	<u>% Bitumen</u>	<u>Thorium</u>	<u>Chromium</u>	<u>Lanthanum</u>
2B17	3.3	7.8	43	27
1F5	4.4	9.6	42	32
1D5	5.8	6.1	28	20
1D3	6.5	7.1	30	24
1D16	8.0	6.4	24	22
1F50	9.3	3.7	20	14
1F32	10.3	4.1	22	15
4A5	12.2	1.6	5	6
4A15	14.1	1.1	5	5
<u>Sample ID</u>	<u>% Bitumen</u>	<u>Hafnium</u>	<u>Arsenic</u>	<u>Antimony</u>
2B17	3.3	11.8	1.4	0.45
1F5	4.4	16.7	1.7	0.41
1D5	5.8	9.7	1.6	0.36
1D3	6.5	14.4	2.1	0.45
1D16	8.0	13.9	1.5	0.36
1F50	9.3	6.2	1.6	0.27
1F32	10.3	7.7	1.4	1.40
4A5	12.2	1.5	0.8	0.75
4A15	14.1	1.5	0.7	0.65
<u>Sample ID</u>	<u>% Bitumen</u>	<u>Terbium</u>	<u>Neodymium</u>	<u>Selenium</u>
2B17	3.3	0.6	21	1.2
1F5	4.4	0.7	20	1.6
1D5	5.8	0.4	13	1.1
1D3	6.5	0.5	14	1.0
1D16	8.0	0.4	13	1.0
1F50	9.3	0.3		0.8
1F32	10.3	0.3	11	0.9
4A5	12.2	0.1		
4A15	14.1	0.1	4	0.3

**Data for concentrations of long-lived elements in ten gram portions
of oil sand**

Sample ID	% Bitumen	Zirconium	Rubidium	Zinc
2B17	3.3	172	49	25
1F5	4.4	216	52	36
1D5	5.8	142	34	19
1D3	6.5	184	36	24
1D16	8.0	189	19	16
1F50	9.3	85	25	17
1F32	10.3	99	23	14
4A5	12.2	21	8	6
4A15	14.1	24	7	-
Sample ID	% Bitumen	Lutetium	Tungsten	Scandium
2B17	3.3	0.31	1.4	5.6
1F5	4.4	0.38	1.3	5.0
1D5	5.8	0.23	1.5	3.3
1D3	6.5	0.29	0.9	3.4
1D16	8.0	0.24	0.8	2.4
1F50	9.3	0.16	0.8	2.2
1F32	10.3	0.17	0.6	2.1
4A5	12.2	0.05		0.5
4A15	14.1	0.04	0.3	0.4
Sample ID	% Bitumen	Caesium	Tantalum	
2B17	3.3	1.9	0.7	
1F5	4.4	2.0	0.8	
1D5	5.8	1.3	0.5	
1D3	6.5	1.2	0.6	
1D16	8.0	0.6	0.6	
1F50	9.3	0.8	0.4	
1F32	10.3	0.7	0.5	
4A5	12.2	0.1	0.1	
4A15	14.1	0.1	0.1	

Data for concentrations of elements (microg/g) in thirty gram test portions of oil sand

<u>ID</u>	<u>% bitumen</u>	<u>V</u>	<u>Al</u>	<u>Ti</u>	<u>Na</u>	<u>Dv</u>	<u>Mn</u>	<u>Ba</u>	<u>Eu</u>	<u>K</u>
2B17	3.3	58	48346	4506	1326	3.5	291	237	0.79	9466
1F5	4.4	52	44841	5087	1159	4.4	83	259	0.87	8374
1D5	5.8	38	28901	3585	726	2.8	58	223	0.57	6615
1D3	6.5	42	37250	1989	949	3.0	75	250	0.60	7684
1D16	8.0	32	16389	2718	405	1.6	40	162	0.38	4224
1F50	9.3	39	19538	2983	517	1.9	52	145	0.43	5419
1F32	10.3	32	14161	2515	372	1.3	41	140	0.37	3795
4A5	12.2	34	5253	1169	167	0.6	14	116	0.15	2263
4A15	14.1	31	5108	595	202	0.5	8	108	0.13	2258

RSD's of concentrations of eleven elements over nine transverse sections of oil sand core: (plot shown in Fig. 7.1)

<u>Transverse section (ID)</u>	<u>Dv</u>	<u>Sm</u>	<u>Eu</u>	<u>Ba</u>	<u>Ti</u>	<u>Mn</u>	<u>Na</u>	<u>V</u>	<u>K</u>	<u>Cl</u>	<u>Al</u>
2B17	5	11	7	11	5	9	2	3	20	13	2
1F5	3	20	18	11	7	4	3	6	20	10	3
1D5	11	8	18	11	13	14	27	9	11	60	13
1D3	8	14	4	8	4	3	11	5	11	27	5
1D16	8	13	10	12	4	13	17	6	15	23	16
1D50	11	11	8	14	11	26	14	8	12	53	12
1F32	4	16	11	15	3	11	7	4	12	17	2
4A5	6	11	19	4	7	4	6	6	5	39	6
4A15	9	11	6	9	10	4	9	5	4	45	2

Data for concentrations (microg/g) of elements in bitumen determined via their long-lived isotopes

<u>Unfiltered</u>		Co	Hg	Sm	La	Ni	Fe	Zn	Cr
	Sc								
1	0.195	3.65	0.07	0.080	0.64	67	227	19	3.8
2	1.380	4.03	0.48	0.357	2.12	100	955	30	13.9
3	0.831	2.22	0.19	0.181	1.08	55	1064	32	8.4
4	1.069	4.75	0.17	0.128	1.93	65	756	44	10.8
5	1.159	4.23	0.18	0.315	1.94	67	985	87	12.2
6	0.776	5.39	0.10	0.225	1.27	64	767	40	7.9
7	3.021	6.21	0.10	0.688	4.24	65	2654	86	24.3
8	0.194	1.80	0.12	0.072	0.46	69	176	40	5.1

<u>Filtered</u>		Co	Hg	Sm	La	Ni	Fe	Zn	Cr
	Sc								
1	0.019	1.10	0.13	0.008	0.05	74	23	20	1.1
2	0.019	1.47	0.60	0.011	0.07	45	37	33	0.8
3	0.021	0.53	0.17	0.010	0.09	40	71	24	1
4	0.024	0.82	0.30	0.013	0.10	50	69	53	0.9
5	0.017	0.86	0.21	0.008	0.07	41	72	17	1.3
6	0.018	2.09	0.08	0.004	0.07	51	45	25	1.2
7	0.012	0.75	0.11	0.006	0.03	50	29	11	1
8	0.011	0.80	0.08	0.003	0.04	51	21	11	0.6